DEPARTMENT OF CHEMISTRY, UNIVERSITY OF JYVÄSKYLÄ
RESEARCH REPORT No. 153

EXPLORING THE SELF-ASSEMBLY OF RESORCINARENES: FROM MOLECULAR LEVEL INTERACTIONS TO MESOSCOPIC STRUCTURES

BY

KAISA HELTTUNEN

Academic dissertation
for the degree of
Doctor of Philosophy

To be presented, by permission of the Faculty of Mathemathics and Science of the University of Jyväskylä, for public examination in Auditorium YAA303, on April 13th 2012, at 12 noon.

UNIVERSITY OF JYVÄSKYLÄ

Jyväskylä, Finland
ISBN 978-951-39-4675-3 (print)
ISBN 978-951-39-4676-0 (pdf)
ISSN 0357-346X

ABSTRACT

Helttunen, Kaisa
Exploring the self-assembly of resorcinarenes: from molecular level interactions to mesoscopic structures
Jyväskylä: University of Jyväskylä, 2012, 79 p.
(Department of Chemistry, University of Jyväskylä Research Report
ISSN 0357-346X; 153)
ISBN 978-951-39-4675-3 (print)
ISBN 978-951-39-4676-0 (pdf)

The research described in this thesis covers the synthesis, characterization, complexation, structural properties, and self-assembly of new amphiphilic resorcinarenes, as well as their application as functional materials.

Resorcinarene octols and tetramethoxy resorcinarenes were used as a macrocyclic platform for new amphiphilic hosts, resorcinarene bis-crowns, resorcinarene octapodands and aminomethylated resorcinarenes. The resorcinarene bis-crowns with preorganized and conformationally fixed binding sites are selective cation hosts for caesium and silver forming 1:1 and 1:2 host-guest complexes in the solid state and in solution. The resorcinarene octapodands contain flexible upper rims, and undergo *boat-to-boat* interconversion and rotation of the *o*-nitroaniline side arms. The complexation and conformational properties were investigated in solution using NMR spectroscopy and in the solid state by single crystal X-ray diffraction.

The lower rim alkyl chain length of the resorcinarene hosts had an effect on their crystal packing and self-assembly, namely on the stability and density of the Langmuir films and diameters of the solid lipid nanoparticles. The crystal structure analysis of the resorcinarene bis-crowns and their alkali metal and silver complexes showed that a pentyl group is the limiting alkyl chain length for bilayered packing in the solid state.

Self-assembled monolayers of resorcinarenes and their interaction with fluorescent dyes were studied in order to create functional materials and sensor applications. The Langmuir-Blodgett films of resorcinarene bis-crown silver complex provided antibacterial coatings, which inhibit the growth of *E. coli* with nanomolar silver concentration. The interaction of aminomethylated resorcinarenes with rhodamine B affects the lactone-zwitterion equilibrium and thus the absorbance and emission of the dye. In addition, the fluorescence intensity of anthracene resorcinarene conjugate can be enhanced by protonation in an acidic medium.

Keywords: antibacterial silver, fluorescence spectroscopy, host-guest chemistry, Langmuir-Blodgett film, NMR spectroscopy, resorcinarene, solid lipid nanoparticle, structural chemistry, supramolecular chemistry, UV-vis spectroscopy, X-ray crystallography

Author's address

Kaisa Helttunen
Department of Chemistry
Nanoscience Center
University of Jyväskylä
P.O. Box 35
FI-40014 University of Jyväskylä
Finland
kaisa.j.helttunen@jyu.fi

Supervisor

Professor Maija Nissinen
Department of Chemistry
Nanoscience Center
University of Jyväskylä
P.O. Box 35
FI-40014 University of Jyväskylä
Finland

Reviewers

Dr. Susan E. Matthews
School of Pharmacy
University of East Anglia
Norwich, UK

Professor Alexander Wei
Department of Chemistry
Purdue University
West Lafayette, USA

Opponent

Professor Pablo Ballester
Catalan Institution for Research and Advanced Studies
& Institute of Chemical Research of Catalonia
Tarragona, Spain

PREFACE

This work was carried out at the Department of Chemistry, University of Jyväskylä, Finland between 2007 and 2012. Funding was received from the Academy of Finland, national graduate school GSOCCB, Orion-Farmos Research Foundation and the Emil Aaltonen Foundation. In addition, grants from the Magnus Ehrnrooth Foundation, Alfred Kordelin Foundation and the Finnish Concordia Fund allowed me to participate in excellent conferences and meet many interesting people.

I am very grateful to my supervisor Professor Maija Nissinen, whose expertise, support and guidance have been essential for completing this work. Working in Maija's group has been a pleasure thanks to the delicately balanced ratio of responsibility and freedom. I wish to thank the other members of Maija's group, Aku Suhonen, Tiia-Riikka Tero, and in particular Kirsi Salorinne and Elisa Nauha for help and friendship throughout the project.

I wish to express my warmest gratitude to Professor Patrick Shahgaldian at FHNW Switzerland for a very fruitful collaboration and support, which shaped this project towards material applications. In addition, I wish to thank Patrick and his group at FHNW for the two months I spent in Basel and Muttenz during this project.

Coworkers in the Nanoscience Center and Department of Chemistry are warmly thanked for creating a pleasant working environment; it has been rewarding to share ideas about science and everything else with you. During these years, the list of people I would like to thank has grown vast. Especially, I would like to acknowledge Professor Erkki Kolehmainen, Professor Mika Pettersson, Professor Janne Ihalainen, Professor Kari Rissanen, Dr. Andreas Johansson, Dr. Ngong Kodiah Beyeh, Dr. Jussi Toppari, Dr. Pasi Myllyperkiö, Dr. Manu Lahtinen, Dr. Piotr Prus and Dr. Nonappa for your help and advice. I also wish to thank all students who have assisted in this project: M.Sc. Anni Riikonen (née Kurronen), Riia Annala, M.Sc. Tahnie Barboza, Hélène Campos Barbosa and M.Sc. Jenna Virkkala.

Laboratory technicians Mirja Lahtiperä and Elina Hautakangas are thanked for the assistance in mass spectrometry and elemental analyses. Laboratory technicians Reijo Kauppinen and Esa Haapaniemi are warmly thanked for the valuable help with the NMR. Laboratory technician Hannu Salo is acknowledged for operating the SEM. Laboratory technicians Pia Petriläinen and Leena Koskela are warmly thanked for their assistance in the day-to-day maintenance of the synthesis laboratory. The assistance of Riitta-Liisa Kuittinen, amanuensis of the Nanoscience Center, has been invaluable, as well as the help of the administrative personnel at the Department of Chemistry.

I would like to express my most sincere gratitude to the reviewers of this thesis, Dr. Susan Matthews and Professor Alexander Wei for their valuable comments. I feel privileged to have such experts of supramolecular chemistry as the referees of my work. I would also like to acknowledge University of Jyväskylä Language Services for revising the language.

To all my friends in Jyväskylä and further away, thank you for your support and good times during these years. In particular, very warm thanks go to Suvi V., Suvi S., Johanna P., Anni M. and Kirsi V. for your friendship and discussions, and to the girls of Dancegroup Meret for such a nice way of taking my mind off work.

Finally, I want to thank my family for the support throughout my studies: Kiitos äiti ja isä, Juuso ja Riikka, ja Antti.

Last but not least, special thanks to Tuomas for giving me moments of joy during these intensive years.

Jyväskylä, March 16th 2012

Kaisa Helttunen

LIST OF ORIGINAL PUBLICATIONS

I Kaisa Helttunen and Patrick Shahgaldian, Self-assembly of amphiphilic calixarenes and resorcinarenes in water, *New. J. Chem.*, **2010**, *34*, 2704–2714.

II Kaisa Helttunen, Kirsi Salorinne, Tahnie Barboza, Hélène Campos Barbosa, Aku Suhonen and Maija Nissinen, Cation binding resorcinarene bis-crowns: the effect of lower rim alkyl chain length on crystal packing and solid lipid nanoparticles, *New. J. Chem.*, **2012**, *36*, 789-795.

III Kaisa Helttunen, Negar Moridi, Patrick Shahgaldian and Maija Nissinen, Resorcinarene bis-crown silver complexes and their application as antibacterial Langmuir-Blodgett films, *Org. Biomol. Chem.*, **2012**, *10*, 2019-2025.

IV Kaisa Helttunen, Elisa Nauha, Anni Kurronen, Patrick Shahgaldian and Maija Nissinen, Conformational polymorphism and amphiphilic properties of resorcinarene octapodands, *Org. Biomol. Chem.*, **2011**, *9*, 906–914.

V Kaisa Helttunen, Piotr Prus, Minna Luostarinen and Maija Nissinen, Interaction of aminomethylated resorcinarenes with rhodamine B, *New J. Chem.*, **2009**, *33*, 1148–1154.

The author is the primary author of papers II-V. She carried out most of the experimental work in papers II–V apart from the LB films and antibacterial tests in paper III. In paper I, the author has written the chapter about micelles.

ABBREVIATIONS

9-BBN	9-borabicyclo[3.3.1]nonane
AFM	atomic force microscopy
AIBN	azodiisobutyronitrile
BSA	bovine serum albumin
CIC	complete inhibitory concentration
CMC	critical micelle concentration
D_H	hydrodynamic diameter
DNA	deoxyribonucleic acid
DLS	dynamic light scattering
DMF	*N,N*-dimethylformamide
DMSO	dimethyl sulfoxide
DOTA	1,4,7,10-tetra(carboxymethyl)-1,4,7,10-tetraazacyclododecane
EDC	1-(3-dimethylaminopropyl)-3-ethylcarbodiimide
IR	infrared
LB	Langmuir-Blodgett
MRI	magnetic resonance imaging
NBS	*N*-bromosuccinimide
NHS	*N*-hydroxysuccinimide
NMR	nuclear magnetic resonance
PEG	polyethylene glycol
PET	photoinduced electron transfer
PGSE NMR	pulsed gradient spin-echo nuclear magnetic resonance
QCM	quartz crystal microbalance
SAM	self-assembled monolayer
SEM	scanning electron microscopy
SLN	solid lipid nanoparticle
SPR	surface plasmon resonance
TEM	transmission electron microscopy
THF	tetrahydrofuran
UV-vis	ultraviolet-visible
VOC	volatile organic compound
XRD	X-ray diffraction

CONTENTS

1 LITERATURE REVIEW

1.1 Introduction

Resorcinarenes and calixarenes form a group of macrocyclic supramolecular hosts, which consist of resorcinol- or phenol-derived aromatic rings connected by carbon bridges.[1-3] After the discovery of these synthetic oligomers as condensation products of phenol, resorcinol and pyrogallol with aldehydes by Adolf von Baeyer[4,5] in the late 19th century, it took several decades before more detailed analysis of resorcinarenes[6] and calixarenes[7] led to a proposal of their macrocyclic structure.[8,9] The ability of calixarenes to form inclusion complexes and retain water within their crystals was realized quite early,[6] but the modern days of calixarene chemistry started at the turn of the 1970s and 1980s when their potential as synthetic enzyme mimics was proposed by Gutsche[10] and the first crystal structures of their solid state inclusion complexes were solved.[11,12] Ever since, the unique properties of resorcinarenes and calixarenes, that is, a hollow aromatic cavity inside the macrocycle, large but defined molecular size and shape, and the possibility of different conformations, which direct the orientation of the functional groups, have been intensively studied.[1-3] These properties, in addition to versatile synthetic routes that allow the introduction of new features, such as water solubility,[13-15] as well as the affinity and selectivity towards guest molecules and ions led to applications of calixarenes and resorcinarenes in molecular recognition,[16,17] ion transport,[18,19] catalysis[20-22] and as enzyme mimics.[23,24]

The emergence of nanoscience and nanochemistry in the 1990s, after the development of scanning probe microscopic techniques, directed the chemistry of calixarene type of macrocycles towards nanoscale materials and applications. Research of resorcinarenes and calixarenes in the 21st century is based on self-assembly[25-27] as a method for the preparation of nanoscale materials,[I,2,3] such as monolayers, thin films, micelles, vesicles and fibers, scaffolds for metal nanoparticles[28] and preparation of crystalline solids.[29] The molecular recognition properties enable the development of calixarene sensors for various

analytes, as well as encapsulation and transportation of drugs, biomolecules and ions.[23,24,30-32] The literature review of this thesis focuses on the structural properties governing the self-assembly of amphiphilic resorcinarenes and calixarenes, and how the complexation properties of these macrocyclic compounds can be utilized in biochemical and sensor applications.

1.2 Resorcinarenes and calixarenes as supramolecular hosts

1.2.1 Synthesis and structure

Resorcinarenes, also known as resorcarenes or calix[4]resorcinarenes, are synthesized by an acid-catalyzed condensation of resorcinol and aliphatic or aromatic aldehydes.[1,3] The major product is a tetrameric macrocycle **1** (Fig. 1), which is derived in the aforementioned conditions under thermodynamic control, but examples of five- and six-membered resorcinarenes are also known.[33-36] The most important structural features of the resorcinarenes include the bowl-shaped, aromatic binding cavity, eight phenolic hydroxyl groups, which form intramolecular hydrogen bonds at the upper rim of the resorcinarene cavity, and pendant aliphatic or aromatic groups (*R*) attached to the bridging methine carbons at the lower rim.[1]

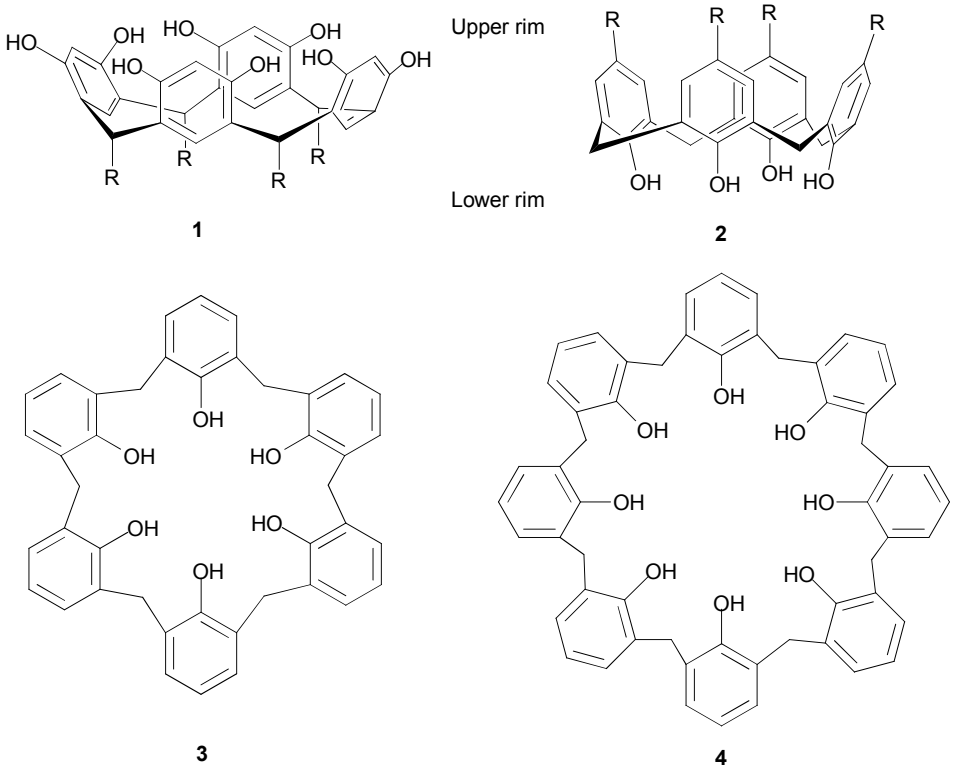

Figure 1. Molecular structure of resorcinarene **1** and calix[4]arene **2**, indicating their upper and lower rims, *p*-H calix[6]arene **3** and *p*-H calix[8]arene **4**.

Calix[n]arenes are synthesized by a base-catalyzed condensation of *p*-substituted phenols, usually *p-tert*-butyl phenol, and formaldehyde, which produces a tetrameric macrocycle (**2,** n = 4)[37] along with larger hexameric (**3**, n = 6)[10] and octameric (**4**, n = 8)[38] structures depending on the reaction conditions

(Fig. 1). In addition, 5-, 7- and 9-membered rings can be prepared.[3] Calix[4]arenes contain four phenolic hydroxyl groups located at the lower rim (narrow rim) of the calixarene bowl, and the *p*-alkyl groups at the upper rim (wide rim) of the calixarene.

Synthetic modifications of the resorcinarene upper rim can be divided into three categories. First of all, resorcinarenes can be synthesized from 2-substituted resorcinols, which have an electron donating group, such as methyl,[39] ethyl,[40] or hydroxyl,[41] in *ortho* position to the hydroxyl groups, whereas a condensation reaction with electron withdrawing groups (-Br, -NO_2, -COOH) does not form tetrameric products (Scheme 1).[39] The second method comprises the functionalization of the hydroxyl groups at the resorcinarene upper rim, which can be alkylated, acylated or tosylated.[1,3,42] Examples of regioselective functionalization of the four distal hydroxyl groups are also known.[43] The third category of reactions includes electrophilic substitution of the aromatic ring, for example, by bromination,[44,45] diazo coupling[46,47] and Mannich reaction.[48] The Mannich reaction with a secondary amine and formaldehyde introduces tertiary amino groups at the 2-position of the resorcinol ring. Similar and even more versatile synthetic routes are available for calixarenes, which can be *O*-alkylated or acylated in a regioselective manner. Combined with electrophilic substitution reactions to the upper rim *p*-position, facile synthetic routes to numerous calixarene hosts are obtained.[2,3]

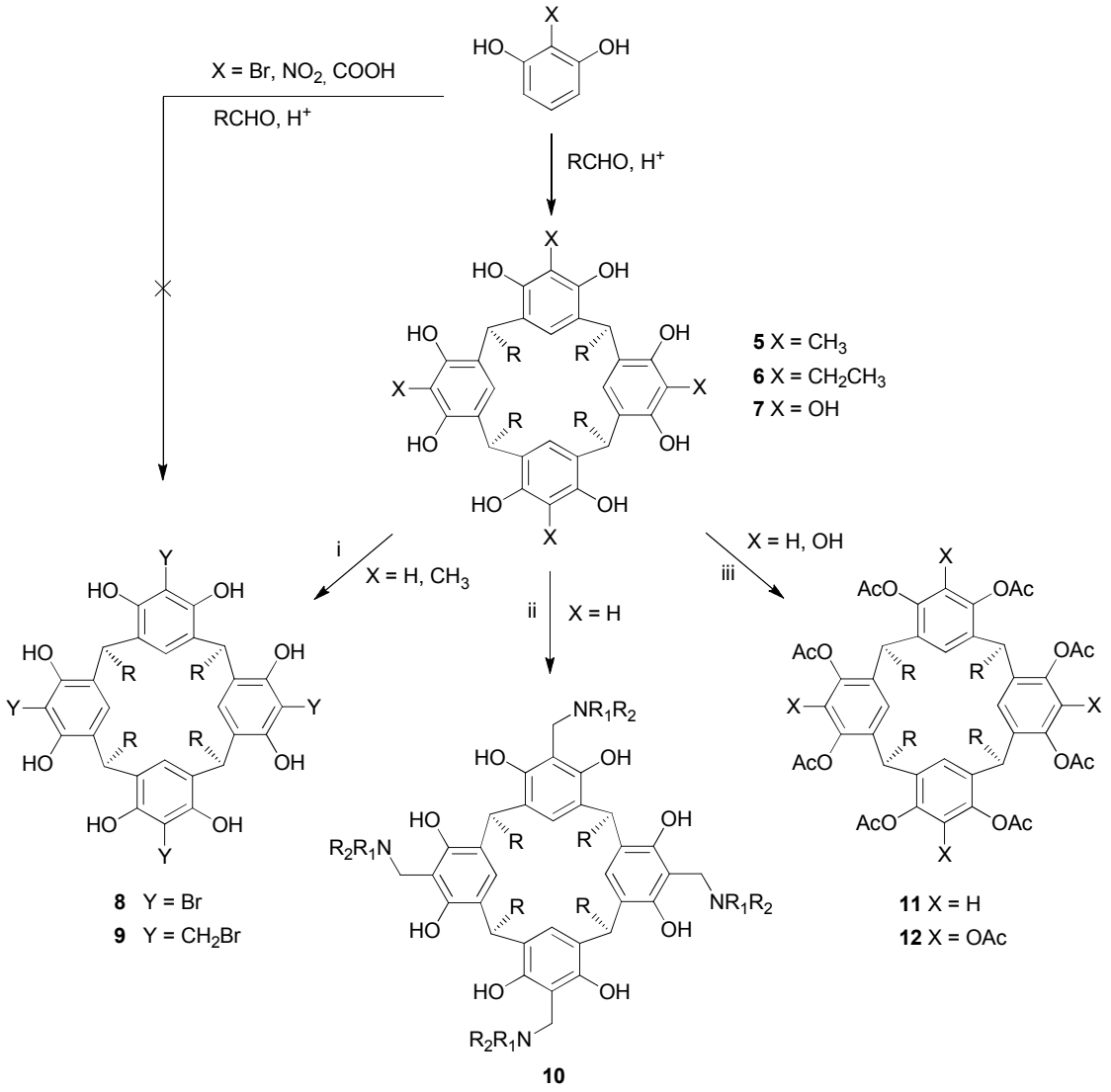

Scheme 1. Synthesis of upper rim functionalized resorcinarenes by bromination (i, NBS),[44,45,49] Mannich reaction (ii, NHR_1R_2, CH_2O)[48] and *O*-acetylation (iii, Ac_2O).[6,50]

Resorcinarenes, which have been prepared from long chain aliphatic aldehydes are inherently amphiphilic, which means that they contain a polar and non-polar head within a single molecule (Fig. 2).[51] The solubility of resorcinarenes can be tuned by the choice of the lower rim alkyl chain length, and the short alkyl chain derivatives, such as C-methyl resorcinarene, can be made water soluble by the addition of polar or ionic groups at the upper rim.[46] Water soluble calixarenes are prepared by functionalizing the upper or lower rim with ionic groups, such as carboxylate,[13,52] sulfonyl,[14,15] phosphate,[53-55] amino[15] or amido[56] groups. The addition of lipophilic alkyl or acyl groups to the opposite rim of the calixarene makes them amphiphilic (Fig. 2).

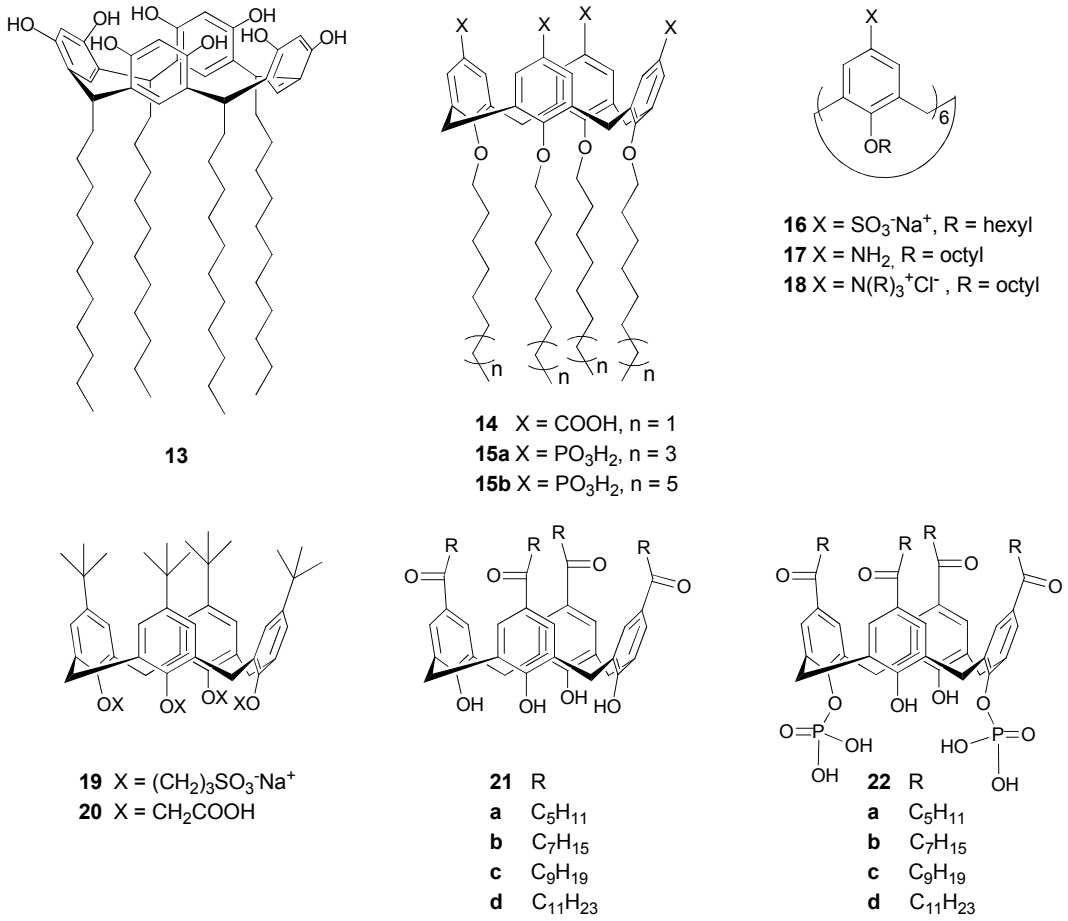

Figure 2. Amphiphilic C-undecyl resorcinarene **13**,[51] amphiphilic calix[4]arenes (**14**-**15**)[52,55,56] and calix[6]arenes (**16**-**18**)[14,15] with polar groups at the upper rim; calix[4]arenes with polar groups at the lower rim (**19**-**20**),[13,15] *p*-acyl calix[4]arenes **21a**-**d** and *p*-acyl dihydroxyphosphoryloxy calix[4]arenes **22a**-**d**.[53]

The lower rim of resorcinarenes can be functionalized by using bifunctional aldehydes such as Ω-alkene,[57-59] acetal protected 11-hydroxydocecanal[60] or sodium 2-formylethane-1-sulfonate formed *in situ*,[17] to provide double bonds, hydroxyl or sulfonate groups at the lower rim, respectively. The alkene functionality can be transformed into thiols[61] or thioethers[58] (Scheme 2), which enables covalent attachment of the resorcinarenes on gold to produce self-assembled monolayers (SAMs). Synthetic transformations or attachment to surfaces often require protection of the upper rim hydroxyls with acetyl[58] or silyl groups.[62] The upper rim hydroxyl groups can also be protected by covalent bridging of the adjacent hydroxyls, which produces resorcinarenes with rigidified binding cavities, also called resorcinarene cavitands (Scheme 2).[44,45,57]

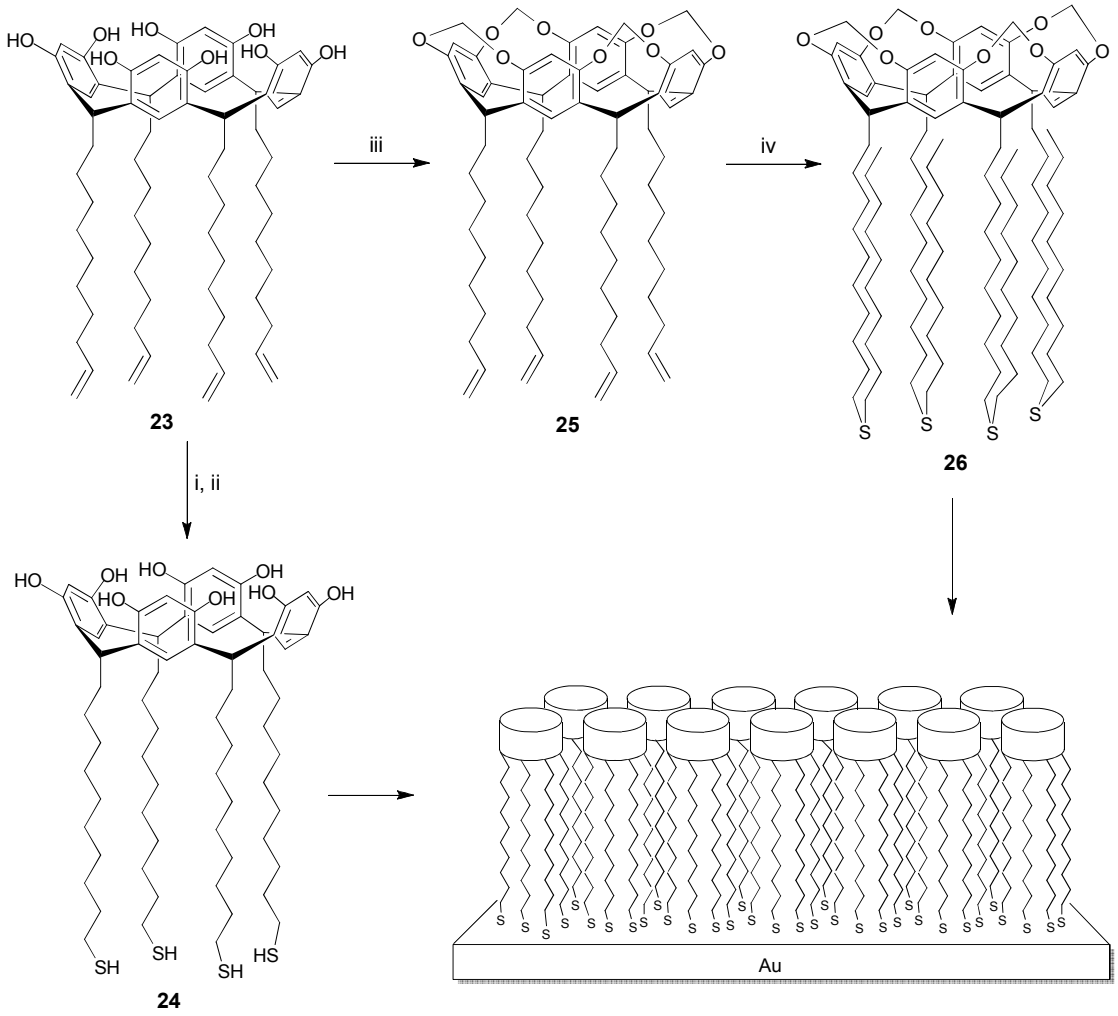

Scheme 2. Functionalization of the lower rim of C-(9-decenyl) resorcinarene **23** to produce thiol terminated resorcinarene **24**,[61] resorcinarene cavitand **25** and thioether terminated cavitand **26**,[58] and preparation of self-assembled monolayers (SAMs) on Au: i) thiolacetic acid, AIBN, ii) NaOH, MeOH, iii) $BrCH_2Cl$, K_2CO_3, iv) decanethiol, 9-BBN.

1.2.2 Conformational mobility

Resorcinarenes and calixarenes can exist in many conformations besides the most common *crown* conformation of resorcinarene and the corresponding *cone* conformation of calixarene (shown in Fig. 1).[1,3] The resorcinarene configuration is classified according to the orientation of the lower rim substituents, *R*, which can be either axial or equatorial, *endo* or *exo*, relative to the resorcinarene cavity. The resorcinarene conformation is assigned by the orientation of the aromatic rings relative to the methine carbon plane. When all *R*s are in the *endo* position, which thermodynamically is the most stable orientation for aliphatic alkyl chains, *crown*, *boat* and *scoop* conformations have been observed (Fig. 3).[39,50,63-66] In the *crown* conformation, all hydroxyl groups point upwards forming a ring of intramolecular hydrogen bonds which stabilizes the crown structure,[39] whereas in the *boat* conformation two opposing aromatic rings face up and the another

two lay almost parallel to the methine carbon plane.[50,63] The scoop is a hybrid of the two previous conformations and it has been observed in the solid state.[66] By studying the kinetic products of the resorcinarene condensation, where at least one aliphatic *R* is in the *exo* orientation, *chair* and *diamond* conformations with one or two aromatic rings pointing down, respectively, have been found.[50,64,65] However, since only all-*endo* conformations—*crown*, *boat* and *scoop*—provide more or less bowl-shaped binding cavity, they are more favorable in host-guest complexation.

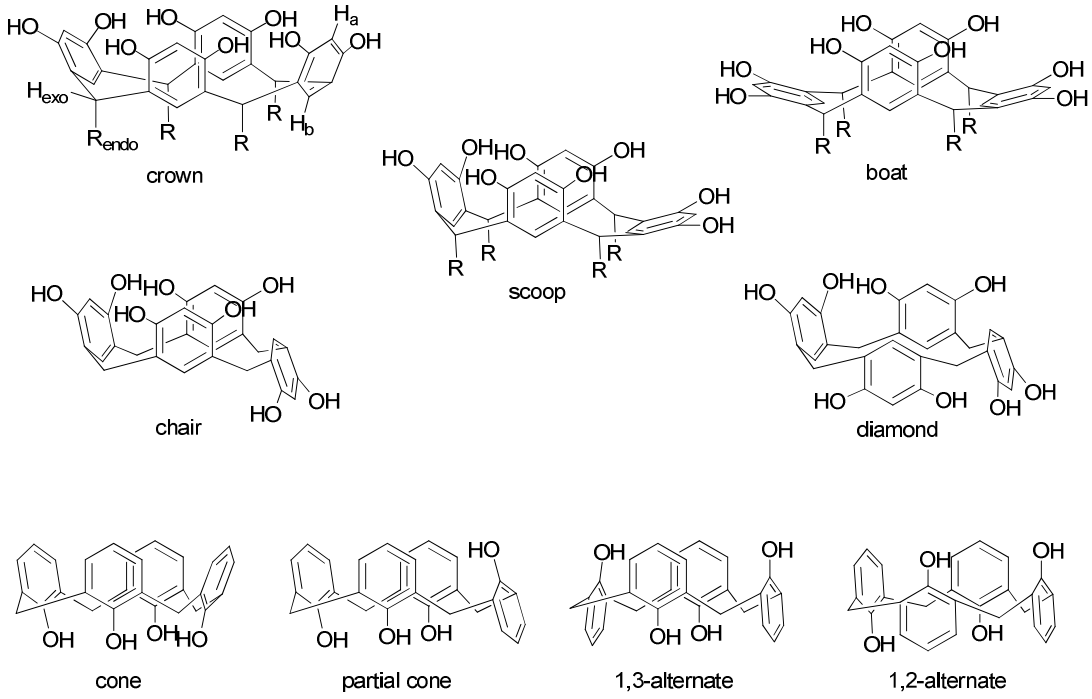

Figure 3. The resorcinarene and calixarene conformations.

A similar classification of conformations is applied to calix[4]arene conformations with different names.[2,3] In addition to the *cone* conformation where all *R* substituents point up (Fig. 1), they can obtain *partial cone*, *1,3-alternate* or a less common *1,2-alternate* conformation, in which one, the two distal, or the two adjacent phenol rings, respectively, are rotated relative to the methylene bridges (Fig. 3). The *flattened cone* conformation is reminiscent of the resorcinarene *boat* conformation. For calix[6]arenes and larger calixarenes (higher calixarenes), the up-down orientation of the phenol rings is no longer sufficient to describe the conformation since the macrocycles can bend or fold relative to the core, and the phenolic rings can tilt inward or outward.[2] Therefore, in addition to larger cavity size, higher calixarenes also present increased conformational flexibility.

Due to the relative flexibility of resorcinarenes and calixarenes, two or more conformations can convert in equilibrium. True *crown* conformation can be distinguished from a *boat-to-boat* conversion, where two different *boat* conformations interconvert in equilibrium, by two sharp aryl proton signals in

^{1}H NMR spectra at a wide temperature range.[64,65] The *boat-to-boat* conversion, also called pseudorotation, can be deduced from the collapse of the lower rim aryl proton H_b and broadening of the upper rim aryl proton H_a (Fig. 3) close to room temperature.[50,63] At lower temperatures the pseudorotation slows down and the aryl signals separate into two singlets.[50,63-65]

Conformation and conformational mobility is an interesting structural feature of resorcinarenes and calixarenes, which can be somewhat utilized and controlled. It affects their host-guest complexation, and by restricting conformational mobility—by covalent bridging, for example—higher preorganization of the host and therefore improved selectivity and affinity can be obtained.[67-71] In addition, conformational mobility also affects the self-assembling properties of amphiphilic calixarenes and resorcinarenes, such as water solubility,[15,72] dimerization,[73] shape and size of calixarene conjugates and their aggregates,[72,74-76] and the flexibility and packing of monolayers.[60] On the other hand, self-assembly also reduces the conformational mobility of resorcinarenes and calixarenes by, for example, directing the hydrophilic groups towards water.[77,78] A controlled change in the conformation of the resorcinarenes can also be utilized for creating molecular motors and switches.[79,80]

1.3 Self-assembly of amphiphilic calixarenes and resorcinarenes

1.3.1 Micelles[I]

The self-assembly of amphiphilic molecules into micelles—i.e. small molecular aggregates with a hydrophobic interior in an aqueous solution (Fig. 4)—is a spontaneous dynamic process which is usually said to occur when the concentration of the amphiphile reaches the critical micelle concentration (CMC). The conditions of self-assembly are controlled by several parameters, with the conical shape of the amphiphile being considered as a prerequisite for forming spherical micelles. Calixarenes and resorcinarenes offer intriguing synthetic possibilities for preparing conically shaped amphiphiles, as demonstrated, for instance, with mono-*O*-alkyl *p*-carboxymethyl (**27**) and *p*-aminomethyl calix[4]arenes (**28**, Fig. 5).[81,82] The *p*-carboxymethyl calix[4]arenes **27** are ionic at the physiological pH 6-8, and their CMC values decrease with increasing alkyl chain length, from C_1 to C_{12}; this is a common trend for surfactants.[81] The aminomethylated calix[4]arenes **28** also formed micelles at pH 2, where all aminogroups are protonated.[82] However, their CMC values do not follow a similar trend. At higher pH, where the amphiphiles are not ionic, the short alkyl chain derivatives form larger aggregates with hydrodynamic diameters >500 nm, whereas the long chain derivatives still assemble as micelles. Based on these observations, the macrocyclic structure and aromatic binding cavity of calixarenes and resorcinarenes differentiate them from linear one- or two-legged surfactants.

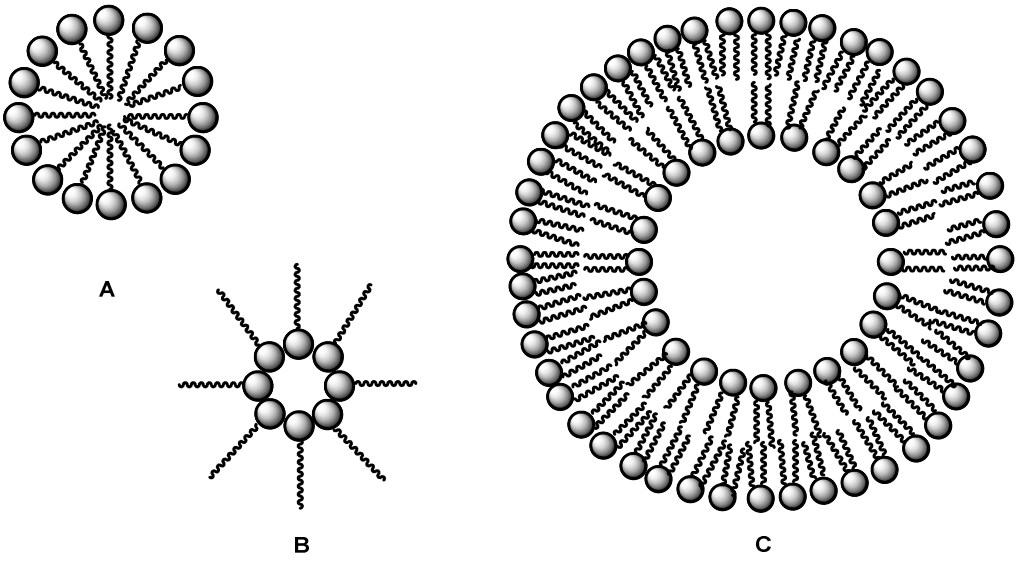

Figure 4. Schematic structure of A) a micelle, B) a reverse micelle and C) a vesicle.

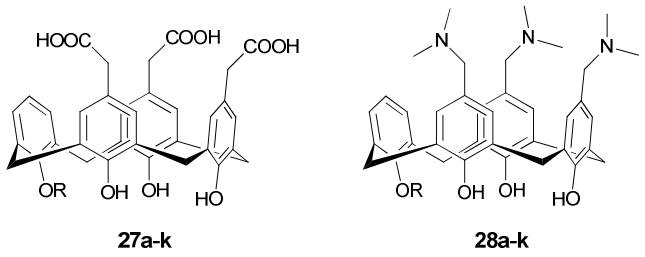

27a-k **28a-k**

Figure 5. Mono-*O*-alkyl *p*-carboxymethyl (**27a-k)** and *p*-aminomethyl calix[4]arenes (**28a-k**), **a**: R = CH_3, **b**: R = C_2H_5, **c**: R = C_3H_7, **d**: R = C_4H_9, **e**: R = C_5H_{11}, **f**: R = C_6H_{13}, **g**: R = C_7H_{15}, **h**: R = C_8H_{17}, **i**: R = C_9H_{19}, **j**: R = $C_{10}H_{21}$, **k**: R = $C_{12}H_{25}$.[81,82]

The dynamic aggregation process can happen stepwise when the monomers form dimers or trimers well below the CMC at a very low concentration, and these precursors assemble as micelles when the concentration is increased. For example, water soluble calix[4]arenes with four 2′-deoxythymidine (**29a**) or 2′-deoxyadenosine (**29b**) groups at their narrow rim (Fig. 6) self-assemble as dimers, which aggregate into micellar structures with hydrodynamic diameters (D_H) of 3.8 and 3.9 nm, respectively.[83] Adenine bases show stronger π-stacking interactions which lead to lower CMC value of **29b** (0.22 mM) compared to the thymine functionalized amphiphile **29a** (0.51 mM). The micelles aggregate into larger clusters when dried on a solid substrate. In the solid state, only **29b** forms spherical and well-defined aggregates of 700 nm diameter; in contrast, **29a** tends to form smaller clusters which assemble into grapelike superstructures, as observed by SEM.

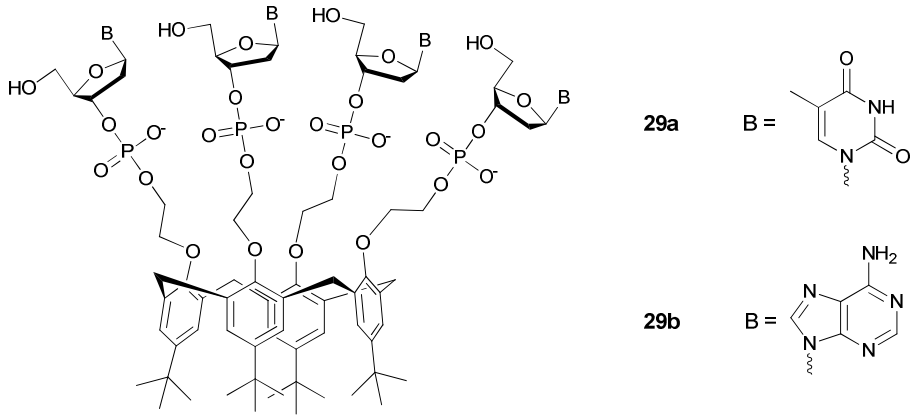

Figure 6. Molecular structure of calix[4]arene tetra-2′-deoxythymidine (**29a**) and tetra-2′-deoxyadenosine (**29b**) conjugates.[83]

Also gadolinium-chelating calix[4]arene **30** (Fig. 7) forms small preaggregates, which assemble into micelles with a hydrodynamic radius of 2.2 nm.[84] The calixarene conjugate was synthesized as a magnetic resonance imaging (MRI) contrast agent, where the toxic gadolinium must be strongly chelated to prevent its release in the body. Therefore, the chelator also has an effect on the performance of the substance.[24] The micellization of the calixarene **30** was found to improve its properties in MRI in comparison to the monomer.[84]

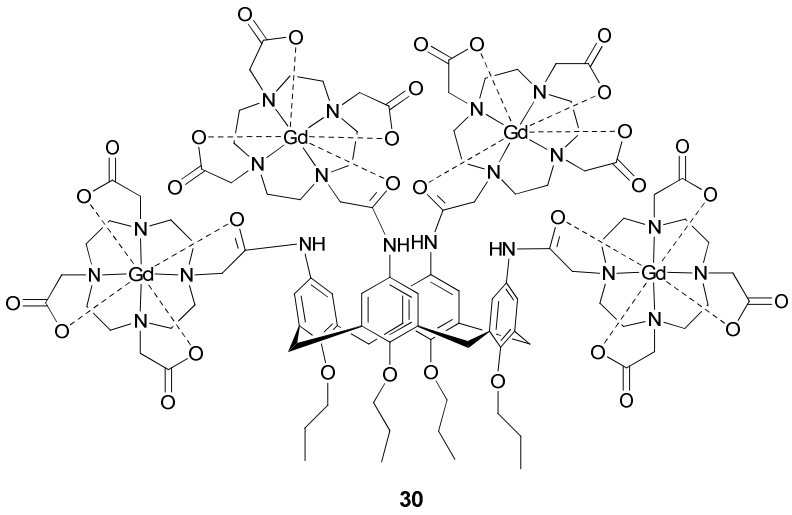

Figure 7. Structure of calix[4]arene gadolinium 1,4,7,10-tetra(carboxymethyl)-1,4,7,10-tetraazacyclododecane (DOTA) conjugate **30**.[84]

Aoyama et al.[85,86] have studied water soluble, non-ionic amphiphiles, which are synthesized from resorcinarenes and which contain extremely large oligosaccharide head groups (Fig. 8). The conjugates do not affect the surface tension of water due to rapid aggregation into micellar structures; this, however, is a clear indication of their amphiphilic nature. The formation of micelles cannot be explained by hydrophobic interactions alone, since the micelle

formation is found to be irreversible even at very low concentrations and the aggregates do not dissociate into monomers. Therefore, in addition to aggregation due to hydrophobic effect between the lower rim alkyl chains, steep curvature in the shape of the conjugates along with hydrogen bonding between the oligosaccharide chains drives the formation of small micelles consisting of 4–6 molecules instead of lamellar assemblies. Interestingly, phosphate anions promote agglutination of the micelles (Fig. 9). ^{31}P NMR studies indicate that phosphate anions are effectively hydrogen-bonded by the oligosaccharide moieties, precipitating two water-soluble species, sugar and salt, out of the solution.

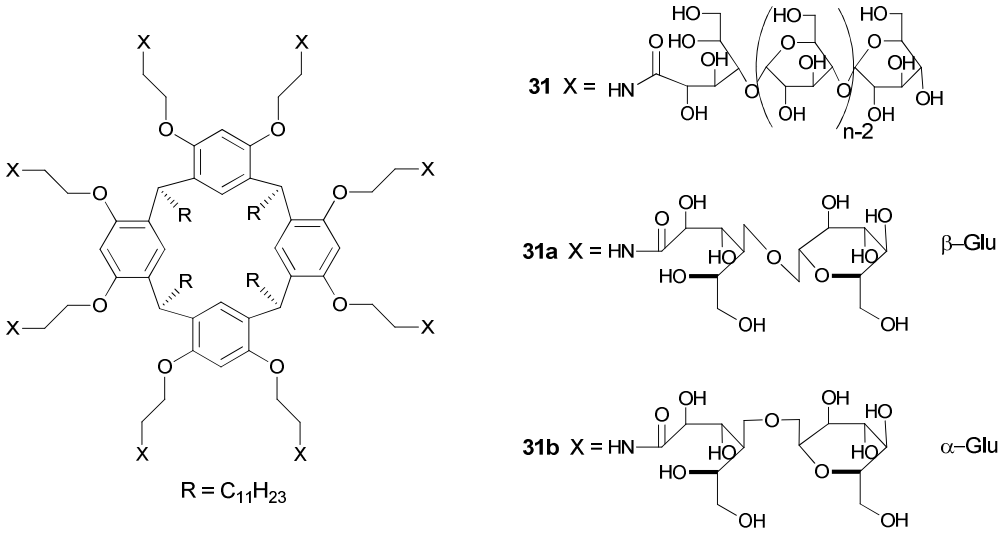

Figure 8. Molecular structure of oligosaccharide resorcinarene conjugates **31**. The head group contains 15-56 glucose residues giving MW of 4 000-10 000 g/mol for the conjugates.[85,86]

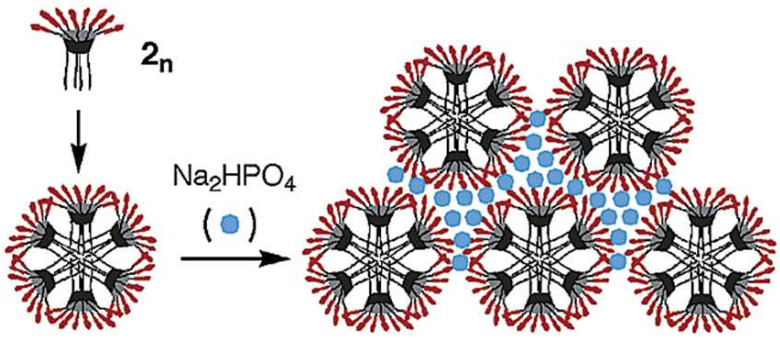

Figure 9. Schematic representation of the self-assembly and phosphate-induced agglutination of amphiphilic resorcinarene oligosaccharide conjugates.[85] (Reprinted with permission from reference 85. Copyright (2003) American Chemical Society.)

Another example of irreversible micellization in water was found with an amphiphilic water soluble tris(hydroxymethyl)amide resorcinarene **32** (Fig. 10), which is not surface active but nevertheless forms small aggregates as indicated by the broad NMR resonances in D_2O.[87] The micelles consist of 3-4 molecules based on PGSE NMR (diffusion) and molecular simulations, and they can be destabilized with organic solvents, such as DMSO or DMF, leading to monomer micelle exchange and reduced size of the aggregates.

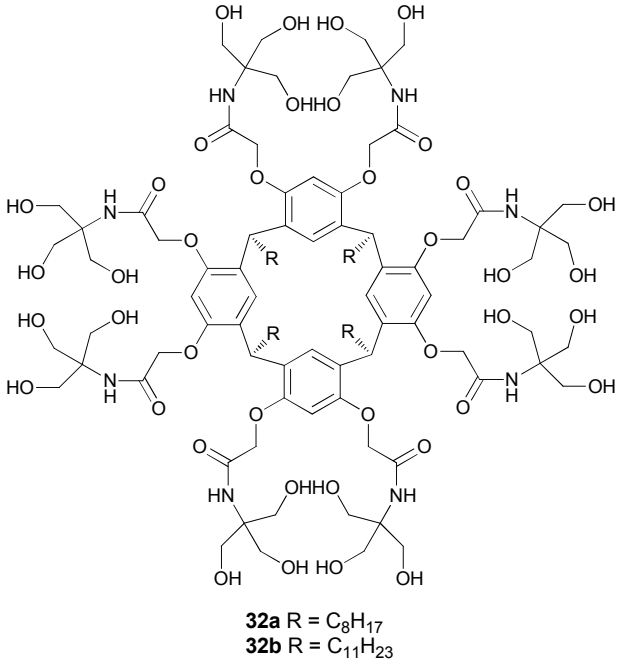

Figure 10. Tris(hydroxymethyl)amide resorcinarene **32a-b**.[87]

The dendrocalixarene **33** (Fig. 11) with a large anionic head group self-assembles at neutral pH and very low concentration (<40 μM) into robust and uniform micelles with hydrodynamic diameters of 6 nm.[88] The structure of the micelles was determined at 12 Å resolution by cryo-TEM and 3D-reconstruction (Fig. 12), and a model with seven subunits was proposed. The interior of these micelles was disordered and not visible in the TEM images. Time-resolved spectroscopy using pyrene as a guest molecule showed that a hydrophobic guest can experience different environments inside the micelle, i.e. the aromatic part of calixarene macrocycle in addition to the hydrophobic tails.[89] However, the calixarene **33** does not quench the pyrene fluorescence as efficiently as 2,6-dimethylanisole, which was used as a non-macrocyclic control for the calixarene walls, but instead protects the embedded fluorophore from the quenchers present in the solution.

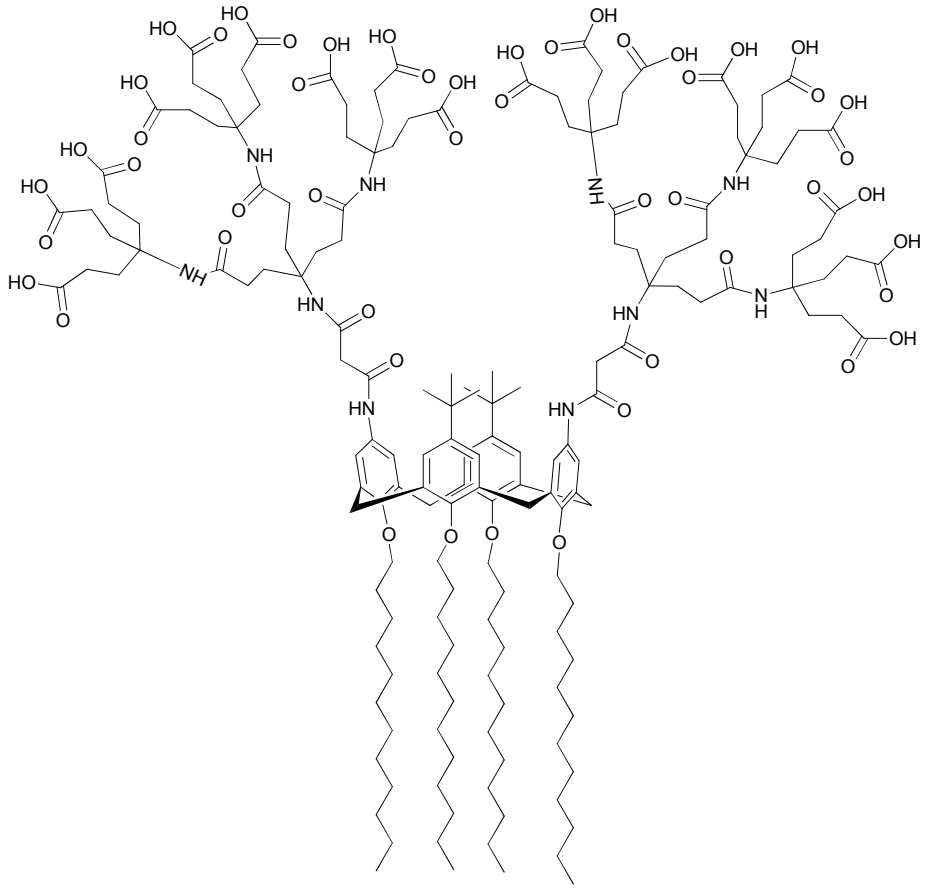

33

Figure 11. Structure of amphiphilic dendrocalixarene **33**.[88]

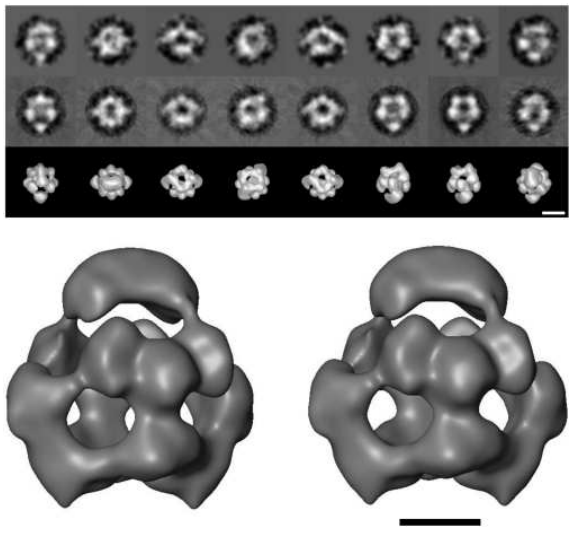

Figure 12. Electron micrographs of dendrocalixarene micelles and their 3D reprojections (above), stereoview of the 3D structure (below).[88]

The aggregation of amphiphilic resorcinarenes with carboxymethyl (**34**), 2-hydroxyethyl (**35**), methylamino acetal (**36**) or dialkylaminogroups (**37-38**) was studied in chloroform, where they form reverse micelles (Fig. 13).[90,91] The reverse micelles form by intramolecular hydrogen bonding between the upper rims, and all of the investigated derivatives show lower CMC values than unsubstituted resorcinarene octol. In addition, the carboxymethyl (**34**) and hydroxyethyl (**35**) resorcinarenes formed intramolecular hydrogen bonds more efficiently than the aminomethylated derivatives, because the strong intramolecular O-H···N hydrogen bonds of **37-38** compete with intermolecular interactions.

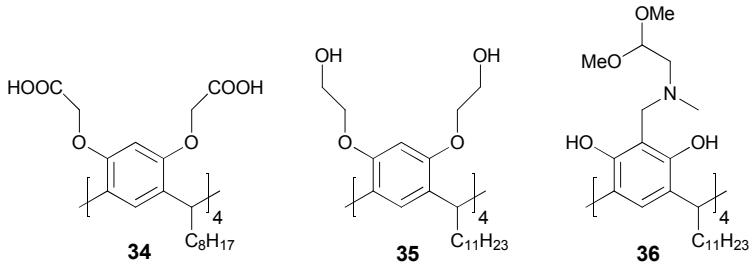

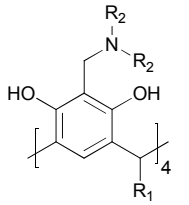

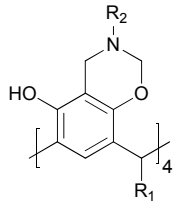

37a R_1 = -C_6H_{13}, R_2 = -CH_3
37b R_1 = -C_9H_{19}, R_2 = -CH_3
37c R_1 = -$C_{11}H_{23}$, R_2 = -CH_3
37d R_1 = -C_9H_{19}, R_2 = -C_2H_5
37e R_1 = -$C_{11}H_{23}$, R_2 = -C_2H_5

38a R_1 = -CH_3, R_2 = -$C_{10}H_{21}$
38b R_1 = -$C_{11}H_{23}$, R_2 = -C_4H_9

Figure 13. Structure of amphiphilic resorcinarenes **34**-**38**.[90,91]

Calixarenes and resorcinarenes are convenient building blocks for supramolecular amphiphiles, in which the hydrophobic and hydrophilic parts of the supramolecule are linked by weak interactions. As a hydrophilic building block, calixarenes and resorcinarenes can be utilized in the dispersion hydrophobic pharmacological compounds.[92] For example, a water-soluble calix[4]arene PEG-conjugate **39** forms an inclusion complex with hydrophobic phenyl palmitate (guest), and the complex forms aggregates in a mildly polar medium (Fig. 14).[93] The morphology of the aggregates can be controlled by changing the ratio of hydrophobic and hydrophilic counterparts in the system. Increasing the amount of hydrophobic guest changes the equilibrium from vesicles with a diameter of 270 nm to micellar species with a diameter of 130 nm at the 1:1 ratio. Finally, an excess of guest leads to the formation of fibrous network aggregates.

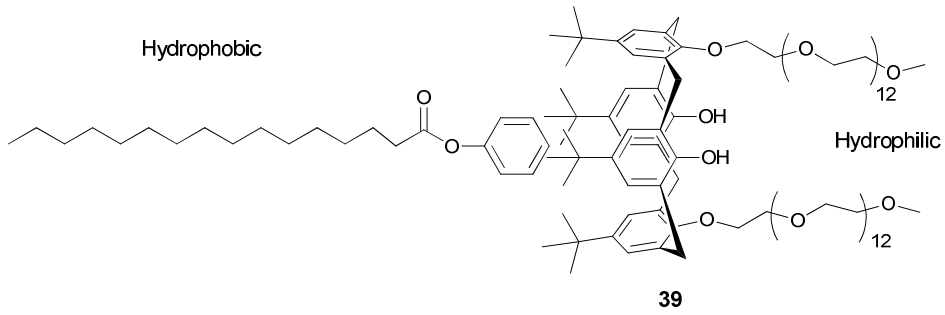

39

Figure 14. Schematic structure of a supramolecular amphiphile formed by an inclusion complex of calix[4]arene PEG-conjugate **39** and phenyl palmitate.[93]

1.3.2 Vesicles[I]

Cylindrical amphiphiles can assemble as vesicles (or liposomes), which have bilayered walls and a hydrophilic solvent-filled interior (Fig. 4). Unmodified *p*-H calix[6]arene (**3**) forms unilamellar vesicles of 0.5-1 μM in diameter by injection of THF solution in water.[77] The shape of the calix[6]arene **3** is cylindrical when all of the lower rim hydroxyl groups are directed towards water, and the aggregation is promoted by π-stacking interactions between the aromatic walls of the macrocycle. *p-tert*-Butyl calix[6]arene did not form vesicles, probably because the shape of the molecule is not perfectly cylindrical.

Resorcinarene octol (**1**) and pyrogallarene (**7**) with long C_{17} alkyl chains formed vesicles by injection of THF solution in aqueous buffer.[94] Small vesicles with a mean diameter of 50 nm (range of 30-240 nm) were obtained. A reference compound lacking the macrocyclic structure, 4-octadecylresorcinol, assembled as micelles under identical conditions.

Relatively minor differences in the geometry of two structurally related calix[4]arenes (**40**-**41**) lead to self-assembly, either into vesicles or into very small aggregates, presumably micelles.[95] The *p*-carboxylic acid derivative **40** (Fig. 15) spontaneously assembles as unilamellar but polydisperse vesicles with a mean diameter of 86 nm in basic solution. The quaternary ammonium derivative **41** did not form large vesicles; the authors suspected that the aggregates were too small to be detected with their light scattering or TEM equipment. It was concluded that the larger head group of the ammonium derivative promotes the formation of micelles rather than vesicles even though no direct observation of the micelles was made.

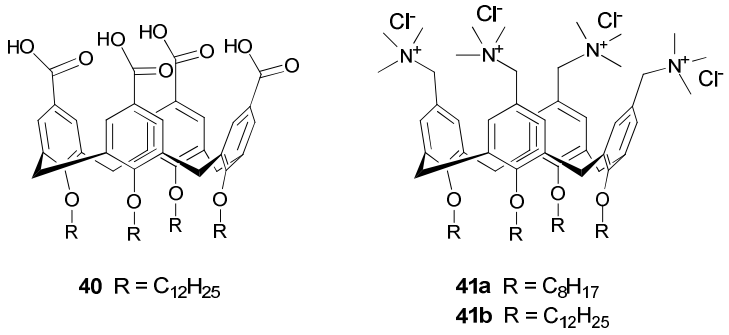

Figure 15. Amphipilic calix[4]arenes **40**-**41**.[95]

When the polar head group contains ionic groups, the pH of the solution affects the charge density and the shape of the molecules. If the amphiphiles do not precipitate due to the pH change,[81] they can form pH sensitive assemblies. Lee et al.[75] have studied aminoalcohol derivatives of calix[4]arene (**42**-**44**, Fig. 16) and discovered that the length of the polar chains at the upper rim affects the size distribution of the vesicles. The calixarene **42** with short 2-hydroxyethylene chains apparently adopts a more cylindrical structure, since it assembled as large vesicles (D_H = 200 nm), than calixarene **44** with long tri(ethylene glycol) chains, which formed micelles of 5-7 nm diameter. However, the intermediate chain length produced the most interesting small vesicles, which, upon protonation in acidic conditions, transformed into micelles. The pH-triggered vesicle-to-micelle transition can be used to release hydrophilic guests carried by the vesicles (Fig. 17).

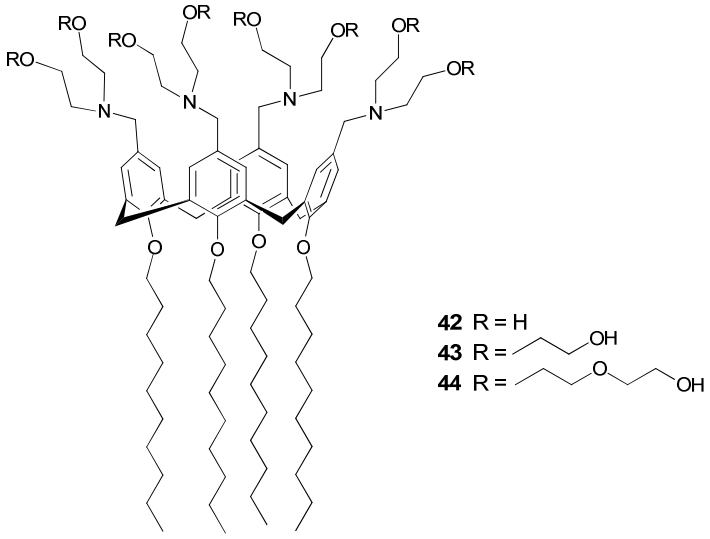

Figure 16. Amphiphilic calix[4]arenes **42**-**44**.[75]

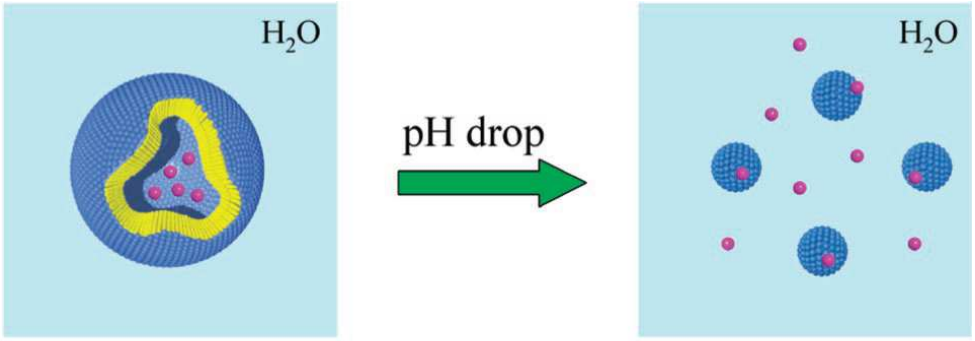

Figure 17. Schematic representation of the pH-controlled vesicle to micelle transition of **43**.[75] (Reprinted with permission from reference 75. Copyright (2004) American Chemical Society.)

Calix[4]arene and calix[8]arene glycoconjugates (**45**-**48**) were synthesized in order to compare their lectin binding abilities (Fig. 18).[96,97] It was expected that calix[8]arene derivatives (**47**-**48**) would show higher affinity, due to more binding units within single host, but instead calix[4]arene derivatives (**45**-**46**) were more efficient. It was proposed that the calix[4]arenes **45**-**46**, which are locked in the *cone* conformation had a more favorable presentation of *N*-acetyl-glucosamine chains than the conformationally mobile calix[8]arenes **47**-**48**. In addition, it was shown that **47**-**48** aggregate spontaneously into vesicles. The structure of the vesicles was investigated in more detail by varying the pH.[98] In neutral and basic solutions, the vesicles had a diameter of 200-400 nm, but below pH 3, the vesicles transformed to micelles with ca. 10 nm diameter. This transition is most likely induced by increased positive charge density after protonation of the thioureido groups, since the isoelectric point of the molecules was at pH 3.2.

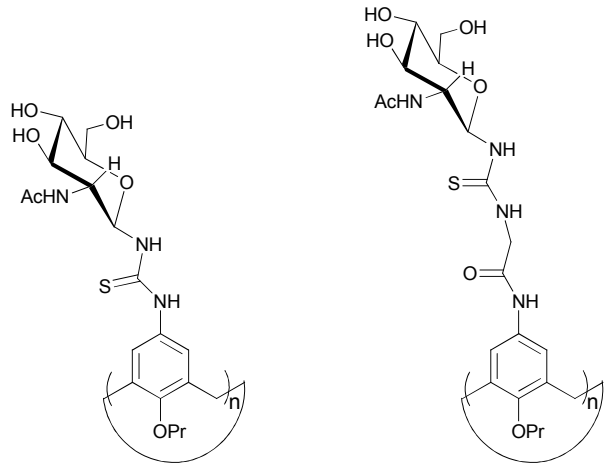

45 n = 4
47 n = 8

46 n = 4
48 n = 8

Figure 18. Structure of calix[4]arene glycoconjugates **45**-**46**, and calix[8]arene glycoconjugates **47**-**48**.[96,97]

The *tris*(imidazolyl) calix[6]arene **49** with three anionic sulfonate groups at the wide rim and three imidazolyl arms at the narrow rim formed aggregates that are sensitive to pH and silver ions (Fig. 19).[99,100] The conformation of **49** is flexible and the imidazole groups point out of the calixarene cavity, creating a roughly cylindrical shape for the amphiphile. The calixarenes assemble into unilamellar 50 nm vesicles at pH 6.5 when the imidazole groups are partially protonated, whereas at higher pH, polydisperse and less durable vesicles were observed.[74] The shape of the calixarene became conical upon complexation to Ag^+, which directs all imidazolyl ligands inwards. The calixarene silver complexes assembled into small (2.5 nm) micelles.

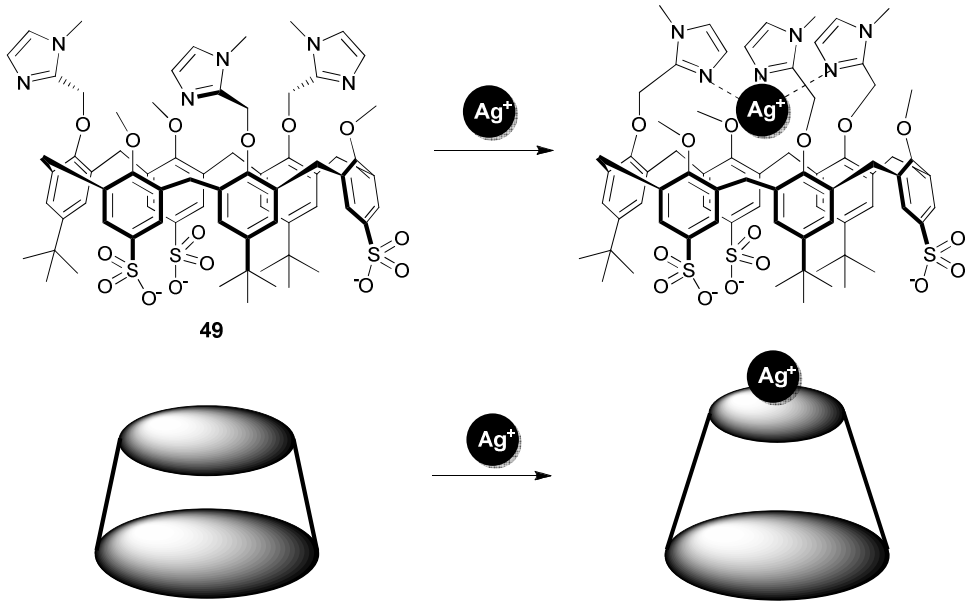

Figure 19. *Tris*(imidazolyl) calix[6]arene **49**, complexation of Ag^+ changed the shape of the molecule into conical.[74]

1.3.3 Solid lipid nanoparticles[I]

Solid lipid nanoparticles (SLN) differ from micelles by their larger diameter (50-1000 nm) and from vesicles by containing a lipid-filled solid interior.[101] Solid lipid nanoparticles have been developed for drug carriers in pharmaceutical and cosmetic products, where they have several advantages, such as increased protection of a drug against the environment and flexible possibilities to control the drug release.[101,102] Solid lipid nanoparticles are prepared on an industrial scale from solid lipids using high pressure homogenization and on smaller scales by microemulsion techniques. The solvent replacement method, where the amphiphile is first dissolved in an organic solvent and then rapidly mixed with water, has been successfully applied for many amphiphilic calixarenes[55,103,104] and resorcinarenes.[105,106]

p-Acyl calix[4]arenes (**21a-d**, Fig. 2) and *p*-phosphonate calix[4]arenes (**15a-b**, Fig. 2) form monodisperse SLNs with hydrodynamic diameters of 130-150 nm.[55,103,107] The solubility and amphiphilic properties of these calixarenes favor the preparation of SLNs, since they are soluble in water miscible organic solvents—such as THF, acetone and ethanol—and readily assemble into nanoparticles without any need for cosurfactants.[107] The acyl chain length (R = C_5H_{11}-$C_{11}H_{23}$) had no effect on the nanoparticle size of the *p*-acyl calix[4]arenes **21a-d**.[107] For tetra *p*-phosphonate calix[4]arenes (**15a-b**), a minor increase in the alkyl chain length from C_{10} to C_{12} affected their agglomeration, suggesting that the shorter chained derivative produced slightly more densely packed and rigid particles.[55] Also *p*-acyl calix[9]arene (**50a-e**, Fig. 20) based SLNs have been prepared, which had a negative correlation between the acyl chain length and the SLN diameter—i.e. shorter chain lengths gave larger particles.[108] This could result from the different conformation and packing of the larger and more flexible calix[9]arene framework during the nanoparticle self-assembly.

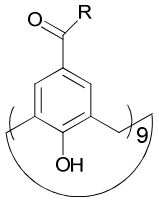

50	**R**
a	C_5H_{11}
b	C_7H_{15}
c	C_9H_{19}
d	$C_{11}H_{23}$
e	$C_{13}H_{27}$

Figure 20. The *p*-acyl calix[9]arenes **50a-e**.[108]

The AFM images of dried nanoparticles on a solid substrate, such as glass or mica, showed slightly flattened nanoparticles (Fig. 21).[55,103,105] They can be differentiated from collapsed vesicles by the much larger height of the assemblies[94] and by comparing their volume to the hydrodynamic diameters measured in solution. The structure is amorphous,[109] even though it probably contains some degree of order due to the packing of the hydrophobic domains of the amphiphiles.[107]

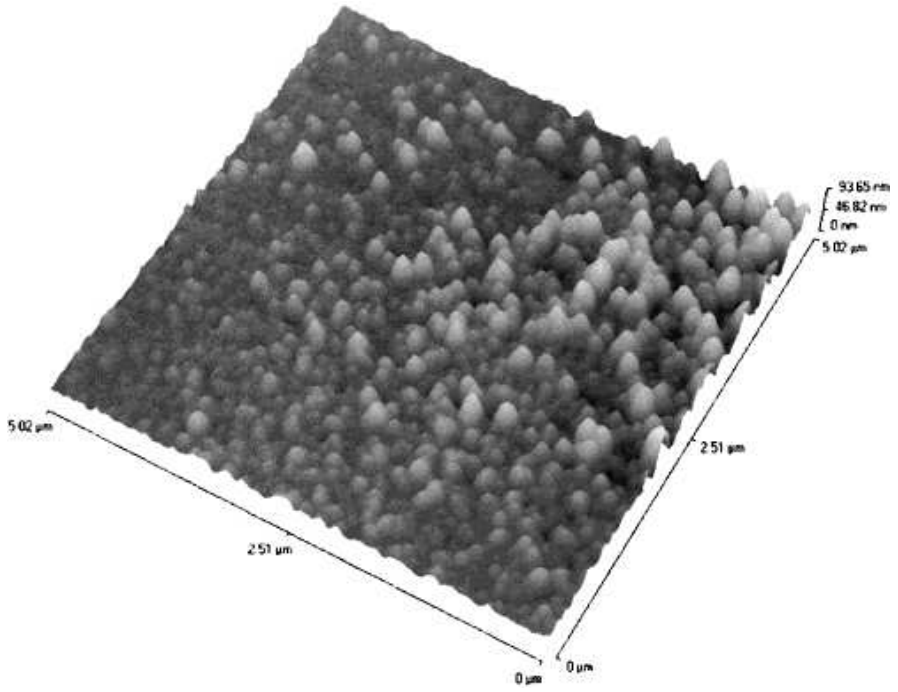

Figure 21. An AFM image (5x5 µm) of solid lipid nanoparticles of **15a** on mica.[55] (Reprinted with permission from reference 55. Copyright (2002) American Chemical Society.)

The guest inclusion into *p*-acyl calixarene cavities on the surface of the particles has been studied for freeze-dried SLN powders by hyperpolarized ^{129}Xe NMR.[109] The results show that the cavities are to some extent available for guest inclusion, depending on the acyl chain length. The longer and more flexible the chains, the fewer cavities are free due to backfolding and interdigitation of the aliphatic chains within the cavities. However, the SLNs can undergo minor changes in the chain packing, which results in increased volume of free cavities. The change was induced, for example, by absorbing gaseous dichloromethane, DMSO, $CHCl_3$, *o*- and *p*-xylene, or tetrachloromethane in the SLNs, after which the signals for hyperpolarized Xe in the cavities increased. Since these experiments were conducted with dried SLNs, some of the observed intercalation of the alkyl chains may have taken place during the removal of the solvent, whereas in the hydrated state some of the cavities could be engaged in hydrogen bonding interactions with water.[110]

Very interesting results have been obtained with the apparently hydrophobic *p*-H dodecanoyl calix[4]arene **51**. Despite a lack of hydrophilic groups, **51** showed surfactant properties, self-assembling into a well-packed monolayer at the air-water interface, and formed SLNs with a D_H of 235 nm.[111] The crystal structure of the compound shows organized packing of the alkyl chains with a head-to-tail arrangement of the amphiphiles (Fig. 22). Since the acyclic reference compound dodecyloxybenzene showed no sign of surfactant behavior, the amphiphilic nature of the calixarene **51** can be attributed to the interactions of the macrocyclic aromatic cavity with water by π-electron cloud.[110]

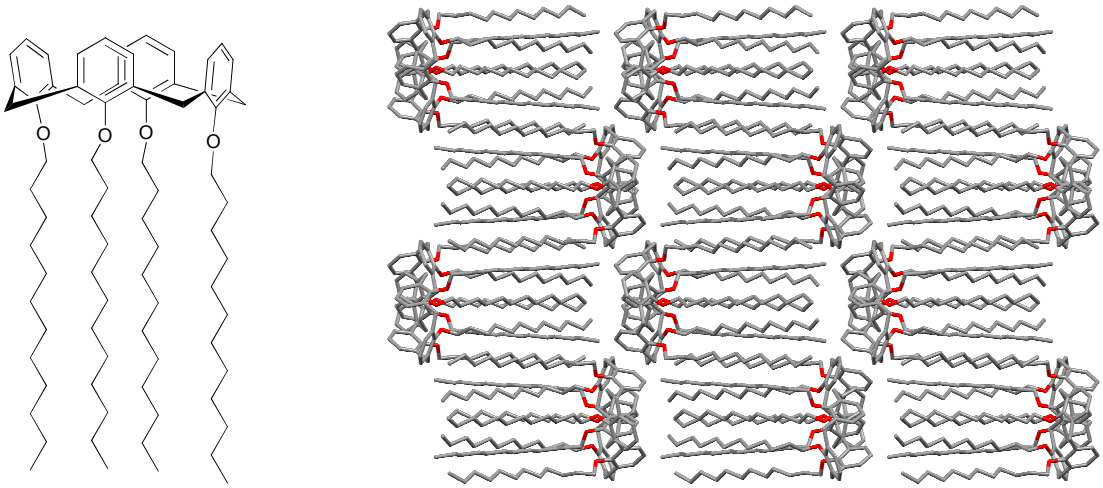

51

Figure 22. Molecular and X-ray crystal structure of *p*-H dodecanoyl calix[4]arene **51**.[111]

The stability and toxicity of calixarene SLNs have been studied in order to elucidate their biocompatibility and potential as drug carriers. Most of the calixarene and resorcinarene SLNs are stable against UV-radiation and physiological salt concentration at a pH range of 2-8.[105,107] The only structurally weak point of the calixarene based SLNs is their limited stability against freeze-drying and redispersion, where they tend to agglomerate.[107] For calix[4]arenes, this can be prevented by using simple sugars, such as glucose, as cryoprotectants.[112] The calix[4]arene SLNs showed no haemolytic tendencies up to 150 mM concentration, since the parent calixarenes have no affinity to lipids, especially to cholesterol of the cell membranes.[113]

The surface of the L-prolyl resorcinarene (**52**) SLNs was coated with bovine serum albumin, BSA, to produce SLNs for drug targeting.[106] Bovine serum albumin was linked to the surface of the particles using 1-(3-dimethylaminopropyl)-3-ethylcarbodiimide (EDC) and *N*-hydroxysuccinimide (NHS) coupling. The BSA on the surface of these particles was in its native conformation and the protein-SLN conjugates were attached on a gold substrate using an antibody (anti-BSA) linker. Successful preparation of the conjugates showed that the resorcinarene SLNs maintain their shape and size well under these reaction conditions (Fig. 23) and have significant potential for nano- and bioapplications.

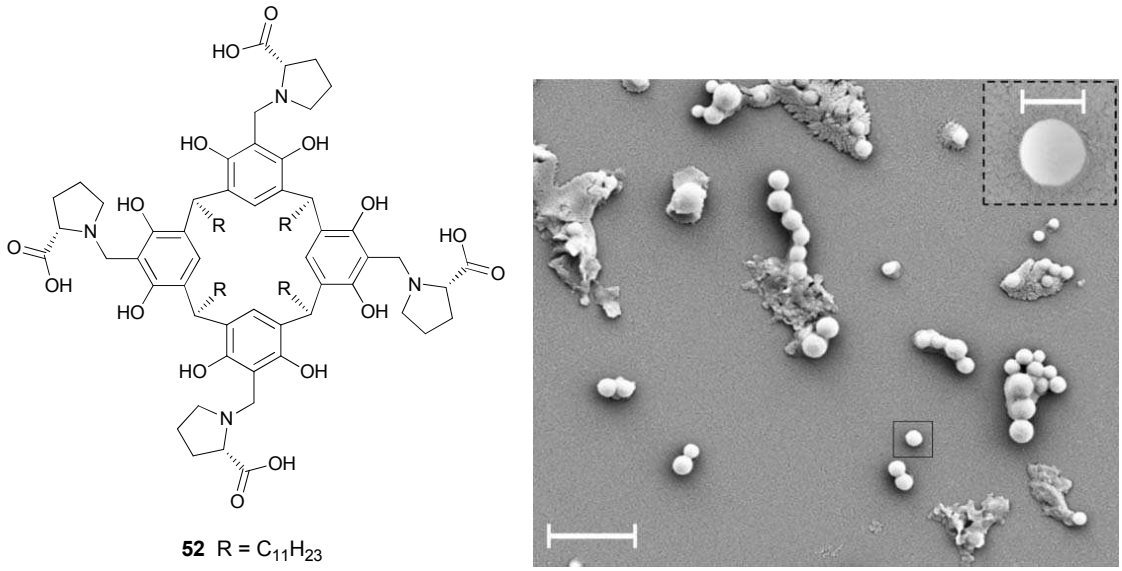

Figure 23. Structure of L-prolyl resorcinarene **52** and a SEM image of BSA-coated SLNs (scale bar 1 μM).[106]

1.3.4 Fibers

Self-assembled nano- and microfibers enable preparation of fibrous materials for applications in nanoscience and nanotechnology. Three types of fiber forming calixarenes and resorcinarenes are discussed: cylindrical *p*-phosphonate calixarenes (**53**),[114] relatively rigid and hydrophobic calix[6]arene crown ethers (**54**-**55**),[76] and *N*-(2-aminoethyl) acetamido resorcinarenes (**59**-**60**) containing very large ionic head groups.[115]

The self-assembly of the cylindrical *p*-phosphonate calix[4]arene (**53**) with long C_{18} alkyl chains in the *cone* conformation was studied in toluene.[114] Toluene solution of the calixarene assembled as nanofibers when dried on moderately polar mica or a less polar graphite surface, whereas hydrophilic silicon oxide did not promote assembly into fibers. The fibers are uniform in diameter (6 nm) with the proposed structure consisting of discs of micellar assemblies stacked as long fibers with a 6-8 Å pore in the middle (Fig. 24). Some toluene is incorporated inside the tubes between the alkyl chains, and its removal under high vacuum resulted in collapse of the fibers into small particles of 3-4 nm in diameter. The assembly process is quite robust, and presumably the calixarene forms micellar preaggregates in toluene, which during toluene evaporation assemble into a fibrous network.

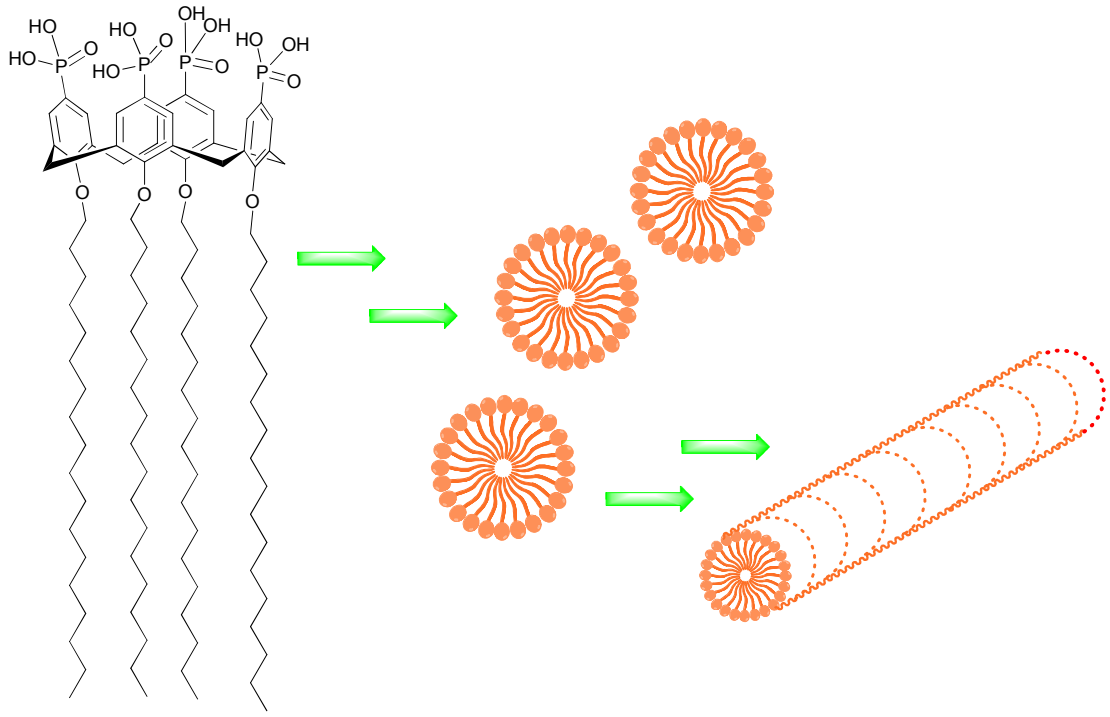

53

Figure 24. The self-assembly of *p*-phosphonate calix[4]arene **53** into nanofibers.[114]

The water insoluble calix[6]arene bis-crowns in an *1,4-alternate* conformation containing polar *N*-(3-aminopropyl) acetamido arms (**54**, Fig. 25) formed vesicles (D_H = 290 nm) in ethanol-water solution, which changed into fibers after an increase in the water content.[76] The fibers were about 10 μm in length and 100-200 nm in width, and they contained a hollow interior. The fibers showed a peak in the XRD pattern, indicating periodic order in the packing.

The structural conditions for the vesicle-fiber transition was studied by preparing a series of calixarenes (**55-58**, Fig. 25).[76,116] The crown ether loops proved to be essential for the formation of fibers, since they provide sufficient conformational rigidity to the calixarene framework. The transformation into fibers can be attributed to minor conformational changes condensing the hydrophobic parts of the molecule when the hydrophilicity of the solution is increased. More importantly, the amido functionalities were discovered to be crucial to the fiber structure: they form intermolecular hydrogen bonds visible in IR spectra and in the X-ray crystal structure (Fig. 26). The hydrogen bonding most likely rigidifies the structure of **54**-**55** in comparison to the calixarenes **57**-**58**, which can change their shape into a more curved structure and thus compensate for the need for dense packing of the hydrophobic volume by assembling into smaller vesicles in hydrophilic solvent. The vesicle-to-fiber transition of **54** can be compared with the transition observed for supramolecular amphiphile **39**, in which the inclusion complexation of the hydrophobic counterpart most likely provides similar rigidity to the structure.[93]

The fibers formed also in the presence of caesium, an effective guest for **54**. The position of caesium within the fibers was not investigated, but it most likely occupies the crown ether loops and aromatic cavity of the calixarene.

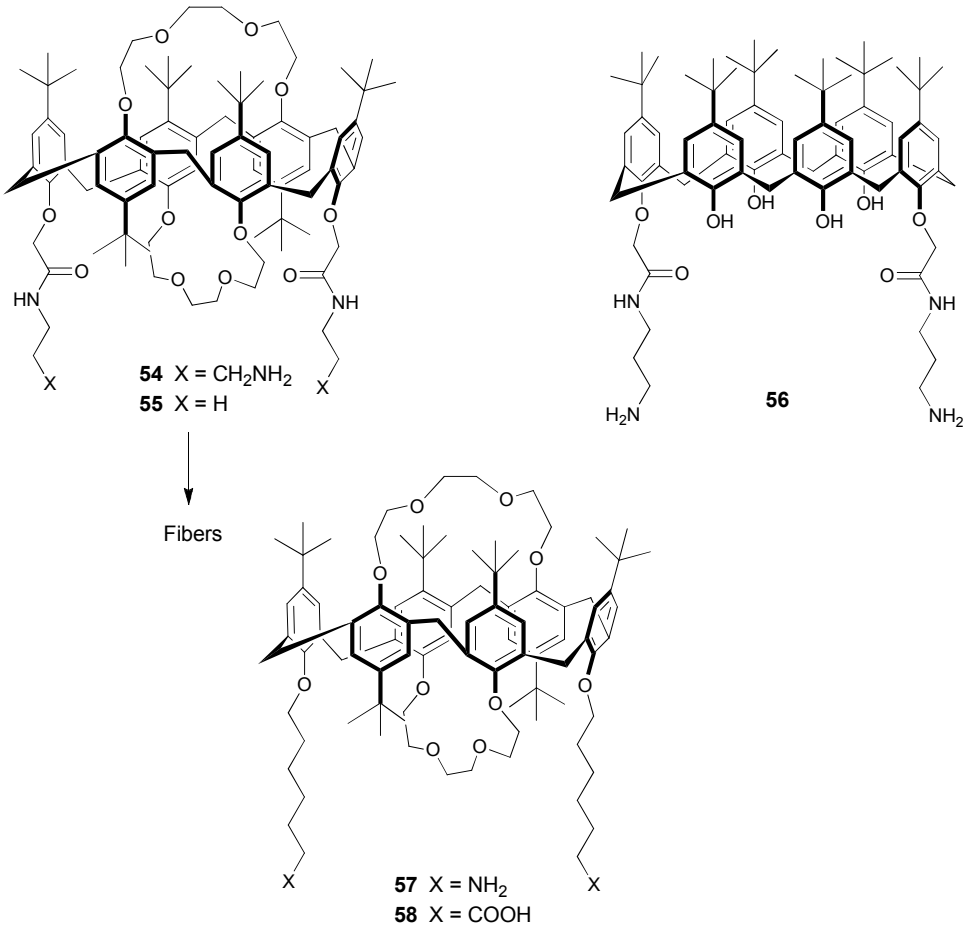

Figure 25. Structure of calix[6]arene bis-crowns **54**-**58**.[76,116]

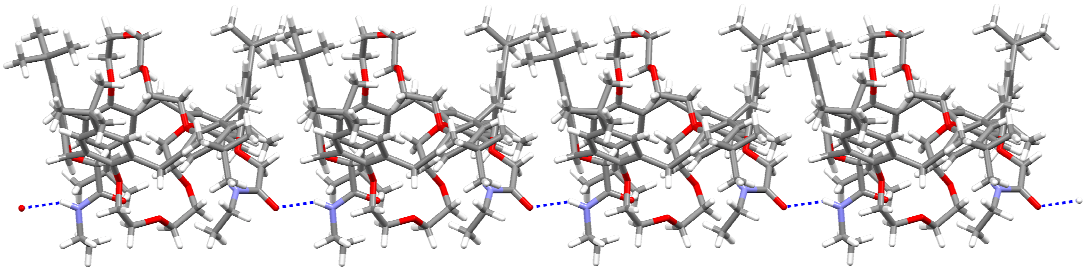

Figure 26. X-ray crystal structure of calix[6]arene bis-crown **55** showing intermolecular hydrogen bonds.[116]

The self-assembly of resorcinarenes with eight *N*-(2-aminoethyl) acetamido substituents at the upper rim was studied in water (**59**, Fig. 27).[115]

The molecules are hydrogelators in their non-ionic form and soluble in water when partially or completely protonated at acidic pH. The effect of lower rim (hydrophobic) and upper rim (hydrophilic) chain length on self-assembly was studied. During aging of the resorcinarene water solutions, a small fraction of the resorcinarenes aggregated into larger clusters, which had a sheet-like morphology. After four weeks, tubular assemblies emerged in solution. The tubes were 1-2 μM in diameter, and had a soft and amorphous structure consisting of multilamellar sheets and hydrogen-bonded water. The lower rim alkyl chain length did not have any remarkable effect on the assembly of **59a-f**, whereas the upper rim 2-aminoethyl chains proved to be important as hydrogen bonding units for the sheet-microtube transition. The amido groups showed distinct shifts in the IR spectra indicating hydrogen bonds. When replaced with hydrazine structure (**60**), only sheets but no tubes were formed. Thus, it was concluded that the hydrophobic interactions and aromatic π-stacking of resorcinarene cavities are needed for aggregation in water, but the hydrophilic head group dominates in the assembly of fibers.

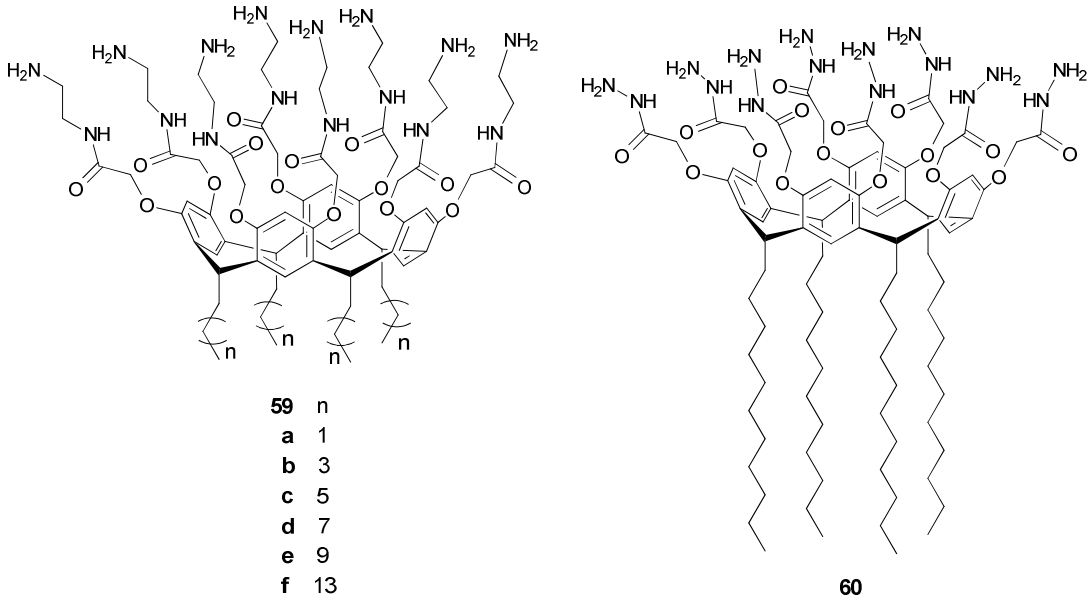

59 n
a 1
b 3
c 5
d 7
e 9
f 13

60

Figure 27. Resorcinarene *N*-(2-aminoethyl) acetamido derivatives **59a-f** and *N*-amino acetamido derivative **60**.[115]

1.3.5 Langmuir-Blodgett films

The self-assembly of amphiphiles into well-organized monolayers at the air-water interface has been observed for many calixarene and resorcinarene derivatives.[2,3] The most important structural features required for the preparation of stable Langmuir films include hydrophilic groups, which point towards water, and hydrophobic chains, which form intra- and intermolecular hydrophobic interactions (Fig. 28). The monolayers of concave resorcinarenes and calixarenes are porous, which makes them interesting materials for sensing

and thin film materials.[117,118] The shape and flexibility of the aromatic cavity, hydrophilicity of the head group functionalities, and length and branching of the hydrophobic alkyl chains all affect the film properties, such as compressibility, stability, density, transferability, and molecular recognition properties.[60,119-121]

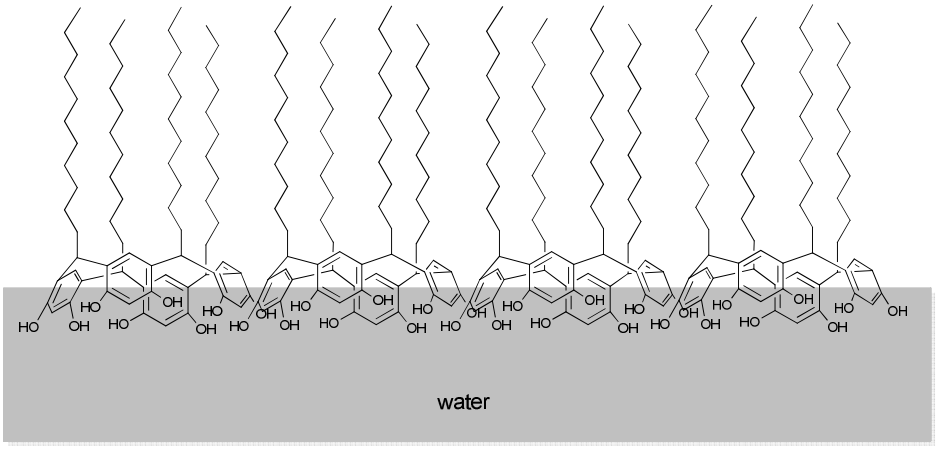

Figure 28. Schematic presentation of a resorcinarene monolayer at the air-water interface.

The limiting molecular areas at the condensed phase of monolayer depend on the cross-sectional area of the molecule. For resorcinarene octols (**1**) and pyrogallarenes (**7**) with unbranched alkyl chains, the macrocyclic cavity determines the limiting molecular area.[60,121] Dense hexagonal packing occupies approximately 130-140 Å^2 per molecule in the *crown* conformation, and it can compress down to 110 Å^2 before collapsing. The area occupied by the alkyl chains is smaller, and surface potential–area isotherms have shown that the chains arrange in a tilted orientation relative to the surface normal during compression[122] as well as in deposited Langmuir-Blodgett multilayers (55-60°).[60] The lower rim alkyl chain length can vary from C_5 to C_{11},[60,119,122] or even from C_3 for pyrogallarenes,[121] or contain distal double bonds without severe effects to the isotherms, whereas long C_{17} alkyl chains promote formation of a bilayer.[60] The branching of the alkyl chains can increase the molecular areas or induce tilted orientation of the molecules with respect to the surface normal.[121]

The esterification of the phenolic hydroxyl groups has significant effects on the isotherms by increasing the molecular areas and decreasing the collapse pressure.[60,119,120] The acetylated resorcinarenes (**11**) had a *boat* conformation at the interface, which explains the enlarged molecular areas. Even when the lower rim contains bulky azobenzene units, as in resorcinarene **61** (Fig. 29), the cross-sectional area of the resorcinarene cavity determines the molecular areas.[123] A comparison of octol **61** and the acetylated compound **62** revealed that the larger molecular area of the acetylated resorcinarene allows more space for the *trans-to-cis* photoisomerization in the compressed films.

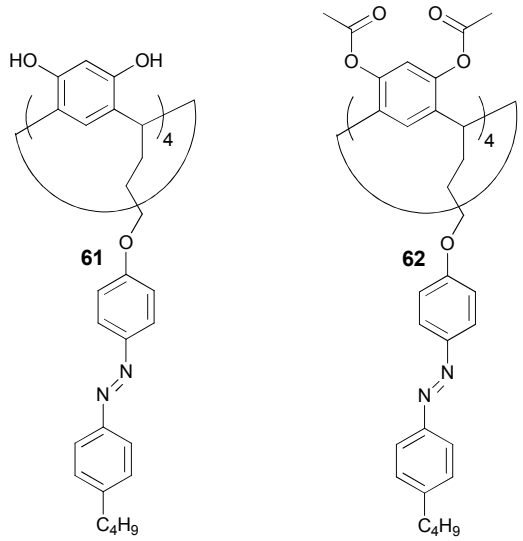

Figure 29. Azobenzene resorcinarenes **61** and **62**.[123]

The rigidity of the resorcinarene cavitands induced steep isotherms, which indicate high stability and relatively low compressability of the Langmuir films.[60] When the Langmuir-Blodgett multilayers of cavitand **63** (Fig. 30), resorcinarene octols **13** (Fig. 2) and **23** (Scheme 2), and acetylated resorcinarenes (**64**-**65**, Fig. 30) were deposited, the flexible acetylated resorcinarenes formed the most ordered multilayers, whereas the rigid cavitand formed poorly organized multilayers, as indicated by the X-ray diffraction peaks.[60] The deposition of Langmuir-Blodgett multilayers has also been successful with C-phenyl resorcinarenes, providing that the head group has sufficient polarity, such as in the aminomethylated resorcinarene **66**.[124]

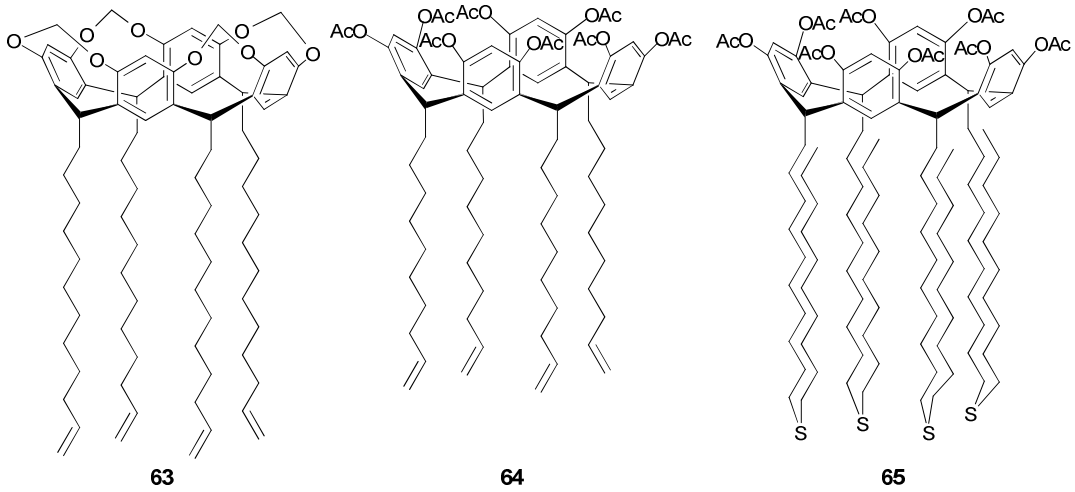

Figure 30. Resorcinarene cavitand **63** and acetylated resorcinarenes **64**-**65**.[60]

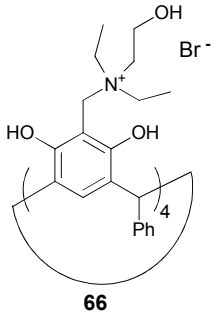

66

Figure 31. Aminomethylated resorcinarene **66**.[124]

O-alkylated resorcinarene octapodands with ester and amido functionalities (**67-68**, Fig. 32) formed complexes with alkali and transition metal cations mediated by ion-dipole and cation-π interactions to the carbonyl groups and resorcinarene cavity.[120] The podands differ in their molecular area responses to the guest cations in the subphase. The ester derivative **67** showed no change in the limiting areas, whereas the amide derivative **68** responded to almost all investigated analytes. The rotation of the upper rim podand arms of **67** upon complexation induces only a small change in the cross-sectional area, which explains the observation. UV-vis and IR spectra of the transferred films indicated that the hosts are in the *boat* conformation for films deposited on pure water, whereas they have a distorted conformation in films deposited on guest ions. The ester and amide derivatives **67** and **68** formed complexes with Cu^{2+}, Cd^{2+}, Na^{+} and K^{+}, but not with Ag^{+} and Ba^{2+}, as indicated by IR spectra of the films. In addition, only **67** formed a complex with Hg^{2+}.

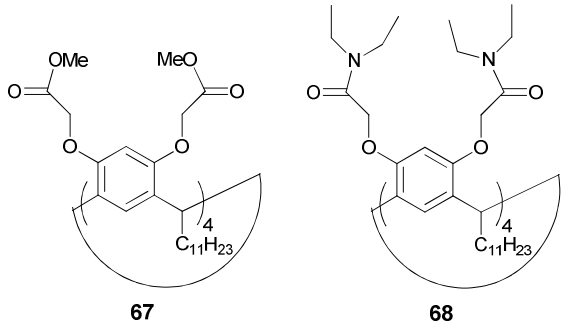

67 68

Figure 32. Resorcinarene podands **67-68**.[120]

The structure and the molecular recognition abilities of films prepared by spin-coating and LB multilayer deposition of resorcinarene octol **13** were compared using surface plasmon resonance (SPR).[125] Both films respond similarly to toluene vapor, indicating that they have similar short range structures. It was proposed that the occurrence of head-to-head dimerization in chloroform prior to spin-coating, followed by interdigitation of the alkyl groups, creates small areas of stacked bilayers within the spin-coated film. Similar interactions form during the Langmuir-Blodgett multilayer deposition,

inducing long-range order for the films due to organized packing at the interface.

1.4 Application of amphiphilic calixarenes and resorcinarenes

1.4.1 Ion channels

Amphiphilic calixarenes and resorcinarenes have numerous applications in nanoscience and nanomaterials, biosensors, and biomimetic and biochemical systems.[23,24,30-32] Amphiphilic calixarenes, resorcinarenes and their assemblies can interact with lipid membranes forming synthetic ion channels that allow the passage of ions through lipid bilayers. Alternatively, they can inhibit the function of biological ion channels.[23,24,31] Synthetic ion channels, which show selectivity towards Na^+, K^+ or Cl^-, are interesting as biological mimics for understanding the mechanism of their biological counterparts.

Calixarenes and resorcinarenes are excellent compounds for synthetic channel formers because their three-dimensional structure can be synthetically controlled with high precision.[24] Resorcinarene **1** with C_{18} alkyl chains formed a potassium channel across soybean lecithin bilayers.[126] It was observed that the long alkyl chains capable of spanning the bilayer were essential for the function of the channel. Therefore, it was proposed that the structure of the ion channel consists of a tail-to-tail resorcinarene dimer. Higher ion fluxes were obtained with resorcinarene cavitands with C_{11} alkyl chains and amino acid residues at the upper rim.[127] Consequently, instead of a dimeric structure the ion channels were probably formed by aggregation of the resorcinarene cavitands, which formed tetrameric, pentameric and hexameric pores through the membrane.

It is difficult to obtain direct information about the structure of ion channels from ion current measurements. Therefore, research on the structure-function relationship of synthetic channel formers can reveal new insights into the interaction of amphiphilic calixarenes and resorcinarenes with the lipid membranes. Davis et al.[128] have studied calixarene based chloride channels and shown that the conformation and small modifications in the structure of the host can affect its function. In the case of a *partial cone* calixarene **69**, addition of *p-tert*-butyl groups (**70**) affects the conformation of the amide substituents, leading to a different mode of assembly and a non-functional ion channel (Fig. 33).[129]

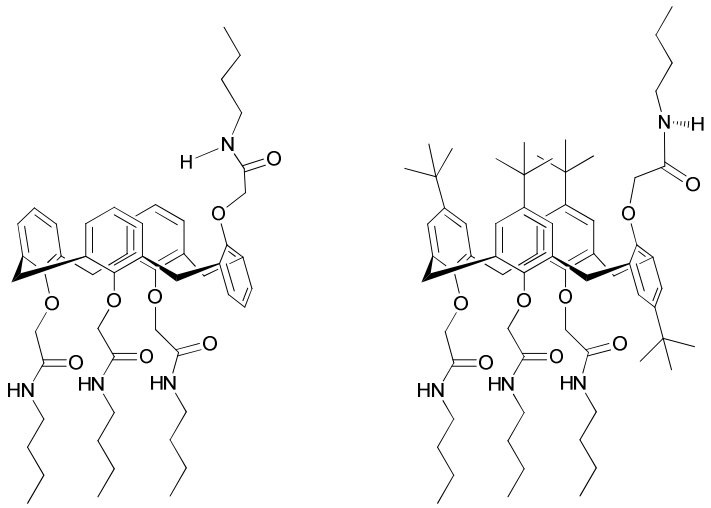

Figure 33. Structure of the chloride channel-forming calix[4]arene **69** and a reference compound **70**.[129]

1.4.2 DNA transfection

Studies of cellular uptake of calixarenes,[130] calixarene-DNA aggregates[72,86,131,132] and DNA-loaded solid lipid nanoparticles[133] have been undertaken in order to develop better transfecting agents and new biochemical imaging tools and to discover the effects of calixarene conjugates on living cells. The resorcinarene glycoconjugates **31** and their micelles shown in Fig. 8 form complexes with DNA by means of sugar-phosphate hydrogen bonding.[86] Cellobiose (β-glucose) resorcinarene conjugate **31a** and DNA form small, 50 nm particles, which are suitable for transfection, whereas α-glucose- (**31b**) and β-galactose-DNA complexes aggregate, reducing their transfection efficiency.

Several cationic calixarenes bearing guanidinium (**71-73**) groups at the upper rim have also been investigated (Fig. 34).[72] The amphiphilicity and conformational mobility of the calixarene had a very important role, since only the conformationally locked calix[4]arenes with long hexyl or octyl chains (**71b-c**) at the lower rim were able to induce DNA transfection. The *cone* conformation of **71** aligns the cationic groups in the same direction and the long alkyl chains at the lower rim form hydrophobic interactions, which efficiently condense DNA into small 50 nm clusters. Similar results have been obtained for hydroxyethyl ammonium calix[4]arenes (**74**, Fig. 35) when propyl and octyl derivatives were compared.[132] The conformationally mobile calix[6]arene- and calix[8]arene-guanidinium derivatives (**72-73**) formed links between several DNA strands, creating large aggregates unable to induce transfection.[72]

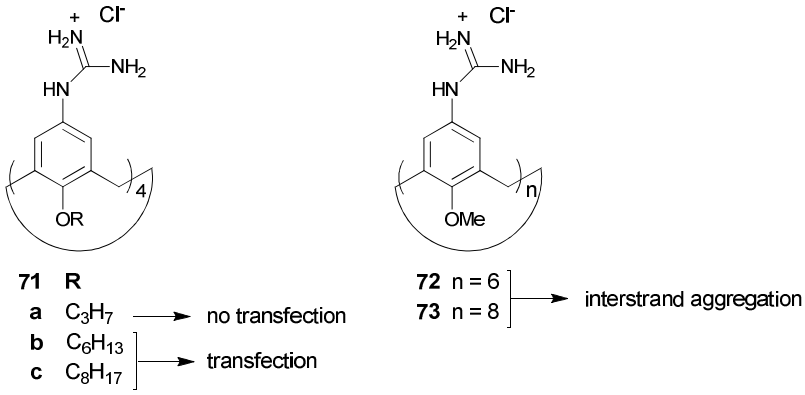

Figure 34. The guanidinium calixarenes **71-73**.[72]

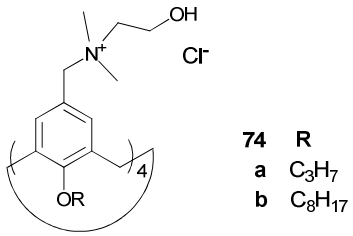

Figure 35. Hydroxyethyl ammonium calix[4]arene **74**.[132]

Covalently linked calix[4]arenes or multicalixarenes were prepared by connecting five cationic alkylamino and arylamino functionalized calix[4]arenes either at symmetrical (**75-76**), or asymmetrical arrangement (**77**).[131] The highest DNA binding affinity was obtained with the amphiphilic, asymmetrical multicalixarene **77**. However, only the alkylamino derivative **76**—which had a symmetrical structure—was able to induce gene transfection.

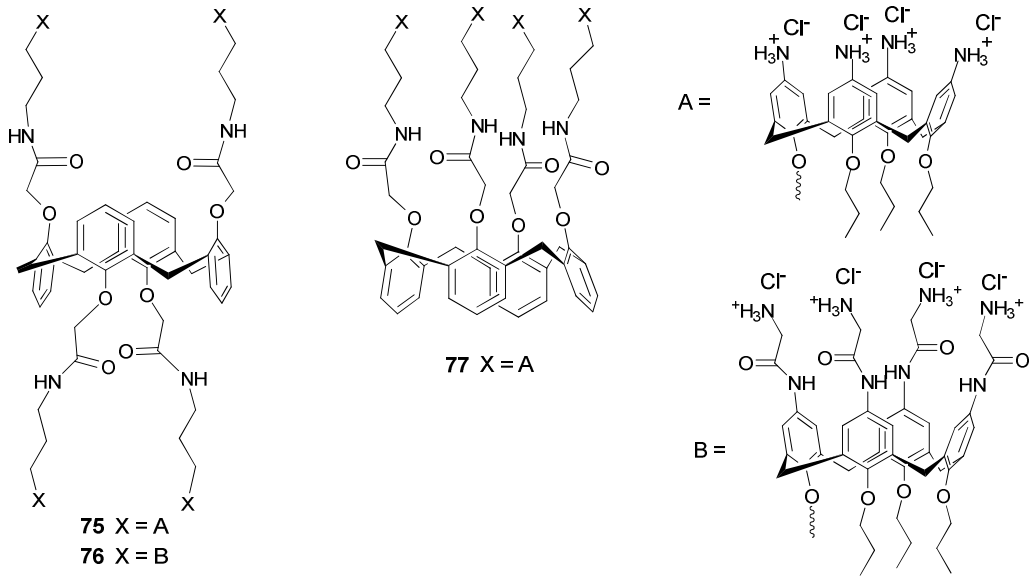

Figure 36. Multicalixarenes **75-77**.[131]

1.4.3 Sensors

Numerous sensor applications have utilized the affinity and selectivity of resorcinarene and calixarene based hosts for metal cations,[120,134,135] anions,[136] carbon dioxide,[137] organic acids,[138] chlorohydrocarbons,[139-141] alcohols,[141,142] amines,[143] aromatics[119,125,141,144] and other small organic compounds,[119,137,138,140,141,144-147] sugars,[138,148] aminoacids,[31,32,149] and proteins.[23,31,32,150,151] Molecular recognition at the air-water interface illustrates the role of an aqueous environment on the stability of the complex.[148] Chiral resorcinarene and cavitand conjugates recognize amino acids enantioselectively, probably due to stereochemically different orientation of D- and L-amino acid side chains, either into lipophilic layer or towards water.[149,152] Mixed monolayers of lipids and cationic and anionic calixarenes showed response in the limiting molecular areas for nanomolar protein concentration.[150] The proposed response mechanism was based on partial water solubility of the charged calixarenes, which formed neutral complexes with oppositely charged proteins in water, and upon complexation returned to the lipid layer, increasing significantly the molecular areas.

Calixarenes can also provide incomparable selectivity in guest binding within their cavities, in comparison to bare Au or polymer coatings.[144] Self-assembled monolayers of resorcinarenes and calixarenes on a gold surface (Scheme 2) have been tested for quartz crystal microbalance (QCM)[140,144,147,137] and surface plasmon resonance sensors[125,140,146,153] for detection of organic molecules in aqueous solutions[144,146,153] and in the gas phase.[125,140,147] The specific binding of calixarenes provides low detection limits at the picomolar or ppm range,[135,147] and enables the separation of closely related isomers.[142,144-146]

The organization of films is important for selectivity when the binding takes place within the cavity, which has been shown to be the case for *p-tert*-butyl calix[4]arene films.[144] Well-organized SAMs of thiol-functionalized calix[4]arene **78** had better selectivity between *o*-, *m*- and *p*-xylenes than spray coated, amorphous layers of *p-tert*-butyl calix[4]arene (Fig. 37). Furthermore, SAMs of resorcinarene tetrasulfide **79** prepared at room temperature were poorly organized and showed irreversible binding behavior with a cyclic guest molecule, α-hydroxy-γ-butyrolactone.[153] Therefore it seems that well-organized SAMs form complexes within the calixarene or resorcinarene binding cavity, whereas the disordered assembly of the monolayers enhances nonspecific binding in the interstitial space.[144,153]

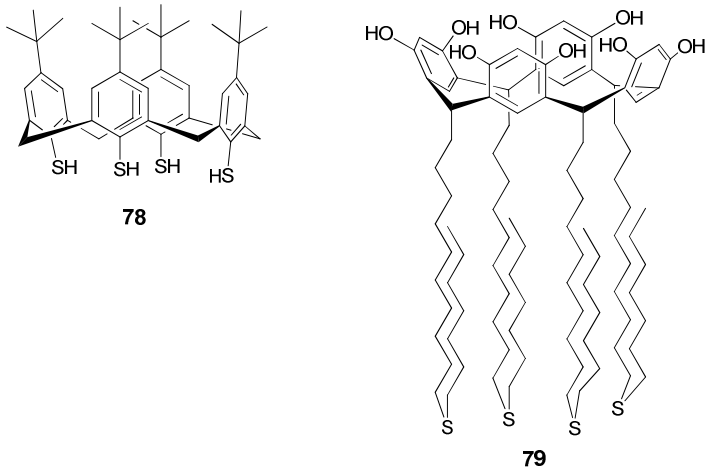

Figure 37. Thiol-functionalized calix[4]arene **78** and resorcinarene tetrasulfide **79** used in the preparation of SAM sensing units.[144,153]

On the other hand, variation in the strength of lipophilic interactions between resorcinarenes and volatile organic compounds was utilized to build a VOC sensor array based on a QCM sensor.[141] The quartz crystals were spin-coated with ethanol solutions of resorcinarene octols **1** with C_1, C_5, C_{11} and C_{17} alkyl chains, which had different responses to analytes. Even though the selectivity of resorcinarene cavity was not utilized, pattern recognition with a sensor array consisting of sensors coated with different resorcinarenes seems to offer potential for VOC detection.

1.4.4 Ligands and scaffolds for metal nanoparticles

Resorcinarenes and calixarenes have unique properties as ligands for metal nanoparticles in comparison to linear thiols.[28] They are able to stabilize larger (10-100 nm) Au particles; the chain spacing at the lower rim generates conformational freedom which prevents aggregation, and co-operative binding of the upper rim groups to the surface of the nanoparticle produces stable bonds (Fig. 38).[154,155] In addition, resorcinarene ligands promote the assembly of 2D nanoparticle arrays for sensor applications,[154,156] and thiacalixarenes can be used as ligands and reducing agents in Au nanoparticle synthesis.[157]

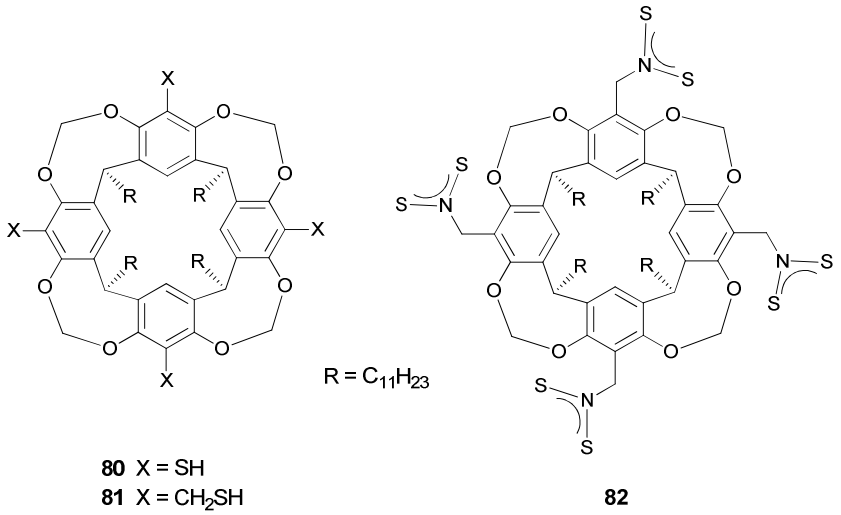

Figure 38. Resorcinarene ligands **80-82** for gold nanoparticles.[155,158]

Self-assembled calixarene fibers can be used as templates for metal nanoparticle synthesis.[159] A mixture of amphiphilic calixarene **54** with metal salt and $NaBH_4$ produced gold nanoparticles with an average diameter of 3-8 nm, depending on the calixarene/metal ratio during the nanofiber assembly. The $AuCl4^-$ is coordinated to the amino groups of the calixarene, and after reduction forms nanoparticles on the surface of the fibers. The nanoparticle fibers were used as catalysts for hydrogenation.

Moreover, the pre-assembled resorcinarene microtubes of **59** were used to stabilize Au nanoparticles.[115,160] When colloidal suspension of Au was mixed with the microtubes, Au nanoparticles were attached only to the outer surface of the tubes. The *in situ* formation of Au nanoparticles during the self-assembly of C_{15} derivative **59f** resulted in localization of the nanoparticles within the tubes, indicating that the attachment of the nanoparticles preceded the microtube assembly.[160]

1.5 Concluding remarks

Resorcinarenes and calixarenes are supramolecular hosts which offer unique molecular recognition properties for metal cations, anions, organic molecules, and small biomolecules, as well as for large biomacromolecules such as proteins and DNA. Self-assembly of amphiphilic resorcinarenes and calixarenes produces nanoscale materials with versatile shapes and morphologies, such as micelles, vesicles, nanoparticles, fibers and monolayers. Self-assembly can be controlled by the upper and lower rim functionalities and by conformation and conformational mobility of the host—which affect the balance between lipophilicity and hydrophilicity—and by the three-dimensional shape and size of the calixarene type of compounds. Conical shape of the calixarenes and resorcinarenes promotes the formation of micelles. Very large polar or ionic

head groups induce self-assembly into small, monodisperse structures. Cylindrical shape of the host promotes self-assembly into vesicles, and when the polar head groups contain ionic functionalities whose charge density depends on the pH of the medium, pH-sensitive vesicle-to-micelle transitions are obtained.

The self-assembled calixarene and resorcinarene based materials are useful in many biochemical, biomimetic and sensor applications, such as synthetic ion channels, encapsulation and transportation of drugs and DNA, and stabilization of metal nanoparticles in catalytic or sensor systems. The selectivity of resorcinarene and calixarene hosts have been utilized in SAM-based sensors, where the organized packing of the monolayers improves selective binding of the analytes. In addition, functional materials which respond to external stimuli—such as solvent, ionic strength, metal ions, or pH—can be prepared by utilizing the selective binding sites, the conformational changes of the calixarene or resorcinarene framework, and shape-changing functionalities at the upper rim.

2 RESULTS AND DISCUSSION

The structure of resorcinarenes with a concave, aromatic binding cavity and tunable upper and lower rim functionalities makes them useful building blocks for host-guest chemistry and self-assembling materials. Amphiphilic resorcinarenes can be easily prepared by using long aliphatic aldehydes in their synthesis. The upper rim of the resorcinarene bowl has an innate hydrophilic character because of its derivation from the resorcinol; in addition, the upper rim is readily available for further functionalization to improve binding affinity and selectivity. The goal of this project was to study the complexation, structural properties, self-assembly, and potential applications of amphiphilic resorcinarenes. These goals were addressed by synthesizing three types of resorcinarene hosts with different lower rim alkyl chain lengths[II,IV,V] and studying their conformational and cation binding properties in solution by means of NMR spectroscopy,[II-IV] examining their solid state packing by single-crystal X-ray diffraction,[II-IV] studying their self-assembly and amphiphilic properties by preparing Langmuir films[III,IV] and solid lipid nanoparticles,[II] and finally, testing their potential as antibacterial coatings[III] and examining their interaction with fluorescent dyes.[V]

2.1 Synthesis of the resorcinarenes

Resorcinarene octols **1** and *O*-methyl resorcinarenes (hence termed tetramethoxy resorcinarenes, **83** in Fig. 39)[161] were used as a macrocyclic platform for new amphiphilic hosts. *O*-Alkylation of the upper rim hydroxyl groups produced resorcinarene bis-crowns[II,III] and resorcinarene octapodands.[IV] A major goal of this study was to explore the effect of lower rim alkyl groups on the self-assembly and amphiphilic properties of resorcinarene hosts. Therefore, resorcinarene bis-crowns and resorcinarene octapodands with identical upper rim (binding site) and different alkyl groups at the lower rim were prepared.

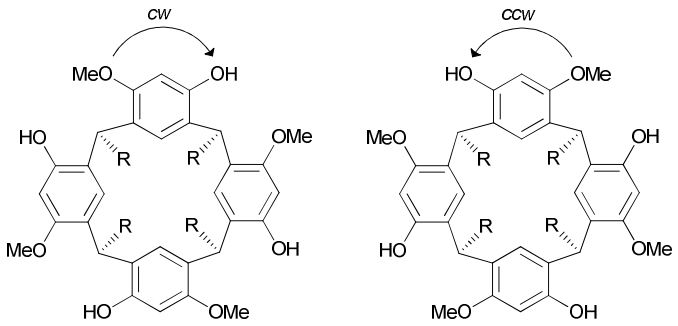

Figure 39. Structure of tetramethoxy resorcinarene (*O*-methyl resorcinarene) **83** showing clockwise (*cw*) and counterclockwise (*ccw*) enantiomers.[161]

Resorcinarene bis-crowns were prepared by attaching two crown ether bridges to the free hydroxyl groups of tetramethoxy resorcinarene **83**, a procedure which locks the resorcinarene in the *boat* conformation and creates two binding pockets for complexation of cations. The resorcinarene bis-crowns **84–91** were synthesized with 15–30% yields using tetraethylene glycol ditosylate and Cs_2CO_3, according to the procedure previously used for resorcinarene bis-crown **84** (Scheme 3).[II,162]

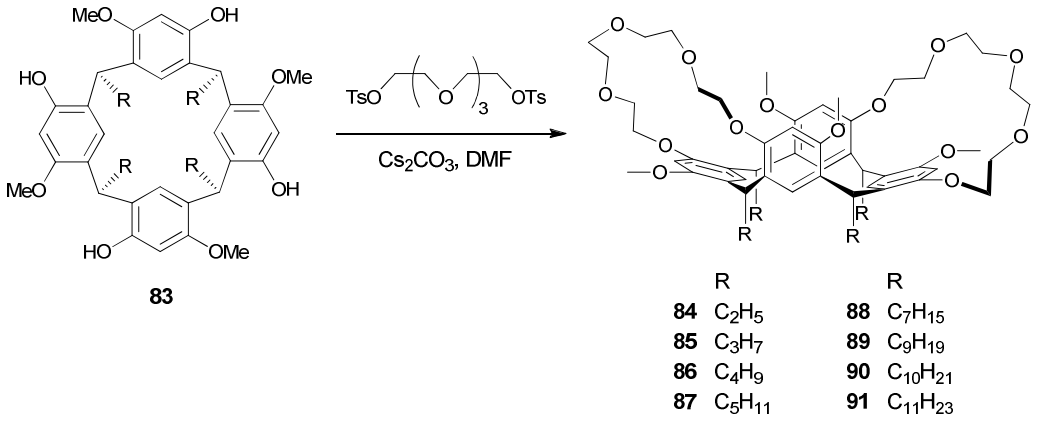

Scheme 3. Synthesis of the resorcinarene bis-crowns **84-91** (*cw* enantiomers shown).[II,162]

O-alkylation of resorcinarene octol **1** with *o*-nitroaniline side arms breaks the hydrogen bonded crown conformation of the octol and produces flexible host structures, resorcinarene octapodands.[IV] Resorcinarene octapodands (**92–96**) were prepared with 40–65% yields using *o*-nitro-*N*-(2-toluenesulfonyloxyethyl)aniline or *o*-nitro-*N*-(2-methanesulfonyloxyethyl)-aniline, according to the procedure previously used to prepare resorcinarene tetrapodands (Scheme 4).[IV,163]

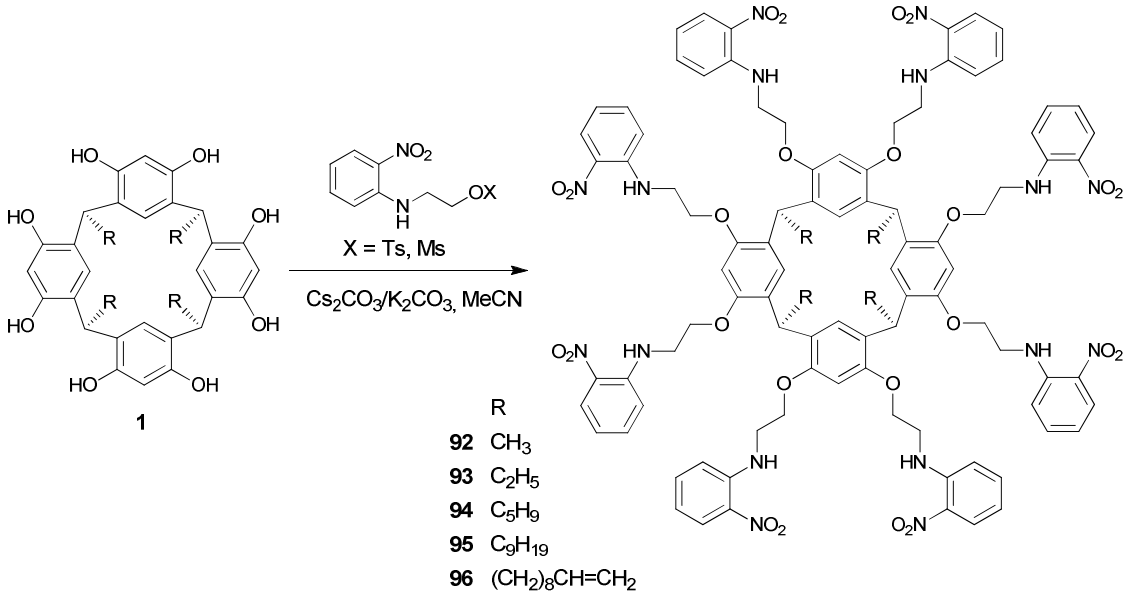

Scheme 4. Synthesis of the resorcinarene octapodands **92-96**. [IV]

Aminomethylation of resorcinarenes provides hosts which contain hydrogen bonded, extended binding cavities in crown conformation.[48,164] The tertiary amino groups can form hydrogen bonds with solvent or guest molecules, and they can be protonated in acidic conditions. Aminomethylated resorcinarenes **97–98** (Fig. 40) were prepared from resorcinarene octol **13**, secondary amine and formaldehyde.[V,165]

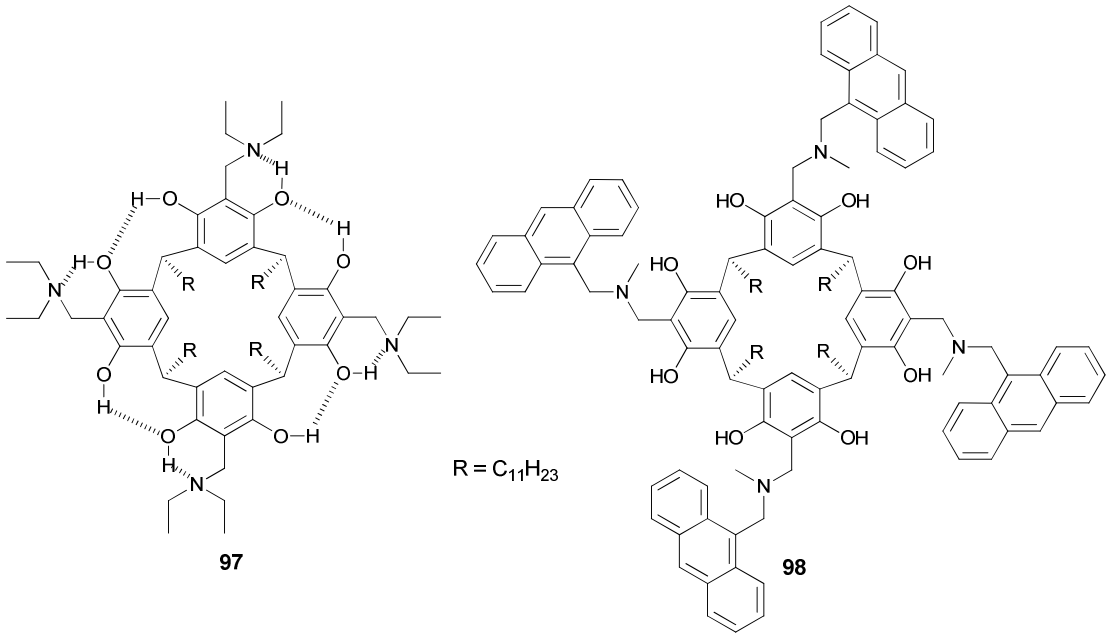

Figure 40. Aminomethylated resorcinarenes **97-98**.[V] Dashed bonds depict intramolecular hydrogen bonds.

2.2 Cation binding of the resorcinarene bis-crowns[II,III]

Resorcinarene bis-crowns **84-91** have two preorganized binding pockets for cationic guests. They form 1:2 host-guest complexes with alkali metal cations and silver.[162,166-168,II,III] The effects of the lower rim alkyl chain length of **85**, **87** and **89-91** on complexation of $CsPF_6$ and $AgPF_6$ were investigated by NMR titration in acetone-D_6, where binding constants for the Cs^+ and Ag^+ complexes were obtained (Table 1).[II,III] Extraction of cations from water to chloroform upon complexation was studied using picrate extraction (Table 2).[II]

Table 1. Binding constants as log K values in acetone-D_6 at 30 °C. [a]

	Cs^+			Ag^+		
Host	K_{11}	K_{12}	$K_{11}K_{12}$	K_{11}	K_{12}	$K_{11}K_{12}$
84	1.75[166]	-	-	1.9[168]	-	-
85	1.04	3.39	4.43	2.16	1.97	4.13
87	1.59	3.03	4.62	-	-	-
89	1.49	2.57	4.06	2.22	1.90	4.12
90	-	-	-	2.22	2.00	4.22
91	2.21	2.82	5.03	2.07	1.93	4.00

[a] Errors ≤ 15 %, R-values ≤ 8 %. Data fitted using WINEQNMR2.[169]

Table 2. Picrate extraction % from water to chloroform (standard deviation ≤ 0.5%).

Guest	**85**	**89**	**90**	**91**
Ag^+	1.6	1.7	1.6	2.8
Cs^+	10	10	10	10

The self-evident hypothesis was that the lower rim alkyl chains should not affect the binding constants since they are not involved in guest coordination. Indeed, the binding constants for the caesium complexes of **85**, **87**, **89** and **91** were between log $K_{11}K_{12}$ = 4.06–5.03,[II] and for the silver complexes of **85** and **89-91** between log $K_{11}K_{12}$ = 4.00–4.22,[III] indicating that the lower rim alkyl chain did not have a significant effect. The titration data fit well for the 1:2 binding model, whereas the previously investigated **84** fit best for the 1:1 binding model.[166,168]

The Job plot of **91** with Ag^+ indicated the simultaneous presence of 1:1 and 1:2 complexes, which is in agreement with the titration data, where the binding constants for 1:1 and 1:2 complexes were almost equal. The Job plot of **91** with Cs^+ also indicated the presence of 1:1 and 1:2 complexes. Previous experiments with **84** have shown that when the intrinsic water concentration of the solution exceeds 1 molar equivalent relative to host, 1:1 complex is dominant.[166] For the bis-crowns **85**, **87**, **89** and **91** such a strong trend was not observed, water content being 1-2.5 molar equivalents—and even 13 molar equivalents for **91** in

the titration. Therefore, the lower rim alkyl chains may have an indirect effect on complexation by playing a role during the desolvation of the cation.

Picrate extraction of caesium picrate from water to chloroform with **85** and **89-91** was 10% regardless of alkyl chain length.[III] The extraction percentage for silver picrate was lower (1.6–2.8%). However, the solid-liquid extraction of Cs^+ and Ag^+ were 10% and 9%, respectively, indicating that the higher cation dehydration enthalpy of silver[170] lowers the liquid-liquid extraction value of Ag^+ in comparison to Cs^+.

2.3 Crystal structures of the resorcinarene bis-crowns[II]

The crystal structures of the resorcinarene bis-crowns were studied in order to investigate the effect of lower rim alkyl chain length on crystal packing, where it can (a) influence the conformation of the host and (b) induce a bilayer packing when the hydrophobic effect of the alkyl chains becomes dominant. The resorcinarene bis-crowns **86** and **87** were crystallized from ethanol without any solvent inside the binding cavity or in the crystal lattice (Table 3, crystal structure composition). Since the crown ether bridges are relatively flexible, the molecules adopt a very compact structure where the upright aryl rings are tilted towards the cavity with -8.3– -10.7˚ dihedral angles (Table 4), the crown ether bridges are folded on top of the binding cavities, and the lower rim butyl and pentyl chains fill the voids between the cavities. The resorcinarene framework of *86*, and especially *87*, show slight twisting of the *boat* conformation (Fig. 41). In *86*, the molecules pack in a pillar-type fashion, where separation into polar and non-polar regions does not occur. In *87*, however, molecules form a "squeezed" bilayer assembly, which shows clear separation of polar and non-polar layers (Fig. 42). This is an indication of the pentyl chain being a limiting size for amphiphilic bilayer packing in the resorcinarene bis-crowns.

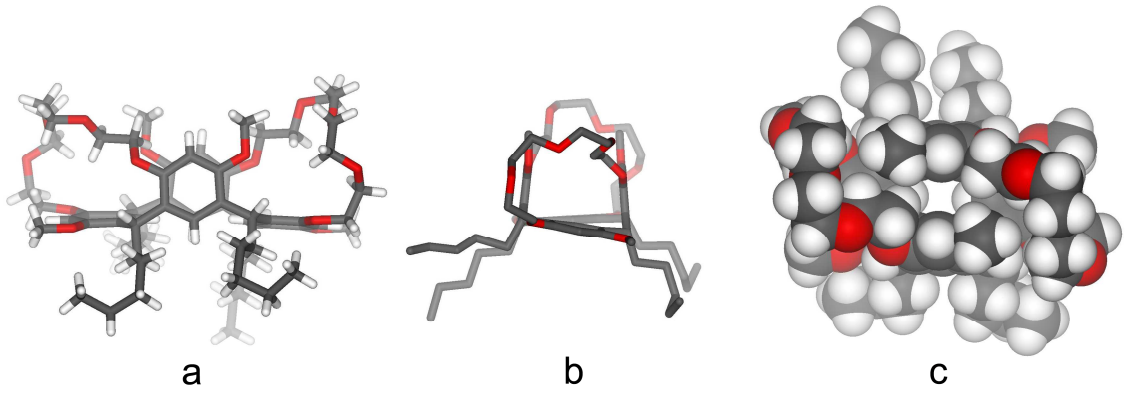

Figure 41. The *twisted boat* conformation of *87*, (a) a front view shows tilting and (b) side view twisting of the resorcinarene skeleton; (c) structure of the *87* viewed from top.

Table 3. Crystal structure composition and codes.

Resorcinarene	Composition	Crystal structure	Reference
84	**84**·$(KPF_6)_2$	*84K2*	II
85	**85**·$(CsPF_6)_2$·$(EtOH)_2$·H_2O	*85Cs2*	II
85	**85**·$(AgPF_6)_2$·$(CH_3CH_2CH_2OH)_2$	*85Ag2*	III
86	**86**	*86*	II
87	**87**	*87*	II
87	**87**·$(KPF_6)_2$	*87K2*	II
90	**90**·$(CsPF_6)_2$	*90Cs2*	II
91	**91**·$(AgPF_6)$·$[(CD_3)_2CO]_2$	*91Ag*	III
92	**92**	*92a*	IV
92	**92**·$(CH_3)_2CO$	*92b*	IV
93	**93**·$(CH_3)_2CO$	*93a*	IV
93	**93**·$(CH_3)_2CO$	*93b*	IV
93	**93**[a]	*93c*	IV
93	**93**·CH_3CN	*93d*	IV
96	**96**·$(H_2O)_{1.5}$	*96*	IV

[a] Disordered solvent molecule removed using SQUEEZE.[171]

Table 4. Conformational properties of the resorcinarene bis-crowns.

	86 [a]		
	I	II	*87*
Crystal packing	*pillar*	*pillar*	*squeezed bilayer*
Conformation	*boat*	*boat*	*twisted boat*
Tilt/°	3.7	5.7	8.9
Twist/°	3.9	5.7	8.7
Distance/Å[b]	4.79 / 8.01	4.87 / 8.00	4.80 / 7.98
Dihedral angle/°[c]	-10.7 / 175.2	-8.3 / 173.3	-10.3 / 167.3

[a] Two molecules in the asymmetric unit. [b] Between opposite aromatic ring centroids. [c] Between opposite aromatic ring planes: upright/ horizontal.

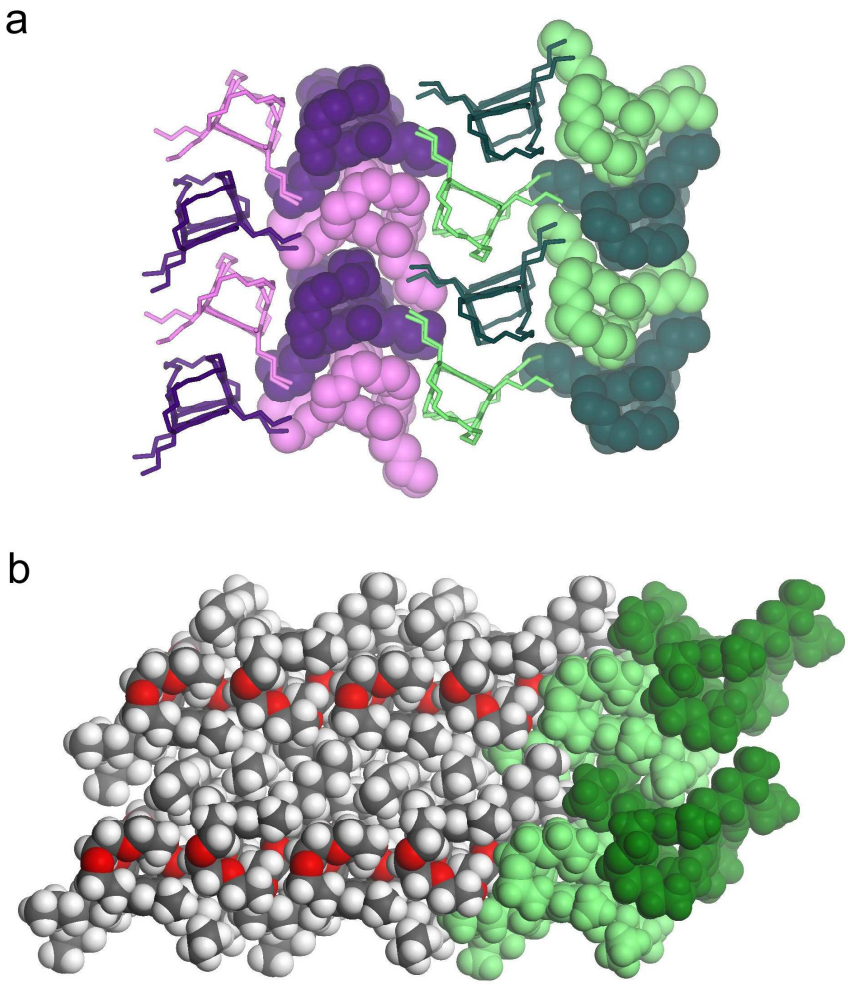

Figure 42. Pillar-packing of *86* (a) and squeezed bilayer packing of *87* (b).

Long chain bis-crowns **89**, **90** and **91** crystallized readily from ethanol in a monoclinic lattice. The structures had well-organized alkyl groups in a bilayered assembly at the lower rim but very severe disorder at the crown ether bridges (Fig. 43). This can be interpreted as stronger hydrophobic interactions at the lower rim, which drive the alkyl chains into ordered packing, whereas the crown ether bridges have more conformational freedom.

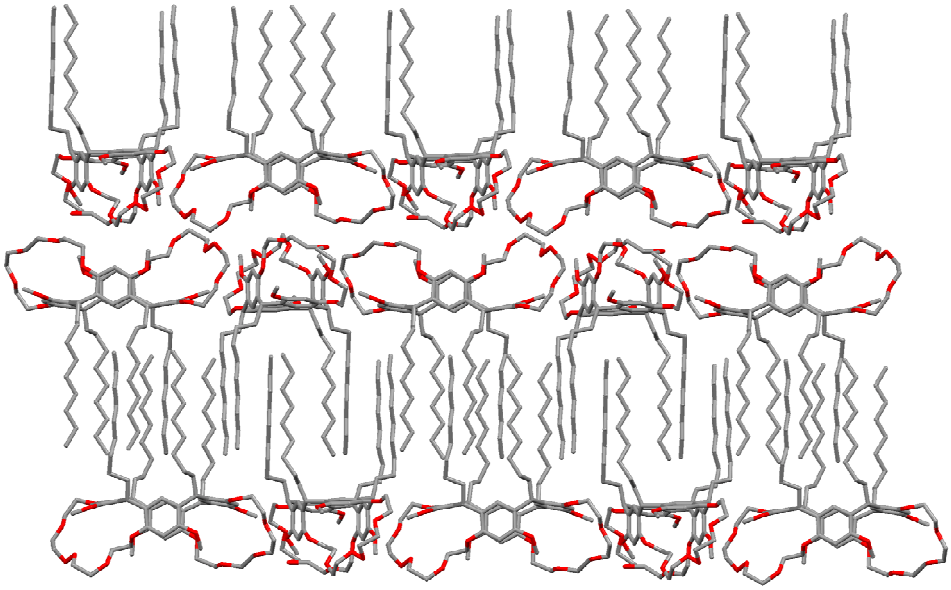

Figure 43. Bilayered packing of **89** (disorder not shown).

A comparison of the crystal structures of the bis-crowns shows that the conformation and twisting of the resorcinarene core mainly depends on the overall packing of the molecules, not on the alkyl chain length, and thus, twisting of the *boat* conformation is not limited to short ethyl chains.[162,166,167,172] However, twisting is more likely with short and medium C_2–C_5 alkyl chains, since the pronounced bilayer packing associated with the longer alkyl chains seems to direct the resorcinarene skeleton closer to a symmetrical *boat* conformation.

2.4 Crystal structures of the resorcinarene bis-crown complexes[II,III]

Crystal structures of the alkali metal (Cs^+, K^+) and silver complexes of the resorcinarene bis-crowns were investigated in order to obtain detailed information about guest coordination and to investigate the role of cation size and lower rim alkyl chain length on the conformation of the host and on the crystal packing of the complexes. Although the affinity of the bis-crowns towards K^+ in solution is quite low,[166] they form solid-state potassium complexes.[162] The structural properties of the K^+ complexes were compared to the Cs^+ complexes with the purpose of exploring alternative crystal packing forms due to smaller cation radius (K^+ 1.52 Å, Cs^+ 1.81 Å).[173] As a transition metal cation, silver has different coordination properties, and thus, not only cation size (1.23 Å)[173] but coordination to the solvent affects the crystal packing of the Ag^+ complexes.[167]

Crystallization of the resorcinarene bis-crowns **84**, **85**, **87** and **90** with excess of potassium, cesium or silver hexafluorophosphate from alcohols provided 1:2 host-guest complexes (Table 3).[II,III] Crystallization of the bis-crown **91** with 1.5 molar equivalents of $AgPF_6$ yielded a 1:1 host-guest complex.[III] Cations bind to the host by $M^+\cdots O$ coordination to the methoxy groups and to the crown ether bridge oxygens, and by cation···π interaction to the horizontal aryl rings (as illustrated in Fig. 44 for *84K2*, *85Cs2* and *85Ag2)*. Alkali metal cations reside roughly in the center of the aromatic rings by η^6 coordination, whereas silver is coordinated to the aromatic rings by η^1 coordination.

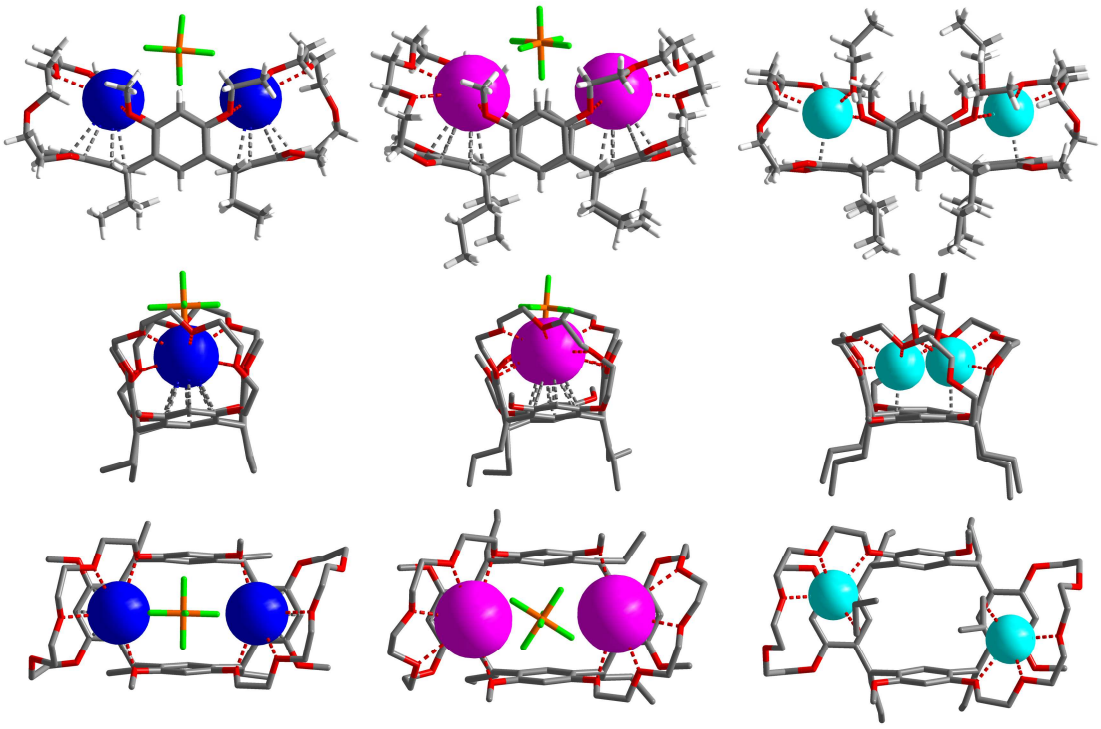

Figure 44. Cation coordination in K^+, Cs^+ and Ag^+ complexes *84K2*, *85Cs2* (H_2O excluded from the picture) and *85Ag2* from left to right; front, side and top views illustrate the size of the binding cavity and the *twisted boat* conformation of the host in Cs^+ and Ag^+ complexes.[II,III]

The binding pockets of the bis-crowns are able to adjust their size slightly according to the size of the guest cation giving K^+ complexes smaller cavity diameters than Cs^+ complexes (Table 5). In the alkali metal complexes, a PF_6^- anion is coordinated between the two cations inside the binding pocket, which reduces the charge repulsion between the cations. Instead of an anion, silver complexes *85Ag2* and *91Ag* have a solvent molecule coordinated to each cation inside the binding cavity. This enlarges the size of the binding cavity of these complexes and induces twisting of the *boat* conformation in *85Ag2*, which contains two propanol molecules inside the resorcinarene cavity. Furthermore, *85Cs2* also has a *twisted boat* conformation, which is caused by a water molecule coordinated to the cation and crystal packing into anion/solvent-coordinated

shifted capsules. Based on the results, it seems that the size of the cation does not have a direct influence on packing or the conformation of the host. Instead, solvent coordination, together with cation size, plays a more important role on packing.

Table 5. Conformational properties of the resorcinarene bis-crown complexes.

	84K2	*85Cs2*	*85Ag2*
Crystal packing	*layer*	*layer/ shifted capsule*	*layer*
Conformation	*boat*	*twisted boat*	*twisted boat*
Tilt/°	1.4	7.0	7.6
Twist/°	2.1	6.4	6.2
Distance/Å[a]	5.28/7.98	5.46/7.95	6.15/7.56
Dihedral angle/°[b]	14.4/151.4	22.2/148.8	31.3/168.5
Cavity diameter/Å[c]	4.80/5.15	5.42/5.28	6.18[d]
Average M^+···O/Å	2.86/2.98	3.17/3.28	2.56 [d]
M^+···Ar/Å[f]	3.05/3.03 (Ct)	3.30/3.30 (Ct)	2.55 (η^1)[d]

	87K2	*90Cs2*	*91Ag*
Crystal packing	*bilayer/ shifted capsule*	*bilayer/ shifted capsule*	*bilayer*
Conformation	*boat*	*boat*	*boat*
Tilt/°	3.3	1.1	5.9
Twist/°	3.5	0.5	5.0
Distance/Å[a]	5.26/7.98	5.49/7.94	5.81/7.84
Dihedral angle/°[b]	11.8/147.0	21.1/148.3	34.2/143.7
Cavity diameter/Å[c]	4.90/4.69	5.08/5.23	5.54/6.06[e]
Average M^+···O/Å	2.87/3.01	3.15/3.07	2.66
M^+···Ar/Å[f]	3.11/3.07 (Ct)	3.22/3.26 (Ct)	2.37 (η^1)

[a] Between opposite aromatic ring centroids. [b] Between opposite aromatic ring planes: upright/ horizontal. [c] Average cavity diameter measured as O–O distances. [d] Identical due to symmetry. [e] Ellipsoidal. [f] Ct = aryl ring centroid.

84K2 and *85Cs2* complexes with short ethyl and propyl chains, respectively, pack in a layered assembly without separation into polar and non-polar sides (Fig. 45). *85Ag2* forms a layered packing, which differs from the other layered assemblies by the relative positions of complexes to each other. Within a layer, each complex is surrounded by six adjacent complexes that form a 'chain mail' pattern (Fig. 46).

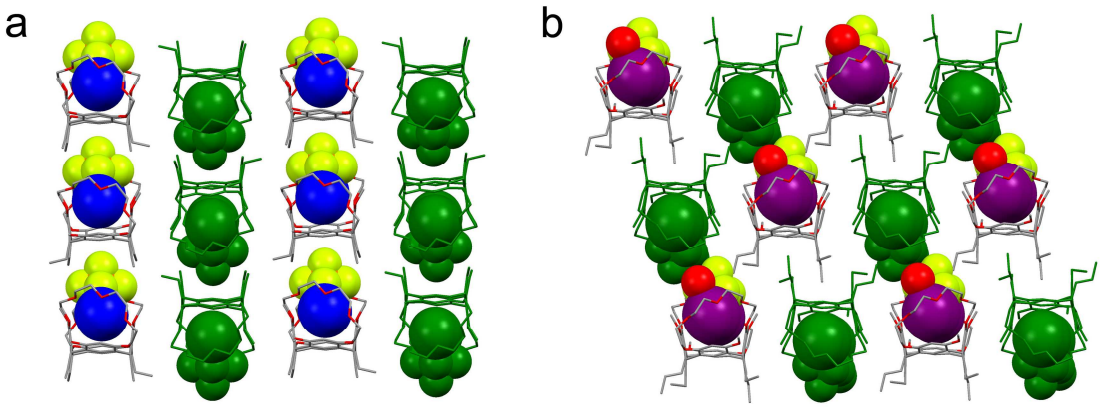

Figure 45. Side view of layered packing in *84K2* (a) and *85Cs2* shifted capsules (b), all *ccw* enantiomers colored green.

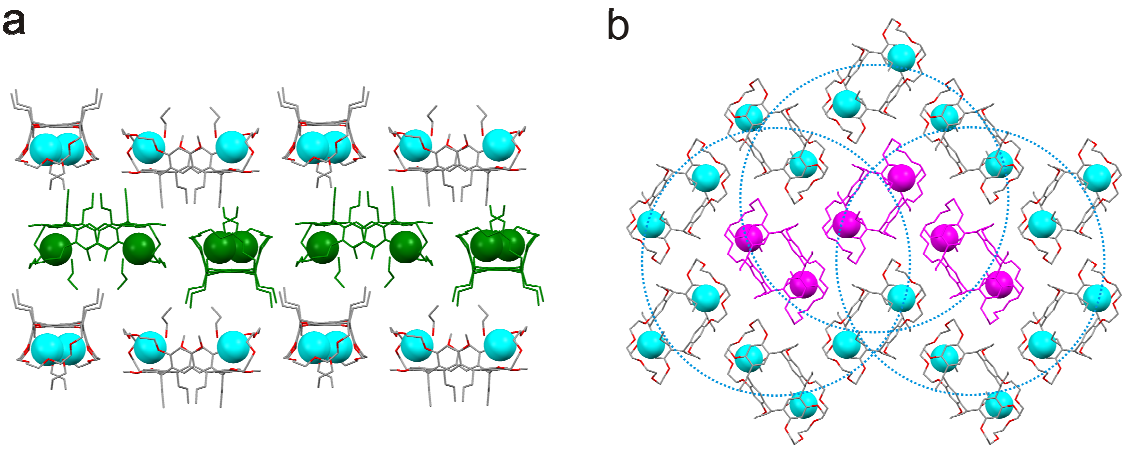

Figure 46. Side (a) and top (b) views of 85Ag2 layers, *ccw* enantiomers in green, anions omitted for clarity.

The resorcinarene bis-crowns **87**, **90** and **91** with longer pentyl, decyl and undecyl chains at the lower rim, formed complexes *87K2*, *90Cs2* and *91Ag*, which pack in bilayered fashion with alternating polar and non-polar layers (Fig. 47). Thus, the effect of alkyl chain length on inducing bilayered packing and on conformation of the complexes is similar to the effect observed with the resorcinarene bis-crown structures *86* and *87*. Complexation of cations in the binding pocket rigidifies the crown ether bridges, reducing the disorder

observed in the crystal structures of long chain bis-crowns **89-91** and enabling the crystal structure analysis of these molecules.

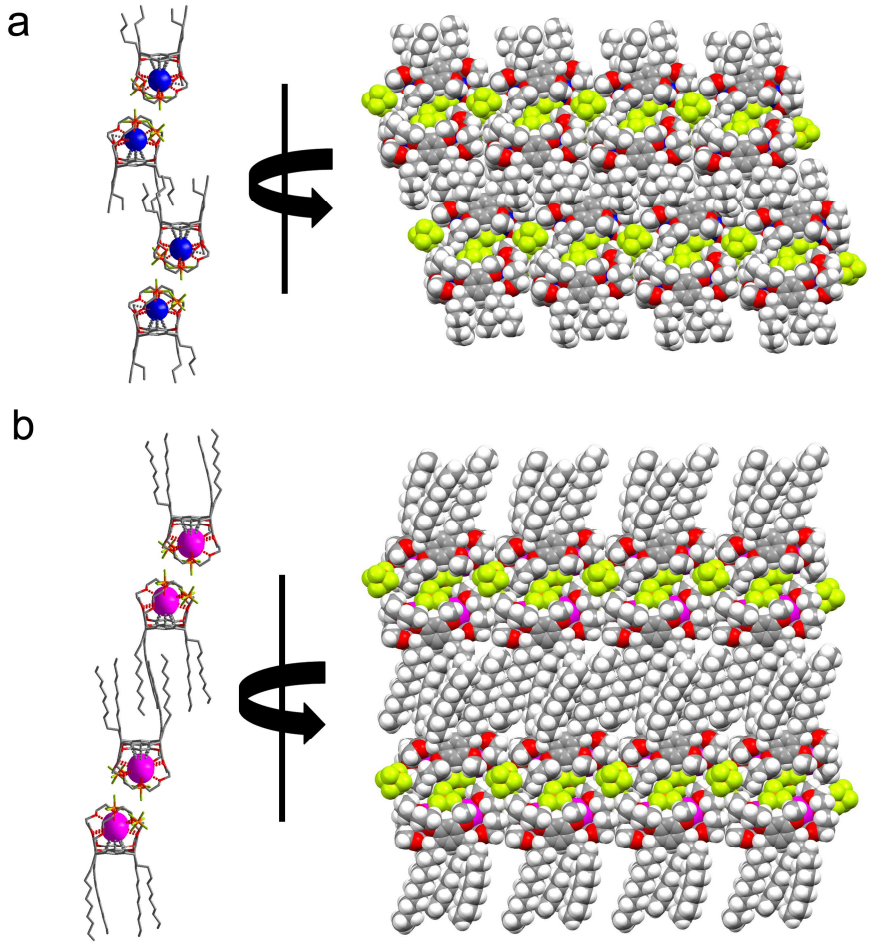

Figure 47. Bilayered packing of (a) *87K2* and (b) *90Cs2*.

2.5 Conformational properties of the resorcinarene octapodands[IV]

The resorcinarene octapodands **92-96** display a flexible *boat-to-boat* interconversion of the resorcinarene skeleton due to the absence of an intramolecular hydrogen bonding network, or bridging, which restricts the bis-crowns in a fixed *boat* conformation (Fig. 48). The speed of the conversion is affected by temperature, medium polarity and lower rim alkyl chain length. This can be deduced from the ^{1}H NMR spectra as broadened resorcinol ring proton signals in a non-polar solvent, $CDCl_3$, in comparison to polar solvents such as acetone or DMSO (Fig. 49). The octapodand **92** with methyl groups at the lower rim had a distinctively reduced speed of conversion in comparison to longer alkyl chain podands, as observed by the presence of two sets of aromatic

proton signals as a description of C_{2v} symmetrical *boat* conformation in $CDCl_3$ at 30 ˚C (Fig. 50).

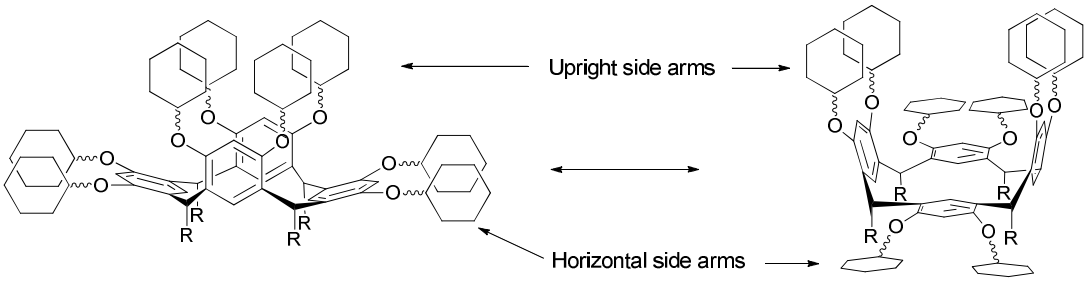

Figure 48. Schematic presentation of the *boat-to-boat* conversion of resorcinarene octapodands.

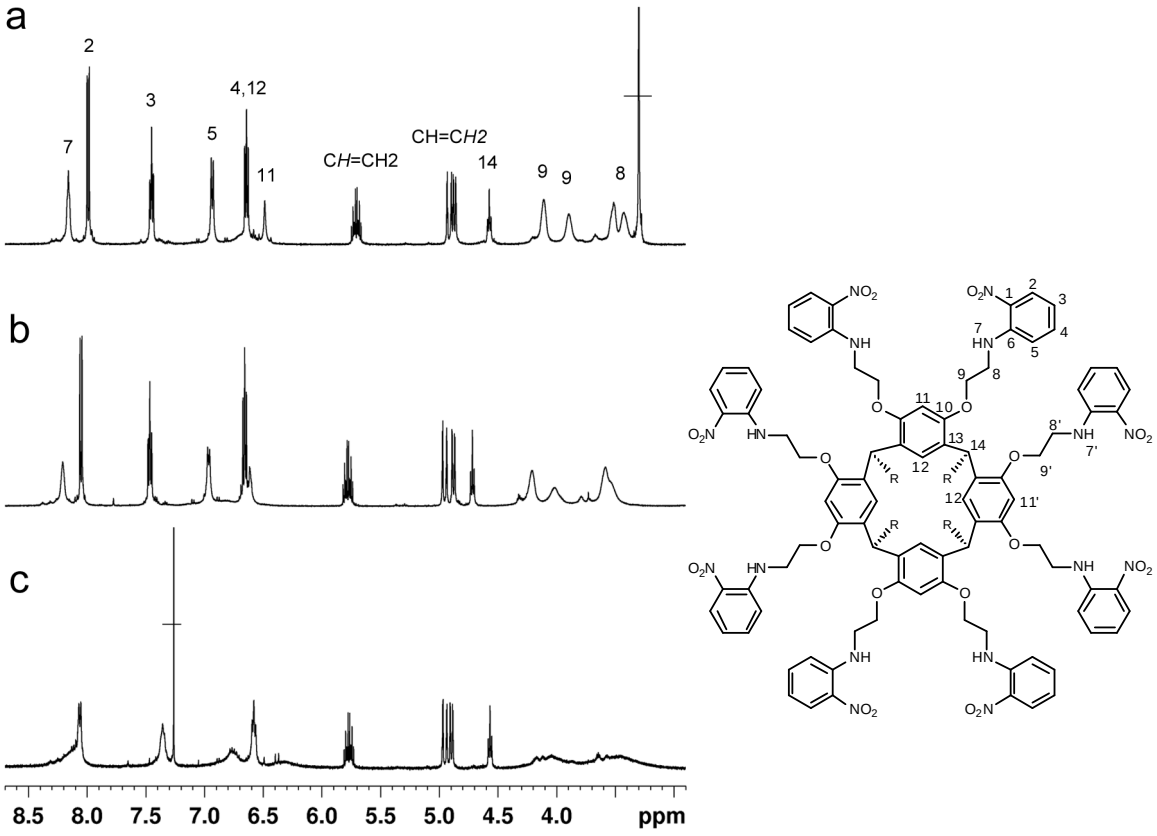

Figure 49. ^{1}H NMR spectra of **96** in a) DMSO-D_6, b) acetone-D_6, c) $CDCl_3$ at 30 °C from 2.9–8.5 ppm.

In addition to the changes in the resorcinarene conformation, the *o*-nitroaniline side arms are able to rotate around the -OCH_2CH_2N- linkers, which in coordination to the *boat-to-boat* conversion produces particular conformational mobility. However, since the eight *o*-nitroaniline side arms are confined in close contact to one another, the rotation around the linkers is restricted by sterical proximity of the other side arms in comparison to a

reference compound, 1,3-bis-2-(*N*-(2-nitrophenyl)-amino)-ethoxy benzene (**99**, Appendix). Whereas **99** shows well-resolved triplet and multiplet patterns for -OCH_2CH_2N- linker protons, the linker protons in octapodands have broad signals resulting from decelerated rotational movement.

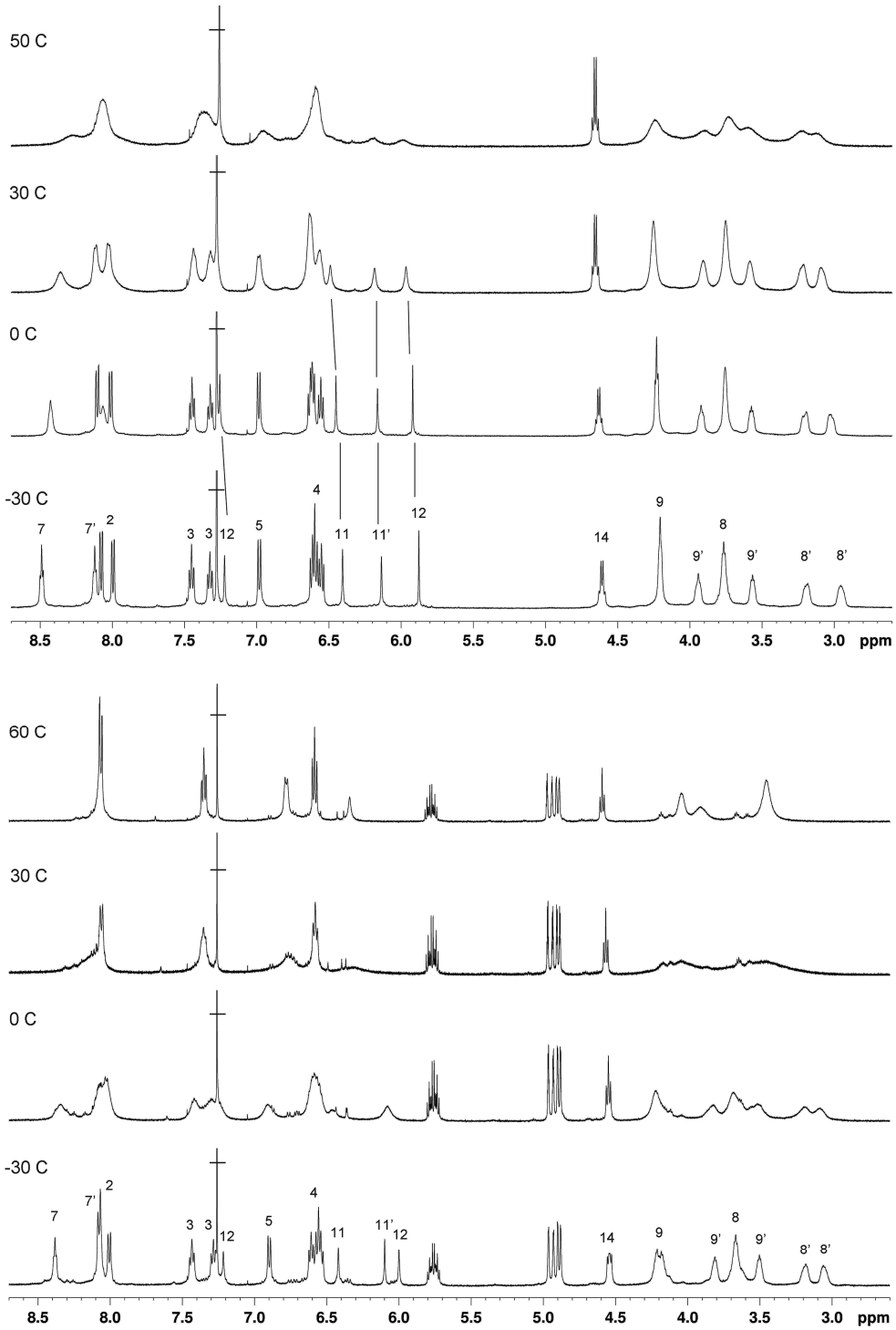

Figure 50. ^{1}H NMR spectra of **92** (top) and **96** (bottom) in $CDCl_3$ at different temperatures, labeled as in Fig. 49.

2.6 Crystal structures and polymorphism of the resorcinarene octapodands[IV]

Crystal structures of the resorcinarene octapodands show the three-dimensional design of the macrocycles in the *boat* conformation. The octapodands **92** and **93** crystallized quite readily from acetone, acetonitrile, nitromethane, and from their mixtures with CH_2Cl_2 (Table 3). Two different crystal forms were found for octapodand **92**, *92a* without the solvent in the crystal lattice, and *92b* with an acetone molecule trapped between the upright side arms, forming a clathrate (Fig. 51). The two crystal forms may be called pseudopolymorphs when the focus is on the crystal structure and conformation of the octapodand.

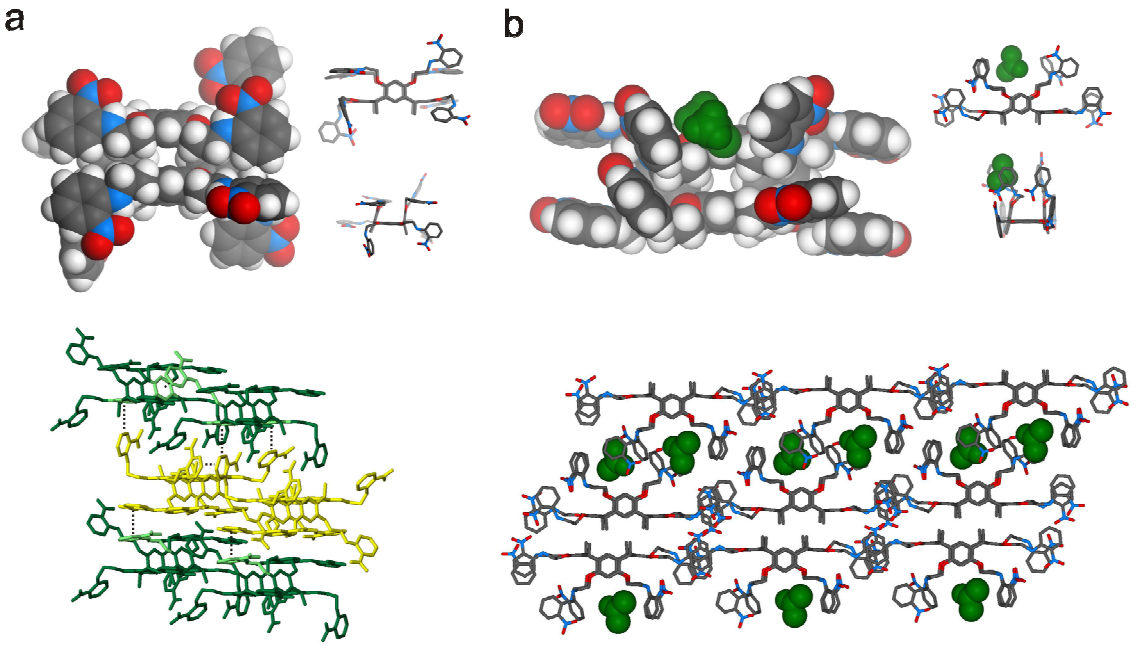

Figure 51. Crystal structures of a) *92a* top view and packing with π···π interactions as dashed lines, b) *92b*, where acetone molecules are shown in green.

Octapodand **93** crystallized as acetone (*93a*, *93b*) and acetonitrile (*93d*) solvates (or clathrates). The conformational polymorphs *93a* and *93b* formed concomitantly in the same crystallization batch, where *93a* was obtained from a plate and *93b* from a needle crystal. The difference between *93a* and *93b* is in the relative orientation of upright side arms and intermolecular interactions between a pair of octapodands (Fig. 52). The upper rim interface of *93a* is connected by intermolecular hydrogen bonding between the *o*-nitroaniline side arms, whereas in *93b* the upper rim interface is connected by π···π interactions.

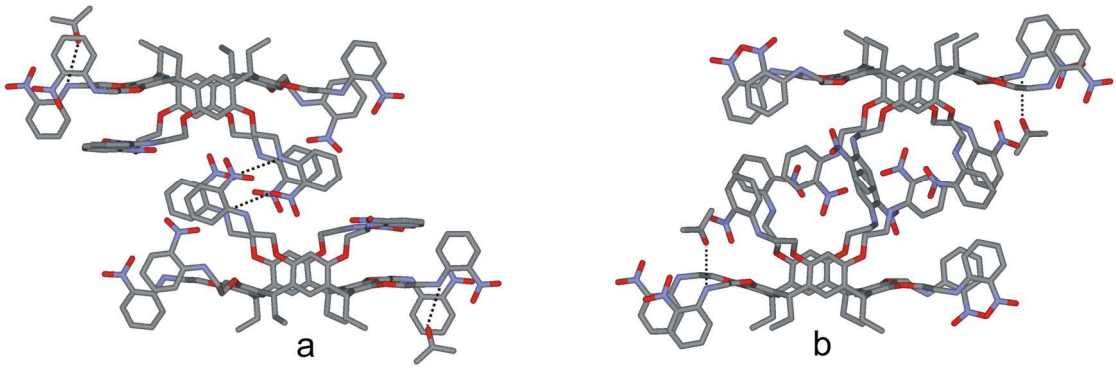

Figure 52. Crystal structure of two polymorphs of **93** acetone solvate, *93a* and *93b*; intermolecular hydrogen bonds marked with dashed lines.

The effect of crystallization conditions on the relative abundance of *93a* and *93b* crystal forms was investigated by powder XRD. Crystallization of the octapodand **93** from acetone was repeated by changing solvent quantity, speed of evaporation and temperature. A comparison of powder XRD data with calculated diffraction patterns of *93a* and *93b* by Rietveld refinement[175] showed that both forms were always present, and that *93b* was more abundant at crystallization performed at 4 °C, whereas *93a* was more abundant in samples which were crystallized at ambient temperature (20 °C). However, the experiments did not lead to unambiguous control over a single crystal form.

In all crystal structures of **92** and **93**, the upper rims of the podands face against upper rims, forming a head-to-head assembly which provides favorable π···π interactions. The upper rim of the octapodands is sterically crowded, as seen in the space-filling model of *92a* and *92b* (Fig. 51). In all crystal structures except *92a*, the octapodands formed row-like assemblies, which are held together by π-stacking interactions between the horizontal side arms. Similar π-stacking was observed for octapodand **96** with long 1-decenyl alkyl chains at the lower rim (*96*, Fig. 53). In addition, *96* shows bilayered packing typical of amphiphilic molecules, forming alternating aliphatic (hydrophobic) and aromatic (more hydrophilic) layers.

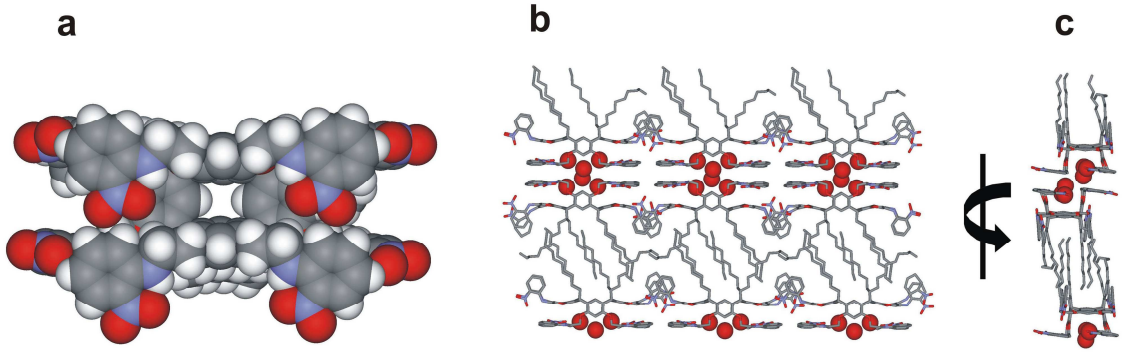

Figure 53. Crystal structure of *96* (a, top view) and bilayered packing (b,c).

2.7 Self-assembly of resorcinarenes

2.7.1 Langmuir films[III,IV]

The self-assembly of resorcinarene bis-crown **91** and resorcinarene octapodands **93–96** as a monolayer at the air-water interface was studied with the Langmuir-Blodgett trough.[III,IV] Resorcinarene bis-crowns and resorcinarene octapodands are non-ionic amphiphiles with a different upper rim polarity and conformational flexibility. However, both resorcinarene octapodands and bis-crowns self-assembled as monolayers at the air-water interface as observed from their π/A isotherms, which indicates their surfactant properties.

The lower rim alkyl chain length of the resorcinarene octapodands had a significant influence on their π/A isotherms (Fig. 54).[IV] The octapodand **93** did not form a monolayer on water due to weak hydrophobic interactions between the short ethyl chains. The octapodand **94** with pentyl groups at the lower rim formed a monolayer, but the collapse pressure was lower and the molecular areas were larger than in the monolayer of **95** with nonyl groups at the lower rim (Table 6). The terminal alkene functionality in **96**, on the other hand, lowered the collapse pressure and increased the molecular areas (in comparison to **95**) by disturbing the organized packing of the alkyl chains.

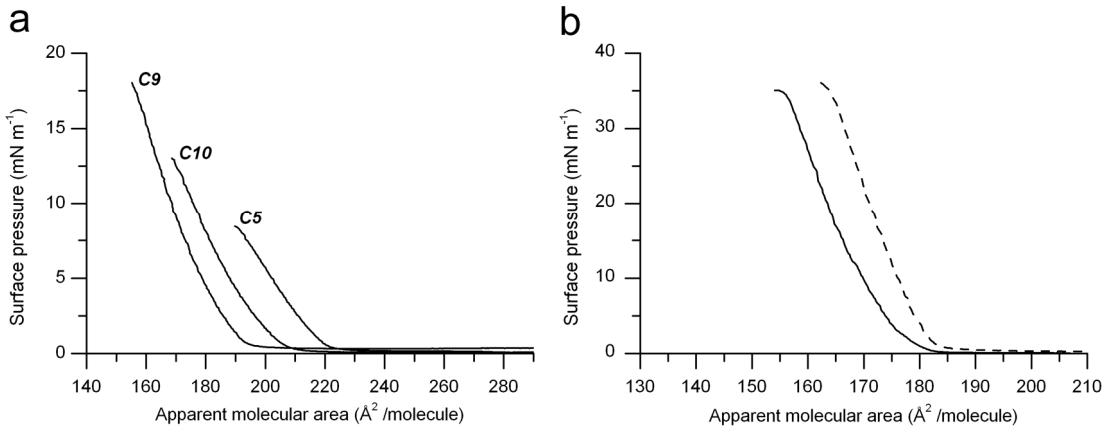

Figure 54. Langmuir isotherms of a) the octapodands **94–96**, b) bis-crown **91** on water (solid line) and on 100 μM $AgNO_3$ (dashed line).

Table 6. Langmuir isotherm data for resorcinarene octapodands **94–96** and bis-crown **91** on water and on aqueous $AgNO_3$ (100 μM).[a]

	94	**95**	**96**	**91**	**91**
Subphase	water	water	water	water	$AgNO_3$ (aq)
$\prod_c$[b]	9	18	13	33	35
A_c[c]	191	157	166	157	163
A_{lim}[d]	221	187	197	174	181

[a] Surface tension values are expressed in mN m^{-1} and areas in $Å^2$/molecule. [b] Surface pressure at the collapse point, [c] molecular area at the collapse point, [d] extrapolation of the linear part of the isotherm on the *x* axis.

The resorcinarene bis-crown **91** with the longest alkyl chains was chosen for the preparation of Langmuir and Langmuir-Blodgett films to optimize the monolayer stability.[III] Accordingly, **91** formed well-organized and stable monolayers, which collapsed at 33 mN m^{-1} surface pressure and show less compressibility than the octapodand **95** (Fig. 54, Table 6). Whereas the molecular areas at the collapse are the same (157 $Å^2$/molecule) the increase in collapse pressure and decrease in the limiting molecular area of **91** probably results from the increased polarity and decreased flexibility of the head group in comparison to the octapodand **95**.

The complexation of silver in a monolayer of **91** was investigated by recording π/A isotherms with 100 μM $AgNO_3$ in the subphase (Fig. 54, Table 6). The slight increase in surface pressure as well as the increase in surface area, indicates that the bis-crown is interacting with silver ions at the air-water interface. The increase of molecular area of pure host, from 157 $Å^2$/molecule to 163 $Å^2$/molecule with silver in the subphase, is consistent with the difference of pure host (159 $Å^2$/molecule) and 1:1 silver complex (166 $Å^2$/molecule) in the crystal structure, suggesting that 1:1 complexation is plausible also at the monolayers.

2.7.2 Solid lipid nanoparticles[II]

The ability of the resorcinarene bis-crowns **84-91** to form solid lipid nanoparticles (SLN) was tested in order to assess their self-assembling properties in water. Bis-crown SLNs were prepared by solvent diffusion (solvent replacement) method,[107] where a few milligrams of bis-crown was dissolved in a small amount of THF and water was added to the solution by vigorous stirring. The resulting cloudy suspension indicated the formation of SLN. The diameters of the SLNs were analyzed by dynamic light scattering method, which gave hydrodynamic diameters of 220–320 nm (Fig. 55) and polydispersity indexes of 0.05–0.34. Particle shape and size were confirmed by SEM images, which revealed spherical particles at a size distribution corresponding to the DLS measurements (Fig. 56).

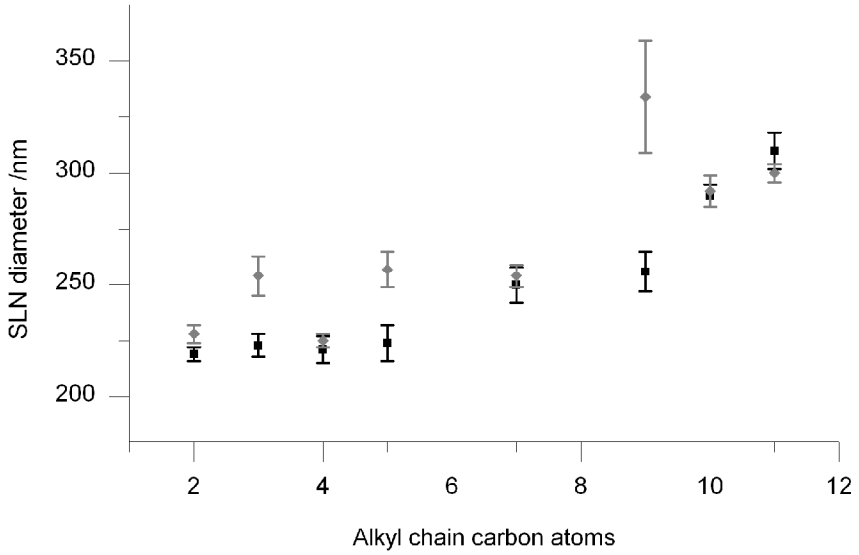

Figure 55. SLN diameters plotted against alkyl chain length (mean size of distribution from DLS showing standard deviation, N = 3); 0.1 mM resorcinarene concentration in black, 100 mg/L in grey.

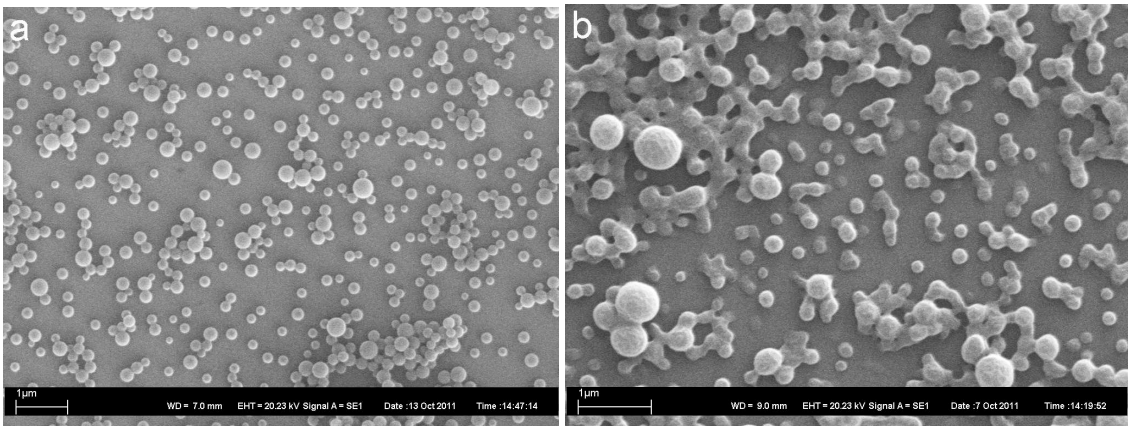

Figure **56**. SEM images for SLNs a) **85**, b) **91** (scale bar 1 µm).

It is noteworthy that bis-crowns **84-86** with short C_2, C_3 and C_4 alkyl chains also formed nanoparticles. Previously, SLNs have been prepared with calixarenes and resorcinarenes with at least five carbon atoms in the alkyl or acyl chains.[107] The ability of the short alkyl chain bis-crowns **84-86** to form SLNs probably arises from their macrocyclic structure, which separates the hydrophilic side of the compound from the hydrophobic side.

The diameter of the SLNs slightly increased when the length of the lower rim alkyl chain increased, which is in fact the opposite result from that obtained by Coleman et al.[108] for *p*-acyl-calix[9]arene SLNs. However, calix[9]arenes have a larger, nine-membered macrocyclic ring with enhanced conformational flexibility, which can lead to different arrangement of the amphiphiles during their self-assembly.

2.8 Antibacterial properties of the bis-crown silver complexes[III]

The antibacterial effect of Langmuir-Blodgett films of resorcinarene bis-crown silver complex deposited on a solid substrate was tested on *E. coli* (isolated from human intestinal flora bacteria) using the setup shown in Fig. 57. The area covered by *E. coli* was measured from the microscopic images after incubation (Fig. 58). Comparison of the resorcinarene bis-crown silver complex **91**-Ag to the reference samples, a hydrophobic glass slide, a monolayer of **91** without silver, and a hydrophobic glass dipped in $AgNO_3$ without resorcinarene, showed almost tenfold reduction in the bacterial growth in the LB film of the bis-crown silver complex. This clearly indicates that the antibacterial effect results from the presence of silver in the LB films, not from the resorcinarene alone. The slight reduction of bacterial viability on top of the hydrophobic glass slide dipped in $AgNO_3$ may be attributed to the presence of hydrophilic areas on the glass slide that bind silver ions via electrostatic interactions and release it when in contact with bacteria.

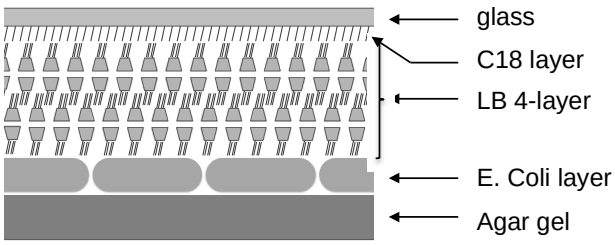

Figure 57. A schematic representation of the experimental setup used to test the antibacterial properties of the **91**-Ag complex.

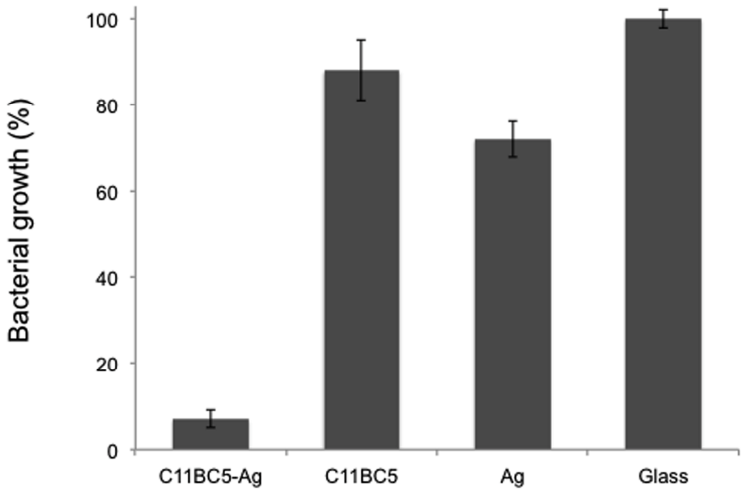

Figure 58. *E. coli* growth (normalized results) on a agar plate submitted to a Langmuir-Blodgett multilayer of **91** transferred from a sub-phase containing silver (C11BC5-Ag) or pure water (C11BC5); hydrophobic glass slides (glass) and hydrophobic glass slides dipped in silver nitrate (100 μM, Ag).

The antibacterial effect of the LB films is remarkable because of the very low silver concentration of the films. Even if the "best-case" scenario where **91** forms a 1:1 complex at the interface were fulfilled, the density of silver ions at the surface would be approximately 0.4 nmol/cm^2, giving a bulk concentration in the medium of 90 nM; this value is 210-fold lower than the complete inhibitory concentration of silver for *E. coli* (CIC = 18.9 μM).[175] The low concentration does not allow a bulk effect of silver ions in the culture medium, but instead suggests that the antibacterial effect results from close contact between the **91**-Ag layer and the bacteria, where the silver is released from the bis-crown complexes in the presence of thiol groups on the bacterial surface. This leads to bacterial death and inhibits overall bacterial growth, as observed in these experiments. The antibacterial effect of **91**-Ag complex serves as proof of principle for the development of supramolecular antibacterial materials, which may well find applications where low silver concentrations are preferred and where silver nanoparticles would be too toxic or silver salts too prone to diffusion.

2.9 Interaction with fluorescent dyes[V]

Aminomethylated resorcinarenes **97** and **98** with *N*,*N*-diethyl or *N*-methyl-*N*-methylanthracene funtionalities are basic compounds, which can be protonated at the tertiary amino groups. Fluorescent dyes, on the other hand, are useful counterparts for acid-base reactions because they are quite often prepared and used as hydrochloride salts, and their reactions can be followed with UV-vis or fluorescence spectroscopy. In addition, since the fluorescent dyes are sensitive to their chemical environment, deprotonation of the dye can dramatically influence its absorption and emission spectra.

Rhodamine B belongs to a group of xanthene dyes which are known for their special chemical equilibrium between open, zwitterionic, and closed lactone form.[176,177] Rhodamine B is stable both as a hydrochloride salt (always present in the zwitterionic form) and rhodamine B base, which has zwitterion and lactone isomers (Fig. 59). The chemical equilibrium between the lactone and zwitterion forms can be changed by protonation, and it is sensitive to solvent polarity and temperature.[178-180] The lactone ring of rhodamine B base opens in protic solvents, such as alcohol or water, and the colorless lactone form is observed in aprotic solvents, such as chloroform.

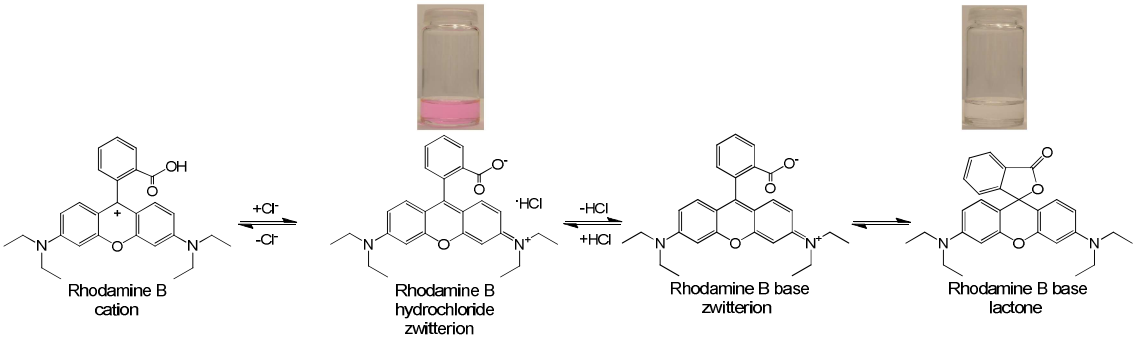

Figure 59. Rhodamine B isomers.

The effect of aminomethylated resorcinarenes **97–98** on rhodamine B absorbance and fluorescence was investigated by UV-vis and fluorescence measurement, and the structures of the reaction products were studied using NMR spectroscopy. When aminomethylated resorcinarenes were added to the solution of rhodamine B hydrochloride in chloroform, a rapid decrease of rhodamine B absorbance at 552 nm was observed, which corresponds to the lactone ring closure of the rhodamine B.

The reaction is more effective with resorcinarene **97** than with **98** (Fig. 60) which probably results from the stronger basicity of **97**, whereas Job's method indicated that both have the same 1:2 host-dye stoichiometric ratio. In a protic solvent (MeOH-$CHCl_3$ 1:1), the lactonization does not occur, but an 8 nm blue shift was observed instead. This corresponds to the absorbance of zwitterionic rhodamine B base and shows that deprotonation of the rhodamine B hydrochloride has occurred. In addition, the NMR spectra of the host **97** in the presence of rhodamine B hydrochloride closely resembles the NMR spectra of protonated host **97**, which was prepared by treating the host **97** with HCl.

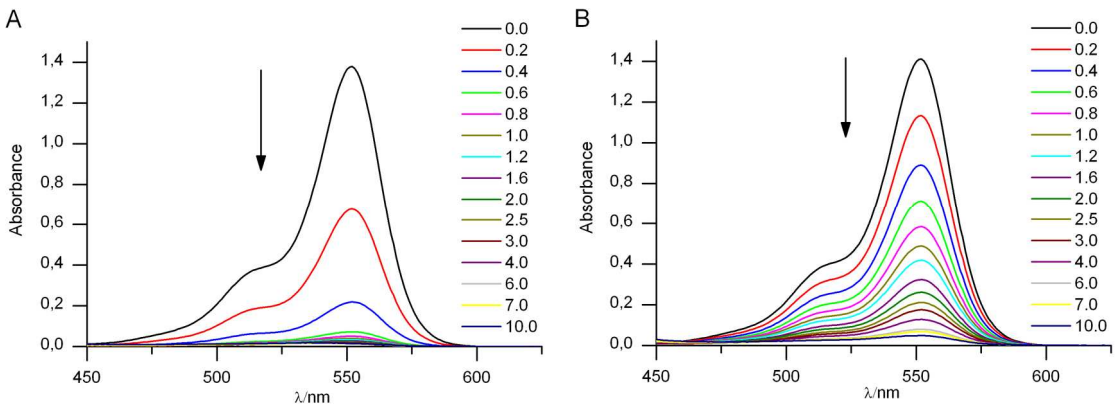

Figure 60. UV-vis spectra of rhodamine B solutions in chloroform titrated with resorcinarenes **97** (a) and **98** (b), units in molar equivalents.

Aminomethylated resorcinarene **98** contains fluorescent anthracene groups at the upper rim of the resorcinarene framework, and itself it can be used as a fluorescent sensor. The fluorescence intensity of the anthracene groups is quenced by a photoinduced electron transfer process (PET), which is caused by the presence of tertiary nitrogen atoms containing a free electron pair next to the fluorophore in host **98**. The quencing is reduced by protonation of the nitrogens, which was observed as approximately 95% increase in the fluorescence intensity by 10 molar equivalents of HCl (Fig. 61). The same phenomena was observed when the fluorescence of host **98** was measured after addition of rhodamine B hydrochloride, which gives yet further evidence of the acid-base reactions between resorcinarene **98** and the dye.

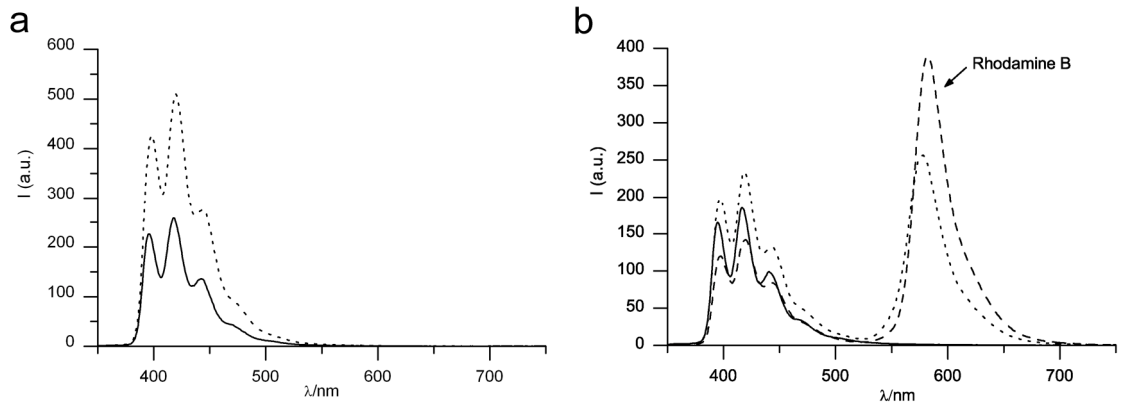

Figure 61 Fluorescence spectra of **98** in chloroform (solid line) at 258 nm excitation, a) with 10 molar equivalents of HCl (dotted line), b) with rhodamine B (1 eq. dotted and 2 eq. dashed line).

3 SUMMARY AND CONCLUSIONS

In this thesis, the self-assembly and complexation properties of eight resorcinarene bis-crowns and five resorcinarene octapodands with identical binding sites and varying alkyl chain lengths were studied. The resorcinarene bis-crowns with preorganized and conformationally fixed binding sites selectively complex caesium and silver cations, forming 1:1 and 1:2 host-guest complexes in the solid state and in solution, regardless of lower rim alkyl chain length. However, the lipophilicity—and thus, the self-assembly of the resorcinarene bis-crowns—can be tuned by changing the length of the lower rim alkyl chains. Long alkyl chains provided strong hydrophobic interactions, which along with the conformationally rigid and polar head group led to well-organized Langmuir monolayers with high stability and low compressibility. In addition, resorcinarene bis-crowns assembled as solid lipid nanoparticles, potential drug carrier structures, in which the particle diameters increased with increasing lower rim alkyl chain length. The crystal structure analysis of two resorcinarene bis-crown structures and six alkali metal and silver complexes revealed interesting details about the packing and amphiphilic nature of the molecules, for instance showing that a pentyl group is the limiting alkyl chain length for bilayered packing in the solid state.

In addition to the lower rim alkyl chain length, the mobility and structure of the resorcinarene upper rim affects the self-assembly of resorcinarenes. Resorcinarene octapodands contain a flexible upper rim binding site, which undergoes *boat-to-boat* interconversion, and rotation of the *o*-nitroaniline side arms around the ethylene linkers. The rate of the conformational movement depends on temperature as well as medium polarity, increasing in more polar solvents. The mobile and relatively non-polar upper rim reduced the stability of the Langmuir monolayers of the octapodands in comparison to the conformationally locked resorcinarene bis-crowns. Seven crystal forms obtained for the resorcinarene octapodands, including solvates and conformational polymorphs, illustrated that the upper rim podand arms can appear in different orientations relative to the resorcinarene cavity also in the solid state.

Self-assembled monolayers of the resorcinarenes and their interaction with fluorescent dyes were studied in order to create functional materials and sensor

applications. The Langmuir-Blodgett films of the resorcinarene bis-crown silver complex provided antibacterial coatings which inhibit *E. coli* with nanomolar silver concentration. The interaction of aminomethylated resorcinarenes with rhodamine B affects the lactone-zwitterion equilibrium and, accordingly, the absorbance and emission of the dye. In addition, the fluorescence intensity of anthracene resorcinarene conjugate can be enhanced by protonation in an acidic medium.

REFERENCES

1 P. Timmerman, W. Verboom and D.N. Reinhoudt, *Tetrahedron,* **1996**, *52*, 2663-2704.
2 L. Mandolini and R. Ungaro, (ed.), *Calixarenes in Action,* Imperial College Press, Singapore, **2000**, pp.271.
3 Z. Asfari, V. Böhmer, J. Harrowfield and J. Vicens, (ed.), *Calixarenes 2001,* Kluwer Academic Publishers, The Netherlands, **2001**, pp.683.
4 A. Baeyer, *Ber. Dtsch. Chem. Ges.,* **1872**, *5*, 25-282.
5 A. Baeyer and V. Villiger, *Ber. Dtsch. chem. Ges.,* **1902**, *35*, 1201-1212.
6 J.B. Niederl and H.J. Vogel, *J. Am. Chem. Soc.,* **1940**, *62*, 2512-2514.
7 A. Zinke and E. Ziegler, *Ber. Dtsch. Chem. Ges.,* **1944**, *77*, 264-272.
8 See for a history of calixarenes: C.D. Gutsche, *Acc. Chem. Res.,* **1983**, *16*, 161-170.
9 See for a history of calixarenes: T. Kappe, *J. Inclusion Phenom. Mol. Recognit. Chem.,* **1994**, *19*, 3-15.
10 C.D. Gutsche, B. Dhawan, K.H. No and R. Muthukrishnan, *J. Am. Chem. Soc.,* **1981**, *103*, 3782-3792.
11 G.D. Andreetti, R. Ungaro and A. Pochini, *J. Chem. Soc. , Chem. Commun.,* **1979**, 1005-1007.
12 M. Coruzzi, G.D. Andreetti, V. Bocchi, A. Pochini and R. Ungaro, *J. Chem. Soc., Perkin Trans. 2,* **1982**, 1133-1138.
13 A. Arduini, A. Pochini, S. Reverberi and R. Ungaro, *J. Chem. Soc., Chem. Commun.,* **1984**, 981-982.
14 S. Shinkai, S. Mori, T. Tsubaki, T. Sone and O. Manabe, *Tetrahedron Lett.,* **1984**, *25*, 5315-5318.
15 S. Shinkai, T. Arimura, K. Araki, H. Kawabata, H. Satoh, T. Tsubaki, O. Manabe and J. Sunamoto, *J. Chem. Soc., Perkin Trans. 1,* **1989**, 2039-2045.
16 Y. Kikuchi, K. Kobayashi and Y. Aoyama, *J. Am. Chem. Soc.,* **1992**, *114*, 1351-1358.
17 K. Kobayashi, Y. Asakawa, Y. Kato and Y. Aoyama, *J. Am. Chem. Soc.,* **1992**, *114*, 10307-10313.
18 R.M. Izatt, J.D. Lamb, R.T. Hawkins, P.R. Brown, S.R. Izatt and J.J. Christensen, *J. Am. Chem. Soc.,* **1983**, *105*, 1782-1785.
19 S.R. Izatt, R.T. Hawkins, J.J. Christensen and R.M. Izatt, *J. Am. Chem. Soc.,* **1985**, *107*, 63-66.
20 S. Shinkai, S. Mori, H. Koreishi, T. Tsubaki and O. Manabe, *J. Am. Chem. Soc.,* **1986**, *108*, 2409-2416.
21 S. Shinkai, Y. Shirahama, T. Tsubaki and O. Manabe, *J. Am. Chem. Soc.,* **1989**, *111*, 5477-5478.
22 M. Komiyama, K. Isaka and S. Shinkai, *Chem. Lett.,* **1991**, 937-940.
23 R.V. Rodik, V.I. Boyko and V.I. Kalchenko, *Curr. Med. Chem.,* **2009**, *16*, 1630-1655.
24 D.T. Schühle, J.A. Peters and J. Schatz, *Coord. Chem. Rev.,* **2011**, *255*, 2727-2745.
25 G.M. Whitesides, J.P. Mathias and C.T. Seto, *Science,* **1991**, 39-1319.
26 R.E. Gillard, F.M. Raymo and J.F. Stoddart, *Chem. Eur. J.,* **1997**, *3*, 1933-1940.
27 J.W. Steed and J.L. Atwood, *Supramolecular chemistry,* 2nd edition, Wiley, Chichester, UK, **2009**.
28 A. Wei, *Chem. Commun.,* **2006**, 1581-1591.
29 J.L. Atwood, L.J. Barbour, M.J. Hardie and C.L. Raston, *Coord. Chem. Rev.,* **2001**, *222*, 3-32.
30 F. Perret, A.N. Lazar and A.W. Coleman, *Chem. Commun.,* **2006**, 2425-2438.

31 A.W. Coleman, F. Perret, A. Moussa, M. Dupin, Y. Guo and H. Perron, *Top. Curr. Chem.*, **2007**, *277*, 31-88.
32 F. Perret and A.W. Coleman, *Chem. Commun.*, **2011**, *47*, 7303-7319.
33 H. Konishi, T. Nakamura, K. Ohata, K. Kobayashi and O. Morikawa, *Tetrahedron Lett.*, **1996**, *37*, 7383-7386.
34 B.W. Purse, A. Shivanyuk and J. Rebek, *Chem. Commun.*, **2002**, 2612-2613.
35 M. Luostarinen, A. Åhman, M. Nissinen and K. Rissanen, *Supramol. Chem.*, **2004**, *16*, 505-512.
36 I. D'Acquarica, L. Nevola, G. Delle Monache, E. Gács-Baitz, C. Massera, F. Ugozzoli, G. Zappia and B. Botta, *Eur. J. Org. Chem.*, **2006**, 3652-3660.
37 C.D. Gutsche, R. Muthukrishnan and K.H. No, *Tetrahedron Lett.*, **1979**, 2213-2216.
38 C.D. Gutsche and R. Muthukrishnan, *J. Org. Chem.*, **1978**, *43*, 4905-4906.
39 L.M. Tunstad, J.A. Tucker, E. Dalcanale, J. Weiser, J.A. Bryant, J.C. Sherman, R.C. Helgeson, C.B. Knobler and D.J. Cram, *J. Org. Chem.*, **1989**, *54*, 1305-1312.
40 J.A. Bryant, C.B. Knobler and D.J. Cram, *J. Am. Chem. Soc.*, **1990**, *112*, 1254-1255.
41 G. Cometti, E. Dalcanale, A. Du vosel and A.M. Levelut, *J. Chem. Soc., Chem. Commun.*, **1990**, 163-165.
42 J.R. Fransen and P.J. Dutton, *Can. J. Chem.*, **1995**, *73*, 2217-2223.
43 A. Shivanyuk, E.F. Paulus, V. Böhmer and W. Vogt, *J. Org. Chem.*, **1998**, *63*, 6448-6449.
44 J.R. Moran, S. Karbach and D.J. Cram, *J. Am. Chem. Soc.*, **1982**, *104*, 5826-5828.
45 D.J. Cram, S. Karbach, H. Kim, C.B. Knobler, E.F. Maverick, J.L. Ericson and R.C. Helgeson, *J. Am. Chem. Soc.*, **1988**, *110*, 2229-2237.
46 O. Manabe, K. Asakura, T. Nishi and S. Shinkai, *Chem. Lett.*, **1990**, 1219-1222.
47 V.K. Jain and P.H. Kanaiya, *J. Inclusion Phenom. Macrocyclic Chem.*, **2008**, *62*, 111-115.
48 Y. Matsushita and T. Matsui, *Tetrahedron Lett.*, **1993**, *34*, 7433-7436.
49 T.N. Sorrell and F.C. Pigge, *J. Org. Chem.*, **1993**, *58*, 784-785.
50 A.G.S. Högberg, *J. Org. Chem.*, **1980**, *45*, 4498-4500.
51 Y. Aoyama, Y. Tanaka and S. Sugahara, *J. Am. Chem. Soc.*, **1989**, *111*, 5397-5404.
52 C.D. Gutsche and P.F. Pagoria, *J. Org. Chem.*, **1985**, *50*, 5795-5802.
53 P. Shahgaldian, A.W. Coleman and V.I. Kalchenko, *Tetrahedron Lett.*, **2001**, *42*, 577-579.
54 M.A. Tairov, M.O. Vysotsky, O.I. Kalchenko, V.V. Pirozhenko and V.I. Kalchenko, *J. Chem. Soc., Perkin Trans. 1*, **2002**, 1405-1411.
55 E. Houel, A. Lazar, E. Da Silva, A.W. Coleman, A. Solovyov, S. Cherenok and V.I. Kalchenko, *Langmuir*, **2002**, *18*, 1374-1379.
56 M. Conner, V. Janout and S.L. Regen, *J. Am. Chem. Soc.*, **1991**, *113*, 9670-9671.
57 E.U. Thoden van Velzen, J.F.J. Engbersen and D.N. Reinhoudt, *J. Am. Chem. Soc.*, **1994**, *116*, 3597-3598.
58 E.U. Thoden van Velzen, J.F.J. Engbersen and D.N. Reinhoudt, *Synthesis*, **1995**, 989-997.
59 G.G. Condorelli, A. Motta, M. Favazza, I.L. Fragala, M. Busi, E. Menozzi, E. Dalcanale and L. Cristofolini, *Langmuir*, **2006**, *22*, 11126-11133.
60 F. Davis, A.J. Lucke, K.A. Smith and C.J.M. Stirling, *Langmuir*, **1998**, *14*, 4180-4185.
61 H. Adams, F. Davis and C.J.M. Stirling, *J. Chem. Soc., Chem. Commun.*, **1994**, 2527-2529.
62 E. Menozzi, R. Pinalli, E.A. Speets, B.J. Ravoo, E. Dalcanale and D.N. Reinhoudt, *Chem. Eur. J.*, **2004**, *10*, 2199-2206.

63 A.G.S. Högberg, *J. Am. Chem. Soc.*, **1980**, *102*, 6046-6050.
64 L. Abis, E. Dalcanale, A. Du vosel and S. Spera, *J. Org. Chem.*, **1988**, *53*, 5475-5479.
65 L. Abis, E. Dalcanale, A. Du vosel and S. Spera, *J. Chem. Soc., Perkin Trans. 2*, **1990**, 2075-2080.
66 B. Ma and P. Coppens, *Chem. Commun.*, **2002**, 424-425.
67 P.J. Dijkstra, J.A.J. Brunink, K.E. Bugge, D.N. Reinhoudt, S. Harkema, R. Ungaro, F. Ugozzoli and E. Ghidini, *J. Am. Chem. Soc.*, **1989**, *111*, 7567-7575.
68 E. Ghidini, F. Ugozzoli, R. Ungaro, S. Harkema, A. Abu El-Fadl and D.N. Reinhoudt, *J. Am. Chem. Soc.*, **1990**, *112*, 6979-6985.
69 G. Barrett, M.A. McKervey, J.F. Malone, A. Walker, F. Arnaud-Neu, L. Guerra, M.J. Schwing-Weill, C.D. Gutsche and D.R. Stewart, *J. Chem. Soc., Perkin Trans. 2*, **1993**, 1475-1479.
70 A. Ikeda and S. Shinkai, *J. Am. Chem. Soc.*, **1994**, *116*, 3102-3110.
71 S. Kunsági-Máté, Z. Csók, K. Iwata, E. Szász and L. Kollár, *J. Phys. Chem. B*, **2011**, *115*, 3339-3343.
72 F. Sansone, M. Dudic, G. Donofrio, C. Rivetti, L. Baldini, A. Casnati, S. Cellai and R. Ungaro, *J. Am. Chem. Soc.*, **2006**, *128*, 14528-14536.
73 G.M.L. Consoli, G. Granata, D. Garozzo, T. Mecca and C. Geraci, *Tetrahedron Lett.*, **2007**, *48*, 7974-7977.
74 S. Houmadi, D. Coquière, L. Legrand, M.C. Fauré, M. Goldmann, O. Reinaud and S. Rémita, *Langmuir*, **2007**, *23*, 4849-4855.
75 M. Lee, S. Lee and L. Jiang, *J. Am. Chem. Soc.*, **2004**, *126*, 12724-12725.
76 B. Guan, M. Jiang, X. Yang, Q. Liang and Y. Chen, *Soft Matter*, **2008**, *4*, 1393-1395.
77 M.A. Markowitz, R. Bielski and S.L. Regen, *Langmuir*, **1989**, *5*, 276-278.
78 G. De Miguel, J.M. Pedrosa, M.T. Martín-Romero, E. Muñoz, T.H. Richardson and L. Camacho, *J. Phys. Chem. B*, **2005**, *109*, 3998-4006.
79 B. Huisman, F.C.J.M. van Veggel and D.N. Reinhoudt, *Pure Appl. Chem.*, **1998**, *70*, 1985-1992.
80 V.A. Azov, A. Beeby, M. Cacciarini, A.G. Cheetham, F. Diederich, M. Frei, J.K. Gimzewski, V. Gramlich, B. Hecht, B. Jaun, T. Latychevskaia, A. Lieb, Y. Lill, F. Marotti, A. Schlegel, R.R. Schlittler, P.J. Skinner, P. Seiler and Y. Yamakoshi, *Adv. Funct. Mater.*, **2006**, *16*, 147-156.
81 K. Suwinska, O. Shkurenko, C. Mbemba, A. Leydier, S. Jebors, A.W. Coleman, R. Matar and P. Falson, *New J. Chem.*, **2008**, *32*, 1988-1998.
82 C. Mbemba, K. Sigaud, F. Perret, K. Suwinska, O. Shkurenko and A.W. Coleman, *J. Inclusion Phenom. Macrocyclic Chem.*, **2008**, *61*, 29-40.
83 G.M.L. Consoli, G. Granata, R. Lo Nigro, G. Malandrino and C. Geraci, *Langmuir*, **2008**, *24*, 6194-6200.
84 D.T. Schühle, J. Schatz, S. Laurent, L. Vander Elst, R.N. Müller, M.C.A. Stuart and J.A. Peters, *Chem. Eur. J.*, **2009**, *15*, 3290-3296.
85 O. Hayashida, K. Mizuki, K. Akagi, A. Matsuo, T. Kanamori, T. Nakai, S. Sando and Y. Aoyama, *J. Am. Chem. Soc.*, **2003**, *125*, 594-601.
86 Y. Aoyama, *Chem. Eur. J.*, **2004**, *10*, 588-593.
87 I.S. Ryzhkina, T.N. Pashirova, W.D. Habicher, L.A. Kudryavtseva and A.I. Konovalov, *Macromol. Symp.*, **2004**, *210*, 41-48.
88 M. Kellermann, W. Bauer, A. Hirsch, B. Schade, K. Ludwig and C. Böttcher, *Angew. Chem. , Int. Ed.*, **2004**, *43*, 2959-2962.
89 Y. Chang, M. Kellermann, M. Becherer, A. Hirsch and C. Bohne, *Photochem. Photobiol. Sci.*, **2007**, *6*, 525-531.

90 I.S. Ryzhkina, K.M. Enikeev, A.P. Timosheva, T.N. Pashirova, S.S. Lukashenko, L.A. Kudryavtseva and A.I. Konovalov, *Russ. Chem. Bull.*, **2004**, *53*, 1528-1535.

91 I.S. Ryzhkina, A.P. Timosheva, A.V. Chernova, R.R. Shagidullin, A.A. Gazizova, W.D. Habicher, T. Krause, L.I. Vagapova and A.I. Konovalova, *Russ. Chem. Bull.*, **2007**, *56*, 475-483.

92 A.W. Coleman, A.N. Lazar and J.P.P. Renault, Supramolecular co-colloids obtained using polyanionic macrocyclic systems. *US Patent,* US 0292272, **2010**.

93 X. Yu, C. Tu, L. He, R. Wang, G. Sun, D. Yan and X. Zhu, *J. Macromol. Sci., Part A: Pure Appl. Chem.*, **2009**, *46*, 360-367.

94 Y. Tanaka, M. Mayachi and Y. Kobuke, *Angew. Chem., Int. Ed.*, **1999**, *38*, 504-506.

95 M. Strobel, K. Kita-Tokarczyk, A. Taubert, C. Vebert, P.A. Heiney, M. Chami and W. Meier, *Adv. Funct. Mater.*, **2006**, *16*, 252-259.

96 G.M.L. Consoli, F. Cunsolo, C. Geraci, T. Mecca and P. Neri, *Tetrahedron Lett.*, **2003**, *44*, 7467-7470.

97 G.M.L. Consoli, F. Cunsolo, C. Geraci and V. Sgarlata, *Org. Lett.*, **2004**, *6*, 4163-4166.

98 N. Micali, V. Villari, G.M.L. Consoli, F. Cunsolo and C. Geraci, *Phys. Rev. E,* **2006**, *73*, 051904-1-051904-8.

99 O. Sénèque, M. Rager, M. Giorgi and O. Reinaud, *J. Am. Chem. Soc.*, **2000**, *122*, 6183-6189.

100 D. Coquière, H. Cadeau, Y. Rondelez, M. Giorgi and O. Reinaud, *J. Org. Chem.*, **2006**, *71*, 4059-4065.

101 R.H. Müller, K. Mäder and S. Gohla, *Eur. J. Pharm. Biopharm.*, **2000**, *50*, 161-177.

102 R.H. Müller, M. Radtke and S.A. Wissing, *Adv. Drug Delivery Rev.*, **2002**, *54*, S131-S155.

103 P. Shahgaldian, M. Cesario, P. Goreloff and A.W. Coleman, *Chem. Commun.*, **2002**, 326-327.

104 P. Shahgaldian, M.A. Sciotti and U. Pieles, *Langmuir,* **2008**, *24*, 8522-8526.

105 J. Gualbert, P. Shahgaldian, A. Lazar and A.W. Coleman, *J. Inclusion Phenom. Macrocyclic Chem.*, **2004**, *48*, 37-44.

106 S. Ehrler, U. Pieles, A. Wirth-Heller and P. Shahgaldian, *Chem. Commun.*, **2007**, 2605-2607.

107 P. Shahgaldian, E. Da Silva, A.W. Coleman, B. Rather and M.J. Zaworotko, *Int. J. Pharm.*, **2003**, *253*, 23-38.

108 S. Jebors, A. Leydier, Q. Wu, B.B. Ghera, M. Malbouyre and A.W. Coleman, *J. Microencapsul.*, **2010**, *27*, 561-571.

109 A. Dubes, I.L. Moudrakovski, P. Shahgaldian, A.W. Coleman, C.I. Ratcliffe and J.A. Ripmeester, *J. Am. Chem. Soc.*, **2004**, *126*, 6236-6237.

110 J.L. Atwood, F. Hamada, K.D. Robinson, G.W. Orr and R.L. Vincent, *Nature,* **1991**, *349*, 683-684.

111 P. Shahgaldian, A.W. Coleman, S.S. Kuduva and M.J. Zaworotko, *Chem. Commun.*, **2005**, 1968-1970.

112 P. Shahgaldian, J. Gualbert, K. Aïssa and A.W. Coleman, *Eur. J. Pharm. Biopharm.*, **2003**, *55*, 181-184.

113 P. Shahgaldian, E. Da Silva and A.W. Coleman, *J. Inclusion Phenom. Macrocyclic Chem.*, **2003**, *46*, 175-177.

114 A.D. Martin, R.A. Boulos, K.A. Stubbs and C.L. Raston, *Chem. Commun.*, **2011**, *47*, 7329-7331.

115 Y. Sun, C. Yan, Y. Yao, Y. Han and M. Shen, *Adv. Funct. Mater.*, **2008**, *18*, 3981-3990.

116 Q. Liang, G. Chen, B. Guan and M. Jiang, *J. Mater. Chem.*, **2011**, *21*, 13262-13267.
117 M.A. Markowitz, R. Bielski and S.L. Regen, *J. Am. Chem. Soc.*, **1988**, *110*, 7545-7546.
118 M.A. Markowitz, V. Janout, D.G. Castner and S.L. Regen, *J. Am. Chem. Soc.*, **1989**, *111*, 8192-8200.
119 A.V. Nabok, A.K. Hassan, A.K. Ray, O. Omar and V.I. Kalchenko, *Sens. Actuators, B*, **1997**, *B45*, 115-121.
120 W.C. Moreira, P.J. Dutton and R. Aroca, *Langmuir*, **1995**, *11*, 3137-3144.
121 M.M. Daschbach, O.V. Kulikov, E.F. Long and G.W. Gokel, *Chem. Eur. J.*, **2011**, *17*, 8913-8921.
122 A.V. Nabok, N.V. Lavrik, Z.I. Kazantseva, B.A. Nesterenko, L.N. Markovskiy, V.I. Kalchenko and A.N. Shivaniuk, *Thin Solid Films*, **1995**, *259*, 244-247.
123 K. Ichimura, N. Fukushima, M. Fujimaki, S. Kawahara, Y. Matsuzawa, Y. Hayashi and K. Kudo, *Langmuir*, **1997**, *13*, 6780-6786.
124 M.W. Sugden, T.H. Richardson, F. Davis, S.P.J. Higson and C.F.J. Faul, *Colloids Surf. Physicochem. Eng. Aspects*, **2008**, *321*, 43-46.
125 A.K. Hassan, A.V. Nabok, A.K. Ray, A. Lucke, K. Smith, C.J.M. Stirling and F. Davis, *Mater. Sci. Eng., C*, **1999**, *8-9*, 251-255.
126 Y. Tanaka, Y. Kobuke and M. Sokabe, *Angew. Chem., Int. Ed. Engl.*, **1995**, *34*, 693-694.
127 I. Elidrisi, S. Negin, P.V. Bhatt, T. Govender, H.G. Kruger, G.W. Gokel and G.E.M. Maguire, *Org. Biomol. Chem.*, **2011**, *9*, 4498-4506.
128 O.A. Okunola, J.L. Seganish, K.J. Salimian, P.Y. Zavalij and J.T. Davis, *Tetrahedron*, **2007**, *63*, 10743-10750.
129 J.L. Seganish, P.V. Santacroce, K.J. Salimian, J.C. Fettinger, P. Zavalij and J.T. Davis, *Angew. Chem. , Int. Ed.*, **2006**, *45*, 3334-3338.
130 R. Lalor, H. Baillie-Johnson, C. Redshaw, S.E. Matthews and A. Mueller, *J. Am. Chem. Soc.*, **2008**, *130*, 2892-2893.
131 R. Lalor, J.L. DiGesso, A. Mueller and S.E. Matthews, *Chem. Commun.*, **2007**, 4907-4909.
132 R.V. Rodik, A.S. Klymchenko, N. Jain, S.I. Miroshnichenko, L. Richert, V.I. Kalchenko and Y. Mély, *Chem. Eur. J.*, **2011**, *17*, 5526-5538.
133 L. Nault, A. Cumbo, R.F. Pretôt, M.A. Sciotti and P. Shahgaldian, *Chem. Commun.*, **2010**, *46*, 5581-5583.
134 S. Zhang, F. Song and L. Echegoyen, *Eur. J. Org. Chem.*, **2004**, 2936-2943.
135 M. Oh, K. Kim, J. Lee, H. Chen and K. Koh, *Appl. Phys. Lett.*, **2006**, *89*, 251104/1-251104/3.
136 S. Zhang, A. Palkar and L. Echegoyen, *Langmuir*, **2006**, *22*, 10732-10738.
137 L. Baldini, M. Melegari, V. Bagnacani, A. Casnati, E. Dalcanale, F. Sansone and R. Ungaro, *J. Org. Chem.*, **2011**, *76*, 3720-3732.
138 F. Davis and C.J.M. Stirling, *Langmuir*, **1996**, *12*, 5365-5374.
139 K.D. Schierbaum, T. Weiss, E.U. Thoden van Velzen, J.F.J. Engbersen, D.N. Reinhoudt and W. Göpel, *Science*, **1994**, *265*, 1413-1415.
140 Z. Özbek, R. Çapan, H. Göktaş, S. Şen, F.G. İnce, M.E. Özel and F. Davis, *Sens. Actuators, B*, **2011**, *158*, 235-240.
141 A.F. Holloway, A. Nabok, A.A. Hashim and J. Penders, *Sens. Transducers J.*, **2010**, *113*, 71-81.
142 F. Maffei, P. Betti, D. Genovese, M. Montalti, L. Prodi, R. De Zorzi, S. Geremia and E. Dalcanale, *Angew. Chem. , Int. Ed.*, **2011**, *50*, 4654-4657.
143 S. Zhang and L. Echegoyen, *Org. Lett.*, **2004**, *6*, 791-794.

144 M.T. Cygan, G.E. Collins, T.D. Dunbar, D.L. Allara, C.G. Gibbs and C.D. Gutsche, *Anal. Chem.*, **1999**, *71*, 142-148.
145 J.D. Faull and V.K. Gupta, *Langmuir*, **2001**, *17*, 1470-1476.
146 J.D. Faull and V.K. Gupta, *Thin Solid Films,* **2003**, *440*, 129-137.
147 I.A. Koshets, Z.I. Kazantseva, Y.M. Shirshov, S.A. Cherenok and V.I. Kalchenko, *Sens. Actuators, B,* **2005**, *B106*, 177-181.
148 K. Kurihara, K. Ohto, Y. Tanaka, Y. Aoyama and T. Kunitake, *J. Am. Chem. Soc.*, **1991**, *113*, 444-450.
149 P. Shahgaldian, U. Pieles and M. Hegner, *Langmuir*, **2005**, *21*, 6503-6507.
150 R. Zadmard and T. Schrader, *J. Am. Chem. Soc.*, **2005**, *127*, 904-915.
151 S. Friedman, S. Kolusheva, R. Volinsky, L. Zeiri, T. Schrader and R. Jelinek, *Anal. Chem.*, **2008**, *80*, 7804-7811.
152 P. Prus, M. Pietraszkiewicz and R. Bilewicz, *Mater. Sci. Eng., C,* **2001**, *C18*, 157-159.
153 J.D. Faull and V.K. Gupta, *Langmuir*, **2002**, *18*, 6584-6592.
154 A. Wei, B. Kim, S.V. Pusztay, S.L. Tripp and R. Balasubramanian, *J. Inclusion Phenom. Macrocyclic Chem.*, **2001**, *41*, 83-86.
155 R. Balasubramanian, B. Kim, S.L. Tripp, X. Wang, M. Lieberman and A. Wei, *Langmuir,* **2002**, *18*, 3676-3681.
156 B. Kim, S.L. Tripp and A. Wei, *J. Am. Chem. Soc.*, **2001**, *123*, 7955-7956.
157 C. Tu, G. Li, Y. Shi, X. Yu, Y. Jiang, Q. Zhu, J. Liang, Y. Gao, D. Yan, J. Sun and X. Zhu, *Chem. Commun.*, **2009**, 3211-3213.
158 Y. Zhao, W. Pérez-Segarra, Q. Shi and A. Wei, *J. Am. Chem. Soc.*, **2005**, *127*, 7328-7329.
159 B. Guan, Q. Liang, Y. Zhu, M. Qiao, J. Zou and M. Jiang, *J. Mater. Chem.*, **2009**, *19*, 7610-7613.
160 Y. Sun, Y. Yao, C. Yan, Y. Han and M. Shen, *ACS Nano,* **2010**, *4*, 2129-2141.
161 M.J. McIldowie, M. Mocerino, B.W. Skelton and A.H. White, *Org. Lett.*, **2000**, *2*, 3869-3871.
162 K. Salorinne and M. Nissinen, *Org. Lett.*, **2006**, *8*, 5473-5476.
163 K. Salorinne, D.P. Weimann, C.A. Schalley and M. Nissinen, *Eur. J. Org. Chem.*, **2009**, 6151-6159.
164 A. Shivanyuk, T.P. Spaniol, K. Rissanen, E. Kolehmainen and V. Böhmer, *Angew. Chem., Int. Ed.*, **2000**, *39*, 3497-3500.
165 S. Nummelin, D. Falabu, A. Shivanyuk and K. Rissanen, *Org. Lett.*, **2004**, *6*, 2869-2872.
166 K. Salorinne and M. Nissinen, *Tetrahedron,* **2008**, *64*, 1798-1807.
167 K. Salorinne, O. Lopez-Acevedo, E. Nauha, H. Häkkinen and M. Nissinen, *CrystEngComm,* **2012**, *14*, 347-350.
168 K. Salorinne, E. Nauha and M. Nissinen, *Chem. Asian J.,* **2012**, DOI: 10.1002/asia.201100969.
169 M.J. Hynes, *J. Chem. Soc., Dalton Trans.*, **1993**, 311-312.
170 N. Ichieda, M. Kasuno, K. Banu, S. Kihara and H. Nakamatsu, *J. Phys. Chem. A,* **2003**, *107*, 7597-7603.
171 P. Van der Sluis and A.L. Spek, *Acta Crystallogr., Sect. A: Found. Crystallogr.*, **1990**, *A46*, 194-201.
172 K. Salorinne and M. Nissinen, *CrystEngComm,* **2009**, *11*, 1572-1578.
173 R.D. Shannon, *Acta Crystallogr., Sect. A,* **1976**, *A32*, 751-767.
174 H.M. Rietveld, *J. Appl. Crystallogr.*, **1969**, *2*, 65-71.
175 G. Zhao and S.E. Stevens Jr, *BioMetals,* **1998**, *11*, 27-32.
176 R.W. Ramette and E.B. Sandell, *J. Am. Chem. Soc.*, **1956**, *78*, 4872-4878.

177 U.K.A. Klein and F.W. Hafner, *Chem. Phys. Lett.*, **1976**, *43*, 141-145.
178 I. Rosenthal, P. Peretz and K.A. Muszkat, *J. Phys. Chem.*, **1979**, *83*, 350-353.
179 D.A. Hinckley, P.G. Seybold and D.P. Borris, *Spectrochim. Acta, Part A*, **1986**, *42A*, 747-754.
180 D.A. Hinckley and P.G. Seybold, *Spectrochim. Acta, Part A*, **1988**, *44A*, 1053-1059.

APPENDIX

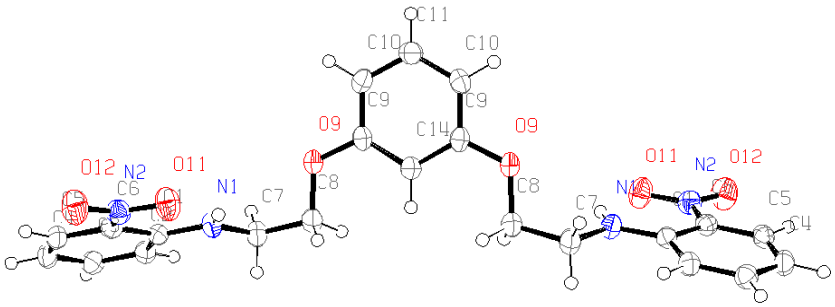

1,3-bis-2-(*N*-(2-nitrophenyl)-amino)-ethoxy benzene **99**

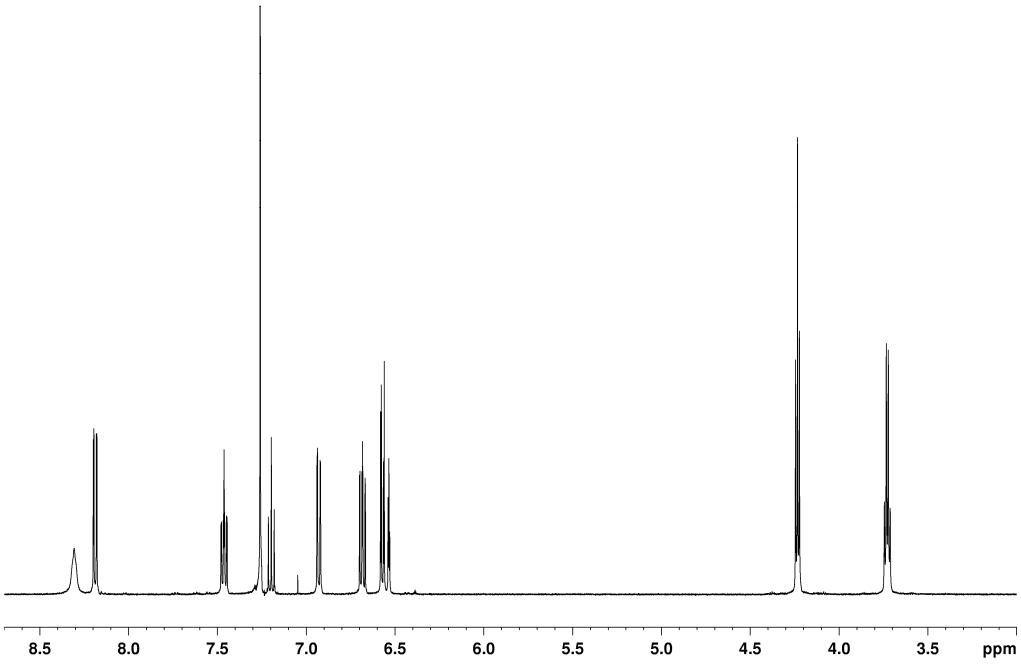

^{1}H NMR spectra of **99** at 500 MHz in $CDCl_3$ at 30 °C

ORIGINAL PAPERS

I

Self-assembly of amphiphilic calixarenes and resorcinarenes in water

by

Kaisa Helttunen and Patrick Shahgaldian, 2010

New. J. Chem. 34 (2010), 2704–2714, DOI: 10.1039/C0NJ00123F.

Self-assembly of amphiphilic calixarenes and resorcinarenes in water

Kaisa Helttunen[a] and Patrick Shahgaldian*[b]

Received (in Montpellier, France) 15th February 2010, Accepted 29th June 2010
DOI: 10.1039/c0nj00123f

The calixarenes and resorcinarenes are macrocyclic phenolic molecules that can be modified "*à façon*" and a wide range of chemical modification strategies have been published over the last 30 years. Because of their remarkable structural properties and their relative ease of chemical modification, they represent excellent and highly versatile bases to design complex building blocks capable of self-assembly and molecular recognition. They have been widely studied for their ability to form supramolecular structures targeting a wide range of applications. The possibility to regio(rim)-selectively modify these macrocycles with different polar and apolar moieties provides synthetic chemists with an unlimited range of possibilities for the design of complex amphiphiles with a high control over the position of the grafted moieties in the three dimensions. These amphiphiles have been shown to possess outstanding self-assembling and/or molecular recognition properties. This short review describes the developments of the chemistry of amphiphilic calixarenes and resorcinarenes with a clear focus on the synthetic paths used for their production and their self-assembly properties in water.

1. Introduction

1.1 Amphiphiles

Self-assemblies of amphiphiles, in addition to their tremendous theoretical interest, have found their place in the exponentially growing fields of drug delivery[1] and more recently of bio-nanotechnology.[2] Indeed, these assemblies give the possibility to encapsulate a pharmaceutically active compound in their core (or at their surface) and to cargo this compound to its therapeutic target.[3] This strategy presents the following advantages: (i) protection of the carried compound against degradation (*e.g.* enzymatic); (ii) possibility of controlled or triggered release; (iii) transport of the drug to its therapeutic target with the main benefit to decrease the doses given to the patient and therefore the possible side effects of these compounds.

In addition to a vast series of natural amphiphiles, a number of "engineered" synthetic amphiphiles have been designed. They include large molecules such as polymers[4] and peptides,[5] amphiphiles designed using a macrocyclic core such as cyclodextrins,[6] and crown-ethers,[7] to name but a few. An additional class of macrocycle that can serve as a basis to design amphiphiles are the calixarenes; the present review focuses on the use of calixarene (or resorcinarene) as an organizing basis

[a] *University of Jyväskylä, Nanoscience Center, Department of Chemistry, Jyväskylä FIN-40014, Finland. E-mail: kaisa.helttunen@jyu.fi*
[b] *University of Applied Science Northwestern Switzerland, Department of Chemistry and Bioanalytics, Gründenstrasse 40, 4132 Muttenz, Switzerland. E-mail: patrick.shahgaldian@fhnw.ch*

Kaisa Helttunen

Kaisa Helttunen was born in 1981 in Mikkeli, Finland. She received her master's degree in chemistry at master's programme in nanoscience from University of Jyväskylä, Finland, in 2006. She is currently pursuing a PhD in chemistry at University of Jyväskylä (Finland) under the supervision of Professor Maija Nissinen.

Patrick Shahgaldian

Patrick Shahgaldian graduated in Biochemistry at the University Claude Bernard Lyon I (France) in 2000; he obtained his PhD in 2002 working under the supervision of Dr Anthony W. Coleman at the Institute of Biology and Chemistry of Proteins in Lyon. In 2003, he joined the group of Prof. Hans-Joachim Güntherodt at the University of Basel as a post-doctoral fellow. In 2005, he moved to the group of Prof. Uwe Pieles at the University of Applied Sciences Northwestern Switzerland (FHNW) in Basel where he was appointed at the Senior Research Scientist level in 2007. His main scientific interests include the design of supramolecular nanomaterials possessing specific recognition or catalytic properties.

for the design of synthetic amphiphiles and the study of the self-assembly of these molecules in water.

1.2 Introducing calixarenes and resorcinarenes

Generalities. The historical origin of calixarenes and resorcinarenes might be attributed to Adolf von Baeyer and the results he reported in 1902 on the reaction of pyrogallol and resorcinol with aldehydes.[8] The development of calixarene chemistry has seen the involvement of a number of chemists over the 20th century such as Lederer and Manasse, Baeckeland, Zinke and Ziegler, to name but a few. The detailed history of the discovery of calixarenes has been described in detail elsewhere.[9] The modern age of calixarene chemistry certainly started with the understanding and rationalization of the synthetic procedures by Gutsche and Muthukrishnan in the late 1970s.[10] The 1980s have seen the emergence of supramolecular chemistry[11] as a field of modern chemical sciences and a proof of the recognition of this new field is the Nobel prize shared by Lehn,[12] Cram[13] and Pedersen[14] for their pioneering work in the field. Supramolecular chemistry aims at designing complex multi-molecular systems where all the components are held together by non-covalent interactions.[11] As these interactions are widespread in biological systems, supramolecular chemistry largely overlaps biomimetic chemistry and numbers of supramolecular architectures mimicking or inspired by natural systems have been developed.[15] In this context, the calixarenes, because of their outstanding structural properties, rapidly took a predominant position in the field.

Calix[*n*]arenes[16,17] are macrocyclic molecules produced by the base-catalyzed reaction of *para*-substituted phenols and formaldehyde; *n* refers to the number of phenolic units that form the macrocycle and depends on the synthetic conditions and the ionic template used for their synthesis, *cf*. Fig. 1. The most commonly studied calixarenes, certainly because of their ease of synthesis, are that composed of 4, 6 or 8 phenolic units; their chemical modifications have been widely studied and reviewed recently.[18] The resorcinarenes (also called resorcinolarenes or resorcarenes) are commonly produced by the Brønsted acid-catalyzed reaction of resorcinol and an aromatic or aliphatic aldehyde in the absence of template;[19] synthetic strategies based on Lewis acid-promoted condensation have also been reported, *cf*. Fig. 1.[20]

Synthetic strategy. The use of macrocyclic compounds as a basis to design synthetic amphiphiles is mainly driven by the possibility given by these molecules to act as organizing entities for introducing and orienting, in the same complex

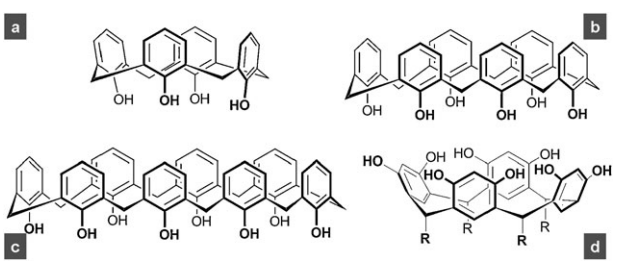

Fig. 1 Molecular formulas of calix[4]arene (a), calix[6]arene (b), calix[8]arene (c) and general formula of resorcinarenes (d).

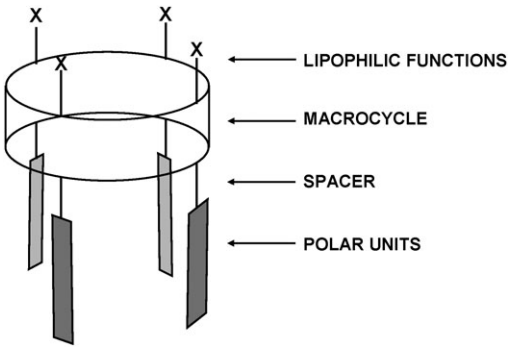

Fig. 2 Schematic representation of a macrocyclic amphiphile.

molecule, lipophilic and polar (molecular recognition) functions. Good candidates should exhibit, in addition to a relative conformational rigidity, the possibility to be chemically modified in a regio-selective fashion. The synthetic strategy may then be adapted in order to introduce on one rim of the macrocycle the needed lipophilic moieties and on the other rim the polar molecular recognition functions with or without spacing groups; a schematic representation is given in Fig. 2.

The calix[4]arenes, composed of four phenolic units, form a fairly rigid truncated cone-shaped molecule when adequately modified to "lock" the structure to avoid conformational changes to partial cone conformations.[16] In this molecule, the aromatic alcohol functions are exposed at the narrow rim, and the *para*-phenolic positions at the wide rim. Applying different chemistries, the macrocycle can be selectively modified either on one rim or the other. The regio-selectivity of the chemical modifications is not restricted to the selection of the modified rim, the number and the position within a rim could also be controlled.

The resorcinarenes, in addition to their rigid structure and the possibility to perform rim-selective modification, possess the advantage to exhibit, on the wide rim, sites of different chemical nature which may thus be differentially modified, giving the possibility to access more straightforwardly the molecules having on their polar side two different kinds of hydrophilic functions. Indeed, the native macrocycle, in addition to the 8 aromatic alcohol functions, can be also modified at the *ortho*-position in order to introduce up to 4 additional polar functions. A number of synthetic routes to amphiphilic calixarenes and resorcinarenes have been published and their self-assembly in water as liposomes, micelles and nanoparticles studied. The present manuscript will detail those three different classes of self-assembly; the formation of amphiphilic concentrated phases such as liquid crystalline phases will not be reviewed here.

2. Calixarene-based vesicles

The first report describing the possibility to form unilamellar vesicles with calixarenes has been published by Regen *et al*.[21] The self-assembly of the native calix[6]arene (unmodified on both rims) has been achieved by injecting a tetrahydrofuran (THF) solution of this macrocycle in water. Dynamic light scattering and transmission electron microscopy (TEM) revealed the monolamellar vesicular structure of the formed

objects with a broad size distribution ranging from 0.5 to 1 μm in diameter. Regarding resorcinarenes, the first report describing the possibility to self-assemble an amphiphilic derivative in water was published by Tanaka *et al.*[22] In this paper, it was described that a resorcinarene bearing C_{16} alkyl chains at the lower rim, previously shown to form ion channels when embedded in lipid bilayers,[23] has the ability to form vesicular systems in water. The self-assembly process used is fairly simple and similar to that used by Regen *et al.*[21] The amphiphile, dissolved in THF, was injected in a buffer at 60 °C which spontaneously led to the formation of a colloidal suspension. After removal of the organic solvent, the formed objects had been analyzed by negative staining TEM and atomic force microscopy (AFM). The results confirmed the unilamellar structure of the produced vesicles that, when dried on a surface, are flattening to form structures having a height of around 4 resorcinarene molecules (*ca.* 10 nm, 2 bilayers).

Lee *et al.* have demonstrated that a series of calix[4]arenes, bearing aliphatic (C_{10}) chains at the lower rim and tertiary amino-alcohol functions at the upper rim, possess amphiphilic self-assembly properties in water.[24] The modification of the parent calix[4]arene has been carried out as follows: (i) alkylation of the lower rim in basic conditions; (ii) chloromethylation of the *para*-positions; (iii) nucleophilic substitution of the chlorine by an amino alcohol, *cf.* Fig. 3.

The self-assembly of these amphiphiles in water had been studied by photon correlation spectroscopy, scanning and transmission electron microscopy. The results showed that these amphiphiles can self-assemble into stable colloidal suspensions with a narrow size distribution and decreasing hydrodynamic diameter (D_H) with increasing the size of the hydrophobic moieties. Indeed, when R′ = H (**1a**), the vesicles have a D_H of 200 nm; while the amphiphiles with R′ = $(CH_2)_2OH$ (**1b**) and R′ = $(CH_2)_2O(CH_2)_2OH$ (**1c**) self-assemble in structures having D_H values of 36 and 6 nm, respectively. The evidence that **1a** and **1b** form vesicles was obtained from the contrast observed in TEM, *cf.* Fig. 4. Because of the small D_H measured for **1c** that corresponds to the double length of the amphiphile, the authors postulated on the micellar structure of the formed aggregates. Using calcein as a hydrophilic fluorescent tag encapsulated into the vesicles, it was demonstrated that the amphiphiles undergo a phase transition and the vesicles transform into micelles of smaller D_H.

Two calix[8]arenes bearing 8 propyl chains at the lower rim and 8 *N*-acetyl glucosamine functions at the upper rim have

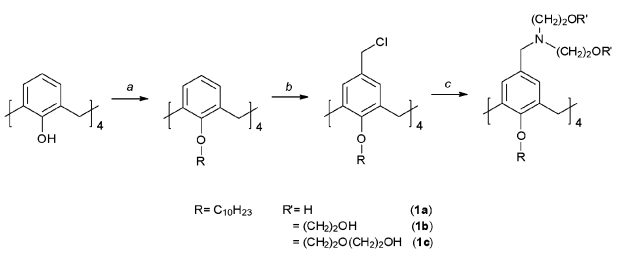

Fig. 3 Synthetic route to amino-alcohol-modified calix[4]arenes **1a**, **1b** and **1c** [a: *n*-$C_{10}H_{23}Br$, NaH; b: $ClCH_2OC_8H_{17}$, $SnCl_4$, c: Na_2CO_3, Bu_4NI, $(R'O(CH_2)_2)_2NH$].

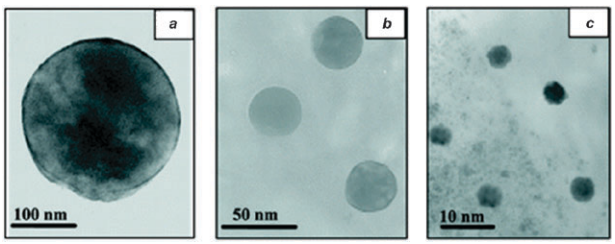

Fig. 4 TEM images of *p*-amino-alcohol-modified calix[4]arenes self-assembled in water (a: **1a**, b: **1b** and c: **1c**, as described in Fig. 3). [Reproduced with permission from ref. 24. Copyright 2004, the American Chemical Society.]

been synthesized,[25] *cf.* Fig. 5. The synthetic route followed consists of an *ipso*-nitration of the *O*-alkylated *p-tert*-butyl-calix[8]arene and the catalytic reduction of the *para*-nitro functions to yield the *para*-amino derivative that can be further modified to introduce the *N*-actetyl glucosamine units on the upper rim of the macrocycle. The produced molecules have been shown to form vesicles at neutral and basic pH. Interestingly, these assemblies are undergoing a vesicle-to-micelle phase transition at acidic pH. This phenomenon was attributed to the protonation of the polar groups of the amphiphiles and the changes of surface charge density.[26]

Reinaud and co-workers have produced[27–29] and studied the self-assembly in water of a calix[6]arene functionalized at the lower rim with three imidazolyl moieties and at the upper rim with sulfonato groups.[30] The synthesis was achieved by first alkylating the lower rim of the macrocycle at three alternate positions following the procedure described by Janssen *et al.*[28] The modification of the three remaining phenolic functions had been carried out using sodium hydride as basis and 2-chloromethyl-1-methyl-1*H*-imidazole hydrochloride.[29] The *ipso*-substitution of the positions in *para* of the methylated

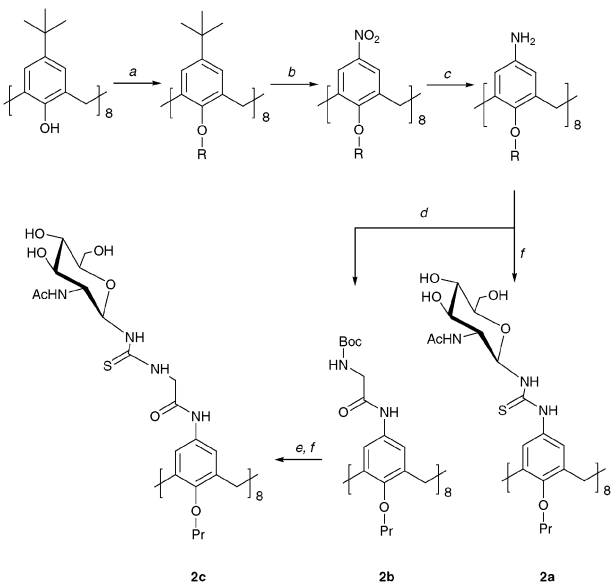

Fig. 5 Synthetic route to *N*-acetyl-glucosamine-bearing-calix[8]-arenes **2a**, **2b** and **2c** (a: NaH, *n*PrI; b: HNO_3, AcOH; c: Pd/C, H_2; d: *N*-Boc-Gly; e: TFA, f: sugar-NCS).[25]

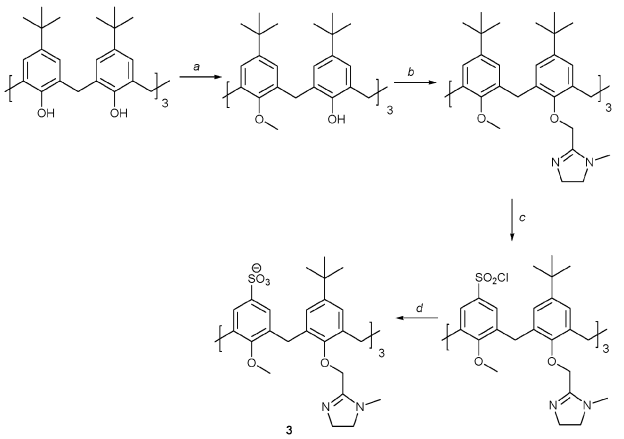

Fig. 6 Synthetic route to imidazolyl-sulfonato-calix[6]arenes, **3** (a: K_2CO_3, MeI; b: NaH, 2-chloromethyl-1-methyl-1*H*-imidazole, c: $ClSO_2OH$; d: TRIS).

phenols had been carried out using chlorosulfonyl acid, *cf*. Fig. 6.

In addition to their properties of biomimetic receptors for neutral molecules, it has been demonstrated that this macrocycle, even if it does not have a "typical" amphiphilic structure, does self-assemble as fairly polydisperse multilamellar vesicles. Ultrasonic treatment of this colloidal suspension has been shown to cause a diminution not only of the size of these assemblies but also of the polydispersity of the suspension. It has also been demonstrated that while decreasing the pH, monodisperse small vesicles are produced, an increase of pH causes the formation of giant vesicles (450 nm). The presence of silver ions drastically affects the self-assembly process causing the formation of micelles. This was attributed to the fact that the complexation with silver ions causes a conformational change of the calixarene which has a more pronounced conical shape and therefore is more prone to form micellar than layered systems, as schematized in Fig. 7.

Calix[4]arenes, modified at the upper rim with carboxy-functions, have been shown to form vesicles in water; interestingly at high concentrations they form layered lyotropic liquid crystalline phases.[31] A calix[4]arene, modified with perfluoro-alkyl chains, has also been shown to form vesicles in water while forming fiber-like structures in methanol.[32]

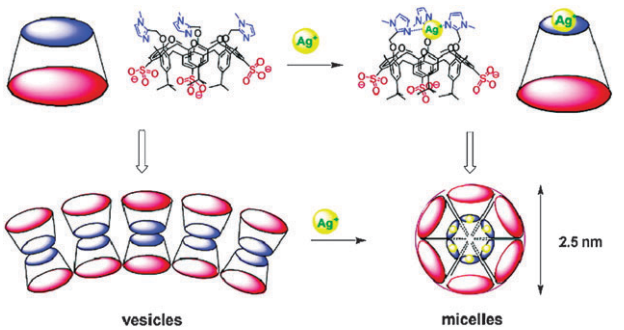

Fig. 7 Schematic representation of the effect of silver ions on the self-assembly of an imidazolyl-modified calix[6]arene. [Reproduced with permission from ref. 30. Copyright 2007, the American Chemical Society.]

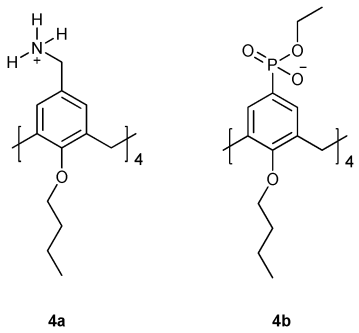

4a **4b**

Fig. 8 Methylammonium (**4a**) and phosphonate (**4b**) modified calixarenes.

The group of Schräder has developed a series of charged calixarene bearing phosphonate (**4a**) or methylammonium (**4b**) groups. It has been shown that these receptors, when embedded in membranes, have the ability to form a "charge imprint" of the target proteins, *cf*. Fig. 8.[33] Using a similar approach but embedding the calixarenes in vesicles comprising phospholipids and a chromatic polydiacetylene polymer, it has been demonstrated that micromolar protein concentrations cause a specific colorimetric response.

3. Micelles

The self-assembly of amphiphilic molecules into micellar structures in aqueous solution is a spontaneous dynamic process which is usually described to occur when the concentration of the amphiphile reaches the critical micelle concentration (CMC). The conditions of self-assembly are controlled by several parameters in which the conical shape of the amphiphile is considered as a prerequisite for forming small spherical micelles. Calixarenes offer intriguing synthetic possibilities for achieving this condition, which has been demonstrated for instance by functionalizing monoalkylated calix[4]arenes with hydrophilic groups by Coleman *et al*.[34] A possible synthetic route to mono-alkylated aminomethyl (**5a**) and carboxymethyl (**5b**) calixarenes is given in Fig. 9. A systematic study of the effect of alkyl chain length and

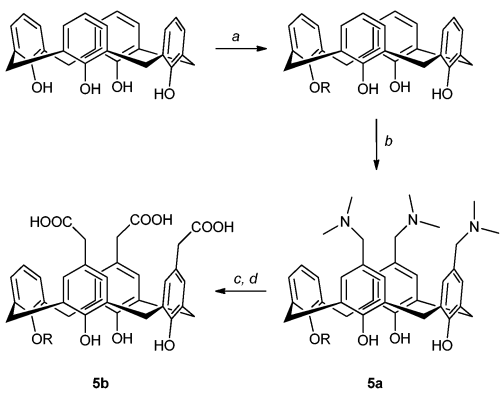

5b **5a**

Fig. 9 Synthesis of monoalkylated calix[4]arene amphiphiles with dimethylaminomethyl (**5a**) and carboxymethyl (**5b**) functionalities, R = CH_3, C_2H_5, C_3H_7, C_4H_9, C_5H_{11}, C_6H_{13}, C_7H_{15}, C_8H_{17}, C_9H_{19}, $C_{10}H_{21}$, $C_{12}H_{25}$; a: K_2CO_3, RI, or CsF, RI; b: $NH(CH_3)_2$, CH_3COOH, HCHO; c: CH_3I; d: KOH.[34]

hydrophilic group on the aggregation properties of the amphiphiles in water revealed that all the calixarene amphiphiles bearing carboxylic acid groups studied form small micelles at physiological pH (*i.e.* 6–8) with CMC values depending on the alkyl chain length—for dodecyl group the value was identical to that of a common surfactant dodecylmaltoside, 0.1 μM. In contrast, for amphiphiles containing less polar aminogroups the micellization does not follow a similar trend.

Water-solubility can be conferred to the calixarenes and resorcinarenes by attaching polar groups to the molecules, which is an appealing approach since it might simultaneously confer the macrocycle the ability to interact with biomolecules and therefore to show a biological activity.[35,36] Amphiphilic calix[4]arenes with four 2′-deoxythymidine or 2′-deoxyadenosine groups were synthesized by linking four phosphoramidite activated nucleotides at the calix[4]arene lower rim (*cf.* Fig. 10) and these molecules were shown to inhibit *in vitro* DNA replication.[37] In aqueous solution, these molecules self-assemble as dimers, which aggregate into micellar structures with D_H of 3.8 and 3.9 nm, respectively.[38] Adenine bases show stronger π-stacking interactions which lead to lower CMC value of **6b**, 0.22 mM compared to 0.51 mM of the thymine functionalized amphiphile **6a**. In the solid state, only **6b** forms spherical well defined aggregates of 700 nm diameter whereas **6a** tends to form smaller clusters which assemble into grapelike superstructures, as observed by SEM.

Multistep synthesis, starting from hydroxy group alkylation of undecyl resorcinarene to produce resorcinarene octaamines which further reacted with maltooligosaccharide lactones, yields amphiphilic resorcinarenes with eight oligosaccharide groups attached at the upper rim with amide linkages, as shown in Fig. 11.[39] The so-produced oligosaccharide conjugates do not show surfactant properties when surface tension is considered but they aggregate in micellar structures in water which is a clear indication of their amphiphilic nature.

In addition, the apparently huge oligosaccharide part with 16–56 glucose residues strongly promotes the formation of

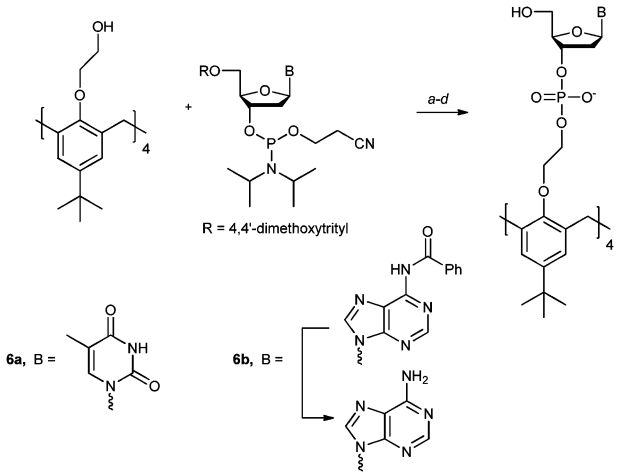

Fig. 10 Synthetic conditions for preparing calixarene nucleotide conjugates starting from *p*-(*tert*-butyl)-*O*-(2-hydroxyethyl) calix[4]arene and protected 2′-deoxynucleoside phosphoramidite; a: tetrazole; b: I_2; c: 30% NH_4OH, pyridine; d: 30% CH_3COOH. Adenosine base (**6b**) is protected with benzoyl group in the starting material.[37]

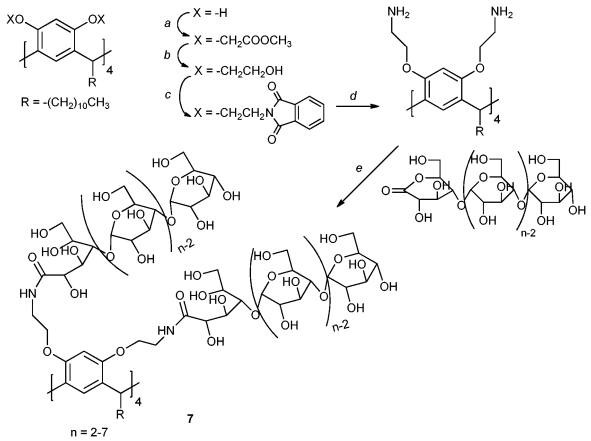

Fig. 11 Synthetic strategy leading to resorcinarene oligosaccharide conjugates; a: $BrCH_2CO_2CH_3$, K_2CO_3, acetone; b: $LiAlH_4$, THF; c: phthalimide, diethyl azodicarboxylate (DEAD), PPh_3, THF; d: $NH_2NH_2{\cdot}H_2O$, THF/EtOH; e: MeOH or MeOH/ethylene glycol.[39]

small micelles consisting of 4–6 molecules instead of lamellar assemblies. The formation of micelles cannot be explained by hydrophobic driving forces alone, since the micelle formation is found to be irreversible and the aggregates are not dissociating into monomers, but interactions between oligosaccharide moieties must also play a role. Phosphate ions promote agglutination of the micelles which indicates that this anion is effectively hydrogen bonded by the oligosaccharide moieties (Fig. 12). The glycosaccharide micelles and their interaction with DNA to form "artificial viruses" have been reviewed elsewhere.[40]

Careful adjustment of the polarity of both the amphiphile and the environment can offer control over the aggregation and micelle formation as observed in systematic experiments conducted with resorcinarenes bearing carboxymethyl (**8**), 2-hydroxyethyl (**9**), methylamino acetal (**10**) or dialkylamino groups (**11–19**) in chloroform and 1,4-dioxane where they form inverted micelles (Fig. 13).[41,42] In addition, mixed micellization of tris(hydroxymethyl)amide resorcinarene with a common cationic surfactant cetyl trimethylammonium bromide has been shown to increase the catalytic activity of the micelles of hydrolysis of phosphoric ester in water when compared to a pure resorcinarene amphiphile (Fig. 14).[43]

Even though aggregation might be considered as a purely random and anarchic way of forming polydispersed material, scientists have recently put a lot of effort in attempts to control the aggregation of many interesting amphiphilic compounds in

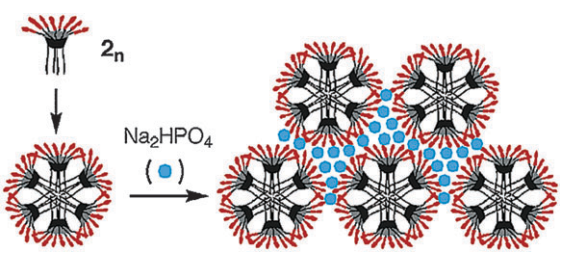

Fig. 12 Schematic representation of the self-assembly and phosphate induced agglutination of amphiphilic resorcinarene oligosaccharide conjugates.[39] [Reproduced with permission from ref. 39. Copyright 2003, the American Chemical Society.]

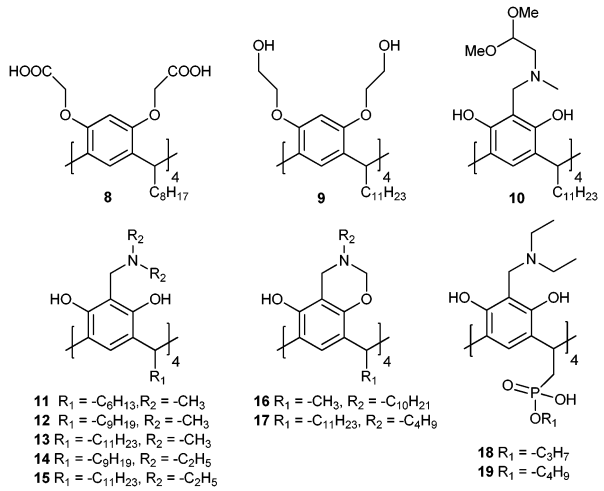

Fig. 13 Structures of amphiphilic resorcinarenes **8–19**.[42–44]

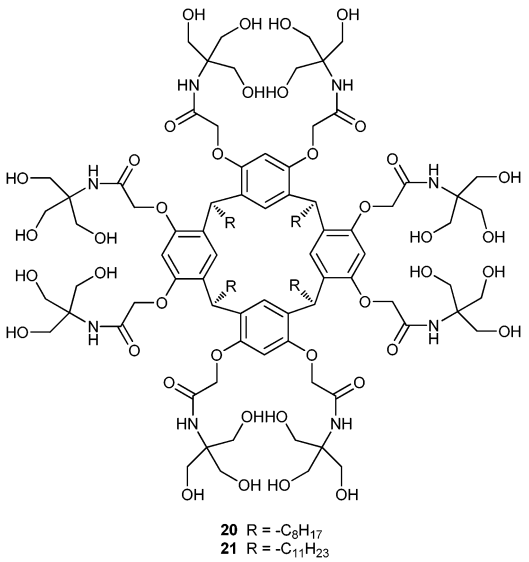

Fig. 14 Tris(hydroxymethyl)amide resorcinarene, **20** and **21**.[43]

order to fully exploit their potential. Aggregation of calix[4]-arene gadolinium chelate conjugates (Fig. 15) into micelles with a hydrodynamic radius of 2.2 nm has a remarkable consequence in improving their properties as a MRI contrast

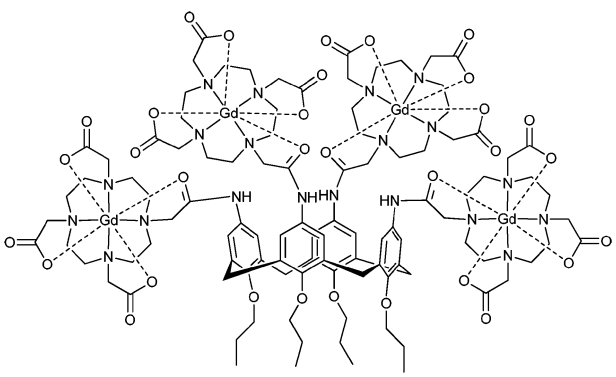

Fig. 15 Structure of calix[4]arene Gd–DOTA conjugate, DOTA = 1,4,7,10-tetra(carboxymethyl)-1,4,7,10-tetraazacyclododecane, **22**.[45]

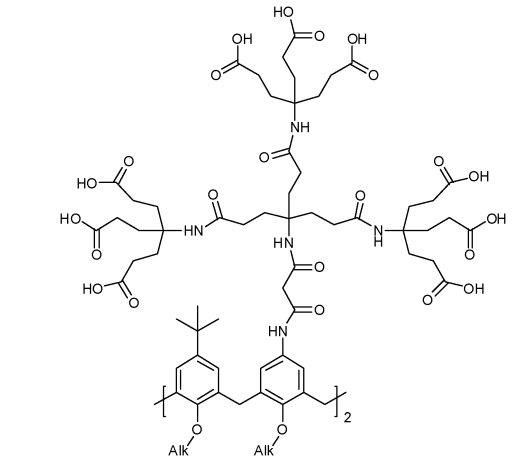

Fig. 16 Structure of amphiphilic dendrocalixarene, **23**.[46]

agent when compared to the monomer.[45] In MRI imaging, the toxic gadolinium must be strongly chelated to prevent its release in the body and therefore the chelator also has an effect on the performance of the substance. In the current study, relaxivity of 18.3 s^{-1} per mM Gd at 37 °C and 20 MHz was obtained for Gd bound to micelles, about twice as much when compared to the monomer.

Another example of micelles forming calixarenes with perfect structural uniformity is presented by the self-assembly of seven subunits of dendrocalixarene (Fig. 16) in aqueous solution into robust and uniform micelles.[46] The structure of the micelles was determined at 12 Å resolution by cryo-TEM and 3D-reconstruction, *cf.* Fig. 17. The interior of these micelles was then probed using pyrene labels for time resolved spectroscopy experiments.[47] The results showed how hydrophobic guest molecule can experience environments inside the micelle, *i.e.* the aromatic part of calixarene macrocycle in addition to the hydrophobic tails. However, calixarene does not quench the pyrene fluorescence as efficiently as 2,6-dimethylanisole, which was used as a model for the calixarene

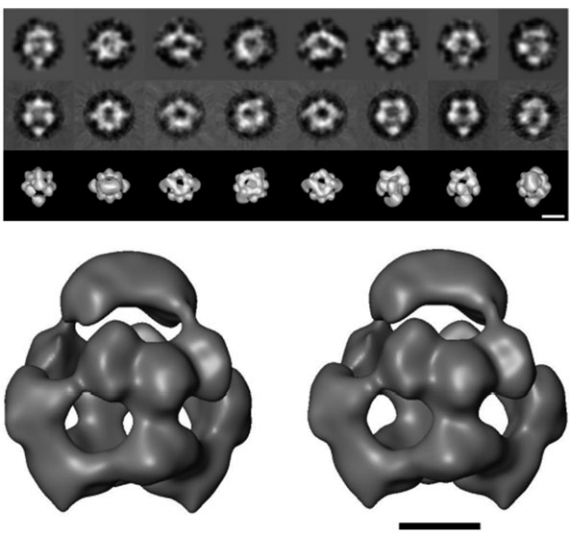

Fig. 17 Electron micrograph of dendrocalixarene micelles; reprojections.[46]

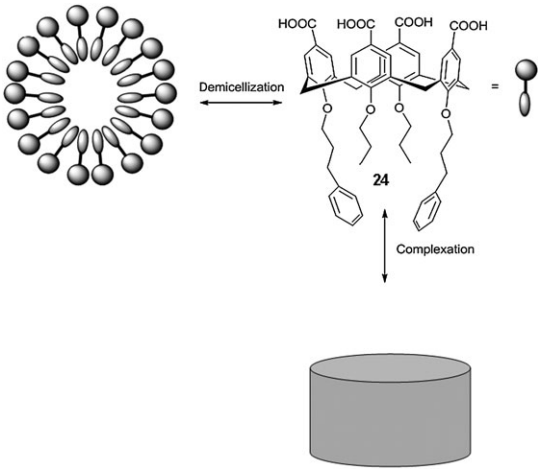

Fig. 18 Demicellization and complexation of calixarenes with γ-cyclodextrin.[48]

walls but rather protects the embedded fluorophore from the quenchers present in the solution. In this study, the CMC of the amphiphiles was found to be only 40 μM, which is 200 times less than for sodium dodecyl sulfate.

Formation of host–guest inclusion complexes in the presence of aggregates has been investigated using calix[4]arene bearing carboxylate groups and cyclodextrins in aqueous solution.[48] Fig. 18 shows a schematic representation of the complexation, where demicellization precedes the 1 : 1 complexation. The study revealed that initial micellization of the amphiphilic calixarenes (guest) did not disturb the inclusion complexation of phenyl groups of the guest inside γ-cyclodextrin cavity, and therefore equilibrium constants for the system could be determined reliably using isothermal titration calorimetry (ITC).

Calixarenes and resorcinarenes can be utilized as building blocks for true supramolecular amphiphiles, *i.e.* the hydrophobic and hydrophilic parts of the supramolecule are linked through weak force interactions.[49,50] Yu *et al.* demonstrated that a hydrophilic calix[4]arene PEG-conjugate forms an inclusion complex with hydrophobic phenyl palmitate (guest), which further assembles in water into vesicles, micelles or network like structure,[49] *cf.* Fig. 19. The elegance of this system lies in the simple way of controlling the equilibrium between each species by changing the ratio of hydrophobic and hydrophilic counterparts in the system. Increasing the amount of hydrophobic guest changes the equilibrium from vesicles with a diameter of 270 nm to micellar species with a diameter of 130 nm at the 1 : 1 ratio and finally the excess of guest leads to the formation of network aggregates.

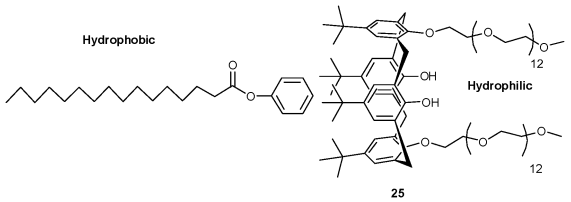

Fig. 19 Structure of a supramolecular amphiphile formed by inclusion complex of calix[4]arene PEG-conjugate and phenyl palmitate.[15]

4. Nanoparticles

The first calix-arene-based solid lipid nanoparticle systems were developed by one of us in the group of Anthony W. Coleman. Using a method pretty similar to that used by Tanaka *et al.* for producing resorcinarene-based liposomes,[22] and inspired from the work done in the group with amphiphilic cyclodextrins,[51] the self-assembly of a series of *p*-acyl-calixarenes in water was studied.[52] Briefly, the preparation method consists of adding water into a solution of the amphiphile dissolved in THF, to keep the formed suspension under stirring for a short time (typically 1 min) and to evaporate the organic solvent under reduced pressure.[53] The AFM studies[52] of these nanoparticles revealed some clear differences with the behaviour of the resorcinarene liposomes described by Tanaka *et al.*[22] Liposomes, when dried on a surface, either collapse to form supported bilayers[54] or get significantly flattened (down to the length of four constitutive amphiphiles in the case of unilamellar liposomes). For the studied systems, not a drastic flattening was observed and the particles revealed a very high stability over time. Indeed, AFM imaging on samples prepared for more than 12 months did not show any difference with the initial images of the fresh samples. From these considerations was postulated a non-lamellar structure of these systems that were then classified as nanoparticles. Additional ^{129}Xe NMR brought additional insights on the structure of these self-assemblies.[55] Having produced a series of *p*-acylated calix[4]arenes as analogues of natural phospholipids modified regioselectively at the lower rim with two phospho-ester groups,[56] it was demonstrated that all these amphiphiles have the ability to self-assemble as stable nanoparticles, *cf.* Fig. 20.

p-Acyl calixarenes have shown remarkable characteristics including high temporal and physical stability,[53] no hemolytic activity,[57] no aggregation in contact with serum albumin,[58] possibility of freeze-drying[59] or possibility of integration in gels used for formulation of topical creams.[60] This work has been recently summarized in a review article and will not be

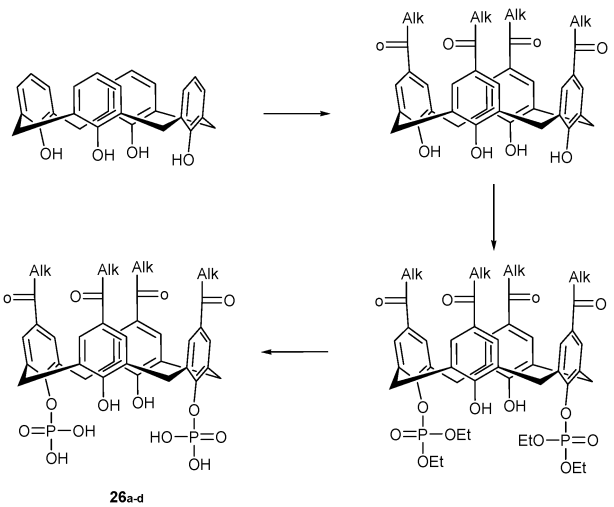

Fig. 20 Synthetic route to *p*-acyl-phospho-calixarenes **26a–d** (a: AlkCOCl, $AlCl_3$; b: $ClPO(OEt)_2$, Et_3N; c: (1) $BrSiMe_3$, (2) MeOH; Alk = $CH_3(CH_2)_n$, n = 5, 7, 9, 11).

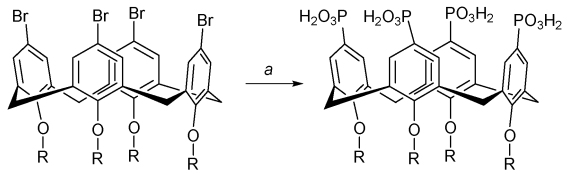

Fig. 21 Synthetic route to *p*-phospho-calix[4]arenes (a: (1) $PO(OiPr_3)$, $NiBr_2$, (2) Me_3SIBr).[62]

detailed here.[61] In a similar approach, the self-assembly of *p*-phospho-calix[4]arenes in water has been studied. Produced by the reaction of the *p*-bromoalkoxycalix[4]arenes with tri-isopropyl phosphite in the presence of $NiBr_2$ and consecutive deprotection with bromotrimethylsilane and methanol, these amphiphiles have been shown to self-assemble as nanoparticles, *cf.* Fig. 21.[62]

This self-assembly method has been expanded to a series of other calixarenes and resorcinarenes. For instance, a synthetic route to a chiral prolyl-bearing resorcinarene has been developed (Fig. 22). In addition to the proof of the chiral recognition properties of these molecules when self-assembled as Langmuir monolayer at the air–water interface *via* the formation of a ternary complex with Cu^{2+} ions,[63] we demonstrated that these molecules self-assemble as stable solid lipid nanoparticles.[64] We have also shown that the formed SLNs can be further modified, using a typical aqueous amide coupling procedure using *N*-hydroxysuccinimide (NHS) and a water soluble carbodiimide (1-ethyl-3-(3-dimethylaminopropyl)-carbodiimide), at their surface with proteins. The integrity of the nanoparticles has been demonstrated by PCS. The *native* state of the protein at the surface of the SLNs has been shown by showing the ability of an antigene directed against this protein to recognize these proteo-SLNs, as demonstrated by surface plasmon resonance experiments.

The high stability of these nanoparticles also allowed us to image them without any further treatment to stabilize the SLNs by means of SEM, *cf.* Fig. 23.

The interest of calixarenes for biomedical applications[35] has shown rapid development during the past decade for applications including anti-viral,[65] anti-thrombotic activities,[66] enzyme inhibition[67] and protein complexation.[68] The first report on the interaction of calixarenes with nucleic acids dates back to 1999 when Shi and Schneider published the synthesis of four different calixarenes bearing (trimethylammonium)-methyl groups at the upper rim of the macrocycle.[69] It was demonstrated

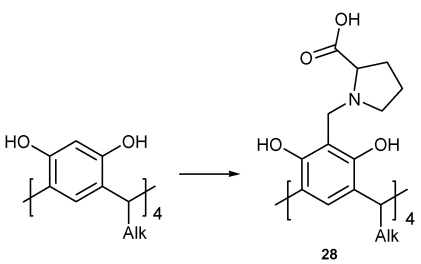

Fig. 22 Synthetic route to prolyl-modified resorcinarenes (HCHO, L-Pro).

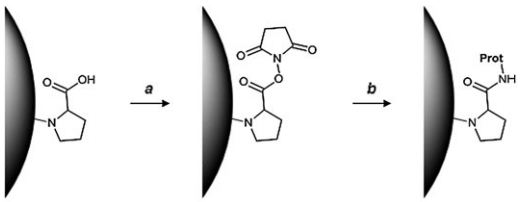

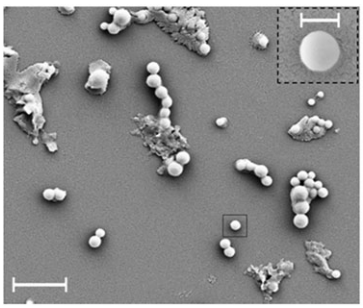

Fig. 23 Chemical modification of prolyl-bearing calix[4]arenes SLNs with serum albumin (top) and scanning electron micrograph of these SLNs spread on a mica surface at a pressure of 10^{-5} Pa (a: 1-ethyl-3-(3-dimethylaminopropyl) carbodiimide, *N*-hydroxysuccinimide; b: bovine serum albumin).

that the two calix[4]arene derivatives produced show greater binding properties than linear polyamines (*e.g.* spermine) which also bear 4 amino functions, suggesting that the interaction was improved by a cooperative effect of the amine groups.[69] Based on these findings and the recent results published by Ungaro *et al.* on the possibility to compact DNA with cationic calixarenes,[70] the self-assembly properties of a polycationic calixarenes, 5,11,17,23-tetramino-25,26,27,28-tetradodecyl-oxycalix[4]arene, at the air–water interface and in water have been studied. The results revealed the ability of these molecules to interact with DNA not only when self-assembled at the air–water interface but also in the form of SLNs.[71] With the ambition to use these systems to cargo DNA for therapeutic purposes, a solution was needed to avoid the exposure of the DNA molecules at the surface of the SLNs to nucleases attacks. It was decided to wrap the DNA with an additional polyelectrolyte (chitosan) layer bound to the DNA *via* electrostatic interactions, this positively charged layer gives the possibility to add, *via* an iterative process, additional layers of DNA, as schematized in Fig. 24.[72] This approach, also known as layer-by-layer (LBL) assembly,[73] additionally allows a significant increase of the quantity of DNA loaded at the surface of the carrier; the choice of the polyelectrolyte used might also favor the uptake of the colloidal particles in the cells. It was demonstrated for the first time the possibility to load calixarene-based SLNs *via* a layer-by-layer assembly

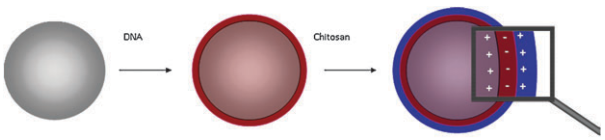

Fig. 24 Schematic representation of the LBL coating of amino-calixarenes.

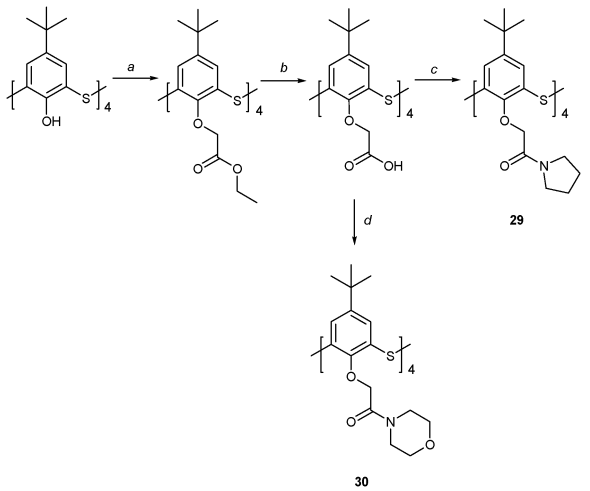

Fig. 25 Synthetic route to morpholine or pyrrolidine modified resorcinarenes; (a) LiOH, H_2O/THF, HCl; (b) $SOCl_2$, reflux; (c) pyrrolidine, RH, NEt_3, CH_2Cl_2, rt; (d) morpholine RH, NEt_3, CH_2Cl_2, rt [from ref. 74].

process and the ability of these systems to enter mammalian cells to release the DNA loaded at their surface.

Thiacalix[4]arenes bearing *p-tert*-butyl groups at the upper rim and functionalized at the lower rim with secondary amide groups have been studied for their ability to dimeric complexes and to recognize metal ions (Li^+, Na^+, K^+, Cs^+, Mg^{2+}, Ca^{2+}, Ba^{2+}, Al^{3+}, Pb^{2+}, Fe^{3+}, Co^{3+}, Ni^{2+}, Cu^{2+}, Ag^+, Cd^{2+}, Hg^{2+}) by the picrate extraction method and photon correlation spectroscopy. Whereas the extraction capabilities have been shown to be fairly poor, these molecules have been shown to form nanoparticulate assemblies in water (Fig. 25).

We have recently reported on the self-assembly of 5,11,17,23-tetra-carboxy-25,26,27,28-tetradodecyloxycalix[4]arene at the air–water interface as monomolecular Langmuir layers and in water.[75] It has been demonstrated that these monolayers have the ability to interact with salicylic acid, acetylsalicylic acid and acetaminophene. As mentioned above, Meier *et al.* demonstrated that this calix-arene has the ability to self-assemble as monomolecular vesicular structures in aqueous medium when dissolved in aqueous ammonia.[31] When using the nanoprecipitation method, the formed assemblies possess properties that suggest that they possess a nanoparticulate structure. Nevertheless, AFM investigations of this calixarene revealed the presence of layered structures coexisting with the nanoparticles at the surface of mica after drying, *cf.* Fig. 26.

Among the relevant number of examples of calix-arenes and forming nanoparticles, one example can be considered non-typical because the macrocycle used as a building block is not amphiphilic but hydrophobic. Indeed, it was demonstrated that *O*-dodecyl-calix[4]arene, even if it does not possess polar functions can self-assemble as fairly stable nanoparticles.[76] This observation might have led to the conclusion that these nanoparticles are formed only because of the insolubility of the lipophilic macrocycle in water. Nonetheless, a series of observation including the ability of this calix-arene to form Langmuir monolayers and that incapacity of the non-cyclic building block (dodecyl-phenol) to form neither Langmuir monolayers nor nanoparticles brought us to qualify this molecule as "pseudo-amphiphilic" (Fig. 27). In other word, the amphiphilic behaviour of this molecule is not due to the presence of polar function but to the capacity of the calix-arene macrocycle to interact with water.[77]

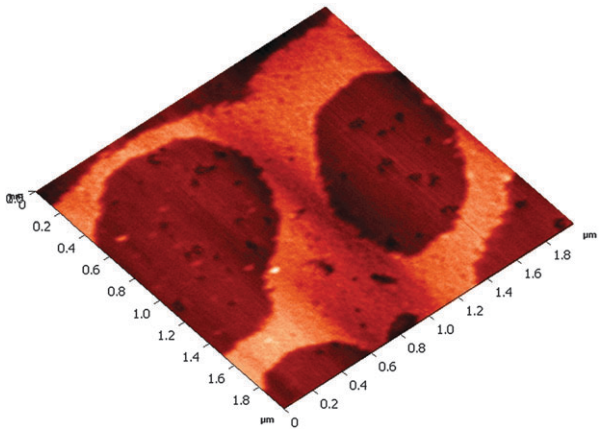

Fig. 26 Supported layer formed by 5,11,17,23-tetra-carboxy-25,26,27,28-tetradodecyloxycalix[4]arene on a mica surface imaged by non-contact AFM in air (2 × 2 µm scan range). [Reproduced with permission from *Chimia*.[75] Copyright 2010, the Swiss Chemical Society.]

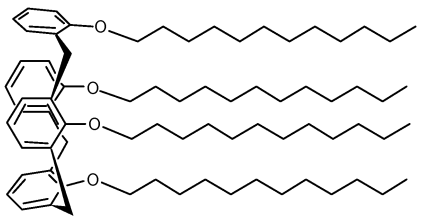

Fig. 27 Molecular formula of *O*-dodecyl-calix[4]arene shown to possess "pseudo-amphiphilic" properties.

5. Summary and outlook

Since the first proof of the possibility to self-assemble amphiphilic calixarenes in water, a relevant number of publications reported the ability of these systems to form self-assemblies in water. Nevertheless, compared to the wide amount of known calixarenes and resorcinarenes and the almost unlimited possibilities given by these macrocycles to design amphiphiles, one can realize that the amount of amphiphilic derivatives is still fairly limited. A more systematic approach of the structure/self-assembly property relations of a wider range of amphiphiles based on macrocyclic molecules might allow us to produce a set of general rules that would help to predict the self-assembly properties of this class of complex amphiphiles and thus allow a rational design of new amphiphiles possessing the desired properties.

As the foremost interest of producing synthetic amphiphilies is oriented toward the use of these self-assemblies for drug transport and targeting, one explanation of the limited amount of data available regarding amphiphilic calixarenes and resorcinarenes is the suspected toxicity of phenolic

compounds and their derivatives. Therefore, we believe that the development of new amphiphilic calixarenes should be accompanied by toxicity tests to definitely open the fertile ground that can represent the chemistry of self-assembled calixarenes and their applications.

Acknowledgements

KH wishes to thank the University of Jyväskylä and National Graduate School of Organic Chemistry and Chemical Biology for funding. PS acknowledges the financial support of the Swiss national science foundation (SNSF) and the Swiss innovation promotion agency (CTI).

Notes and references

1 A. Chonn and P. R. Cullis, *Adv. Drug Delivery Rev.*, 1998, **30**, 73–83; A. Samad, Y. Sultana and M. Aqil, *Curr. Drug Delivery*, 2007, **4**, 297; A. N. Lukyanov and V. P. Torchilin, *Adv. Drug Delivery Rev.*, 2004, **56**, 1273–1289; G. S. Kwon and T. Okano, *Adv. Drug Delivery Rev.*, 1996, **21**, 107–116; V. P. Torchilin, *Adv. Drug Delivery Rev.*, 2006, **58**, 1532–1555; J. E. Kipp, *Int. J. Pharm.*, 2004, **284**, 109–122.
2 D. S. Goodsell, *Bionanotechnology: lessons from nature*, Wiley-Liss, Hoboken, 2004; E. Gazit, *Plenty of Room for Biology at the Bottom: An Introduction to Bionanotechnology*, Imperial College Press, London, 2007; M. Ferrari, *Nat. Rev. Cancer*, 2005, **5**, 161–171.
3 R. B. Gupta and U. B. Kompella, *Nanoparticle Technology for Drug Delivery*, Taylor and Francis, New York, 2006; *Drug delivery: principles and applications*, ed. B. Wang, T. Siahaan and R. Soltero, John Wiley and sons, New York, 2005.
4 J. H. Park, S. Lee, J.-H. Kim, K. Park, K. Kim and I. C. Kwon, *Prog. Polym. Sci.*, 2008, **33**, 113–137; R. Haag and F. Kratz, *Angew. Chem., Int. Ed.*, 2006, **45**, 1198–1215; Y. Kakizawa and K. Kataoka, *Adv. Drug Delivery Rev.*, 2002, **54**, 203–222.
5 S. Cavalli, F. Albericio and A. Kros, *Chem. Soc. Rev.*, 2010, **39**, 241–263; C. R. Yamnitz and G. W. Gokel, *Peptibiotics*, 2009, 657–674; R. M. Capito, A. Mata and S. I. Stupp, *Nanotechnology*, 2009, **5**, 385–412.
6 E. Bilensoy, *J. Biomed. Nanotechnol.*, 2008, **4**, 293–303; R. H. de Rossi, O. F. Silva, R. V. Vico and C. J. Gonzalez, *Pure Appl. Chem.*, 2009, **81**, 755–765; F. Sallas and R. Darcy, *Eur. J. Org. Chem.*, 2008, 957–969.
7 G. W. Gokel, W. M. Leevy and M. E. Weber, *Chem. Rev.*, 2004, **104**, 2723–2750.
8 A. von Baeyer and V. Villiger, *Ber. Dtsch. Chem. Ges.*, 1902, **35**, 1201–1212.
9 T. Kappe, *J. Inclusion Phenom. Mol. Recognit. Chem.*, 1994, **19**, 3–15.
10 C. D. Gutsche and R. Muthukrishnan, *J. Org. Chem.*, 1978, **43**, 4905–4906.
11 *Supramolecular Chemistry*, ed. J. W. Steed and J. L. Atwood, John Wiley and sons, Chichester, 2000; *Core Concepts in Supramolecular Chemistry and Nanochemistry*, ed. J. W. Steed, D. R. Turner and K. Wallace, John Wiley and sons, Chichester, 2007; J.-M. Lehn, *Supramolecular Chemistry: Concepts and Perspectives*, Wiley-VCH, Weinheim, 1995.
12 J.-M. Lehn, *Angew. Chem., Int. Ed. Engl.*, 1988, **27**, 89–112.
13 D. J. Cram, *Angew. Chem., Int. Ed. Engl.*, 1988, **27**, 1009–1020.
14 C. J. Pedersen, *Angew. Chem., Int. Ed. Engl.*, 1988, **27**, 1021–1027.
15 *Supramolecular Chemistry: From Biological Inspiration to Biomedical Applications*, ed. P. J. Cragg, Springer-Verlag, Heidelberg, 2010; Y. Bar-Cohen, *Biomimetics: biologically inspired technologies*, CRC Press, Boca Raton, 2006; *Biomimetic Materials and Design: Biointerfacial Strategies, Tissues Engineering and Targeted Drug Delivery*, ed. A. K. Dilow and A. M. Lowman, Marcel Dekker, New York, 2002; *Biomimetic Materials Chemistry*, ed. S. Mann, John wiley and sons, New York, 1995.
16 C. D. Gutsche, *Calixarenes: an introduction*, RSC Publishing, Cambridge, 2008, and references therein.
17 *Calixarenes 2001*, ed. M.-Z. Asfari, V. Böhmer, J. Harrowfield and J. Vicens, Kluwer Academic Publisher, Dordrecht, 2001; *Calixarenes in the Nanoworld*, ed. J. Vicens and J. Harrowfield, Springer, Heidelberg, 2007; *Calixarenes in action*, ed. L. Mandolini and R. Ungaro, Imperial College Press, London, 2000; C. D. Gutsche, *Calixarenes revisited*, The Royal Society of Chemistry, Cambridge, 1998.
18 L. Baldini, A. Casnati, F. Sansone and R. Ungaro, *Chem. Soc. Rev.*, 2007, **36**, 254–266.
19 P. Timmerman, W. Verboom and D. N. Reinhoudt, *Tetrahedron*, 1996, **52**, 2663–2704.
20 A. D. M. Curtis, *Tetrahedron Lett.*, 1997, **38**, 4295–4296; W. Iwanek, *Tetrahedron*, 1998, **54**, 14089–14094; W. Iwanek and B. Syzdol, *Synth. Commun.*, 1999, **29**, 1209–1216; M. J. McIldowie, M. Mocerino, B. W. Skelton and A. H. White, *Org. Lett.*, 2000, **2**, 3869–3871.
21 M. A. Markowitz, R. Bielski and S. L. Regen, *Langmuir*, 1989, **5**, 276–278.
22 Y. Tanaka, M. Mayachi and Y. Kobuke, *Angew. Chem., Int. Ed.*, 1999, **38**, 504–506.
23 Y. K. Y. Tanaka and M. Sokabe, *Angew. Chem., Int. Ed. Engl.*, 1995, **34**, 693.
24 M. Lee, S.-J. Lee and L.-H. Jiang, *J. Am. Chem. Soc.*, 2004, **126**, 12724–12725.
25 G. M. L. Consoli, F. Cunsolo, C. Geraci, T. Mecca and P. Neri, *Tetrahedron Lett.*, 2003, **44**, 7467–7470; G. M. L. Consoli, F. Cunsolo, C. Geraci and V. Sgarlata, *Org. Lett.*, 2004, **6**, 4163–4166.
26 N. Micali, V. Villari, M. L. Consoli Grazia, F. Cunsolo and C. Geraci, *Phys. Rev. E: Stat. Nonlin. Soft Matter Phys.*, 2006, **73**, 051904.
27 D. Coquiere, H. Cadeau, Y. Rondelez, M. Giorgi and O. Reinaud, *J. Org. Chem.*, 2006, **71**, 4059–4065.
28 R. G. Janssen, W. Verboom, D. N. Reinhoudt, A. Casnati, M. Freriks, A. Pochini, F. Ugozzoli, R. Ungaro and P. M. Nieto, *et al.*, *Synthesis*, 1993, 380–386.
29 O. Seneque, M.-N. Rager, M. Giorgi and O. Reinaud, *J. Am. Chem. Soc.*, 2000, **122**, 6183–6189.
30 S. Houmadi, D. Coquiere, L. Legrand, M. C. Faure, M. Goldmann, O. Reinaud and S. Remita, *Langmuir*, 2007, **23**, 4849–4855.
31 M. Strobel, K. Kita-Tokarczyk, A. Taubert, C. Vebert, P. A. Heiney, M. Chami and W. Meier, *Adv. Funct. Mater.*, 2006, **16**, 252–259.
32 O. M. Martin and S. Mecozzi, *Supramol. Chem.*, 2005, **17**, 9–15.
33 R. Zadmard and T. Schrader, *J. Am. Chem. Soc.*, 2005, **127**, 904–915; S. Friedman, S. Kolusheva, R. Volinsky, L. Zeiri, T. Schrader and R. Jelinek, *Anal. Chem.*, 2008, **80**, 7804–7811.
34 C. Mbemba, K. Sigaud, F. Perret, K. Suwinska, O. Shkurenko and A. W. Coleman, *J. Inclusion Phenom. Macrocyclic Chem.*, 2008, **61**, 29–40; K. Suwinska, O. Shkurenko, C. Mbemba, A. Leydier, S. Jebors, A. W. Coleman, R. Matar and P. Falson, *New J. Chem.*, 2008, **32**, 1988–1998.
35 F. Perret, A. N. Lazar and A. W. Coleman, *Chem. Commun.*, 2006, 2425–2438.
36 R. V. Rodik, V. I. Boyko and V. I. Kalchenko, *Curr. Med. Chem.*, 2009, **16**, 1630–1655.
37 G. M. L. Consoli, G. Granata, E. Galante, I. Di Silvestro, L. Salafia and C. Geraci, *Tetrahedron*, 2007, **63**, 10758–10763.
38 G. M. L. Consoli, G. Granata, R. Lo Nigro, G. Malandrino and C. Geraci, *Langmuir*, 2008, **24**, 6194–6200.
39 O. Hayashida, K. Mizuki, K. Akagi, A. Matsuo, T. Kanamori, T. Nakai, S. Sando and Y. Aoyama, *J. Am. Chem. Soc.*, 2003, **125**, 594–601.
40 Y. Aoyama, *Chem.–Eur. J.*, 2004, **10**, 588–593.
41 I. S. Ryzhkina, K. M. Enikeev, A. P. Timosheva, T. N. Pashirova, S. S. Lukashenko, L. A. Kudryavtseva and A. I. Konovalov, *Russ. Chem. Bull.*, 2004, **53**, 1528–1535.
42 I. S. Ryzhkina, A. P. Timosheva, A. V. Chernova, R. R. Shagidullin, A. A. Gazizova, W. D. Habicher, T. Krause, L. I. Vagapova and A. I. Konovalova, *Russ. Chem. Bull.*, 2007, **56**, 475–483.
43 I. S. Ryzhkina, T. y. N. Pashirova, W. D. Habicher, L. A. Kudryavtseva and A. I. Konovalov, *Macromol. Symp.*, 2004, **210**, 41–48.

44 I. S. Ryzhkina, L. A. Kudryavtseva, K. M. Enikeev, Y. A. Babkina, A. I. Konovalov, Y. F. Zuev and N. L. Zakharchenko, *Russ. J. Gen. Chem.*, 2002, **72**, 1401–1405.
45 D. T. Schuehle, J. Schatz, S. Laurent, L. Vander Elst, R. Mueller, M. C. A. Stuart and J. A. Peters, *Chem.–Eur. J.*, 2009, **15**, 3290–3296.
46 M. Kellermann, W. Bauer, A. Hirsch, B. Schade, K. Ludwig and C. Boettcher, *Angew. Chem., Int. Ed.*, 2004, **43**, 2959–2962.
47 Y. Chang, M. Kellermann, M. Becherer, A. Hirsch and C. Bohne, *Photochem. Photobiol. Sci.*, 2007, **6**, 525–531.
48 J. J. Michels, J. Huskens, J. F. J. Engbersen and D. N. Reinhoudt, *Langmuir*, 2000, **16**, 4864–4870.
49 X. Yu, C. Tu, L. He, R. Wang, G. Sun, D. Yan and X. Zhu, *J. Macromol. Sci., Pure Appl. Chem.*, 2009, **46**, 360–367.
50 A. W. Coleman, A. N. Lazar and J. Y. P. P. Renault, *European Patent* EP 2073783, 2008.
51 J. Hart, D. Rival, N. Terry, S. Bonnet, C. Buffevant and E. Perrier, *J. Cosmet. Sci.*, 2006, **57**, 185–186; D. Rival, N. Terry, S. Bonnet, B. Sohm, E. Perrier and A. Coleman, *SOFW J.*, 2006, **132**, 54, 56, 58, 60–62.
52 P. Shahgaldian, M. Cesario, P. Goreloff and A. W. Coleman, *Chem. Commun.*, 2002, 326–327.
53 P. Shahgaldian, E. Da Silva, W. Coleman Anthony, B. Rather and J. Zaworotko Michael, *Int. J. Pharm.*, 2003, **253**, 23–38.
54 E. T. Castellana and P. S. Cremer, *Surf. Sci. Rep.*, 2006, **61**, 429–444; R. P. Richter, R. Berat and A. R. Brisson, *Langmuir*, 2006, **22**, 3497–3505.
55 A. Dubes, I. L. Moudrakovski, P. Shahgaldian, A. W. Coleman, C. I. Ratcliffe and J. A. Ripmeester, *J. Am. Chem. Soc.*, 2004, **126**, 6236–6237.
56 P. Shahgaldian, A. W. Coleman and V. I. Kalchenko, *Tetrahedron Lett.*, 2001, **42**, 577–579.
57 P. Shahgaldian, E. Da Silva and A. W. Coleman, *J. Inclusion Phenom. Macrocyclic Chem.*, 2003, **46**, 175–177.
58 J. Gualbert, P. Shahgaldian and A. W. Coleman, *Int. J. Pharm.*, 2003, **257**, 69–73.
59 P. Shahgaldian, J. Gualbert, K. Aissa and A. W. Coleman, *Eur. J. Pharm. Biopharm.*, 2003, **55**, 181–184.
60 P. Shahgaldian, L. Quattrocchi, J. Gualbert, A. W. Coleman and P. Goreloff, *Eur. J. Pharm. Biopharm.*, 2003, **55**, 107–113.
61 A. W. Coleman, S. Jebors, P. Shahgaldian, G. S. Ananchenko and J. A. Ripmeester, *Chem. Commun.*, 2008, 2291–2303.
62 E. Houel, A. Lazar, E. Da Silva, A. W. Coleman, A. Solovyov, S. Cherenok and V. I. Kalchenko, *Langmuir*, 2002, **18**, 1374–1379.
63 P. Shahgaldian, U. Pieles and M. Hegner, *Langmuir*, 2005, **21**, 6503–6507.
64 S. Ehrler, U. Pieles, A. Wirth-Heller and P. Shahgaldian, *Chem. Commun.*, 2007, 2605–2607.
65 K. M. Hwang, Y. M. Qi and S.-Y. Liu, *US Patent* 5196452, 1993.
66 K. M. Hwang, Y. M. Qi, S.-Y. Liu, T. C. Lee, W. Choy and J. Chen, *US Patent* 5409959, 1995.
67 J. L. Atwood, R. J. Bridges, R. K. Juneja and A. K. Singh, *US Patent* 5 489 612, 1996.
68 A. W. Coleman, F. Perret, A. Moussa, M. Dupin, Y. Guo and H. Perron, *Top. Curr. Chem.*, 2007, **277**, 31–88.
69 Y. Shi and H.-J. Schneider, *J. Chem. Soc., Perkin Trans. 2*, 1999, 1797–1803.
70 M. Dudic, A. Colombo, F. Sansone, A. Casnati, G. Donofrio and R. Ungaro, *Tetrahedron*, 2004, **60**, 11613–11618; F. Sansone, M. Dudic, G. Donofrio, C. Rivetti, L. Baldini, A. Casnati, S. Cellai and R. Ungaro, *J. Am. Chem. Soc.*, 2006, **128**, 14528–14536.
71 P. Shahgaldian, M. A. Sciotti and U. Pieles, *Langmuir*, 2008, **24**, 8522–8526.
72 L. Nault, A. Cumbo, R. Prétot, M. Sciotti and P. Shahgaldian, *Chem. Commun*, 2010, **46**, 5581–5583.
73 K. Ariga, J. P. Hill and Q. Ji, *Phys. Chem. Chem. Phys.*, 2007, **9**, 2319–2340; N. Benkirane-Jessel, P. Lavalle, V. Ball, J. Ogier, B. Senger, C. Picart, P. Schaaf, J.-C. Voegel and G. Decher, *Macromol. Eng.*, 2007, **2**, 1249–1305.
74 I. I. Stoikov, E. A. Yushkova, A. Y. Zhukov, I. Zharov, I. S. Antipin and A. I. Konovalov, *Tetrahedron*, 2008, **64**, 7112–7121.
75 D. Elend, U. Pieles and P. Shahgaldian, *Chimia*, 2010, **64**, 45–48.
76 P. Shahgaldian, A. W. Coleman, S. S. Kuduva and M. J. Zaworotko, *Chem. Commun.*, 2005, 1968–1970.
77 J. L. Atwood, F. Hamada, K. D. Robinson, G. W. Orr and R. L. Vincent, *Nature*, 1991, **113**, 2760.

II

Cation binding resorcinarene bis-crowns: the effect of lower rim alkyl chain length on crystal packing and solid lipid nanoparticles

by

Kaisa Helttunen, Kirsi Salorinne, Tahnie Barboza, Hélène Campos Barbosa, Aku Suhonen & Maija Nissinen, 2012

New. J. Chem. 36 (2012), 789-795, DOI: 10.1039/C2NJ20981K.

NJC

Dynamic Article Links

Cite this: *New J. Chem.*, 2012, **36**, 789–795

www.rsc.org/njc

PAPER

Cation binding resorcinarene bis-crowns: the effect of lower rim alkyl chain length on crystal packing and solid lipid nanoparticles†

Kaisa Helttunen,* Kirsi Salorinne, Tahnie Barboza, Hélène Campos Barbosa, Aku Suhonen and Maija Nissinen*

Received (in Victoria, Australia) 22nd November 2011, Accepted 19th December 2011
DOI: 10.1039/c2nj20981k

A group of seven resorcinarene bis-crown ethers (C*N*BC5) with two polyether bridges at the upper rim and either propyl, butyl, pentyl, heptyl, nonyl, decyl or undecyl groups at the lower rim were synthesized and their binding properties with Cs^+ were investigated by NMR titration. The bis-crowns form 1 : 2 complexes with Cs^+ with binding constants of log *K* 4–5. Crystal structures of bis-crowns and their Cs^+ and K^+ complexes were studied and different packing motifs were found depending on the alkyl chain length. Short ethyl, propyl and butyl alkyl chains gave a layer or pillar packing where the polar and non-polar regions cannot be distinguished, whereas longer pentyl and decyl chains formed bilayers. Amphiphilic properties and self-assembly in water were studied by preparing solid lipid nanoparticles (SLNs) from the bis-crowns. All investigated compounds formed stable SLNs showing amphiphilic character, which in the case of the short chain bis-crowns probably arises from their locked boat conformation separating the polar face of the molecule from the non-polar face.

Introduction

Combining host–guest chemistry and surfactant properties into a single molecule by structural design of supramolecules, nanoscale materials, *i.e.* films, particles or gels, with host–guest functionality can be obtained. Calixarenes and resorcinarenes are macrocyclic supramolecular hosts well suited for this task since they have a concave binding cavity capable of binding various guest molecules or ions.[1–3] Resorcinarenes can be easily converted into amphiphilic molecules using long aliphatic aldehydes in their synthesis resulting in hydrophobic chains below the binding site. The upper rim of the resorcinarene bowl has innate hydrophilic character because of the OH-functionalities derived from the resorcinol, and in addition, the upper rim is readily available for further functionalization to improve the binding affinity and selectivity. The self-assembly of amphiphilic calixarenes and resorcinarenes in water and at interfaces into mono/bilayers, thin films, vesicles and micelles, and properties of these assemblies have been studied avidly to extend the use of calixarenes.[2,4] Some recent examples of their potential applications include gene delivery,[5,6] catalytic activity,[7] liquid crystals[8] and VOC sensing.[9]

Nanoscience Center, Department of Chemistry, University of Jyväskylä, P.O. Box 35, Jyväskylä FI-40014, Finland. E-mail: maija.nissinen@jyu.fi, kaisa.j.helttunen@jyu.fi; Tel: +358 50 428 0804

† Electronic supplementary information (ESI) available: Synthetic procedures, SEM images for SLN and details of crystal structure refinement. CCDC reference numbers 854053–854058. For ESI and crystallographic data in CIF or other electronic format see DOI: 10.1039/c2nj20981k

In addition to host–guest properties, environmentally responsive functionalities, which change the organized structures from micelles into larger vesicles according to pH, have been prepared.[10–12]

Solid lipid nanoparticles (SLNs), or particles prepared from solid lipids, are the latest addition to the family of drug carrier structures since the introduction of liposomes and polymeric nanoparticles, which are prepared from liquid lipids.[13] The preparation process of SLNs leads to particles with diameters from tens to few hundred or thousand nanometres, which can be loaded with drugs or other sensitive compounds and used for their protection and transport. Since calixarenes and resorcinarenes are usually solid materials at room temperature, they can be used for preparation of solid lipid nanoparticles and studies of their potential in encapsulation of biologically important guests, DNA for cell transfection and surface modification for drug targeting have been published.[14–17]

Calixarenes and resorcinarenes with crown ether bridges connecting the hydroxyl groups are very selective cation receptors called calixcrowns.[18] Depending on the number of oxygen donors and thus the length and geometry of the crown bridge, calixcrowns have very good affinity towards alkali and alkaline earth metal cations and ammonium ions.[19] Resorcinarene bis-crowns and their K^+, Cs^+, Rb^+ and Ag^+ complexes have shown very interesting structural properties such as formation of layers, capsules and nanorods.[20–23] Therefore, we have been interested in studying the effect of alkyl chain length on the crystal packing of the resorcinarene bis-crowns and their metal complexes, where it can (a) influence the twisting of the resorcinarene framework and (b) induce a layer or bilayer

packing when the hydrophobic effect of the alkyl chains becomes strong enough. The alkyl chain length also affects the amphiphilic properties and self-assembly in water, which was studied by preparing SLNs from a series of resorcinarene bis-crowns with short, medium and long alkyl chains.

Results

Synthesis and complexation studies

A group of seven resorcinarene bis-crown ethers or C*N*BC5, where *N* denotes the number of carbons at the lower rim alkyl group and 5 the number of oxygen donors in each polyether bridge, were prepared by O-alkylation of the free hydroxyl groups of various tetramethoxy resorcinarenes[24] (Fig. 1). Propyl, butyl, pentyl, heptyl, nonyl, decyl and undecyl groups at the resorcinarene lower rim were chosen for structural comparison with the previously synthesized C2BC5[20,21] and to create amphiphilic bis-crowns. Synthesis was carried out in dry dimethyl formamide (DMF) using Cs_2CO_3 and ditosylated tetra(ethylene glycol) yielding tetramethoxy resorcinarene bis-crown ethers after purification in 15–30% yields.

Complexation of the bis-crowns with an alkali metal cation, caesium hexafluorophosphate, was carried out using NMR titration in order to investigate if the lower rim alkyl chain length has an effect on the binding affinity. C3BC5, C5BC5, C9BC5 and C11BC5 bind Cs^+ with the affinity of $\log K_{11}$ 1.0–2.2 and a total binding constant of $\log K_{11}K_{12}$ 4.0–5.0 (Table 1). C2BC5 has a binding constant of $\log K_{11}$ 1.75 for a 1 : 1 complex,[21] which falls at the same magnitude of order as

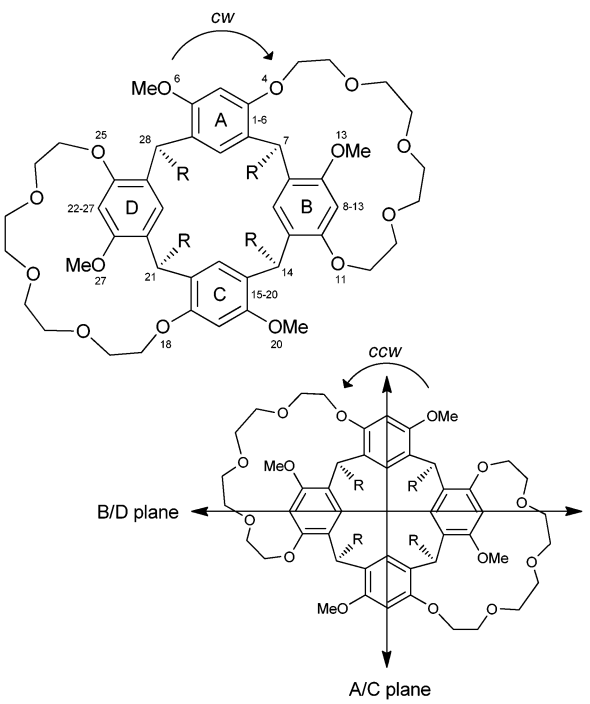

Fig. 1 Structure of the resorcinarene bis-crowns C*N*BC5, R = C_NH_{2N+1} where N = 2, 3, 4, 5, 7, 9, 10, 11 with selected crystallographic numbering. *cw* and *ccw* enantiomers are shown; the A/C plane runs through the upright aryl rings (A and C) and the B/D plane through parallel aryl rings (B and D) respective to the methine plane C7–C14–C21–C28.

Table 1 Binding constants for Cs^+ complexes in acetone-D6[a]

	C3BC5	C5BC5	C9BC5	C11BC5
$\log K_{11}$[b]	1.04 ± 0.18	1.59 ± 0.41	1.49 ± 0.60	2.21 ± 0.09
$\log K_{11}K_{12}$[c]	4.43 ± 0.03	4.62 ± 0.10	4.06 ± 0.19	5.03 ± 0.04
$\log K_{12}$[d]	3.39	3.03	2.57	2.82

[a] NMR titration at 30 °C, *R*-values <7%. [b] Binding constant for reaction H + G ↔ HG. [c] Total binding constant for H + 2G ↔ HG_2. [d] $K_{12} = K_{11}K_{12}/K_{11}$.

now determined $\log K_{11}$ values. The second binding constant $\log K_{12}$ is larger than the first binding constant for all investigated complexes. In the case of C2BC5, K_{12} was not determined because the Job plot showed that intrinsic water concentration over 1 molar equivalent relative to the host leads to 1 : 1 complexation. For C3BC5–C11BC5 such a strong trend was not observed, the water content being 1–2.5 molar equivalents except for the 13 mol. equiv. for C11BC5. In all cases a 1 : 2 binding model gave better fits than the 1 : 1 model.

Crystal structures

Resorcinarene bis-crowns. Single crystals of resorcinarene bis-crowns were grown by slow evaporation from alcohol solutions. C4BC5 (structure **C4**) and C5BC5 (**C5**) crystallized in a triclinic $P\bar{1}$ without any solvent in their binding cavity or in the crystal lattice. Analysis of the conformational properties of individual molecules (Table 2) revealed that the bis-crowns are in a boat or slightly twisted boat conformation and upright aryl rings (A and C) are tilted towards the cavity with −8.3– to −10.7 dihedral angles. Crown ether bridges are folded on top of the binding cavities closing the space inside.

The crystal packing of **C5** can be described as a "squeezed bilayer" where the upper rim interface of two opposing rows appears as if compressed into one layer (Fig. 2). However, the polar and non-polar layers can still be distinguished. Rows are aligned parallel to the A/C aryl plane direction (later A/C direction, Fig. 1). The clockwise (*cw*) counterclockwise (*ccw*) enantiomers of the bis-crowns are related by inversion symmetry. In **C5**, *cw* and *ccw* enantiomers alternate in each bilayer in such a way that each *cw* is facing up and is surrounded by a *ccw* facing down on both sides. **C4** has two molecules in the asymmetric unit, I and II, which could be assigned either a boat or a slightly twisted boat conformation. Molecules pack in a pillar assembly with alternating I and II molecules (Fig. 3). Each pillar consists of either *cw* enantiomers or *ccw* enantiomers, which in turn form layers of *cw* and *ccw* enantiomers, but separation into polar and non-polar regions does not occur.

Long chain bis-crowns C9BC5, C10BC5 and C11BC5 crystallized readily from ethanol in a monoclinic lattice (Z = 8). Interestingly, most of these structures showed straight alignment of the alkyl groups in the bilayer assembly without disorder but had unresolvable disorder at the crown ether bridges and therefore these structures can only be considered as preliminary structures.‡

‡ **C9**: $C2/c$, a = 52.218(1), b = 14.6337(3), c = 21.2980(5), β = 101.245(1), V = 15962.2(6); **C10**: $C2/c$, a = 54.931(2), b = 14.5212(5), c = 21.3574(8), β = 102.354(2), V = 16641.4(1); **C11**: $C2/c$, a = 57.434(2), b = 14.5337(4), c = 21.1864(7), β = 100.590(1), V = 17383.6(1).

Table 2 Conformational properties of the resorcinarene bis-crowns and their alkali metal complexes

	C4[a]						
	I	II	**C5**	**C2K2**	**C3Cs2**	**C5K2**	**C10Cs2**
Crystal packing arrangement	Pillar	Pillar	Squeezed bilayer	Layer	Layer/shifted capsule	Bilayer/shifted capsule	Bilayer/shifted capsule
Conformation	Boat	Boat	Twisted boat	Boat	Twisted boat	Boat	Boat
Tilt/°	3.7	5.7	8.9	1.4	7.0	3.3	1.1
Twist/°	3.9	5.7	8.7	2.1	6.4	3.5	0.5
Distance/Å[b]	4.79/8.01	4.87/8.00	4.80/7.98	5.28/7.98	5.46/7.95	5.26/7.98	5.49/7.94
Dihedral angle between opposite rings/°[c]	−10.7/175.2	−8.3/173.3	−10.3/167.3	14.4/151.4	22.2/148.8	11.8/147.0	21.1/148.3
Dihedral angle against methine plane/°[d]	80.0/89.1, 175.6/176.5	88.9/82.9, 176.2/176.3	86.4/83.2, 173.2/174.0	96.5/97.9, 165.9/165.5	100.3/101.5, 168.3/160.5	96.4/95.3, 166.5/160.5	100.6/100.5, 163.2/165.1
Cavity diameter/Å[e]	5.17/5.11	5.26/5.21	4.59/4.79	4.80/5.15	5.42/5.28	4.90/4.69	5.08/5.23

[a] **C4** has two molecules in the asymmetric unit. [b] Between opposite aromatic ring centroids. [c] Between opposite aromatic ring planes A and C, B and D. [d] Aromatic ring planes A, C, B, D against the methine plane C7–C14–C21–C28. [e] Average cavity diameter measured as O–O distances.

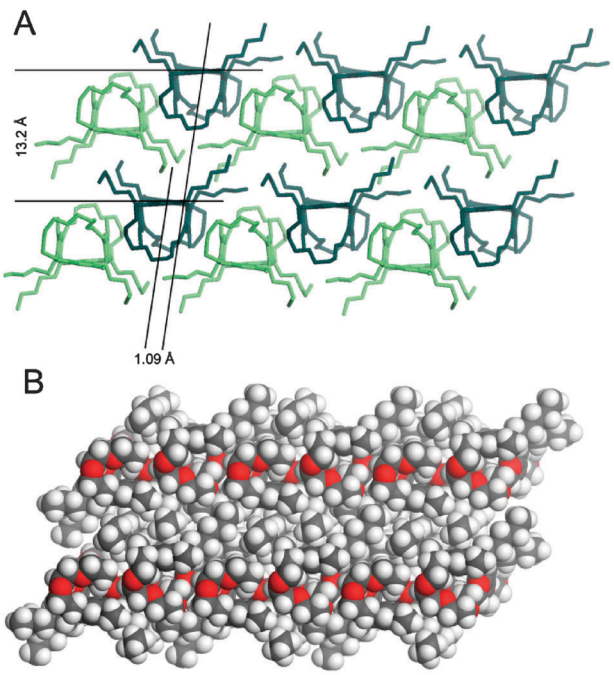

Fig. 2 Crystal packing of **C5**, a flattened bilayer, in a stick model (A) with *cw* enantiomers in light and *ccw* in dark green, respectively, and a CPK representation (B), where the polar and non-polar regions are clearly visible. Disorder not shown for clarity.

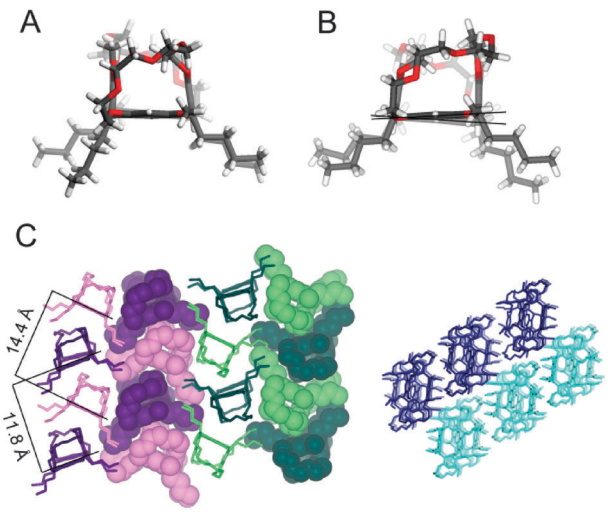

Fig. 3 Crystal structure of **C4** (disorder not shown). **C4** has two molecules, I (A) and II (B) in the asymmetric unit, the twist angle in II indicated. (C) Pillar packing of **C4**: *cw* (up, purple) and *ccw* (down, green) enantiomers are separated in pillars with alternating I (dark shade) and II (light shade). Each pillar consists of a single enantiomer with the methine plane angle (43.6°) and distances indicated; a top view shows pillars of *cw* and *ccw* enantiomers in dark and light color, respectively.

Alkali metal complexes. Alkali metal complexes of the bis-crowns were studied by crystallizing C*N*BC5s with an excess of potassium or caesium hexafluorophosphate in alcohols yielding 1 : 2 (host–guest) complexes. When the binding pockets of the host are filled with cations the dihedral angles of A/C aryl rings are 11.8–22.2° and cavity diameters between 4.69–5.23 Å. The binding pocket of the bis-crowns is flexible and able to adjust its size slightly according to the size of the guest cation giving smaller cavity diameters for K^+ than Cs^+ complexes. Cations bind to the host with cation–π (η^6) interaction with a centroid–cation distance of 3.0–3.1 Å for K^+ and 3.2–3.3 for Cs^+, and with M^+–O interactions with methoxy group oxygens and 3–4 coordination bonds to the bridge (O–M^+ 2.70–3.54 Å). One of the PF_6^- anions is coordinated between the two cations inside the binding pocket, which helps reduce the charge repulsion between the cations. The other anion is located outside the cavity and creates short contacts between the complexes. Depending on the structure, alkyl chain length and the cation, the complexes pack in shifted capsule, layer or bilayer assemblies.

C2BC5 has been previously crystallized as a KPF_6 complex in a capsule assembly.[20] Now, another packing for the C2BC5·2KPF_6 complex (**C2K2**) was obtained, forming layered packing without the capsule formation. When viewed on top, each *cw* enantiomer alternates with *ccw* enantiomers within a layer, and therefore polar and non-polar sides cannot be distinguished. A side view (B/D direction) of the packing reveals that *cw* and *ccw* enantiomers are separated on their own stacks in a parallel alignment (Fig. 4).

C3BC5·2$CsPF_6$ (**C3Cs2**) crystallized with ethanol as a solvate in the crystal lattice. The conformation of the host is a twisted boat in contrast to the boat conformation of all the other

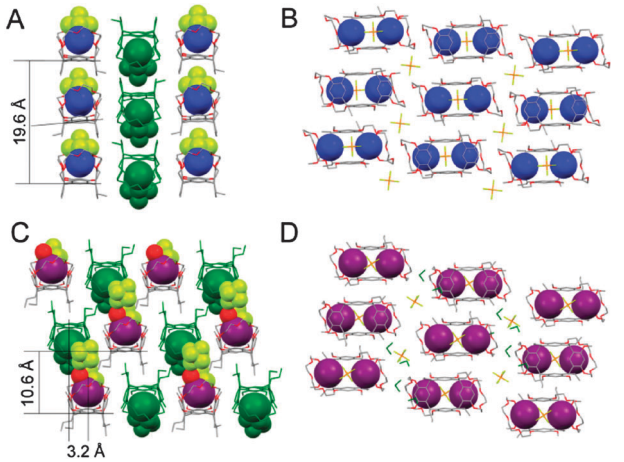

Fig. 4 Side and top views of the crystal packing of **C2K2** layers (A, B) and **C3Cs2** shifted capsules/layers (C, D); side view: *ccw* enantiomers facing down (green); top view of a layer: outlying anions and ethanol molecules (in D, green) shown as a stick model.

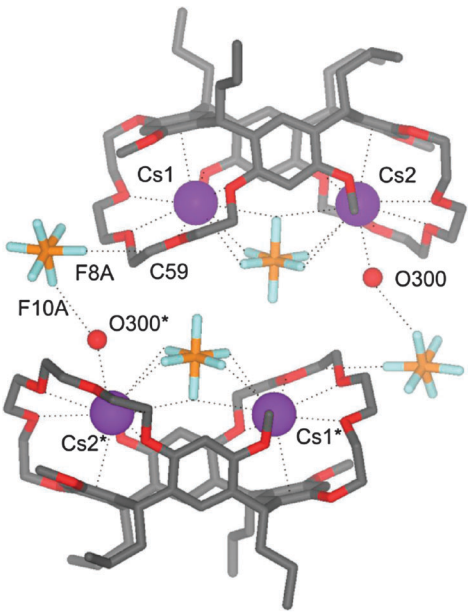

Fig. 5 **C3Cs2** shifted capsule consisting of *cw* and *ccw* enantiomers, short contacts to the solvent and anions shown in dashed lines, atoms labelled with an asterisk are generated by a symmetry operation $-x + 1$, $-y + 2$, $-z + 1$. Disorder not shown for clarity.

complexes, which can be understood by analyzing the anion/solvent coordination of the cation. One of the PF_6^- anions is coordinated between the two Cs^+ inside the cavity. In addition, a water molecule, not found in the other structures, is coordinated to Cs2 with 3.13 Å Cs–O distance and has a short contact of 2.99 Å to the F10A of the (disordered) second PF_6^-, which in turn is located close to the crown ether bridge of the opposite enantiomer with an F8A–C59 distance of 3.12 Å (Fig. 5). A pair of complexes, *cw* and *ccw* enantiomers, form a shifted capsule connected by the solvent–anion contacts. The top view of the complexes shows a similar alternating pattern of *cw* and *ccw* enantiomers as in **C2K2**, and the side view from the B/D direction shows a layered packing, where shifted capsules form

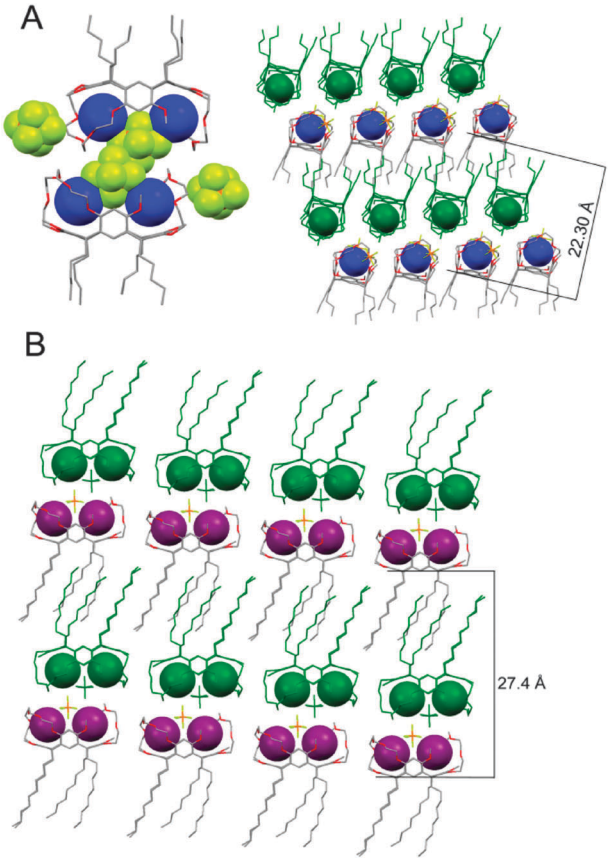

Fig. 6 **C5K2**: a front view of an offset capsule and a bilayer packing (A); **C10Cs2**: a front view of a bilayer (B). *ccw* enantiomers in green color; outlying anions and disorder not shown.

diagonal lines through the crystal. The role of the ethanol solvate is to fill the voids at the B/D edges of the complexes, where they form H-bonded circles of four ethanol molecules without connecting to the host–guest complex.

The C5BC5·2KPF$_6$ complex (**C5K2**) forms layers of single *cw* or *ccw* enantiomer which consist of rows aligned in the A/C direction with a 2.43 Å shift between the molecules (15% of complex width) and in the B/D direction with a 3.28 Å (35%) shift. In contrast to **C5**, all alkyl chains are oriented straight below the methine plane forming a clear bilayer packing. The upper rim interface of **C5K2** forms shifted capsules with a 2.80 Å dislocation of the B/D planes accounting for 30% of the width of a molecule (Fig. 6A). Similar packing was obtained for the C10BC5·2CsPF$_6$ complex (**C10Cs2**) despite the difference in cation size and thus larger cavity diameter, but the longer alkyl groups expand the thickness of the bilayer up to 27.39 Å (Fig. 6B).

Solid lipid nanoparticles

The ability of C*N*BC5's to form solid lipid nanoparticles was tested to assess their self-assembling properties in water. Previously, calixarenes and resorcinarenes bearing long alkyl chains and hydrophilic functionalities at the upper rim have been used to prepare stable SLN's by a solvent diffusion (solvent replacement) method.[25,26] The same method was applied for the C*N*BC5s, where approximately 5–7 mg of C*N*BC5 was dissolved in a small amount of THF and water

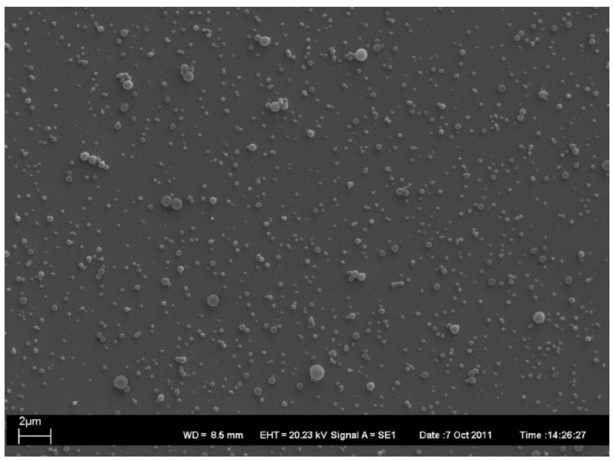

Fig. 7 SEM image of C11BC5 SLN on SiO_x; spherical particles with a mean diameter of 300 nm are shown.

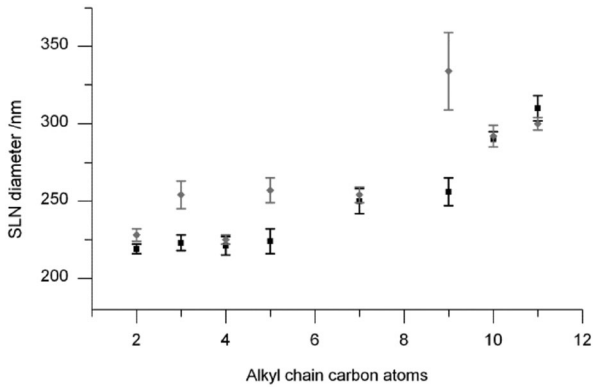

Fig. 8 SLN diameters for all C*N*BC5 (mean of the size distribution from DLS showing standard deviation). SLNs with a constant 0.1 mM concentration (black) and with a constant mass 100 mg L^{-1} (grey) show increasing diameter for longer alkyl chains.

was added to the solution by vigorous stirring, after which a cloudy suspension was formed. The size of the SLN's was analyzed using dynamic light scattering, which gave hydrodynamic diameters of 220–320 nm for the particles with polydispersity indexes of 0.04–0.34. The particle shape and size was confirmed by SEM images, which revealed spherical particles at a size distribution corresponding to the DLS measurements (Fig. 7). For calixarenes and resorcinarenes, it has been discovered that the size of the SLNs is affected by several parameters: THF/water ratio, stirring speed, pH of the solution, and length of the alkyl chains of the calixarene.[25,26] However, changes in the particle size are mostly affected by the final concentration of the calixarene in the suspension. Therefore in this study, other parameters except the length of the alkyl chains and final concentration of the resorcinarene suspensions were kept constant. In the first series (Fig. 8) the molar concentration of the bis-crowns was constant and the diameters of the particles increase when the amount of carbon atoms at the alkyl chains increases. In the second series SLNs were prepared keeping the mg L^{-1} concentration constant to make sure that the increased particle diameter was not originating from the increased amount (in milligrams) of bis-crown in the suspensions. The second series (Fig. 8) has very similar particle sizes than the first one, which indicates that the change in the amount of bis-crowns between the two series has a negligible effect. The variation in the particle size, although quite modest, is most likely caused by the different alkyl chain lengths of the bis-crowns, which affect their amphiphilic properties.

Discussion

Resorcinarene bis-crowns were shown to bind Cs^+ as 1 : 1 and 1 : 2 complexes in solution, 1 : 2 being the dominant species. There is some variation especially between the $\log K_{11}$ values, giving 1.04 for C3BC5 and 3.31 for C11BC5. However, the higher $\log K_{12}$ value for C3BC5 partly compensates this difference when the total binding constants are examined. In contrast to the previously examined C2BC5, all compounds gave 1 : 2 complexes when more than 1 molar equivalent of water relative to the host was present in the solution. Therefore, what at first glance appears to be the effect of the alkyl chain length may well be the indirect result of desolvation of the cation. The sensitivity of the measurement towards water may explain some of the observed differences in the binding constants between the experiments.

Since the affinity of C2BC5 towards K^+ is very low, $\log K$ of 0.23 for the 1 : 1 complex,[21] the binding constant was not determined for the other bis-crown potassium complexes. However, the structural properties of solid state K^+ complexes were compared to the Cs^+ complexes with the purpose of exploring alternative crystal packing forms due to different cation size. Based on the results it seems that the size of the cation does not have a direct influence on the packing, since similar structures were obtained for the different cations (**C2K2** and C2BC5·$CsPF_6$ complex;[21] **C5K2** and **C10Cs2**). Instead, solvent coordination together with the cation size has a more important role in the packing, which is seen by comparing the **C2K2** and **C3Cs2** and a capsule structure of C2BC5·2KPF_6[20] with a water molecule coordinated inside the cavity. **C3Cs2** also contains water, which is involved in the shifted capsule coordination. The larger diameter of Cs^+ probably prevents similar coordination of water and the tilted angle of PF_6^- between the cations inside the binding pocket as in C2BC5·2KPF_6 capsules, and now coordination takes place outside the binding pocket.

Twisting of the resorcinarene skeleton was observed in **C4**, **C5** and **C3Cs2**, and is therefore not limited to short alkyl chain bis-crowns. Rather, all interactions in the lattice determine the conformation of the resorcinarene to provide optimal close packing.

The effect of the lower rim alkyl chain length is connected to the amphiphilic nature of the bis-crowns. When alkyl chains are 2–4 carbon long, they have not been found to form bilayer packing with separated polar and non-polar parts. Instead, layers with alternating upper and lower rims in neighboring molecules or complexes are seen, and in addition, **C4** formed a pillar type assembly with tilted methine carbon planes. For C5BC5 a squeezed bilayer in **C5** and a bilayer in **C5K2** were found, which shows that five carbons is a limiting alkyl chain length for the bilayer type packing. For the long chain bis-crowns increased molecule size made crystallization more

difficult and the structures also tend to show more disorder either at the lower rim alkyl chains or at the crown ether bridges or both. Since C9BC5–C11BC5 had a very bad unresolvable disorder at the upper rim polyether bridges but quite well organized alkyl groups at the lower rim, this can be interpreted as an indication of stronger hydrophobic interactions at the lower rim, which drives the alkyl chains in the ordered packing, whereas the crown ether bridges have more conformational freedom. As a result, complexation of cations in the binding pocket was attempted in order to rigidify the crown ether bridges and, thus, enable the crystal structure analysis of these molecules. This strategy has so far provided the structure of Cs^+ complex of C10BC5 which has a very similar packing compared to **C5K2**.

The second goal of this study was to investigate the self-assembly of C*N*BC5s in water by preparing SLNs. Bis-crowns are neutral amphiphilic molecules without H-bond donors at their polar part. It is noteworthy that also bis-crowns with C_2, C_3 and C_4 alkyl chains, which do not arrange in a bilayered packing, indicating their amphiphilic character in the solid state, form these particles. In addition, SLNs with shorter than C_4 alkyl or acyl chains have not been previously reported for calixarenes or resorcinarenes to the best of our knowledge. The ability of these molecules to form SLNs probably arises from the macrocyclic effect and the locked boat conformation, which separates the hydrophilic side of the compound from the hydrophobic side.

The diameter of the SLNs increased for the longer alkyl chains, which is in fact opposite result to those Coleman *et al.*[27] have obtained for the *para*-acyl-calix[9]arene SLNs. *para*-Acyl-calix[4]arenes on the other hand have not shown a clear trend in the SLN size for different alkyl chain lengths.[25] Calix[9]arenes have larger, nine membered macrocyclic rings with enhanced conformational flexibility compared to resorcinarenes and calix[4]arenes, which can lead to a different arrangement of the amphiphiles during their self-assembly.

The prepared SLNs were stable enough to survive the vacuum treatment needed for the SEM sample preparation (gold coating) and in most cases the SLN suspensions were stable over several months. Some exceptions to this rule were observed, a couple of times the samples formed a visible precipitate within a week or two accompanied with particle size increase. In the SEM images some of the samples showed signs of early aggregation tendency, and in a couple of samples complete assimilation of the smaller <1 μm particles into the substrate was seen. Also, the nature of the substrate has an effect during the sample preparation since on the hydrophobic carbon tape most of the particles deformed in contrast to the hydrophilic SiO_x surface, where hydrophilic interactions with the surface could help maintain the integrity of the particles. According to the preliminary results C11BC5 seemed to give the most stable SLN's. However, further studies are needed to establish a more systematic survey on the properties of the resorcinarene bis-crown SLNs.

In conclusion, resorcinarene bis-crowns bind Cs^+ in solution and form solid state complexes with Cs^+ and K^+. The lower rim alkyl chains affect the crystal packing and the amphiphilic properties since C2BC5–C4BC5 form layered packing, whereas a bilayered packing typical for amphiphilic molecules is observed with C_5 and longer alkyl chains. The locked boat conformation of C*N*BC5 makes also the short chain derivatives behave as amphiphilic molecules, which form stable solid lipid nanoparticles with slight dependence between the SLN size and the alkyl chain length.

Table 3 Crystal structure parameters[a]

Composition	**C4** $C_{64}H_{92}O_{14}$	**C5**[b] $C_{68}H_{100}O_{14}$	**C2K2** $[K_2(PF_6)(C_{56}H_{76}O_{14})]PF_6$	**C3Cs2** $[Cs_2(PF_6)(C_{60}H_{84}O_{14})(H_2O)]PF_6{\cdot}2C_2H_6O$	**C5K2** $[K_2(PF_6)(C_{68}H_{100}O_{14})]PF_6$	**C10Cs2** $[Cs_2(PF_6)(C_{88}H_{140}O_{14})]PF_6$
FW	1085.38	1141.48	1341.31	1695.18	1509.62	1977.76
Crystal system	Triclinic	Triclinic	Monoclinic	Triclinic	Triclinic	Triclinic
Space group	$P\bar{1}$	$P\bar{1}$	$C2/c$	$P\bar{1}$	$P\bar{1}$	$P\bar{1}$
a/Å	15.5428(4)	14.0441(5)	36.7201(7)	12.5169(3)	10.1107(5)	10.4675(4)
b/Å	16.2070(5)	16.3664(6)	19.6013(5)	17.8145(5)	17.014(1)	16.8329(7)
c/Å	28.1062(9)	16.5780(6)	19.4874(6)	18.0005(5)	22.918(1)	27.588(1)
α/°	78.135(2)	99.948(2)	90	70.468(2)	109.330(3)	96.549(2)
β/°	88.922(2)	104.812(2)	116.801(1)	79.987(2)	95.789(3)	97.404(2)
γ/°	62.066(2)	112.067(2)	90	82.768(1)	89.952(3)	93.961(2)
Volume/Å^3	6096.8(3)	3256.7(2)	12519.6(6)	3715.3(2)	3698.9(3)	4771.6(3)
Z	4	2	8	2	2	2
D_{calcd}/Mg m^{-3}	1.182	1.164	1.423	1.515	1.355	1.377
$F(000)$	2352	1240	5600	1732	1592	2056
μ/mm^{-1}	0.661	0.641	2.676	8.867	2.323	6.958
Crystal size/mm	0.15 × 0.10 × 0.07	0.26 × 0.20 × 0.10	0.15 × 0.10 × 0.05	0.30 × 0.20 × 0.10	0.10 × 0.10 × 0.05	0.20 × 0.08 × 0.06
Mean reflns	29 260	15 745	17 010	45 717	16 668	19 576
Indep. reflns	20 072	10 590	10 802	12 755	11 625	13 472
R_{int}	0.0909	0.0593	0.0589	0.0587	0.1246	0.0927
R_1 [$I > 2\sigma(I)$]	0.0792	0.0852	0.0788	0.0449	0.0969	0.0826
wR_2 [$I > 2\sigma(I)$]	0.1761	0.2238	0.2001	0.1125	0.2355	0.1656
GooF on F^2	1.063	1.025	1.029	1.044	1.074	1.055
Largest diff. peak and hole/e Å^{-3}	0.470, −0.378	0.580, −0.335	0.713, −0.646	0.882, −1.338	0.828, −0.457	1.027, −0.634

[a] Unit cell dimensions for C9BC5, C10BC5 and C11BC5 at the endnotes. [b] Isomorphous structures obtained from *tert*-butanol/methanol, *iso*-butanol/methanol, and ethanol solutions.

Experimental

X-Ray crystallography

Single crystal X-ray data were recorded on a Nonius Kappa CCD diffractometer with an Apex II detector using graphite monochromatized CuK_α (λ = 1.54178 Å) radiation at a temperature of 173 K. The data were processed and absorption correction was made to all structures with Denzo-SMN v.0.97.638[28] unless otherwise mentioned. The structures were solved by direct methods (SHELXS-97) and refined (SHELXL-97) against F^2 by full-matrix least-squares techniques using the SHELX-97 software package (Table 3).[29] The hydrogen atoms were calculated to their idealized positions with isotropic temperature factors (1.2 or 1.5 times the C temperature factor) and refined as riding atoms. Crystal structure analysis was done using Mercury CSD 2.4 software.[30] CCDC 854053–854058.

NMR titration

4 mM C*N*BC5 was titrated with $CsPF_6$ solution in acetone-D6 and the ^{1}H NMR spectra were recorded after each addition at 30 °C. The shift in the aromatic resorcinarene signal at 6.005 ppm for the free host was followed and the binding constants were calculated using WinEQNMR2 software.[31]

SLNs

Solid lipid nanoparticles were prepared by a solvent replacement method.[32] 5 mg (or 5.27 μmol, 5.2–7.8 mg) of C*N*BC5 was dissolved in 1.5 ml of THF and 50 ml of purified water (Millipore, resistivity > 18 MΩ) was added at a constant flow during 10 s into the organic solution under vigorous stirring at 800 rpm with a magnetic stirrer. A cloudy suspension formed immediately. The suspension was stirred for an additional minute and THF was removed under reduced pressure by a rotary evaporator (44 °C, 60–70 mbar). The volume of the suspension was adjusted to 50 ml giving the final nanoparticle concentration of 100 mg L^{-1} (or 0.1 mM). The hydrodynamic diameter of the nanoparticles was measured using dynamic light scattering (Beckman Coulter N5 Submicron Particle Size Analyzer) at a 90° angle in water using plastic cuvettes (3 min equilibration, 3 min measurement). Three samples for each SLN were measured. The morphology and size of the SLN's were analyzed using scanning electron microscopy (Zeiss EVO 50). Sample preparation: a drop of SLN suspension was pipetted on a piece of silicon wafer attached by carbon tape to the sample holder and dried under ambient conditions. Samples were coated with gold (JEOL Fine coat Ion Sputter JFC-1100) prior to imaging.

Acknowledgements

Authors wish to thank Hannu Salo for SEM imaging, and Mr Reijo Kauppinen and M.Sc. Esa Haapaniemi for the help with the NMR measurements. Graduate School of Organic Chemistry and Chemical Biology, and Academy of Finland (project 128341) are acknowledged for funding.

Notes and references

1 P. Timmerman, W. Verboom and D. N. Reinhoudt, *Tetrahedron*, 1996, **52**, 2663–2704.
2 L. Mandolini and R. Ungaro, *Calixarenes in Action*, Imperial College Press, Singapore, 2000, p. 271.
3 J. Vicens and V. Böhmer, *Topics in Inclusion Science*, *Calixarenes: A Versatile Class of Macrocyclic Compounds*, Kluwer Academic Publishers, Netherlands, vol. 3, 1991, p. 264.
4 K. Helttunen and P. Shahgaldian, *New J. Chem.*, 2010, **34**, 2704–2714.
5 R. V. Rodik, A. S. Klymchenko, N. Jain, S. I. Miroshnichenko, L. Richert, V. I. Kalchenko and Y. Mély, *Chem.–Eur. J.*, 2011, **17**, 5526–5538.
6 Y. Aoyama, *Chem.–Eur. J.*, 2004, **10**, 588–593.
7 L. Y. Zakharova, V. V. Syakaev, M. A. Voronin, F. V. Valeeva, A. R. Ibragimova, Y. R. Ablakova, E. K. Kazakova, S. K. Latypov and A. I. Konovalov, *J. Phys. Chem. C*, 2009, **113**, 6182–6190.
8 L. Y. Zakharova, Y. R. Kudryashova, N. M. Selivanova, M. A. Voronin, A. R. Ibragimova, S. E. Solovieva, A. T. Gubaidullin, A. I. Litvinov, I. R. Nizameev, M. K. Kadirov, Y. G. Galyametdinov, I. S. Antipin and A. I. Konovalov, *J. Membr. Sci.*, 2010, **364**, 90–101.
9 A. F. Holloway, A. Nabok, A. A. Hashim and J. Penders, *Sens. Transducers J.*, 2010, **113**, 71–81.
10 M. Lee, S. Lee and L. Jiang, *J. Am. Chem. Soc.*, 2004, **126**, 12724–12725.
11 N. Micali, V. Villari, G. M. L. Consoli, F. Cunsolo and C. Geraci, *Phys. Rev. E: Stat., Nonlinear, Soft Matter Phys.*, 2006, **73**, 051904.
12 S. Houmadi, D. Coquière, L. Legrand, M. C. Fauré, M. Goldmann, O. Reinaud and S. Rémita, *Langmuir*, 2007, **23**, 4849–4855.
13 R. H. Müller, K. Mäder and S. Gohla, *Eur. J. Pharm. Biopharm.*, 2000, **50**, 161–177.
14 M. Pojarova, G. S. Ananchenko, K. A. Udachin, M. Daroszewska, F. Perret, A. W. Coleman and J. A. Ripmeester, *Chem. Mater.*, 2006, **18**, 5817–5819.
15 S. Ehrler, U. Pieles, A. Wirth-Heller and P. Shahgaldian, *Chem. Commun.*, 2007, 2605–2607.
16 P. Shahgaldian, M. A. Sciotti and U. Pieles, *Langmuir*, 2008, **24**, 8522–8526.
17 L. Nault, A. Cumbo, R. F. Pretôt, M. A. Sciotti and P. Shahgaldian, *Chem. Commun.*, 2010, **46**, 5581–5583.
18 C. Alfieri, E. Dradi, A. Pochini, R. Ungaro and G. D. Andreetti, *J. Chem. Soc., Chem. Commun.*, 1983, 1075–1077.
19 K. Salorinne and M. Nissinen, *J. Inclusion Phenom. Macrocyclic Chem.*, 2008, **61**, 11–27.
20 K. Salorinne and M. Nissinen, *Org. Lett.*, 2006, **8**, 5473–5476.
21 K. Salorinne and M. Nissinen, *Tetrahedron*, 2008, **64**, 1798–1807.
22 K. Salorinne, O. Lopez-Acevedo, E. Nauha, H. Häkkinen and M. Nissinen, *CrystEngComm*, 2012, **14**, 347–350.
23 K. Helttunen, N. Moridi, P. Shahgaldian and M. Nissinen, 2011, submitted.
24 M. J. McIldowie, M. Mocerino, B. W. Skelton and A. H. White, *Org. Lett.*, 2000, **2**, 3869–3871.
25 P. Shahgaldian, E. Da Silva, A. W. Coleman, B. Rather and M. J. Zaworotko, *Int. J. Pharm.*, 2003, **253**, 23–38.
26 J. Gualbert, P. Shahgaldian, A. Lazar and A. W. Coleman, *J. Inclusion Phenom. Macrocyclic Chem.*, 2004, **48**, 37–44.
27 S. Jebors, A. Leydier, Q. Wu, B. B. Ghera, M. Malbouyre and A. W. Coleman, *J. Microencapsulation*, 2010, **27**, 561–571.
28 Z. Otwinowski and W. Minor, *Methods Enzymol.*, 1997, **276**, 307–326.
29 G. M. Sheldrick, *Acta Crystallogr., Sect. A: Found. Crystallogr.*, 2008, **64**, 112–122.
30 C. F. Macrae, I. J. Bruno, J. A. Chisholm, P. R. Edgington, P. McCabe, E. Pidcock, L. Rodriguez-Monge, R. Taylor, J. van de Streek and P. A. Wood, *J. Appl. Crystallogr.*, 2008, **41**, 466–470.
31 M. J. Hynes, *J. Chem. Soc., Dalton Trans.*, 1993, 311–312.
32 M. Skiba, D. Wouessidjewe, A. Coleman, H. Fessi, J.-P. Devissaguet, D. Duchene and F. Puisieux, *Preparation and use of novel cyclodextrin-based dispersible colloidal systems in the form of nanospheres*, US Patent 5718905, 1998.

III

Resorcinarene bis-crown silver complexes and their application as antibacterial Langmuir-Blodgett films

by

Kaisa Helttunen, Negar Moridi, Patrick Shahgaldian & Maija Nissinen, 2012

Org. Biomol. Chem. 10 (2012), 2019-2025, DOI: 10.1039/C2OB06920B.

Organic & Biomolecular Chemistry

Dynamic Article Links

Cite this: *Org. Biomol. Chem.*, 2012, **10**, 2019

www.rsc.org/obc

PAPER

Resorcinarene bis-crown silver complexes and their application as antibacterial Langmuir–Blodgett films†

Kaisa Helttunen,[a] Negar Moridi,[b] Patrick Shahgaldian*[b] and Maija Nissinen*[a]

Received 14th November 2011, Accepted 12th January 2012
DOI: 10.1039/c2ob06920b

Silver complexes of a cation binding supramolecular host, resorcinarene bis-crown (C*N*BC5) with propyl, nonyl, decyl and undecyl alkyl chains were investigated by NMR titration, picrate extraction and single crystal X-ray diffraction. Binding studies showed that both 1 : 1 and 1 : 2 (host–Ag^+) complexes are present in solution with only a slight effect of the lower rim alkyl chain length on the binding constants (log *K* 4.0–4.2 for 1 : 2 complexes). Solid state complexes of the resorcinarene bis-crowns bearing either C_3 or C_{11} chains were obtained. Single crystal X-ray analyses showed that both derivatives bind silver ions by metal–arene and Ag···O coordination from the crown ether bridges and from the solvent, and pack in layered or bilayered fashion. Furthermore, the amphiphilic nature of C11BC5 was demonstrated using the Langmuir balance technique. Langmuir–Blodgett films of the amphiphilic C11BC5–Ag complex were transferred onto a substrate and shown to possess antibacterial activity against *E. coli*.

Introduction

Calixarenes and their close relatives, resorcinarenes, are a structurally versatile group of macrocyclic supramolecular hosts with a concave binding cavity and high affinity towards various guests, such as cations (alkali and alkaline earth metals, transition metals, ammonium ions), anions and small organic molecules.[1–3] The calixarene framework (Fig. 1) can be easily modified to enhance the binding selectivity and affinity towards cations, for example, by adding polyethylene glycol bridges to the hydroxyl groups at the calixarene lower rim or at the resorcinarene upper rim, binding pockets with tunable size and number of oxygen donors are created.[4] These compounds are called calixcrown ethers,[5] or calixarene bis-crowns[6] when two such bridges are attached to a single host, and they have proven to be very effective and selective hosts *e.g.* for caesium in nuclear waste treatment.[7] Resorcinarene bis-crown ethers[8,9] differ from the calixarene bis-crowns by confining both of the crown bridges on top of the binding cavity and having pendant alkyl groups below the binding site, forming an amphiphilic structure, whereas the calixarene bis-crowns usually exhibit 1,3-alternate conformations in the calixarene skeleton, which directs the two binding pockets to opposite sides of the molecule.

The recent rise of bacterial resistance to synthetic antibiotics and hospital-acquired bacterial infections has promoted the

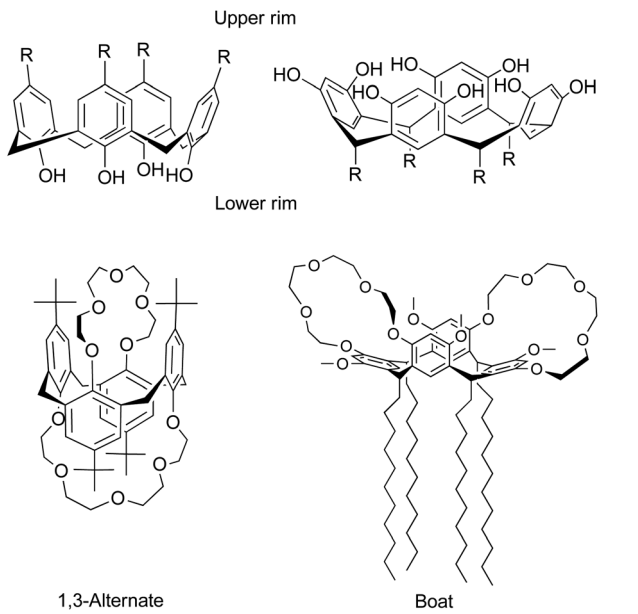

Fig. 1 Comparison of a calix[4]arene (left) with a resorcinarene (right) in the cone conformation, and a *p-tert*-butylcalix[4]arene bis-crown-5[6] with an amphiphilic resorcinarene bis-crown-5 in 1,3-alternate and boat conformations, respectively.

[a]*Nanoscience Center, Department of Chemistry, University of Jyväskylä, P.O. Box 35 Jyväskylä FI-40014, Finland. E-mail: maija.nissinen@jyu.fi; Tel: +358 50 428 0804*
[b]*School of Life Sciences, Institute of Chemistry and Bioanalytics, University of Applied Sciences Northwestern Switzerland, Gründenstrasse 40, CH-4132 Muttenz, Switzerland. E-mail: patrick.shahgaldian@fhnw.ch*

† Electronic supplementary information (ESI) available: Titration curves, Job plot, data for picrate extraction; crystallographic data and figures. CCDC reference numbers 833089 and 833090. For ESI and crystallographic data in CIF or other electronic format see DOI: 10.1039/c2ob06920b

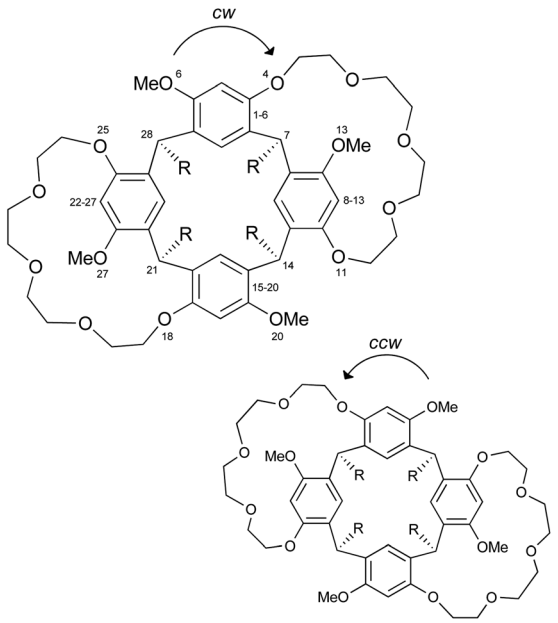

Fig. 2 General molecular formula of C*N*BC5, where N = 3, 9, 10, 11 according to the number of carbons in the alkyl group R, (R = C_NH_{2N+1}). Both clockwise, *cw*, and counterclockwise, *ccw*, enantiomers are shown.

research of alternative methods to control bacterial infections. Silver, a long known antimicrobial agent, has therefore found new applications in antibacterial materials for medical[10–14] and consumer products.[15,16] Many of these products utilize silver nanoparticles (AgNP), which provide an efficient Ag^+ release from the surface and form direct interactions with the bacterial cell wall.[13,14,17] However, silver nanoparticles also have toxic effects on mammalian cells and an extensive release of the AgNPs from the materials could lead to environmental hazards.[18,19]

Even though the exact mechanism of the antibacterial effect of silver, especially silver nanoparticles, is not fully understood, there is strong evidence that silver cations bind to the thiol groups of the proteins in the bacterial cell membrane, penetrate inside the cell and prevent normal cellular functions.[13,17,19,20] The mechanism is non-specific and therefore effective against a wide range of microorganisms. Since the toxicology and antibacterial effect of silver and AgNPs seem to depend on the particle size and the ligand,[21–24] as well as matrix and substrate properties,[25–28] there is a continuous need for new potential antibacterial materials and coatings. Several approaches have been reported; some recent examples include Ag^+ complexes,[29–32] silver clusters,[33] AgNPs with β-cyclodextrin capping,[34] electrochemically produced silver ions[35] and genetically engineered Ag^+ binding phage fibers.[36]

In supramolecular chemistry, silver complexes with macrocyclic hosts, such as crown ethers,[37] calixarenes and resorcinarenes,[38–41] and calixcrowns[42–45] are known. As a soft acid, silver prefers coordination to soft (N, S) donors,[37,40,43,44] but coordination to hard donors (O) and π-basic binding sites has also been observed.[38,39,41,42,45] However, the antibacterial activity of this kind of complex has been scarcely studied.[46] In the present manuscript, the ability of a series of resorcinarene bis-crowns to complex silver(I) in solution, in the solid-state and at the air–water interface is demonstrated. In addition, a new approach for the preparation of antibacterial coatings based on the use of self-assembled Langmuir–Blodgett (LB) films of an amphiphilic bis-crown silver complex is reported. The antibacterial properties of the LB films are assessed by applying the so-produced surface on a bacterial culture of *E. coli*.

Table 1 Binding constants for C*N*BC5:Ag^+ complexes in acetone-D6[a]

	C3BC5	C9BC5	C10BC5	C11BC5
log K_{11}[b]	2.16	2.22	2.22	2.07
log $K_{11}K_{12}$[c]	4.13	4.12	4.22	4.00

[a] NMR titration at 30 °C, *R*-values <4%, errors <8%. [b] Binding constant for the 1 : 1 complex. [c] Total binding constant for the 1 : 2 complex.

Results and discussion

Complexation studies in solution

Tetramethoxy resorcinarene bis-crown ethers, C*N*BC5's, where *N* denotes the number of carbons at the lower rim alkyl group (Fig. 2), have two polyether bridges with five oxygen donors at the resorcinarene upper rim and can thus incorporate either one or two guests into the binding site. The amphiphilic properties of the bis-crowns can be affected by selecting the length of the lower rim alkyl chains. The resorcinarene bis-crowns are known to complex alkali metal cations and silver inside their binding cavity by cation–π or metal–arene interactions and $M^+\cdots O$ coordination.[8,9,47,50] We have studied the silver binding properties of the bis-crowns (N = 3, 9, 10 and 11) in solution by means of NMR titration and picrate extraction. All of the resorcinarene bis-crowns were observed to bind silver with the affinity of log K_{11} 2.1–2.2 and log $K_{11}K_{12}$ 4.0–4.2, demonstrating that the length of the lower rim alkyl chain plays only a minor role in binding (Table 1). According to the Job plot as well as the titration data, both 1 : 1 and 1 : 2 species are present in solution. In an ideal Job plot, the maximum for the 1 : 1 complex should appear at 0.50 and for the 1 : 2 complex at 0.33. However, the obtained data show a maximum at 0.45, which can be interpreted as an indication of an equilibrium between the 1 : 1 and 1 : 2 complexes.[48]

Picrate extraction, where the transport of silver and caesium picrates from water to a chloroform phase upon complexation, was studied, and showed that the bis-crowns had a lower extraction ability towards silver (1.6–2.8%) than caesium (10%), an alkali metal cation used for reference purposes. Nonetheless, since solid liquid extraction in $CDCl_3$ showed similar complexation efficiency for both cations, the lower extraction value for silver could be explained by the differences in the cation hydration enthalpies, which are −483 kJ mol^{-1} for Ag^+ and −283 kJ mol^{-1} for Cs^+, according to Ichieda *et al*.[49]

Crystal structures

Details of the Ag^+ coordination in the bis-crown complexes were studied using single crystal X-ray diffraction. Crystals of **C3Ag2**

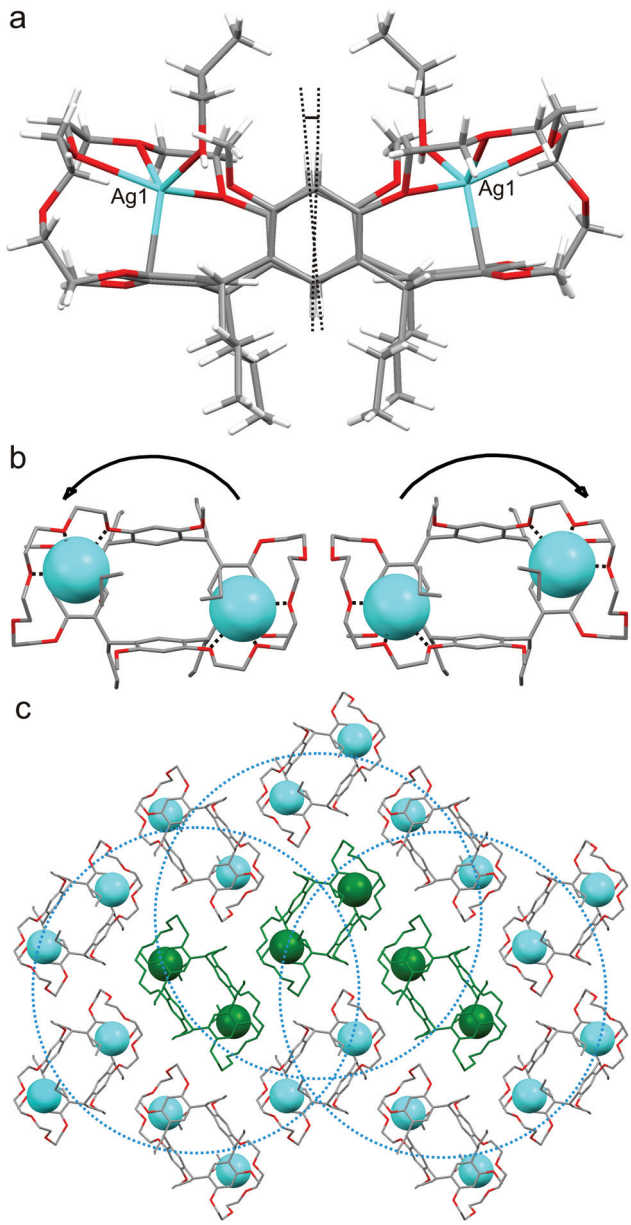

Fig. 3 Crystal structure of **C3Ag2**. (a) A side view showing tilt angle, (b) a top view of both enantiomers, (c) packing of the bis-crown complexes within a layer.

[C3BC5·$(AgPF_6)_2$·$(C_3H_8O)_2$] were grown with excess $AgPF_6$ by slow evaporation from 1-propanol, and **C11Ag1** [C11BC5·$AgPF_6$·$(C_3D_6O)_2$] with 1.5 equivalents of $AgPF_6$ from acetone-D6.

In **C3Ag2** the silver cation is coordinated by three Ag–O bonds to the crown ether bridge with bond lengths of 2.44–2.68 Å and to the 1-propanol with bond length of 2.29 Å (Fig. 3). In addition, Ag^+ is bound by a metal–arene interaction to a corner of the resorcinarene benzene ring with 2.55 Å distance to the C11 (4-position, η^1-coordination), whereas in alkali metal complexes of the bis-crowns, the cation is usually located symmetrically in the middle of the aromatic ring (η^6-coordination).[9] The cavity diameter measured as an average of the O–O distances is 6.18 Å, comparable to the silver complexes of

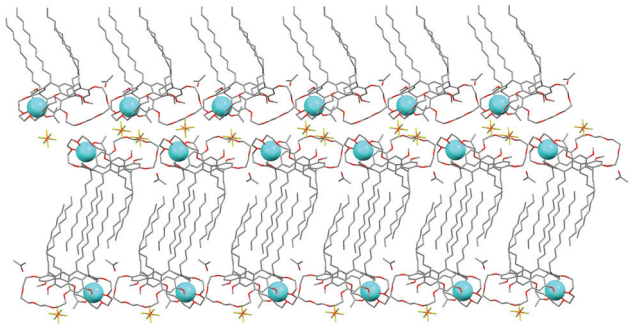

Fig. 4 Bilayer packing of **C11Ag1** with counter anions shown between the layers.

C2BC5.[47] The coordination to the other cation is identical due to symmetry. The resorcinarene core of the C3BC5 is in a slightly twisted boat conformation, which probably arises from the space needed for including the solvent inside the cavity. Interestingly, Ag^+ prefers coordination to alcohols over the PF_6^- anion, contrary to the K^+ and Cs^+ complexes, where the PF_6^- usually coordinates between the two cations inside the binding cavity.[8,9,50]

C3Ag2 packs in parallel layers, which are separated by 10.51 Å (methine carbon planes of superposed complexes). Within a layer, each complex is surrounded by six adjacent complexes with an identical chirality forming a beautiful "chain mail" pattern (Fig. 3c). The counter anions contribute to the crystal packing between the layers by forming short contacts between the crown ether bridges and the lower rim alkyl groups. Because the lower rim alkyl chains are only three carbons long, the complexes form an up-down arrangement and separation into hydrophobic and hydrophilic bilayers does not occur. The structure of **C3Ag2** is similar to the 1-propanol and 2-propanol solvates of C2BC5·$2AgPF_6$,[47] and therefore we can predict that the addition of one carbon, from ethyl to propyl, in the lower rim alkyl chains does not affect the crystal packing of the layered structures.

The amphiphilic C11BC5 crystallized as a 1 : 1 complex with silver (**C11Ag1**), where Ag^+ has very similar coordination in comparison to **C3Ag2** with the exception of acetone instead of 1-propanol as the coordinating solvent (Ag–O 2.28 Å). The silver is bound between alkoxy substituents in the 5-position of the resorcinol ring (2.37 Å) instead of the 4-position observed in **C3Ag2**, and coordinates to the three middle oxygen donors in the crown ether bridge with distances of 2.46–2.84 Å. This is probably due to the increased space at the binding pocket in comparison to **C3Ag2**, which additionally leads to a slight decrease in twisting of the resorcinarene framework. The free binding site is partly filled by a methoxy group C75 pointing inside the cavity. The long alkyl chains of **C11Ag1** pack in organized hydrophobic layers, whereas the upper rims of the complexes are placed on top of each other and connected by the anions, forming a bilayer structure clearly indicating the amphiphilic nature of the complex (Fig. 4).

Langmuir–Blodgett films

The amphiphilic self-assembly properties of C11BC5 were studied by means of the Langmuir balance technique on water or

Table 2 Langmuir isotherm data of C11BC5 on pure water and 100 μM $AgNO_3$[a]

$AgNO_3$[b]	Π_c[c]	A_c[d]	A_{lim}[e]
0	33	157	174
100	35	163	181

[a] Surface tension values are expressed in mN m^{-1} and areas in $Å^2$ per molecule. [b] In μM. [c] The surface pressure at the collapse of the monolayer. [d] The surface area at the collapse of the monolayer. [e] Extrapolation of the linear part of the isotherm on the *x* axis.

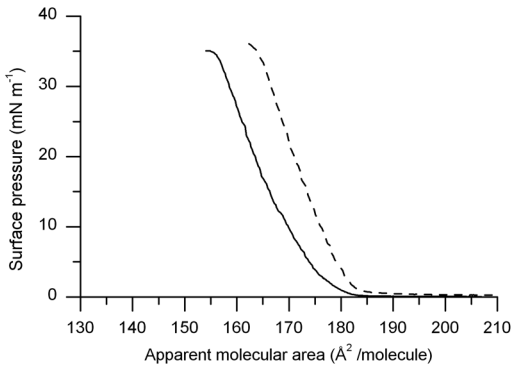

Fig. 5 *Π*/*A* isotherms of C11BC5 on pure water (—) and 100 μM $AgNO_3$ (···) sub-phases.

on an aqueous subphase containing 100 μM $AgNO_3$. From the results (in Table 2, Fig. 5) it could be seen that while the monolayer on pure water subphase collapses at 33 mN m^{-1} at a surface area of 157 $Å^2$ per molecule, the presence of silver ions causes a slight increase in the collapse pressure to a value of 35 mN m^{-1} and an increase in the collapse area to a value of 163 $Å^2$ per molecule suggesting interactions between the amphiphiles spread at the interface and the silver ions. Since the structure of C11BC5 is relatively rigid, and the resorcinarene framework is preorganized in the boat conformation for binding, no dramatic changes in the molecular areas upon complexation are expected. However, the A_c values measured are in excellent agreement with the crystal structure packing. In the solid state the pure C9BC5 shows an "apparent molecular area" of 159 $Å^2$, and C11BC5 has a collapse area of 157 $Å^2$ at the air–water interface. Moreover, the molecular area of 163 $Å^2$ at the air–water interface when the amphiphile is interacting with silver is also consistent with the solid-state packing with values of 166 $Å^2$ and 179 $Å^2$ for the 1 : 1 and 1 : 2 complexes, respectively.

Antibacterial experiments

In order to study the potential antibacterial effects of the produced complexes, four layers of the C11BC5–Ag(I) complex (*Y*-type) were transferred on hydrophobic glass substrates using the Langmuir–Blodgett approach and applied on a bacterial (*E. coli*) carpet grown on agar gel, as shown in Fig. 6. In addition to the samples, control samples with the same treatment of C11BC5 but in the absence of silver were prepared, along with controls of a glass slide dipped in 100 μM $AgNO_3$ solution and a hydrophobic glass slide. The area covered by the bacteria on the agar

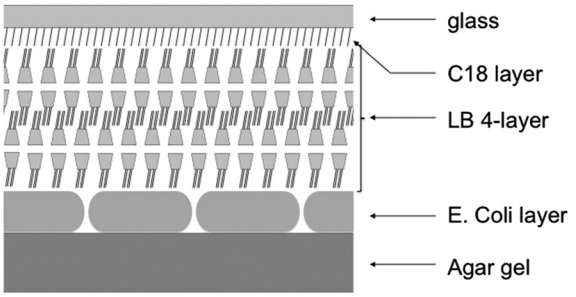

Fig. 6 Schematic representation of the experimental set-up used to test the antibacterial properties of C11BC5–Ag(I) complex.

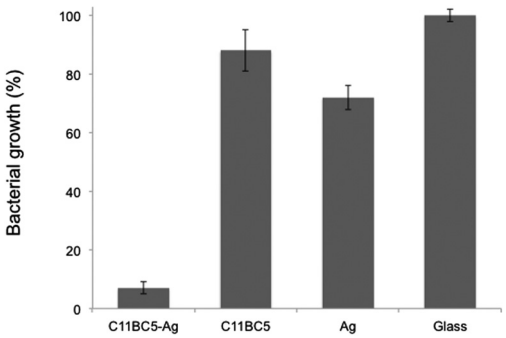

Fig. 7 *E. coli* growth (normalized results) on an agar plate submitted to a Langmuir–Blodgett multilayer of C11BC5 transferred from a subphase containing silver (100 μM, C11BC5–Ag) or pure water (C11BC5); hydrophobic glass slides (glass) and hydrophobic glass slides dipped in silver nitrate (100 μM, Ag).

gel was measured from microscope images after incubation of the samples for 5 hours at 37 °C (93%) and was used to normalize the measured data; the results are given in Fig. 7.

From the results it could be seen that the substrate dipped in silver nitrate shows only a limited loss of bacterial viability with a bacterial growth that remains as high as 72 ± 4%. This result may be attributed to the presence, at the surface of the glass slide, of unmodified areas (hydrophilic) that bind silver ions *via* electrostatic interactions and release it when in contact with bacteria. Nevertheless, the inhibitory effect observed for C11BC5–Ag(I) is relevantly higher with a bacterial growth of only 7 ± 2% while the same LB film in the absence of silver shows a growth of 88 ± 7%. This clearly shows that the antibacterial effect results from the presence of silver in the LB films. Taking into account the isotherm data and assuming the "best case" scenario where C11BC5 forms a 1 : 1 complex at the interface, the density of silver ions at the surface of the treated substrate would be approximately 0.4 nmol cm^{-2} giving a bulk concentration in the medium of 90 nM; this value is 210-fold lower than the complete inhibitory concentration (CIC) of silver for *E. coli* that has been reported to be 18.9 μM.[51]

Conclusions

The resorcinarene bis-crowns bind silver in solution, in the solid state as well as at the air–water interface on LB films. The lower

rim alkyl chain length has an effect on the self-assembling properties of the bis-crowns, as well as their complexes. When the bis-crowns are equipped with long alkyl chains (C_{11}), they show amphiphilic *i.e.* surfactant-like properties forming monomolecular Langmuir–Blodgett films, which enables their use in functional coatings. The LB films of the C11BC5–Ag complex show a relevant antibacterial effect against *E. coli* when compared to pure hydrophobic glass. The solution studies show that the binding constants for Ag^+ complexes are log K_{11} 2.1–2.2 and log $K_{11}K_{12}$ 4.0–4.2, which means that the free host, the guest, and the 1 : 1 and 1 : 2 complexes are in equilibrium and that the silver binding is reversible. Since the estimated concentration of silver in the LB films of the C11BC5–Ag complex is very low, 90 nM, it would not allow a bulk effect of the silver ions in the culture medium, but instead suggests that the antibacterial effect might be due to the close contact between the silver releasing layer and the bacteria. It is also worth noting that the antibacterial effect of silver includes a hypothesis that the Ag^+ ions bind to the thiol groups on the surface of bacteria, which is supported by the ability of the thiol-containing compounds to block the antibacterial activity of silver,[52] and that the affinity of silver for sulfur is much higher than it is for oxygen. Therefore, it is logical to assume that silver is released from the bis-crown complexes in the presence of the thiol groups on the bacterial surface, which leads to bacterial death and inhibits the overall bacterial growth as observed in these experiments. Further experiments are planned to obtain a more detailed understanding of the antibacterial effect of the bis-crown silver complexes, and whether the complex could be transported through bacterial cell membranes, enhancing the toxicity of silver. The preliminary results reported in this paper serve as a proof of principle for the development of supramolecular antibacterial materials, which in comparison to the free silver salts already show the possibility to control the release of silver and the need for lower doses. Work is underway to study the effect of thicker LB multilayers on *E. coli* growth over longer periods of time.

Experimental

Materials

All reagents and solvents were purchased from Sigma-Aldrich and VWR and used without further purification. NMR spectra were recorded with a Bruker Avance DRX 500 spectrometer at 500 MHz for ^{1}H at 30 °C. UV-vis spectra were measured using a Perkin Elmer Lambda 850 spectrometer. Tetramethoxy resorcinarene bis-crown ethers were synthesized according to a previous reference[8] from the corresponding tetramethoxy resorcinarenes.[53] Characterization data were published elsewhere.[50]

Binding studies

4 mM C*N*BC5 was titrated with $AgPF_6$ solution in acetone-D6 and ^{1}H NMR spectra were recorded after each addition at 30 °C. The shift in the aromatic resorcinarene signal at 6.005 ppm for the free host was followed and binding constants were calculated using WinEQNMR2 software.[54] Job plot samples were prepared from 4 mM solutions of C*N*BC5 and $AgPF_6$ in acetone-D6 by mixing host and guest at 9 : 1, 3 : 1, 3 : 2, 1 : 1, 2 : 3, 3 : 7, 2 : 8 and 1 : 9 ratios while keeping the total concentration constant.

Crystallography

Single crystal X-ray data were recorded on a Nonius Kappa CCD diffractometer with Apex II detector using graphite monochromated CuKα (λ = 1.54178 Å) radiation at a temperature of 173 K. The data were processed and absorption correction was made to all structures with Denzo-SMN v.0.97.638[55] unless otherwise mentioned. The structures were solved by direct methods (SHELXS-97) and refined (SHELXL-97) against F^2 by full-matrix least-squares techniques using SHELX-97 software package.[56] The hydrogen atoms were calculated to their idealized positions with isotropic temperature factors (1.2 or 1.5 times the *C* temperature factor) and refined as riding atoms. Crystal structure analysis was done using Mercury CSD 2.4 software.[57] CCDC 833089–833090.

C3Ag2: Crystallization of C3BC5 with excess $AgPF_6$ in 1-propanol by slow evaporation afforded a colorless block crystal (0.20 × 0.20 × 0.06). Orthorhombic *Pbcn*, a = 14.6967(5), b = 21.0360(7), c = 23.8819(9), V = 7383.3(4) Å^3, $C_{60}H_{84}O_{14}\cdot(AgPF_6)_2\cdot(C_3H_8O)_2$, Z = 4, D_{calc} = 1.489, FW = 1655.14, Meas. Reflns = 12333, Indep. Reflns = 6524, R_{int} = 0.0223, $R_1[I > 2\sigma(I)]$ = 0.0503, w$R_2[I > 2\sigma(I)]$ = 0.1358, GooF = 1.029. Disordered 1-propanol over two positions: (C101–C106) with site occupancy of A : B = 0.6 : 0.4. Atoms C104–C106 refined as isotropic. Disordered atoms were restrained using DFIX, DELU and SIMU.

C11Ag1: Crystallization of C11BC5 with 1.5 equiv. of $AgPF_6$ in acetone-D6 by slow evaporation afforded a colorless needle crystal (0.30 × 0.04 × 0.04). Monoclinic $P2_1/n$, a = 12.2817(4), b = 60.688(2), c = 13.4217(4), β = 97.516(2), V = 9918.0(5) Å^3, $C_{92}H_{148}O_{14}\cdot AgPF_6\cdot(C_3D_6O)_2$, Z = 4, D_{calc} = 1.245, FW = 1859.17, Meas. Reflns = 43546, Indep. Reflns = 14946, R_{int} = 0.1307, $R_1[I > 2\sigma(I)]$ = 0.0976, w$R_2[I > 2\sigma(I)]$ = 0.2245, GooF = 1.019. Absorption correction was made using SADABS.‡ C32–C38 were restrained using SADI, DELU and SIMU.

Langmuir–Blodgett films

Experiments were performed using a NIMA 112D system. The trough and the barriers were cleaned with analytical grade chloroform and nanopure water (resistivity ≥18 MΩ cm). Surface tension was monitored using a Wilhelmy plate. Compressions were performed in a continuous mode at a speed rate of 5 cm^2 min^{-1} either on pure water sub-phases or on silver nitrate aqueous solutions (100 μM). All isotherms were measured in triplicate to ensure their reproducibility. In order to ensure the absence of surface-active molecules in the sub-phase, compressions without C11BC5 spread on the surface were performed; in no case could a relevant change in surface tension be observed.

LB transfer experiments were performed using a D1L-75 vertical dipping system at a surface tension-controlled mode and a speed rate of 5 mm min^{-1}. The glass slides used as substrates for the LB deposition were cleaned by immersing them in a piranha solution (H_2O_2, H_2SO_4; 70 : 30, vol : vol)§ at 20 °C for 4 hours

followed by ultrasonic treatment in nanopure water for 30 min. The cleaned glass slides were dried under nitrogen stream and immersed in a 10 mM anhydrous heptane solution of octadecyltrichlorosilane (OTS) for 30 min at 20 °C. The glass slides were thoroughly rinsed with heptane and chloroform, respectively, and dried under nitrogen stream. Four Langmuir–Blodgett monolayers (*Y*-type) of C11BC5:Ag were transferred onto the hydrophobic glass slides at a surface tension 25 mN m^{-1}. Three controls were prepared: a hydrophobic glass slide, a hydrophobic glass slide dipped in the 100 μM $AgNO_3$ solution, and a hydrophobic glass coated with four LB monolayers of C11BC5 in the absence of $AgNO_3$.

Antibacterial experiment

Liquid LB agar (14 mL) was poured into disposable sterilized Petri dishes and allowed to solidify as thin (2.5 mm) LB agar discs. *E. coli* isolated from human intestinal florabacteria was cultivated in LB medium at 37 °C for 24 hour until reaching $OD_{600} = 1$. The bacterial suspension was then diluted 167 times in the LB medium. Diluted bacteria (1 mL) were deposited on the LB agar plate, spread uniformly and dried. The coated glass slides with C11BC5:Ag Langmuir–Blodgett monolayers and the three controls were gently deposited over the solidified agar gel. The prepared samples were incubated at 37 °C. The antibacterial effect was measured from the samples after a 5 hour incubation using a Olympus BX51 light microscope equipped with a 40× objective. The obtained images (6 per sample) were then analyzed using image processing software GIMP 2.6 and ImageJ in order to numerically evaluate the bacterial surface coverage. The obtained data are presented normalized using the results obtained for the unmodified hydrophobic glass slide.

Acknowledgements

This work was supported by the National Graduate School of Organic Chemistry and Chemical Biology and the FHNW research fund. We wish to thank M.Sc. Tahnie Barboza and Ms. Hélène Campos Barbosa for their assistance in the synthesis.

Notes and references

‡SADABS Area-Detector Absorption Correction, Siemens Industrial Automation, Inc., Madison, WI, 1996.
§Warning: piranha solution is highly oxidative; it could explode in contact with organics and must be handled with extreme care.

1 P. Timmerman, W. Verboom and D. N. Reinhoudt, *Tetrahedron*, 1996, **52**, 2663–2704.
2 *Calixarenes in Action*, ed. L. Mandolini and R. Ungaro, Imperial College Press, Singapore, 2000, p. 271.
3 Z. Asfari, V. Böhmer, J. Harrowfield and J. Vicens, *Calixarenes 2001*, Kluwer Academic Publishers, The Netherlands, 2001, p. 683.
4 C. Alfieri, E. Dradi, A. Pochini, R. Ungaro and G. D. Andreetti, *J. Chem. Soc., Chem. Commun.*, 1983, 1075–1077.
5 For a review of calixcrowns: K. Salorinne and M. Nissinen, *J. Inclusion Phenom. Macrocyclic Chem.*, 2008, **61**, 11–27.
6 E. Ghidini, F. Ugozzoli, R. Ungaro, S. Harkema, A. Abu El-Fadl and D. N. Reinhoudt, *J. Am. Chem. Soc.*, 1990, **112**, 6979–6985.
7 See for a review: J. Vicens, *J. Inclusion Phenom. Macrocyclic Chem.*, 2006, **55**, 193–196.
8 K. Salorinne and M. Nissinen, *Org. Lett.*, 2006, **8**, 5473–5476.
9 K. Salorinne and M. Nissinen, *Tetrahedron*, 2008, **64**, 1798–1807.
10 J. Ricco, *J. Vasc. Surg.*, 2006, **44**, 339–346.
11 M. D. Khare, S. S. Bukhari, A. Swann, P. Spiers, I. McLaren and J. Myers, *J. Infect.*, 2007, **54**, 146–150.
12 K. Galiano, C. Pleifer, K. Engelhardt, G. Brössner, P. Lackner, C. Huck, C. Lass-Flörl and A. Obwegeser, *Neurol. Res.*, 2008, **30**, 285–287.
13 H. Cao and X. Liu, *Wiley Interdiscip. Rev.: Nanomed. Nanobiotechnol.*, 2010, **2**, 670–684.
14 K. K. Y. Wong and X. Liu, *Med. Chem. Commun.*, 2010, **1**, 125–131.
15 H. Y. Ki, J. H. Kim, S. C. Kwon and S. H. Jeong, *J. Mater. Sci.*, 2007, **42**, 8020–8024.
16 T. M. Benn and P. Westerhoff, *Environ. Sci. Technol.*, 2008, **42**, 4133–4139.
17 J. Liu, D. A. Sonshine, S. Shervani and R. H. Hurt, *ACS Nano*, 2010, **4**, 6903–6913.
18 X. Chen and H. J. Schluesener, *Toxicol. Lett.*, 2008, **176**, 1–12.
19 C. Marambio-Jones and E. M. V. Hoek, *J. Nanopart. Res.*, 2010, **12**, 1531–1551.
20 N. Silvestry-Rodriguez, E. E. Sicairos-Ruelas, C. P. Gerba and K. R. Bright, *Rev. Environ. Contam. Toxicol.*, 2007, **191**, 23–45.
21 N. V. Ayala-Núñez, H. H. Lara Villegas, L. d. C. Ixtepan Turrent and C. Rodríguez Padilla, *NanoBiotechnology*, 2009, **5**, 2–9.
22 A. Le, L. T. Tam, P. D. Tam, P. T. Huy, T. Q. Huy, N. Van Hieu, A. A. Kudrinskiy and Y. A. Krutyakov, *Mater. Sci. Eng., C*, 2010, **30**, 910–916.
23 H. Liu, S. A. Dai, K.-Y Fu and S. Hsu, *Int. J. Nanomed.*, 2010, **5**, 1017–1028.
24 M. V. D. Z. Park, A. M. Neigh, J. P. Vermeulen, L. J. J. de la Fonteyne, H. W. Verharen, J. J. Briedé, H. van Loveren and W. H. de Jong, *Biomaterials*, 2011, **32**, 9810–9817.
25 A. Travan, C. Pelillo, I. Donati, E. Marsich, M. Benincasa, T. Scarpa, S. Semeraro, G. Turco, R. Gennaro and S. Paoletti, *Biomacromolecules*, 2009, **10**, 1429–1435.
26 P. Pallavicini, A. Taglietti, G. Dacarro, Y. Antonio Diaz-Fernandez, M. Galli, P. Grisoli, M. Patrini, G. Santucci De Magistris and R. Zanoni, *J. Colloid Interface Sci.*, 2010, **350**, 110–116.
27 V. Sedlarik, T. Galya, J. Sedlarikova, P. Valasek and P. Saha, *Polym. Degrad. Stab.*, 2010, **95**, 399–404.
28 X. Zan, M. Kozlov, T. J. McCarthy and Z. Su, *Biomacromolecules*, 2010, **11**, 1082–1088.
29 L. Balogh, D. R. Swanson, D. A. Tomalia, G. L. Hagnauer and A. T. McManus, *Nano Lett.*, 2001, **1**, 18–21.
30 S. Pal, E. J. Yoon, S. H. Park, E. C. Choi and J. M. Song, *J. Antimicrob. Chemother.*, 2010, **65**, 2134–2140.
31 S. Patil, J. Claffey, A. Deally, M. Hogan, B. Gleeson, L. M. Menéndez Méndez, H. Müller-Bunz, F. Paradisi and M. Tacke, *Eur. J. Inorg. Chem.*, 2010, 1020–1031.
32 C. Abbehausen, T. A. Heinrich, E. P. Abrão, C. Costa-Neto, W. R. Lustri, A. L. B. Formiga and P. P. Corbi, *Polyhedron*, 2011, **30**, 579–583.
33 I. Tsyba, B. B. Mui, R. Bau, R. Noguchi and K. Nomiya, *Inorg. Chem.*, 2003, **42**, 8028–8032.
34 S. Jaiswal, B. Duffy, A. K. Jaiswal, N. Stobie and P. McHale, *Int. J. Antimicrob. Agents*, 2010, **36**, 280–283.
35 W. K. Jung, H. C. Koo, K. W. Kim, S. Shin, S. H. Kim and Y. H. Park, *Appl. Environ. Microbiol.*, 2008, **74**, 2171–2178.
36 J. Y. Mao, A. M. Belcher and K. J. Van Vliet, *Adv. Funct. Mater.*, 2010, **20**, 209–214.
37 T. Nabeshima, *J. Inclusion Phenom. Mol. Recognition*, 1998, **32**, 331–345.
38 A. Ikeda and S. Shinkai, *J. Am. Chem. Soc.*, 1994, **116**, 3102–3110.
39 W. Xu, R. J. Puddephatt, K. W. Muir and A. A. Torabi, *Organometallics*, 1994, **13**, 3054–3062.
40 A. F. Danil de Namor, O. E. Piro, L. E. Pulcha Salazar, A. F. Aguilar-Cornejo, N. Al-Rawi, E. E. Castellano and F. J. Sueros Velarde, *J. Chem. Soc., Faraday Trans.*, 1998, **94**, 3097–3104.
41 M. Munakata, L. P. Wu, T. Kuroda-Sowa, M. Maekawa, Y. Suenaga, K. Sugimoto and I. Ino, *J. Chem. Soc., Dalton Trans.*, 1999, 373–378.
42 P. Thuéry, M. Nierlich, F. Arnaud-Neu, B. Souley, Z. Asfari and J. Vicens, *Supramol. Chem.*, 1999, **11**, 143–150.
43 J. Y. Lee, J. Kwon, C. S. Park, J. Lee, W. Sim, J. S. Kim, J. Seo, I. Yoon, J. H. Jung and S. S. Lee, *Org. Lett.*, 2007, **9**, 493–496.
44 J. Y. Lee, H. J. Kim, C. S. Park, W. Sim and S. S. Lee, *Chem.–Eur. J.*, 2009, **15**, 8989–8992.
45 M. S. Wong, P. F. Xia, P. K. Lo, X. H. Sun, W. Y. Wong and S. Shuang, *J. Org. Chem.*, 2006, **71**, 940–946.
46 Y. Yi, Y. Wang and H. Liu, *Carbohydr. Polym.*, 2003, **53**, 425–430.

47 K. Salorinne, O. Lopez-Acevedo, E. Nauha, H. Häkkinen and M. Nissinen, *CrystEngComm*, 2012, **14**, 347–350.
48 V. M. S. Gil and N. C. Oliveira, *J. Chem. Educ.*, 1990, **67**, 473–478.
49 N. Ichieda, M. Kasuno, K. Banu, S. Kihara and H. Nakamatsu, *J. Phys. Chem. A*, 2003, **107**, 7597–7603.
50 K. Helttunen, K. Salorinne, T. Barboza, H. Campos Barbosa, A. Suhonen and M. Nissinen, *New J. Chem.*, 2012, DOI: 10.1039/c2nj20981k.
51 G. Zhao and S. E. Stevens Jr, *BioMetals*, 1998, **11**, 27–32.
52 S. Y. Liau, D. C. Read, W. J. Pugh, J. R. Furr and A. D. Russell, *Lett. Appl. Microbiol.*, 1997, **25**, 279–283.
53 M. J. McIldowie, M. Mocerino, B. W. Skelton and A. H. White, *Org. Lett.*, 2000, **2**, 3869–3871.
54 M. J. Hynes, *J. Chem. Soc., Dalton Trans.*, 1993, 311–312.
55 Z. Otwinowski and W. Minor, *Methods Enzymol.*, 1997, **276**, 307–326.
56 G. M. Sheldrick, *Acta Crystallogr., Sect. A: Found. Crystallogr.*, 2008, **64**, 112–122.
57 C. F. Macrae, I. J. Bruno, J. A. Chisholm, P. R. Edgington, P. McCabe, E. Pidcock, L. Rodriguez-Monge, R. Taylor, J. van de Streek and P. A. Wood, *J. Appl. Crystallogr.*, 2008, **41**, 466–470.

IV

Conformational polymorphism and amphiphilic properties of resorcinarene octapodands

by

Kaisa Helttunen, Elisa Nauha, Anni Kurronen, Patrick Shahgaldian & Maija Nissinen, 2011

Org. Biomol. Chem. 9 (2011), 906–914, DOI: 10.1039/C0OB00602E.

Organic & Biomolecular Chemistry

Dynamic Article Links

Cite this: *Org. Biomol. Chem.*, 2011, **9**, 906

www.rsc.org/obc

PAPER

Conformational polymorphism and amphiphilic properties of resorcinarene octapodands†

Kaisa Helttunen,[a] Elisa Nauha,[a] Anni Kurronen,[a] Patrick Shahgaldian[b] and Maija Nissinen*[a]

Received 18th August 2010, Accepted 25th October 2010
DOI: 10.1039/c0ob00602e

o-Nitroaniline functionalized resorcinarene octapodands **1–5** with pendant methyl, ethyl, pentyl, nonyl or 1-decenyl groups, respectively, were synthesized and their structural properties investigated using X-ray crystallography and NMR spectroscopy. The upper rim of each podand is identical containing flexible side arms, in which rotation around the -OCH_2CH_2N- linkers create excellent possibilities for polymorphism. Two conformational polymorphs of acetone solvate of **2** were identified containing different side arm orientation and crystal packing. Compound **1** crystallized from acetone and nitromethane yielding two pseudopolymorphs with different packing motifs. The longer alkyl chains of **3–5** lead to differences in solubility and induce amphiphilic properties, which were studied at the air–water interface using the Langmuir-film technique. Crystals of amphiphilic compound **5**, which has hydrophobic alkyl tails at the lower rim and hydrophilic nitroaniline groups at the upper rim, showed an interesting packing motif with alternating aromatic and aliphatic layers. Versatile structures of the octapodands in solid state and in solution serve as an example of how conformational flexibility can be utilized in crystal engineering and creating self-assembling monolayer structures.

Introduction

Calixarenes and resorcinarenes are widely utilized building blocks for designing supramolecular hosts and self-assembling structures since they offer a concave binding cavity and diverse synthetic pathways for obtaining desired functionalities.[1–6] Recently, work in this field has continued to produce increasingly elaborate host molecules for cations,[7–12] anions,[13,14] ion-pairs,[15,16] neutral guests[10,15,16] and biomolecules.[17,18] In addition, unique self-assembling properties of resorcinarenes have been used to prepare novel nanomaterials with examples ranging from gold/organic microtubular composites[19,20] and coated gold and cobalt nanoparticles[21–24] to dimeric[25,26] and hexameric capsules[27] and molecular containers.[11,12] The design of amphiphilic calixarenes and resorcinarenes bearing long alkyl chains has provided interesting applications,[26,28] such as templating calcite crystallization under monolayers[29] and preparation of solid lipid nanoparticles which interact with DNA[30,31] or proteins.[32]

Resorcinarenes and calixarenes seem to present unlimited possibilities for crystal engineering and creating new supramolecular architectures such as nanotubes,[33,34] preorganizing arrays of fullerene C_{60}[35,36] and benzil in resorcinarene matrices.[37] However, polymorphism, the existence of two or more different crystal forms of one compound, which is considered a very important aspect of crystal engineering,[38] has hardly been studied in these macrocyclic hosts. Resorcinarenes and calixarenes polymorphs have been found by changing crystallization conditions, such as solvent, temperature or pressure,[39–43] but to our knowledge, there are not any reported cases where resorcinarenes or calixarenes are able to form conformational polymorphs[44] in identical crystallization conditions. However, for calixcrowns,[41] a thermally induced conformational change has been reported, and a case of thermal polymorphic change for amino acid derivative of calixarene has been published.[39] Investigation of new polymorphs of a known macrocyclic compound has already provided interesting applications, such as gas absorption in the crystal lattice of various calixarenes.[45–50] In addition, development of new potentially polymorphic compounds can lead the way to new material innovations and deeper understanding of the principles directing the crystallization process.

Our earlier work with tetramethoxy resorcinarenes has provided a selection of cation and anion binding receptors by adding crown ether bridges or pendant groups in upper rim hydroxyl groups.[51–54] A similar synthetic approach has now been applied to resorcinarenes with the objective of creating novel self-assembling properties for supramolecular hosts.

[a]*Department of Chemistry, Nanoscience Center, University of Jyväskylä, P.O. Box 35, FIN-40014, University of Jyväskylä, Finland. E-mail: maija.nissinen@jyu.fi; Fax: +358 14 260 4756; Tel: +358 14 260 4242*
[b]*School of Life Sciences, Institute of Chemistry and Bioanalytics, University of Applied Sciences Northwestern Switzerland, Gründenstrasse 40, 4132, Muttenz, Switzerland*

† Electronic supplementary information (ESI) available: Synthetic procedures and NMR spectra for each podand; details of X-ray structure analysis and crystallographic data. CCDC reference numbers 781919–781925. For ESI and crystallographic data in CIF or other electronic format see DOI: 10.1039/c0ob00602e

Indeed, a selection of structurally flexible resorcinarene octapodands were obtained, which exhibit conformational polymorphism and in the case of long alkyl chain compounds, amphiphilic properties, which were demonstrated by preparing Langmuir-films at the air–water interface, as well as formation of a crystal structure with alternating aromatic and aliphatic layers.

Results and Discussion

Synthesis

Octapodands **3–5** bearing long alkyl chains were prepared by attaching eight *o*-nitro-*N*-(2-hydroxyethyl)aniline units into a resorcinarene platform using Cs_2CO_3 or K_2CO_3 as a base and dibenzo-18-crown-6 as a phase transfer catalyst in refluxing acetonitrile (Scheme 1).[54] The octapodands were obtained as yellow amorphous powders with 40–65% yields. Instead of the tosyl leaving group (compound **6**), a mesyl group (compound **7**) can be used in the reaction as was discovered in the synthesis of **3** and **5**. TG/DTA analysis of **5** showed gradual decomposition between 273–600 °C without a clear melting point according to the enthalpy values. Melting point measurements of each synthesis batch varied between 56 and 77 °C and therefore the reported melting points for amorphous podands should be considered as rough estimates only.

1 and **2** with pendant methyl and ethyl groups, respectively, were synthesized using the above mentioned reaction conditions, but the product was collected from the filtered reaction mixture by extraction with CH_2Cl_2 unlike **3–5**, which are soluble in acetonitrile and were collected from the filtrate. In addition, **1** and **2** were recrystallized from hot acetone to provide orange crystalline solids at 23–31% yield or alternatively treated as the long chain podands to produce amorphous powders at 44–54% yield.‡

Single crystal X-ray crystallography

The octapodands **1**, **2** and **5** provided single crystals suitable for X-ray analysis from nitromethane–CH_2Cl_2 solution (structures **1A**, **2C** and **5A** respectively). Crystallization from nitromethane was a slow process, and took several months for all the investigated compounds providing a selection of yellow needles, blocks, plates and rods. **1A** and **5A** were crystallized without nitromethane in the lattice but **2C**, using acetone solvate as a starting material incorporated two disordered nitromethane molecules per unit cell. Structure **2D**, which crystallized from acetonitrile–CH_2Cl_2 solution has an isomorphous unit cell and packing with **2C**. Compounds **1** and **2** crystallized from acetone and acetone–CH_2Cl_2 solutions as acetone solvates (structures **1B**, **2A** and **2B**), which were only poorly soluble in acetone. Interestingly, **2A** and **2B** formed simultaneously in the same test tube and are conformational polymorphs of each other.§ Structure **2A** was obtained from a plate and structure **2B** from a needle shaped crystal. Obtaining several polymorphs simultaneously under the same crystallization conditions is quite rare; an example of such a macrocyclic compound is furanotribenzo-21-crown-7 in which the conformation of the macrocycle is however unchanged.[56] Crystallographic data of all structures are presented in Table 1.

The resorcinarene core of all octapodands is in a boat conformation since all phenolic hydroxyl groups are alkylated.[4] The angle of the upright resorcinol rings C1–C6 and C15–C20 against

‡ For some crystallization experiments the amorphous form of **1** and **2** was used.

§ The original crystallization was made from acetone–DCM by dissolving part of the sample in acetone and adding DCM until the sample was fully dissolved. Later on pure acetone and acetone–DCM 3 : 1 were used.

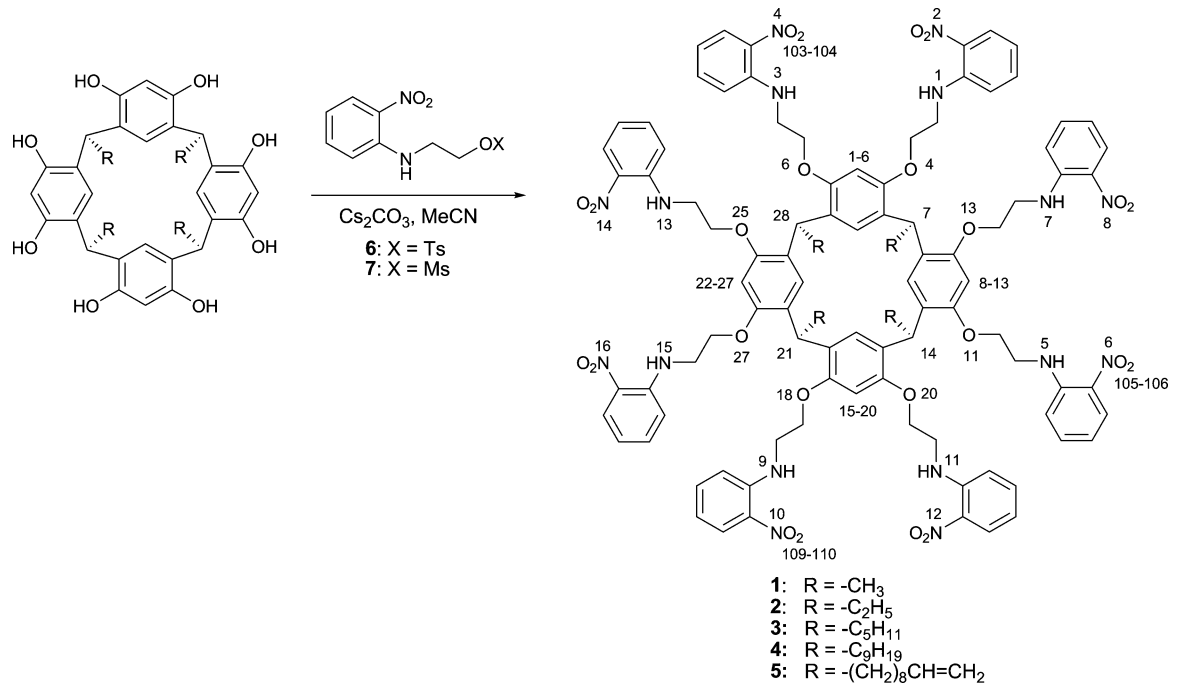

Scheme 1 Synthetic procedure and selected crystallographic numbering for octapodands.

Table 1 X-ray structure parameters

	1A	1B	2A	2B	2C	2D	5A
Crystallization solvent	nitromethane–CH_2Cl_2	acetone	acetone–CH_2Cl_2	acetone–CH_2Cl_2	nitromethane–CH_2Cl_2	acetonitrile–CH_2Cl_2	nitromethane–CH_2Cl_2
Crystal shape	block	plate	plate	needle	needle	block	rod
Crystal size/mm	0.40 × 0.20 × 0.20	0.20 × 0.12 × 0.08	0.18 × 0.14 × 0.02	0.20 × 0.08 × 0.02	0.24 × 0.10 × 0.04	0.20 × 0.10 × 0.10	0.20 × 0.10 × 0.10
Formula	$C_{96}H_{96}N_{16}O_{24}$	$C_{96}H_{96}N_{16}O_{24}\cdot(CH_3)_2CO$	$C_{100}H_{104}N_{16}O_{24}\cdot(CH_3)_2CO$	$C_{100}H_{104}N_{16}O_{24}\cdot(CH_3)_2CO$	$C_{100}H_{104}N_{16}O_{24}$[a]	$C_{100}H_{104}N_{16}O_{24}\cdot C_2H_3N$[a]	$C_{132}H_{160}\ N_{16}O_{24}\cdot 1.5H_2\ O$
FW	1857.89	1915.97	1972.07	1972.07	1913.99	1955.05	2381.78
a/Å	12.2700(3)	11.8003(4)	11.1398(3)	11.8347(3)	11.9965(3)	12.0137(3)	12.6739(5)
b/Å	19.6334(7)	20.6248(7)	22.0112(6)	20.5903(5)	20.2594(5)	20.2750(4)	20.5874(7)
c/Å	20.4221(6)	21.2868(8)	22.5117(6)	22.5132(7)	22.8564(5)	22.8339(4)	25.8506(9)
α (°)	75.230(2)	110.363(2)	113.189(2)	113.258(2)	114.695(1)	115.072(1)	77.841(3)
β (°)	72.675(2)	97.492(2)	100.427(2)	95.992(2)	96.9670(9)	96.578(1)	77.976(2)
γ (°)	75.364(2)	99.820(2)	99.965(1)	100.282(2)	99.770(2)	99.681(2)	74.025(2)
Volume/Å^3	4457.3(2)	4683.8(3)	4804.5(2)	4865.6(2)	4857.9(2)	4857.3(2)	6257.4(4)
D_c/Mg m^{-3}	1.384	1.359	1.363	1.346	1.308	1.337	1.264
μ/mm^{-1}	0.842	0.826	0.820	0.810	0.787	0.802	0.719
Meas. reflns	22810	23546	23754	21729	24568	23282	20941
Indep. reflns	15349	15426	16232	14853	16100	16813	14939
R_{int}	0.0584	0.0833	0.1092	0.1283	0.0743	0.0789	0.1675
R_1 [$I > 2\sigma(I)$]	0.0748	0.0824	0.0979	0.0935	0.0671	0.0651	0.1458
wR_2 [$I > 2\sigma(I)$]	0.2233	0.2008	0.2643	0.2192	0.1581	0.1754	0.3528
GooF on F^2	1.392	1.404	1.323	1.253	1.127	1.230	1.283

[a] Disordered solvent molecules were removed using SQUEEZE.[55]

Table 2 The upright resorcinol ring tilt angles against the C7–C14–C21–C28 plane

Structure	C1–C6 (°)	C15–C20 (°)
1A	76.2	87.1
1B	80.2	89.1
2A	84.4	88.3
2B	80.6	87.1
2C	81.2	86.7
2D	81.2	87.0
5A	100.1	97.6

the methine carbon plane C7–C14–C21–C28 varies between 76.2° and 87.1° in structure **1A** up to 100.1° and 97.6° in structure **5A** (Table 2), which is the only structure where both resorcinol rings are pointing slightly outwards opening the resorcinarene cavity. Structure **5A** differs from the other structures quite remarkably, since **5** is the only podand that has long 1-decenyl groups at the lower rim capable of packing next to each other due to van der Waals interactions. The packing of short alkyl chain podands **1** and **2** is directed by intermolecular hydrogen bonding of nitro and amine groups as well as π–π interactions between aromatic rings.

In general, the eight nitroaniline side arms at phenolic oxygens can be divided into two groups depending on whether they are bound to upright or horizontal resorcinol rings (Fig. 1): 'top' (O4, O6, O18 and O20, named after the oxygen atom they are attached to) which extend on top of the resorcinarene cavity and 'alongside' (O11, O13, O25 and O27) which point to the sides of the cavity. Most structures have their 'alongside' side arms in a vertical position but there is a little more variation in the 'top' side arm positions (see Table 3 for O–C–C–N distortion angles). In addition, podands form an upper rim interface where the resorcinarene cavities of two molecules approach each other, and tail-to-tail interface, where alkyl chains of the podands face each other.

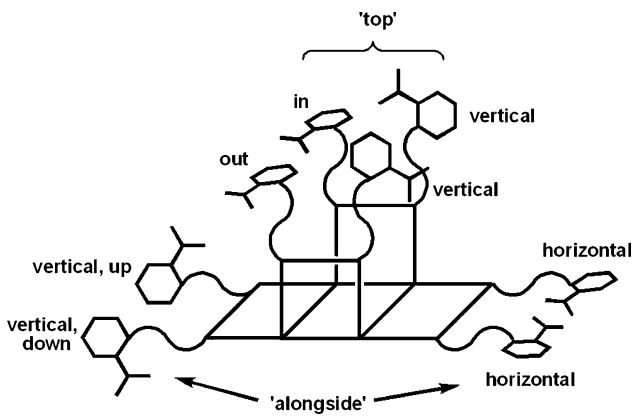

Fig. 1 Different orientations of the 'top' and 'alongside' side arms. The horizontal conformation of 'top' side arms is either 'in' or 'out' of the resorcinarene cavity.

Structure **1A** has three 'top' side arms in horizontal orientation (O4, O6 and O18), where side arms O4 and O6 form an intermolecular π-stack at the upper rim interface (Fig. 2). The remaining side arm O20 forms additional π-stacking with the resorcinol ring (C1–C6) not observed in other structures. Two of the 'alongside' side arms, O25 and O27 have twisted vertical conformations with distortion angles 73.6° and –67.4°, respectively, and they form intermolecular edge-to-face π-interactions between two parallel molecules. In addition, the side arm O25 approaches the resorcinol ring (C8–C13) forming another edge-to-face π-interaction at the tail-to-tail interface. Side arm O13 is horizontally oriented forming a π-stack with side arm O18 of the neighboring parallel molecule. Side arm O11, however, is between a horizontal and a vertical conformation forming an edge-to-face π-interaction with C22–C27 resorcinol ring of another molecule at the tail-to-tail interface, which explains the twisted conformation of the side arm O11.

Table 3 O–C–C–N distortion angles of the side arms

Structure	O4···N1	O6···N3	O11···N5	O13···N7	O18···N9	O20···N11	O25···N13	O27···N15
1A	55.3(4)	−52.1(4)	84.1(4)	−42.0(8)	74.5(4)	171.3(3)	73.6(3)	−67.4(3)
1B	−64.4(5)	56.8(4)	178.8(3)	135.1(8)[a]	63.7(5)	−177.0(3)	150.0(5)[a]	−51.6(9)[a]
2A	−63.1(5)	−165.0(4)	−175.7(4)	−174.5(4)	171.7(4)	−72.7(5)	173.2(5)	75.8(7)
2B	−62.8(6)	68.9(6)	−176.0(5)	152.1(6)[a]	61.0(7)	178.9(4)	−156.9(6)	173.2(4)
2C	61.5(4)	−66.2(3)	168.3(3)	−170.4(3)	−63.4(4)	−176.2(3)	156.2(4)	−179.2(3)
2D	60.4(4)	−66.3(3)	168.3(3)	−171.0(3)	−62.8(4)	−176.9(2)	160.1(3)	178.6(2)
5A	−66.1(10)	70.9(10)	164.0(11)	176.9(8)	76.3(9)	−74.3(10)	−168.3(15)[a]	−170.3(9)

[a] For disordered side arms the distortion angle for the part with higher site occupancy is reported.

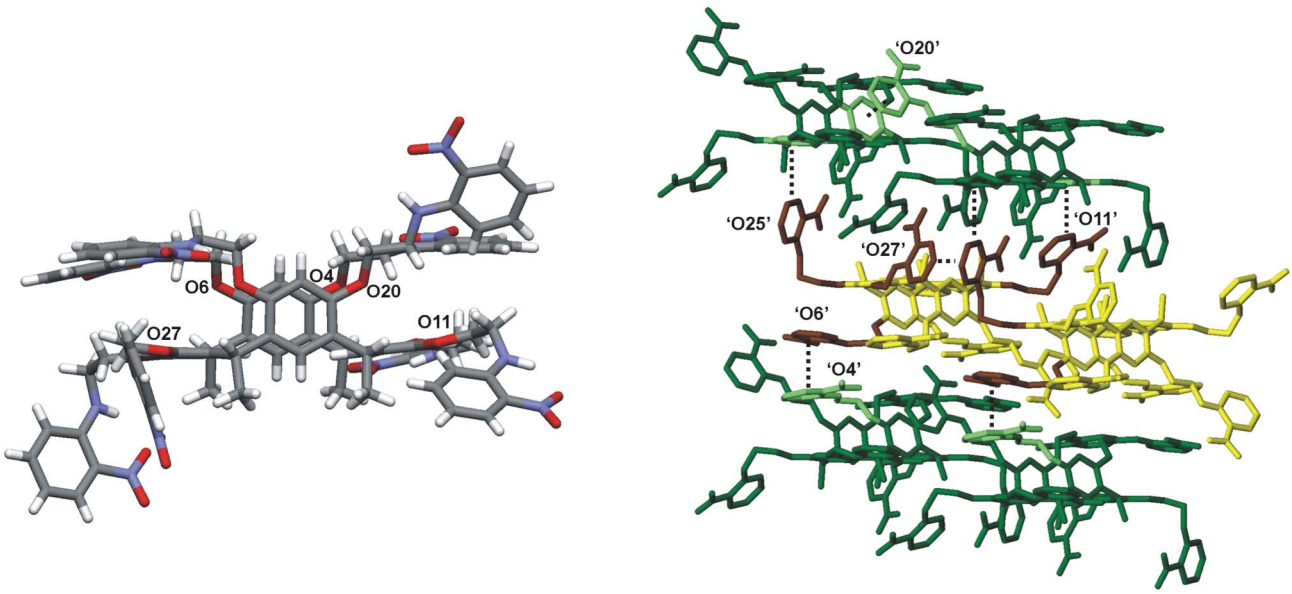

Fig. 2 Structure **1A** (side view) and packing illustrating π–π-interactions between side arms 'O4' and 'O6', 'O11' and C22–27, 'O20' and C1–C6, 'O25' and 'O27' as well as 'O25' and C8–13. π-stacking between side arms 'O13' and 'O18' is not shown.

Altogether, the π–π interactions of **1A** lead to a network like packing instead of rows of parallel molecules found in all other structures.

Acetone solvate **1B** crystallized from acetone providing beautiful block shaped crystals of relatively good quality. **1B** has an isomorphous unit cell and closely related structure to acetone solvate **2B**, structure **2C** and acetonitrile solvate **2D**. All of them can be characterized by rows of molecules joined together by π-stacks of four 'alongside' side arms (Fig. 3). Rows of podands pack next to each other forming an edge-to-face π-interaction between side arms O18 and O4. At the upper rim interface, rows are shifted with respect to each other, and connect through intertwined side arms O20 penetrating into the neighboring resorcinarene cavity (edge-to-face interaction with side arm O18), as well as O4···O4 π-stacking with another podand. At the tail-to-tail interface intermolecular hydrogen bonds between side arms O11 (nitro and amine groups) of nearby molecules connect two layers.

In structure **2B**, an acetone molecule is hydrogen bonded into N–H (N15) group whereas in **1B** the acetone molecule is simply positioned between the side arms O4 and O6 on top of the cavity. In **2A**, which is a conformational polymorph of **2B**, an acetone molecule is hydrogen bonded into N5, and rows of podands pack next to each other forming a more pronounced step like pattern with intermolecular π-interactions between side arms O4 and O20 (Fig. 3). The upper rim interface of **2A** is held together by intermolecular hydrogen bonding between side arms O6 and side arms O18 and O27 (N3–O103 and N15–O109) instead of pairing through side arms O20 (Fig. 4).

Structure **5A** with pendant 1-decenyl groups at the lower rim has a very symmetrical arrangement of the side arms with similar π-stacking of four 'alongside' side arms as structures **1B** and **2B–D**. In addition, the 'top' side arms are folded horizontally on top of the cavity, where each podand finds a pair in the facing row of podands through π–π-interactions of side arms O4 with O18, and O6 with O20. The facing rows of podands pack next to each other forming almost continuous layers of aromatic and aliphatic components through the crystal (Fig. 5) and since the aromatic part contains hydrophilic nitroaniline groups, compound **5** could present amphiphilic properties.

An indication of the versatile possibilities for these molecules to pack in the solid state is yet another structure of **1** obtained from the same crystallization experiment as structure **1A** containing a disordered solvent molecule. The data completeness was too low to provide decent temperature factors, but nevertheless, a different unit cell¶ and packing motif were confirmed, where all side arms

¶ $a = 14.6212(7)$ Å, $b = 16.7373(7)$ Å, $c = 19.5562(10)$ Å, $\alpha = 75.57(3)°$, $\beta = 89.870(2)°$, $\gamma = 87.986(3)°$, $V = 4631.9(4)$ Å^3

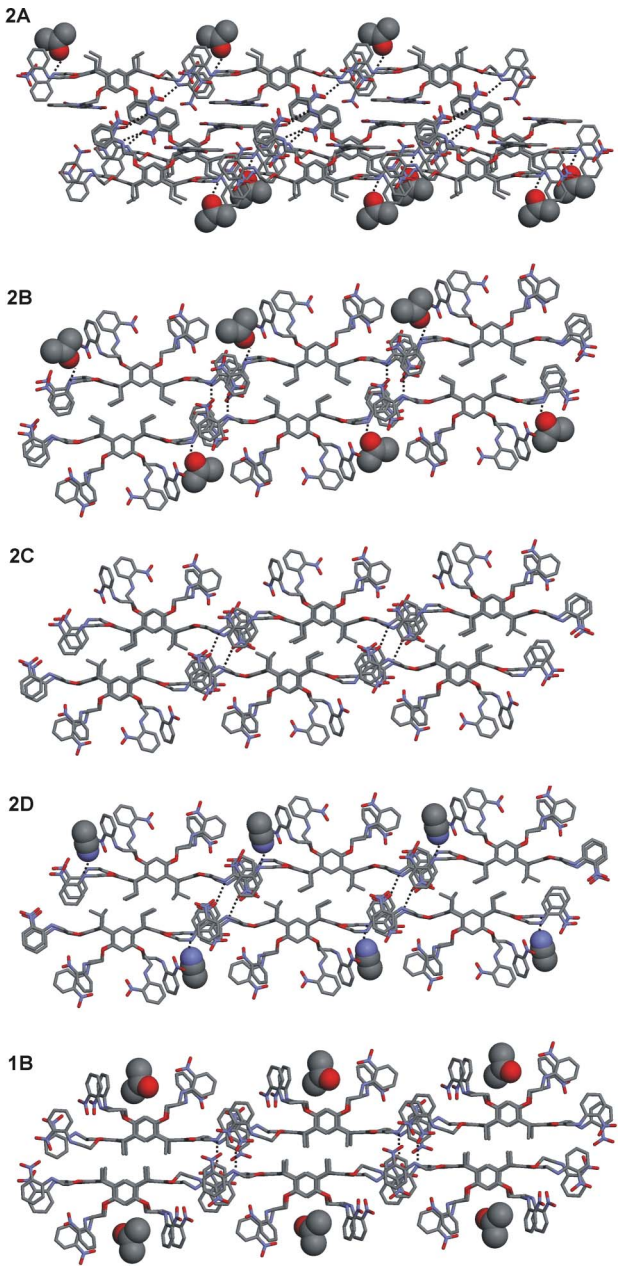

Fig. 3 Packing of structures **2A** (top), **2B**, **2C**, **2D** and **1B** (bottom) showing intermolecular hydrogen bonding (donor–acceptor) and omitting hydrogen atoms; solvent molecules are shown as CPK models except for structure **2C**, in which solvent molecules were removed by SQUEEZE.

have a vertical arrangement and podands are arranged in rows as in acetone solvate **1B** but where the upper rim interface is connected by intermolecular hydrogen bonding as in acetone solvate **2A**.

Powder X-ray diffraction

To elucidate the polymorphism and relative stability of the acetone solvates **2A** (plate) and **2B** (needle) powder X-ray diffraction experiments were carried out. Compound **2** was crystallized several times from acetone varying the crystallization speed and temperature. Fast crystallizations were conducted at room temperature by letting acetone evaporate overnight, which provided microcrystalline products. Slow crystallization was performed at 4 °C and crystals were filtered and dried briefly under vacuum. The X-ray diffraction patterns were compared with the calculated patterns of structures **2A** and **2B** showing that fast crystallization produced more structure **2A** and slow crystallization more structure **2B** (Fig. 6).‖ In addition, when acetone was removed rapidly under vacuum, only amorphous product was obtained indicating that crystallization process does not occur instantaneously.

When samples were placed under vacuum for more extended period, their diffraction pattern changed due to the loss of acetone and resulting changes in the lattice. After drying, unit cell parameters for a plate and a needle were collected and the plate matched still with the unit cell of **2A** but the parameters for a needle did not match either **2A** or **2B**, which indicates that structure **2A** might be more durable against collapse of the lattice when acetone is removed since its upper rim interface is hydrogen bonded. Based on these observations it seems that structure **2A** forms faster than **2B** when the system has more thermal energy (higher T), but both **2A** and **2B** are stable at room temperature and 4 °C, as well as –100 °C where single crystal data were collected. However, visual observation of the microcrystalline samples showed that they all contained both plates and needles, and the amount of plates and needles did not correspond to the ratio of **2A** and **2B** in the powder diffraction pattern.

Amphiphilic properties

The structural mobility and amphiphilic properties of the resorcinarene octapodands in solution were examined using NMR spectroscopy and Langmuir monolayer studies. Broad ^{1}H NMR resonances of **5** in $CDCl_3$ indicate that conformational changes occur approximately at the NMR timescale. Cooling to sub-zero temperatures slowed the movement below the NMR timescale where individual conformers could be observed as separate resonances appearing in the spectrum. Heating the sample to 60 °C, on the other hand, accelerated the movement which was observed as sharpening of individual resonances as well as improved resolution.

Interestingly, the rate of the conformational change could be adjusted by dissolving **5** in a more polar solvent, such as [D_6]acetone, in which sufficient resolution could be obtained at 30 °C (Fig. 7). In [D_6]DMSO the effect was even more profound. The behavior where polar solvent increases the mobility of polar parts of the molecule is known for amphiphiles,[57,58] and is expected to cause the observed changes for the octapodands as well.

For **3** and **4** the polarity of the solvent had a similar effect in the ^{1}H resonances whereas for **2** the effect was not as clear. Podand **1**, which contains short methyl groups at the lower rim, showed separate ^{1}H resonances for upright and horizontal resorcinol rings at 30 °C indicating slower boat-to-boat interconversion than for other podands. At –30 °C all nitroaniline protons except a proton *ortho* to the -NH group appear as two separate patterns in the spectrum and belong either to the upright or horizontal resorcinol ring according to ^{1}H, ^{1}H COSY and NOE spectra. NMR spectra are given in the ESI.†

Amphiphilicity of the podands **3–5** was confirmed by recording isotherms for monolayers of the podands on water, whereas **2** did

‖ Since powder X-ray patterns were measured at ambient temperature and single crystal data at 173 K, it should be noted that comparison between them has some limitations.

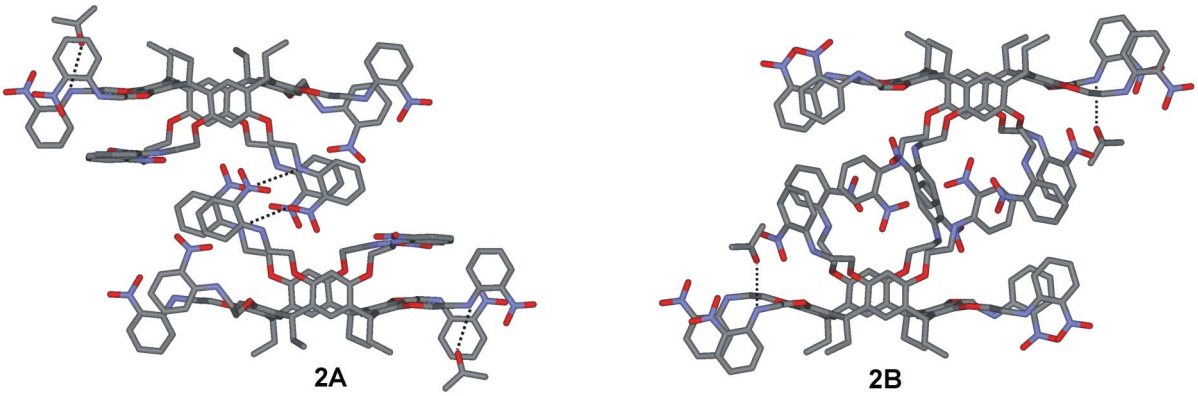

Fig. 4 Comparison of polymorphs **2A** and **2B**; intramolecular hydrogen bonds are shown with dashed lines (donor–acceptor), hydrogens are omitted for clarity.

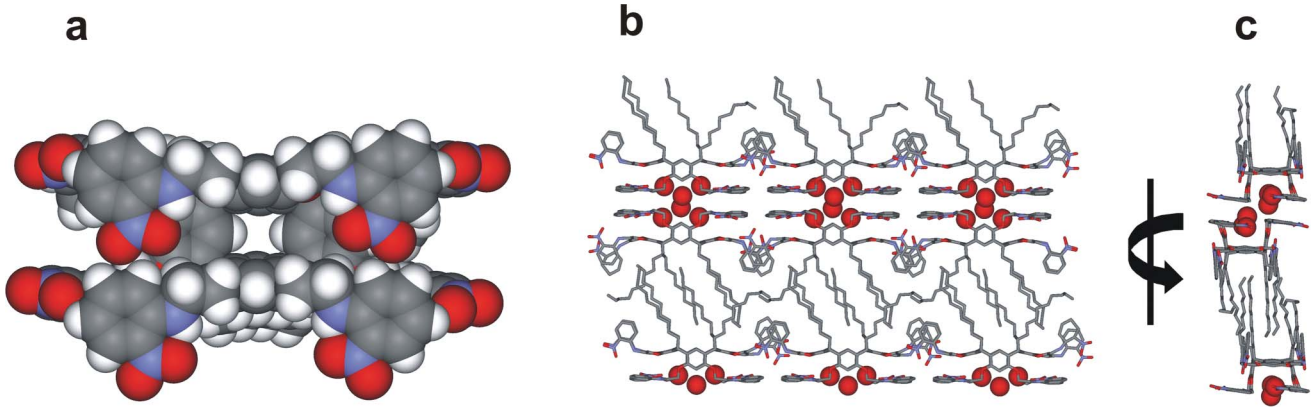

Fig. 5 Structure **5A** top view as a CPK model (a), solvent molecules are omitted for clarity. Packing (omitting hydrogens) viewed perpendicular to the plane of rows of podands (b), 90° rotation counterclockwise (c) illustrating π-interactions between pairs of podands. H_2O is shown as a CPK model and disorder is not shown for clarity.

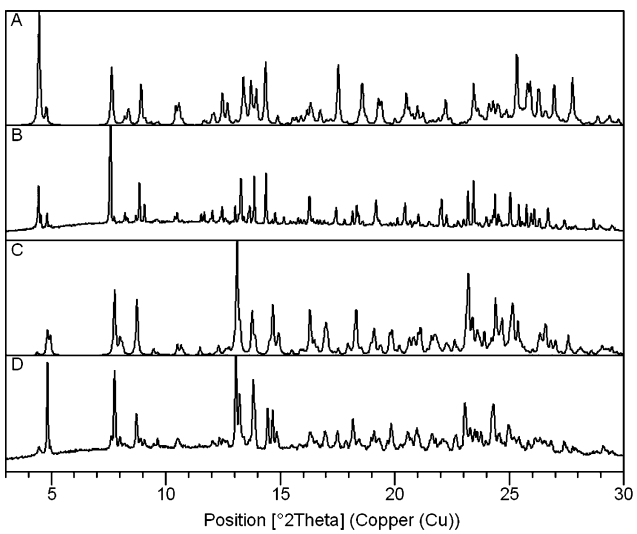

Fig. 6 Powder X-ray diffraction patterns (A) **2A** calculated structure, (B) fast crystallization of **2** at RT (C) **2B** calculated structure, (D) slow crystallization of **2** at 4 °C.

not form a monolayer on water due to the short ethyl chains at the lower rim. Compounds **3** and **4** formed monomolecular layers showing an increase in the collapse pressure from 8.6 to 18.2 mN m^{-1} with increasing chain length but monolayers of compound **5** collapsed at 12.8 mN m^{-1} which is probably caused by the disruption of terminal double bond to the aliphatic layer (Fig. 8). Collapse areas varied between 157 and 191 Å^2/molecule (Table 4), which are consistent when compared with the solid state structures (~170–250 Å^2). The relatively low collapse pressures recorded for these three octapodands can be interpreted as a consequence of the high flexibility of their polar head group preventing the amphiphiles from packing in a two dimensional interfacial solid phase. For compound **4** unexpected behaviour was observed in further studies with different alkali and earth alkali metal salts dissolved in the subphase since the collapse area showed quite large variation when recorded on subsequent days in water. A possible

Table 4 Isotherm parameters of the monolayers, areas are given as Å^2/molecule. A_{lim} is the extrapolation of the linear part of the isotherm on the *x* axis, A_0 and A_1 represent apparent molecular areas for surface tensions at 0 and 1 mN m^{-1} respectively

	3	**4**	**5**
collapse pressure/mN m^{-1}	8.6	18.2	12.8
collapse area/Å^2	191	157	166
A_{lim}/Å^2	221	187	197
A_0/Å^2	227	200	210
A_1/Å^2	219	192	201

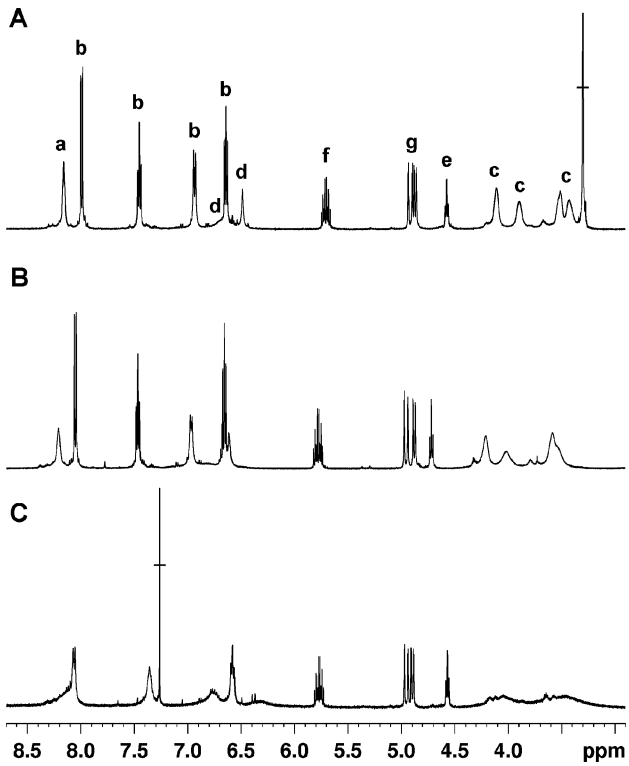

Fig. 7 ^{1}H NMR spectra of **5** in (A) [D6]DMSO, (B) [D6]acetone and (C) $CDCl_3$; resonances at 2.9–8.7 ppm, a: N*H*, b: nitroaniline Ar*H*, c: OCH_2CH_2N, d: resorcinarene core Ar*H*, e: Ar*CH*, f: alkyl tail $CH{=}CH_2$, g: alkyl tail $CH{=}CH_2$.

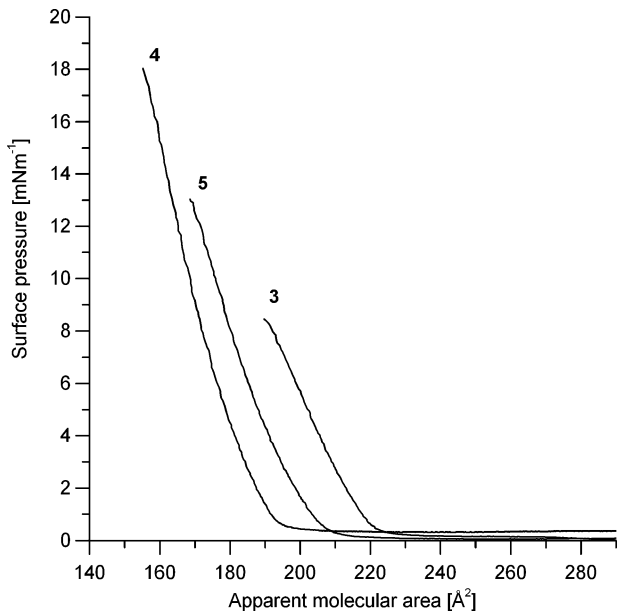

Fig. 8 Isotherms of podands **3**, **4** and **5**.

explanation could be found from the structural properties of the compound, since different conformations of the polar and flexible upper rim might lead to different packing also at the air–water interface. However, further experiments are required to confirm these preliminary observations.

Conclusions

Resorcinarene octapodands **1–5** exhibit versatile self-assembling properties, and show high conformational mobility due to boat-to-boat interconversion as well as the rotation around upper rim side arm -OCH_2CH_2N- linkers. Structural mobility is observed in the solid state as conformational polymorphism of **2**, and as disordered side arms and large temperature factors for nitroaniline groups. The different packing motifs observed for compounds **1** and **2** suggests that there are more than one almost equally favorable conformations in the solid state, probably depending on whether π–π-interactions or H-bonds form first during the crystallization process. The ratio of polymorphs **2A** and **2B** can be controlled by changing crystallization conditions, namely temperature and speed of solvent evaporation, which indicates that these molecules approach the limit where further structural flexibility leads to random precipitation instead of organized crystal structures. The X-ray diffraction data obtained for **2A** and **2B** also implies that **2A** with more extensive hydrogen bonding at the upper rim might be more stable against collapsing when acetone is removed from the lattice.

Compound **5** formed crystals from nitromethane–CH_2Cl_2 with continuous aliphatic and aromatic layers, where aliphatic groups of the molecule as well as π-interactions between side arms control the crystallization process. The conformational mobility, which leads to polymorphism and versatile conformations of the side arms observed in all crystal structures was further demonstrated in solution by ^{1}H NMR, where long chain octapodands **3–5** showed remarkable conformational flexibility and amphiphilic properties, which were confirmed by forming Langmuir monolayers. In contrast to the solid state structures, where the binding cavity of resorcinarenes was quite often blocked by side arms, conformational mobility of boat-to-boat interconversion and side arm rotation could lead to successive opening and closing of the binding cavity of the podands in solution. NMR spectra recorded in various solvents and temperatures showed how the energetics of these events can be tuned when the lower rim substituents are changed from methyl to ethyl or to longer alkyl chains.

Conformational polymorphism of resorcinarenes and other macrocyclic compounds has remained largely unexplored even though the importance of new polymorphs can be easily observed in the field of host–guest chemistry. Further chemical modification of the investigated podands could provide a variety of host molecules in which the binding properties in the solid state could be tuned by changing crystallization conditions. In addition, the amphiphilicity could be utilized in preparing self-assembling structures, such as monolayers, vesicles or micellar structures with novel binding properties.

Experimental Methods

General

All chemicals and solvents were purchased from Sigma–Aldrich and they were used as received. Acetonitrile was dried with $CaCl_2$ and distilled over molecular sieves. NMR spectra were recorded with a Bruker Avance DRX (500 MHz for ^{1}H and 126 MHz for ^{13}C) spectrometer at 30 °C unless otherwise stated. *J* values are given in Hz. ESI-MS spectra were measured with a Micromass

LCT (ESI-TOF) instrument. Melting points were determined with a Metler Toledo FP62 apparatus and are uncorrected. Elemental analyses were performed on a Vario EL III apparatus. Thermogravimetric/differential thermal analysis was measured with a Perkin Elmer Diamond TG/DTA. Samples were placed in a platinum sample pan and measured with a temperature program 25–900 °C at 10 °C min^{-1}.

General procedure for resorcinarene octapodands

Resorcinarene, dibenzo-18-crown-6 (0.16 molar equivalents) and dry Cs_2CO_3 or K_2CO_3 (16 molar equivalents) were suspended in dry acetonitrile under nitrogen atmosphere and refluxed for 15 min followed by an addition of 8 molar equivalents of **6**[54] or **7** in acetonitrile. The yellow suspension was refluxed for 24 h, filtered with suction and evaporated under reduced pressure. The residue was suspended in water and extracted with dichloromethane; organic layer was dried over $MgSO_4$ and evaporated to dryness. The product was purified with flash chromatography (SiO_2; $CHCl_3$–MeOH), dissolved in acetone and precipitated from water with an addition of NaCl, or recrystallized from acetone. The product was filtered with suction and dried under vacuum. Detailed synthetic procedure for each podand along with spectroscopic data is provided in the ESI.†

o-Nitro-*N*-(2-methanesulfonyloxyethyl)aniline 7

o-Nitro-*N*-(2-hydroxyethyl)-aniline[59,60] (2.74 g, 15.0 mmol) was dissolved in 5 ml of pyridine under nitrogen atmosphere and cooled in an ice bath. Methanesulfonylchloride (1.4 ml, 18.1 mmol) was added drop wise into the solution. After mixing one hour in an ice bath and one hour in the room temperature, reaction was quenched by adding 50 ml of water. The orange crystals were filtered with suction, washed with water and dried under vacuum. The product was recrystallized from hot chloroform–hexane, filtered and dried under vacuum to afford yellow–orange crystals (3.0 g, 76%). mp 82–83 °C; (Found: C, 41.55; H, 4.5; N, 10.8. $C_9H_{12}N_2O_5S$ requires C, 41.5; H, 4.65; N, 10.8%); δ_H(500 MHz, $CDCl_3$) 3.05 (s, 3H; CH_3), 3.73 (q, ^3J (H,H) = 5.7, 2H; NCH_2), 4.46 (t, ^3J (H,H) = 5.6, 2H; OCH_2), 6.73 (m, 1H; ArH), 6.89 (dd, ^3J (H,H) = 8.6, ^4J (H,H) = 0.9, 1H; ArH), 7.48 (m, 1H; ArH), 8.18 (br, 1H; NH), 8.20 (dd, ^3J (H,H) = 8.6, ^4J (H,H) = 1.6, 1H; ArH); δ_C(126 MHz, $CDCl_3$) 37.9 (*C*H_3), 42.1 (N*C*H_2), 66.8 (O*C*H_2), 113.5 (*Ar*H), 116.5 (*Ar*H), 127.3 (*Ar*H), 133.0 (*Ar*NO_2), 136.6 (*Ar*H), 144.7 (*Ar*NH); *m*/*z* (ESI-TOF) 283 (M + Na^+, 100%) 261 (M + H^+, 8), 187 (60), 165 ($M^+ - SO_3CH_3$, 38).

X-Ray crystallography

Powder X-ray diffraction patterns were measured on a PANalytical X'Pert Pro system in reflection mode using monochromatized Cu-Kα radiation (λ = 1.54178 Å) at ambient temperature. The 2θ angle range was 3–30°.

Single crystal X-ray data were recorded on a Nonius Kappa CCD diffractometer with Apex II detector using graphite monochromatized Cu-Kα [λ = 1.54178 Å] radiation at a temperature of 173 K. The data were processed and absorption correction was made to all structures with Denzo-SMN v0.97.638.[61] The structures were solved by direct methods (SHELXS-97) and refined (SHELXL-97) against F^2 by full-matrix least-squares techniques using SHELX-97 software package.[62] The hydrogen atoms were calculated to their idealized positions with isotropic temperature factors (1.2 or 1.5 times the C temperature factor) and refined as riding atoms unless otherwise mentioned. All compounds crystallized as triclinic $P\bar{1}$ with Z = 2. Crystal structure analysis was done using Mercury CSD 2.3 software.[63] Crystallographic data (excluding structure factors) for the structures in this paper have been deposited with the Cambridge Structural Data Center as supplementary publication nos. CCDC 781919–781925.† Copies of the data can be obtained free of charge from The Cambridge Crystallographic Data Centre *via* www.ccdc.cam.ac.uk/data_request/cif.

Langmuir monolayer studies

Langmuir isotherms were recorded using a 112D Nima Technology (Coventry, U.K.) system. Spreading solutions were prepared by dissolving **2–5** in chloroform at 2 mg ml^{-1} concentration and diluted to 0.5 mg ml^{-1} by weighing the amount of solvent. Monolayers were prepared on purified water (Millipore Milli-Q water system, resistivity ≥18 MΩ·cm) by adding 20 µl of spreading solution on the surface and recording the isotherm after 15 min with compression rate set at 5 cm^2 min^{-1} from 85 to 14 cm^2 or until a collapse point was observed. Each isotherm was recorded at least three times to ensure the reliability of the results.

Acknowledgements

This work was financially supported by Academy of Finland (projects 117945 and 116503) and National Graduate School of Organic Chemistry and Chemical Biology. We are grateful to Mr Reijo Kauppinen for his help with the NMR studies.

Notes and references

1 J. Vicens and V. Böhmer, *Topics in Inclusion Science, Vol. 3: Calixarenes: A Versatile Class of Macrocyclic Compounds*, Kluwer Academic Publishers, Netherlands, 1991, pp.264.
2 L. Mandolini and R. Ungaro, *Calixarenes in Action*, Imperial College Press, Singapore, 2000, pp.271.
3 C. D. Gutsche, *Calixarenes Revisited*, The Royal Society of Chemistry, UK, 1998, pp. 233.
4 P. Timmerman, W. Verboom and D. N. Reinhoudt, *Tetrahedron*, 1996, **52**, 2663–2704.
5 S. M. Biros and J. Rebek Jr, *Chem. Soc. Rev.*, 2007, **36**, 93–104.
6 W. Sliwa and C. Kozlowski, *Calixarenes and resorcinarenes*, Wiley-VCH, Germany, 2009, pp. 316.
7 Y. Liu, H. Wang, L. Wang, Z. Li, H. Zhang and Q. Zhang, *Tetrahedron*, 2003, **59**, 7967–7972.
8 M. M. Reinoso García, W. Verboom, D. N. Reinhoudt, E. Malinowska, M. Pietrzak and D. Wojciechowska, *Tetrahedron*, 2004, **60**, 11299–11306.
9 M. A. Sarmentero and P. Ballester, *Org. Biomol. Chem.*, 2007, **5**, 3046–3054.
10 U. Darbost, M. Rager, S. Petit, I. Jabin and O. Reinaud, *J. Am. Chem. Soc.*, 2005, **127**, 8517–8525.
11 S. Busi, H. Saxell, R. Fröhlich and K. Rissanen, *CrystEngComm*, 2008, **10**, 1803–1809.
12 H. Mansikkamäki, M. Nissinen and K. Rissanen, *CrystEngComm*, 2005, **7**, 519–526.
13 A. J. McConnell, C. J. Serpell, A. L. Thompson, D. R. Allan and P. D. Beer, *Chem.–Eur. J.*, 2010, **16**, 1256–1264.
14 M. H. Filby, T. D. Humphries, D. R. Turner, R. Kataky, J. Kruusma and J. W. Steed, *Chem. Commun.*, 2006, 156–158.
15 S. Le, Gac and I. Jabin, *Chem.–Eur. J.*, 2008, **14**, 548–557.
16 M. Ménand and I. Jabin, *Chem.–Eur. J.*, 2010, **16**, 2159–2169.

17 F. Perret, A. N. Lazar and A. W. Coleman, *Chem. Commun.*, 2006, 2425–2438.
18 A. W. Coleman, F. Perret, A. Moussa, M. Dupin, Y. Guo and H. Perron, *Top. Curr. Chem.*, 2007, **277**, 31–88.
19 Y. Sun, C. Yan, Y. Yao, Y. Han and M. Shen, *Adv. Funct. Mater.*, 2008, **18**, 3981–3990.
20 Y. Sun, Y. Yao, C. Yan, Y. Han and M. Shen, *ACS Nano*, 2010, **4**, 2129–2141.
21 B. Kim, S. L. Tripp and A. Wei, *J. Am. Chem. Soc.*, 2001, **123**, 7955–7956.
22 A. Wei, B. Kim, S. V. Pusztay, S. L. Tripp and R. Balasubramanian, *J. Inclusion Phenom. Macrocyclic Chem.*, 2001, **41**, 83–86.
23 A. Wei, *Chem. Commun.*, 2006, 1581–1591.
24 J. Liu and A. Wei, *Chem. Commun.*, 2009, 4254–4256.
25 H. Kitagawa, M. Kawahata, R. Kitagawa, Y. Yamada, M. Yamanaka, K. Yamaguchi and K. Kobayashi, *Tetrahedron*, 2009, **65**, 7234–7239.
26 A. W. Coleman, S. Jebors, P. Shahgaldian, G. S. Ananchenko and J. A. Ripmeester, *Chem. Commun.*, 2008, 2291–2303.
27 A. Shivanyuk, *J. Am. Chem. Soc.*, 2007, **129**, 14196–14199.
28 K. Helttunen and P. Shahgaldian, *New J. Chem.*, 2010, DOI: 10.1039/C0NJ00123F.
29 D. Volkmer, M. Fricke, D. Vollhardt and S. Siegel, *J. Chem. Soc., Dalton Trans.*, 2002, 4547–4554.
30 P. Shahgaldian, M. A. Sciotti and U. Pieles, *Langmuir*, 2008, **24**, 8522–8526.
31 L. Nault, A. Cumbo, R. F. Pretôt, M. A. Sciotti and P. Shahgaldian, *Chem. Commun.*, 2010, **46**, DOI: 10.1039/b926025k.
32 S. Ehrler, U. Pieles, A. Wirth-Heller and P. Shahgaldian, *Chem. Commun.*, 2007, 2605–2607.
33 H. Mansikkamäki, M. Nissinen and K. Rissanen, *Angew. Chem., Int. Ed.*, 2004, **43**, 1243–1246.
34 H. Mansikkamäki, S. Busi, M. Nissinen, A. Åhman and K. Rissanen, *Chem.–Eur. J.*, 2006, **12**, 4289–4296.
35 M. Makha, C. W. Evans, A. N. Sobolev and C. L. Raston, *Cryst. Growth Des.*, 2008, **8**, 2929–2932.
36 D. Sun and C. A. Reed, *Chem. Commun.*, 2000, 2391–2392.
37 B. Ma, Y. Zhang and P. Coppens, *J. Org. Chem.*, 2003, **68**, 9467–9472.
38 G. R. Desiraju, *Angew. Chem., Int. Ed.*, 2007, **46**, 8342–8356.
39 E. Nomura, M. Takagaki, C. Nakaoka and H. Taniguchi, *J. Org. Chem.*, 2000, **65**, 5932–5936.
40 T. Gruber, M. Peukert, D. Schindler, W. Seichter, E. Weber and P. Bombicz, *J. Inclusion Phenom. Macrocyclic Chem.*, 2008, **62**, 311–324.
41 P. Thuéry, M. Nierlich, R. Calemczuk, M. Saadioui, Z. Asfari and J. Vicens, *Acta Crystallogr., Sect. B: Struct. Sci.*, 1999, **B55**, 95–103.
42 J. L. Atwood, L. J. Barbour and A. Jerga, *Chem. Commun.*, 2002, 2952–2953.
43 S. H. Dale, M. R. J. Elsegood and C. Redshaw, *CrystEngComm*, 2003, **5**, 368–373.
44 A. Nangia, *Acc. Chem. Res.*, 2008, **41**, 595–604.
45 P. K. Thallapally, G. O. Lloyd, T. B. Wirsig, M. W. Bredenkamp, J. L. Atwood and L. J. Barbour, *Chem. Commun.*, 2005, 5272–5274.
46 J. L. Atwood, L. J. Barbour and A. Jerga, *Science*, 2002, **296**, 2367–2369.
47 J. L. Atwood, L. J. Barbour and A. Jerga, *Angew. Chem., Int. Ed.*, 2004, **43**, 2948–2950.
48 S. J. Dalgarno, J. Tian, J. E. Warren, T. E. Clark, M. Makha, C. L. Raston and J. L. Atwood, *Chem. Commun.*, 2007, 4848–4850.
49 J. L. Atwood, L. J. Barbour, P. K. Thallapally and T. B. Wirsig, *Chem. Commun.*, 2005, 51–53.
50 A. V. Yakimov, M. A. Ziganshin, A. T. Gubaidullin and V. V. Gorbatchuk, *Org. Biomol. Chem.*, 2008, **6**, 982–985.
51 K. Salorinne and M. Nissinen, *Org. Lett.*, 2006, **8**, 5473–5476.
52 K. Salorinne and M. Nissinen, *Tetrahedron*, 2008, **64**, 1798–1807.
53 K. Salorinne, T. Tero, K. Riikonen and M. Nissinen, *Org. Biomol. Chem.*, 2009, **7**, 4211–4217.
54 K. Salorinne, D. P. Weimann, C. A. Schalley and M. Nissinen, *Eur. J. Org. Chem.*, 2009, 6151–6159.
55 P. Van, der Sluis and A. L. Spek, *Acta Crystallogr., Sect. A: Found. Crystallogr.*, 1990, **A46**, 194–201.
56 J. H. Burns, J. C. Bryan, M. C. Davis and R. A. Sachleben, *J. Inclusion Phenom. Mol. Recognit. Chem.*, 1996, **26**, 197–207.
57 K. Miyazawa and F. M. Winnik, *Macromolecules*, 2002, **35**, 9536–9544.
58 T. Kai, X. Sun, K. M. Faucher, R. P. Apkarian and E. L. Chaikof, *J. Org. Chem.*, 2005, **70**, 2606–2615.
59 J. M. McManus and R. M. Herbst, *J. Org. Chem.*, 1959, **24**, 1042–1043.
60 L. Westerheide, F. K. Müller, R. Than, B. Krebs, J. Dietrich and S. Schindler, *Inorg. Chem.*, 2001, **40**, 1951–1961.
61 Z. Otwinowski and W. Minor, *Methods Enzymol.*, 1997, **276**, 307–326.
62 G. M. Sheldrick, *Acta Crystallogr., Sect. A: Found. Crystallogr.*, 2008, **A64**, 112–122.
63 C. F. Macrae, I. J. Bruno, J. A. Chisholm, P. R. Edgington, P. McCabe, E. Pidcock, L. Rodriguez-Monge, R. Taylor, J. van de Streek and P. A. Wood, *J. Appl. Crystallogr.*, 2008, **41**, 466–470.

V

Interaction of aminomethylated resorcinarenes with rhodamine B

by

Kaisa Helttunen, Piotr Prus, Minna Luostarinen & Maija Nissinen, 2009

New. J. Chem. 33 (2009), 1148–1154, DOI: 10.1039/B820409H.

Interaction of aminomethylated resorcinarenes with rhodamine B

Kaisa Helttunen, Piotr Prus, Minna Luostarinen and Maija Nissinen*

Received (in Durham, UK) 14th November 2008, Accepted 12th February 2009
First published as an Advance Article on the web 26th March 2009
DOI: 10.1039/b820409h

The interaction of aminomethylated resorcinarenes with a red xanthene dye, rhodamine B, was investigated in chloroform, methanol and chloroform–methanol solutions using UV-vis, NMR and fluorescence spectroscopy. Aminomethylated resorcinarenes **1** and **2** shift the rhodamine B equilibrium from the zwitterion to the lactone form unlike reference compounds **3** and **4**, which do not contain tertiary amino groups at the upper rim, giving an example of how supramolecular hosts can influence the equilibrium of rhodamine B isomers.

Introduction

Probing host–guest binding and molecular recognition events using fluorescent dye molecules has proven to be a very sensitive and useful technique, and numerous examples of the complexation of fluorescent guests can be found in the literature.[1] A typical example is the formation of an inclusion complex in aqueous solution, where the hydrophobic interactions act as a driving force to induce complexation, which is often accompanied by an increase[2] or decrease[3,4] in the fluorescence intensity resulting from a change in the microenvironment of the dye. Different host molecules, such as cyclodextrins,[2,5–7] cucurbiturils,[7,8] and water-soluble calixarene,[4,5,7,9] and resorcinarene[3,10] derivatives have been used in these studies.

Inclusion of non-fluorescent guests can be monitored using fluorescent probes, for example substituted 3*H*-indole with cyclodextrins,[11] or pyrene labeled guests with phosphonate cavitands[12] or pyrogallarene capsules.[13] When the use of fluorescent guests or probes is not feasible, host molecules can be covalently modified using fluorescent groups, resulting in fluorescence sensing multifunctional host molecules, such as coumarin functionalized cavitand crown ethers[14] or calixarenes.[15]

Rhodamine B, a strongly red xanthene dye, has been commonly used in dye lasers[16] and as a fluorescent label in biological staining.[17] The equilibrium of rhodamine B isomers, *i.e.* red zwitterion and a colorless lactone form (Scheme 1), has been an intensive target of research during the past fifty years due to the need to understand the complicated behavior of the dye in solution,[18] in the solid state,[19] and on catalyst coated surfaces.[20] Different optical properties of the isomers have already been utilized in an ammonia fluorosensor application.[21] The equilibrium of the rhodamine B base isomers depends, among other things, on the hydrogen bonding ability and self-organization of the solvent, where protic solvents favor the zwitterion and aprotic solvents favor the lactone form.[22] However, in a contradicting study, rhodamine B base was found to exist as a zwitterion in chloroform.[23] The equilibrium of rhodamine B hydrochloride salt lies strongly on the zwitterion side in protic solvents as well as in aprotic solvents, such as acetonitrile and chloroform, even though there has been some ambiguity whether the strong red color observed in chloroform results from the absorption of the zwitterion or from the cation form (Scheme 1).[22]

Resorcinarenes are a widely studied group of supramolecular hosts with a shallow and conformationally flexible binding cavity at the upper rim, which is readily available for versatile chemical modifications to introduce structural rigidity and selectivity to the binding properties.[24] Aminomethylation of resorcinarenes using Mannich condensation[25,26] extends the upper rim of the macrocycle with tertiary amino groups, which can be protonated by acidic compounds. Aminomethylated resorcinarenes and their salts have been observed to complex neutral organic guests, such as acetonitrile, formaldehyde and alcohols.[27,28] The size of the amine used in the aminomethylation can vary from simple diethylamine to bulky cyclic structures, which enable the complexation of rather large, chiral ammonium cations,[29] or tetramethylammonium cations with their counter anions.[30]

In the current research we have investigated the interaction of aminomethylated resorcinarenes **1–2** (Scheme 2) and their reference compounds **3–4** with rhodamine B in solution using spectroscopic methods. Special attention is paid to the effect of the aminomethylated resorcinarenes to the rhodamine B equilibrium in protic and aprotic solutions, since there are only a very few examples of such research in aprotic environments.[23] The long alkyl chain resorcinarenes **1** and **2** were chosen as target compounds due to their known ability to form self-assembled monolayers,[31,32] which could have further been utilized in designing functional monolayers.

Results and discussion

Synthesis and characterization of hosts 1–4

Mannich condensation of undecylresorcinarene with 5–10 equivalents of formaldehyde and 4 equivalents of diethylamine or 9-(methylaminomethyl)anthracene in ethanol afforded hosts **1** and **2**, respectively, in crown conformation.

Department of Chemistry, Nanoscience Center, University of Jyväskylä, P.O. Box 35, FIN-40014 JYU, Finland. E-mail: maija.nissinen@jyu.fi; Fax: +358 14 260 4756; Tel: +358 14 260 4242

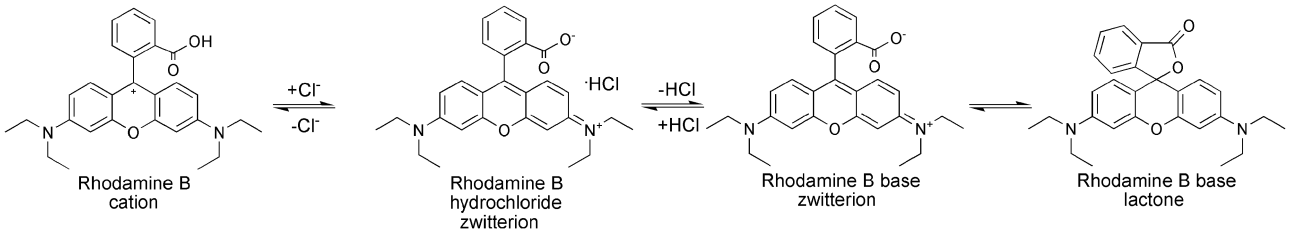

Scheme 1 The equilibrium of rhodamine B isomers.

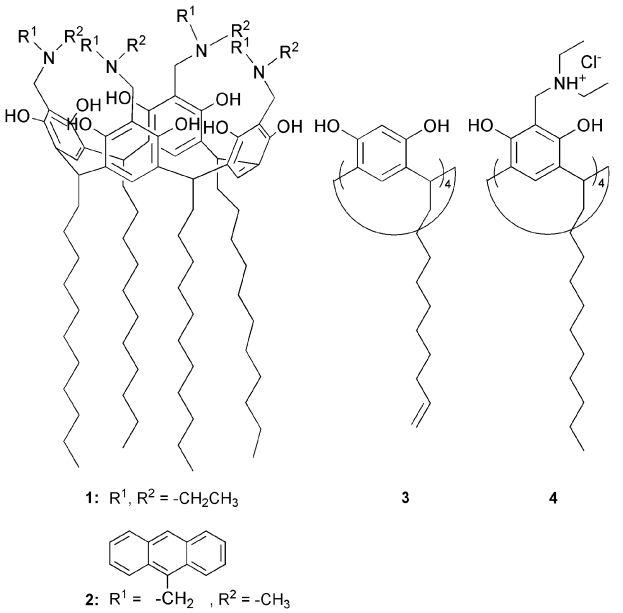

Scheme 2 Structures of aminomethylated resorcinarenes **1–2** and reference compounds **3–4**.

The conformation was confirmed by the ^{1}H NMR spectra, where only one sharp aromatic proton signal arising from the resorcinarene core was observed. The starting material, undecylresorcinarene, has a hydrogen bonded upper rim that keeps the molecule in the crown conformation, which after aminomethylation is further supported by nitrogen atoms participating in the hydrogen bonding array, as illustrated in single crystal X-ray structures of closely related compounds which show how the array of intramolecular hydrogen bonds extends and rigidifies the binding cavity of the host.[26,27,33]

Reference compound **3** was synthesized according to the literature procedure[34] and compound **4** by heating the host **1** at reflux with 5 eq. of aqueous HCl in ethanol and removing the solvent under vacuum. The compound **3** was chosen as a reference compound instead of undecylresorcinarene because of its potential as a starting material for sulfur-functionalized resorcinarenes[32] or for self-assembling monolayers on Si surfaces.[35] The results of the NMR experiments show that the length of the alkyl chain or double bond functionality did not have any observable effect on the interaction with rhodamine B.

^{1}H NMR spectroscopy

The interaction of aminomethylated resorcinarenes **1–2** with rhodamine B hydrochloride was investigated in $CDCl_3$ by titrating samples of rhodamine B with **1** and **2**. The acquired ^{1}H NMR spectra were compared with the spectrum of pure rhodamine B hydrochloride and the spectrum of rhodamine B base in lactone form.

Addition of compound **1** induces dramatic changes in the rhodamine B signals (Fig. 1), indicating a transformation of the rhodamine B zwitterion into the lactone form. In addition, the aromatic proton signal of **1** is shifted from 7.10 to 7.30 ppm, value which corresponds to the aromatic proton signal of reference compound **4** (Fig. 2). This indicates that compound **1** is protonated and the simultaneous decrease in the resolution of the upper rim proton signals at 1 : 1 ratio with rhodamine B suggests that **1** has an equilibrium between protonated and deprotonated forms and potentially some interaction with rhodamine B.

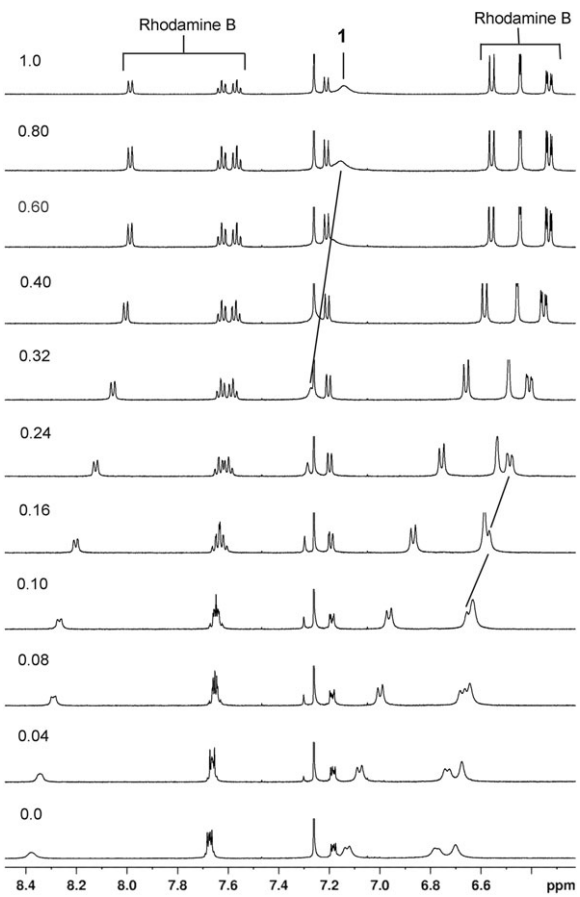

Fig. 1 NMR titration of rhodamine B hydrochloride in $CDCl_3$ with **1** showing lactonization of rhodamine B. Additions as molar equivalents.

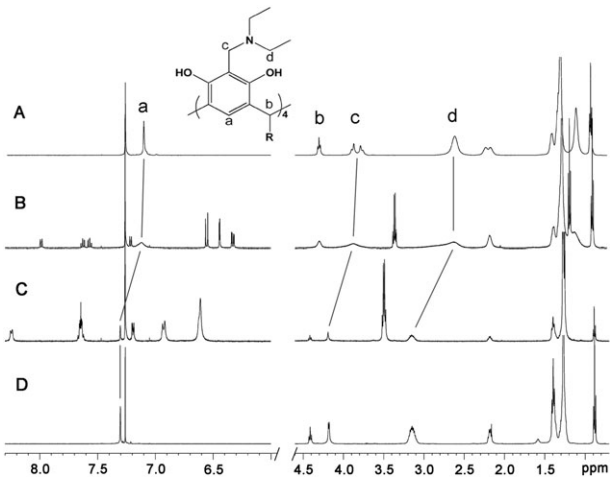

Fig. 2 ^{1}H NMR spectra in $CDCl_3$ of (**A**) **1**, (**B**) **1** with 1 eq. of rhodamine B hydrochloride, (**C**) **1** with 10 eq. of rhodamine B hydrochloride, (**D**) **4**, showing a downfield shift of the aromatic proton signal of **1** and broadening of the upper rim signals upon the addition of rhodamine B.

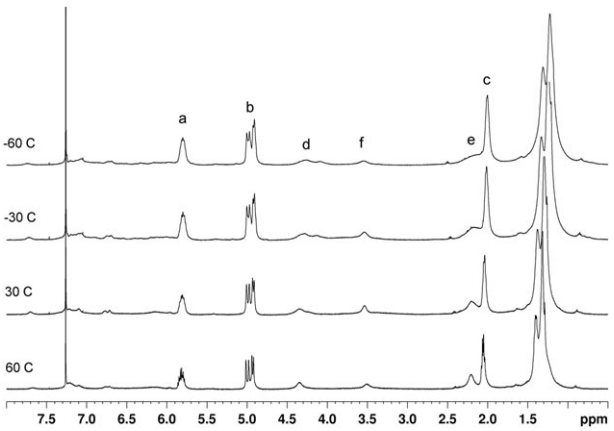

Fig. 3 ^{1}H NMR spectra of compound **3** with 1 eq. of rhodamine B hydrochloride in $CDCl_3$ at −60, −30, 30 and 60 °C. The resolution of the resorcinarene signals **a** (–C*H*═CH_2), **b** (–CH═C*H*$_2$), **c** (–C*H*$_2$CH═CH_2), **d** (Ar–C*H*) and **e** (Ar–CHC*H*$_2$) is increased at 60 °C and decreased at −60 °C, **f** from rhodamine B (–N–C*H*$_2$CH$_3$).

Rhodamine B lactonization was also observed in the presence of **2**, and the aromatic proton signal arising from the host's resorcinarene core was shifted downfield from 6.95 to 7.03 ppm at 1 : 1 ratio of rhodamine B. After addition of excess rhodamine B, the signal was covered under broad signals of the anthracene moieties. Even though the overlapping of proton signals made the analysis of the NMR spectra more complicated, compound **2** was chosen for further study because of the possibility of the aromatic anthracene moieties binding *via* π–π interaction to the rhodamine B molecule, and because of the fluorescence properties of the anthracene substituents. The reference compounds **3** and **4** do not induce rhodamine B lactonization, which proves, as expected, that the tertiary amino groups at the upper rim of resorcinarenes **1–2** are required for lactonization.

Addition of rhodamine B hydrochloride into a sample of **4** does not change the spectrum of the host at all, whereas addition of rhodamine B hydrochloride into a sample of **3** significantly reduces the resolution of all signals of host **3** and rhodamine B compared with the spectra of the pure components. This indicates that the system involves unspecified binding events close to the NMR timescale, which were further studied by varying the temperature of the sample between −60 and 60 °C (Fig. 3). At 60 °C the resolution is partially restored for the signals of **3**, especially at the lower rim, but for the rhodamine B signals no significant change was observed. The interaction was too vague to be specified but it is likely to involve the free hydroxyl groups at the upper rim of resorcinarene **3**, which could hydrogen bond to various functional groups of rhodamine B, and π–π interaction between aromatic rings of rhodamine B and **3**.

The ability of compound **1** to interact with rhodamine B hydrochloride in protic solvent was investigated by measuring a sample of **1** with rhodamine B hydrochloride in deuterated methanol. Protic solvents are known to shift the rhodamine B equilibrium towards the zwitterion form, which is thought to result from the ability of a protic solvent to stabilize the rhodamine B zwitterion through hydrogen bonding.[22] Chemical shifts of rhodamine B hydrochloride proton signals when 1 equivalent of **1** is added (Table 1) correspond quite accurately to the chemical shifts of rhodamine B base in methanol-d_4. The solubility of compound **1** in methanol is poor by itself, but the addition of rhodamine B improves the solubility of **1** by protonation of the nitrogens since sufficient amount of **1** was dissolved in the solvent to induce deprotonation in rhodamine B hydrochloride.

Based on the NMR experiments, the observed interaction between aminomethylated resorcinarenes **1–2** and rhodamine B hydrochloride is an obvious example of an acid–base interaction, where compounds **1–2** act as a base, and rhodamine B hydrochloride acts as an acid, and the result of this interaction is the lactonization of rhodamine B. However, the additional changes in the NMR spectra of **1** mentioned earlier indicate that there could be π–π interaction between the aromatic ring structure of rhodamine B and the aromatic part of resorcinarene, or interaction between the amino or acid groups of rhodamine B and the upper rim of the resorcinarene as observed with compound **3**. To reveal these interactions and eliminate the effect of lactonization in the spectra, rhodamine 6G (Scheme 3), which is an esterified analog of rhodamine B and therefore incapable of forming a lactone ring structure, was mixed with **1** in $CDCl_3$. The resulting NMR spectra did not show any changes in the chemical shifts of rhodamine 6G

Table 1 Comparison of the proton chemical shifts of pure rhodamine B hydrochloride, rhodamine B hydrochloride with 1 eq. of **1** and pure rhodamine B base (zwitterion) in methanol-d_4

	RhB·HCl	RhB·HCl + **1** (1 : 1)	RhB base
–NCH$_2$C*H*$_3$ (12 H)	1.31	1.29	1.29
–NC*H*$_2$CH$_3$ (8 H)	3.68	3.65	3.66
Xanthene-*H* (2 H)	6.97	6.91	6.90
Xanthene-*H* (2 H)	7.03	6.99	6.99
Xanthene-*H* (2 H)	7.14	7.28	7.28
Phenyl-*H* (1 H)	7.41	7.25	7.24
Phenyl-*H* (2 H)	7.82	7.62	7.62
Phenyl-*H* (1 H)	8.34	8.09	8.09

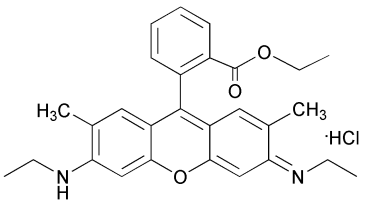

Scheme 3 Rhodamine 6G.

or aromatic proton signal of **1**, which was slightly surprising since protonation of **1** by rhodamine 6G hydrochloride could have been expected. Therefore we can conclude that rhodamine B hydrochloride has a much better ability to protonate compound **1** than rhodamine 6G, and changes in the spectra of rhodamine B hydrochloride in the presence of **1** in aprotic solvent are induced by lactonization, not by deprotonation.

UV-vis spectroscopy

Rhodamine B hydrochloride presents an intense absorbance maximum at 552 nm in $CHCl_3$ with a shoulder at 516 nm and additional bands in the UV region at 353, 307, 282 and 261 nm, whereas the lactone form presents only UV absorbance bands at 317, 278, and 242 nm (Fig. 4). Titration of rhodamine B hydrochloride solution in chloroform with increasing amounts of **1** or **2** showed a rapid decrease in the intensity of the rhodamine B absorbance maximum at 552 nm and bleaching of the pink color indicating a shift in the rhodamine B equilibrium from the zwitterion to the lactone form. The effect is comparable to that observed by Barra *et al*. in a study of rhodamine B with erythromycin A.[23]

Bleaching was more effective with host **1** than with host **2** when the same amount of host solution was added to the sample (Fig. 5), which contradicts our preliminary idea that the aromatic anthracene moieties of **2** would enhance interaction with the dye. Job's method[36] was used to determine the stoichiometry of the investigated interaction and it was found to be 1 : 2 (host–RhB) for both **1** and **2**, which indicates that one host molecule is able to deprotonate two rhodamine B molecules.

Reference compounds **3–4** did not induce rhodamine B lactonization, but addition of **3** to rhodamine B solution shifted the absorbance maximum 1 nm to longer wavelength,

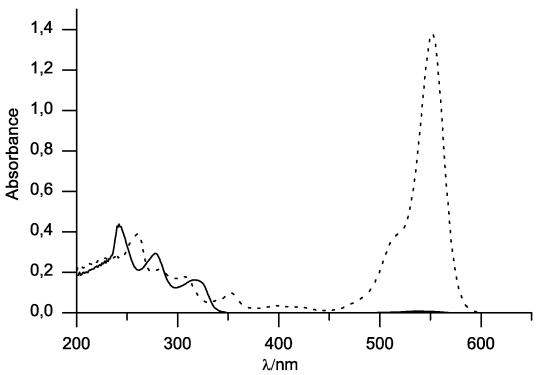

Fig. 4 Absorption spectra of rhodamine B hydrochloride (dotted line) and rhodamine B base in lactone form (solid line) at 1×10^{-5} M concentration in chloroform.

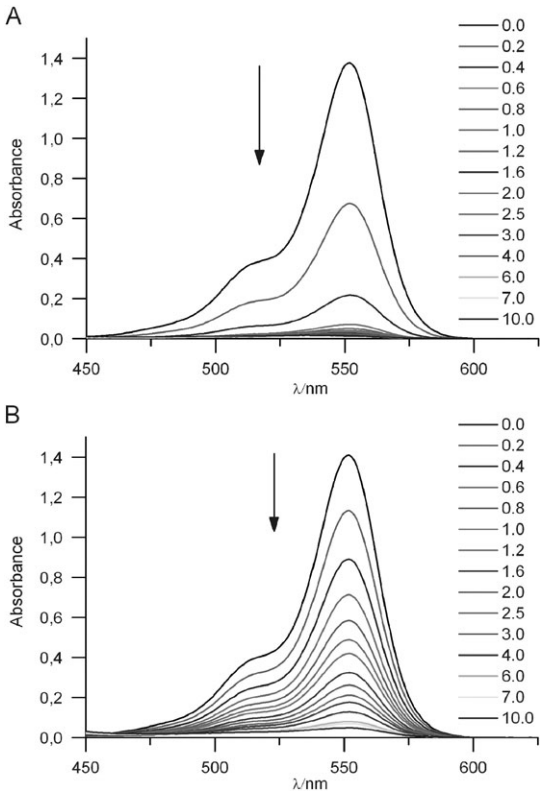

Fig. 5 UV-vis titration of rhodamine B hydrochloride in $CHCl_3$ with (A) **1** and (B) **2**. Additions as molar equivalents.

which is an indication that a cation form of rhodamine B, which exists in acidic conditions,[18] is stabilized in the presence of **3**. In addition, a rhodamine 6G sample was titrated with **1** in $CHCl_3$, but no change in the absorbance spectra of the dye was observed, which together with the NMR experiments confirms that rhodamine 6G does not interact with aminomethylated resorcinarene **1**.

The ability of the aminomethylated resorcinarenes to interact with rhodamine B in protic solvent was also investigated with UV-vis spectroscopy. Rhodamine B hydrochloride samples were titrated with compounds **1–2** in $CHCl_3$–MeOH (1 : 1), and instead of bleaching, an 8 nm blue shift was observed, which corresponds to the peak of zwitterionic rhodamine B base in the same conditions.

The ability of **1**, which was observed to be a stronger lactonizing compound, and reference compound **3** to extract rhodamine B into hexane phase from water phase was examined using hexane–water extraction. Rhodamine B hydrochloride is insoluble in hexane, whereas the long aliphatic chains of resorcinarenes **1** and **3** make them very soluble in non polar organic solvents, but insoluble in water. An aqueous solution of rhodamine B was stirred with a hexane solution of **1** or **3**, and after separation of the phases, the decrease in the rhodamine B absorbance in the water phase was used to calculate the amount of the dye transported. Compound **1** did not transport any rhodamine B but compound **3** transported 15.2 ± 0.9% when the rhodamine concentration was ten times higher than the host concentration. The results show that resorcinarene **3**, which has an open binding cavity,

aggregates with rhodamine B as depicted in the NMR experiments and therefore has better ability to transport rhodamine B than **1**. In case of compound **1** the interaction between **1** and rhodamine B is mainly acid–base interaction and requires that the components are in the same phase.

Fluorescence spectroscopy

The effect of **1** in rhodamine B hydrochloride fluorescence spectrum was investigated in $CHCl_3$. Rhodamine B hydrochloride has an emission maximum at 580 nm, but in the presence of compound **1**, the maximum is shifted to 558 nm, and the emission intensity is decreased close to the values observed for rhodamine B base. Furthermore, rhodamine B lactonization was confirmed as an appearance of a new emission band at 487 nm at excitation wavelength 286 nm, which corresponds to the maximum absorption of resorcinarene core and rhodamine B lactone. With 350 nm excitation, which corresponds to the absorption of rhodamine B hydrochloride, the emission intensity was very low. The fluorescence spectra of rhodamine B hydrochloride, rhodamine B base (lactone form) and a sample of rhodamine B with 1 equivalent of **1** at 286 nm excitation are presented in Fig. 6.

Host **2**, which contains four anthracene units connected by $–CH_2–N(CH_3)–CH_2–$ bridges to the upper rim, has fluorescence maxima at 395, 418 and 442 nm wavelengths in $CHCl_3$. Tertiary nitrogen atoms next to anthracene are known to cause fluorescence quenching by PET (photoinduced electron transfer) processes.[37] When acid was added to the sample of **2** in chloroform, the fluorescence intensity was increased. After 1 equivalent of HCl was added, the increase of intensity was roughly 70% accompanied by a 1–2 nm red shift of the fluorescence bands, and after 10 equivalents of HCl were added, the increase was 95%. The observed increase is likely induced by protonation of the nitrogens, which hinders PET and therefore promotes fluorescence. When rhodamine B hydrochloride was added to the sample of **2**, the fluorescence intensity of **2** was first increased as well (~25%), but after addition of more than 1 eq. of rhodamine B, the fluorescence intensity was decreased, which probably indicates that rhodamine B absorbance becomes a dominating factor (Fig. 7).

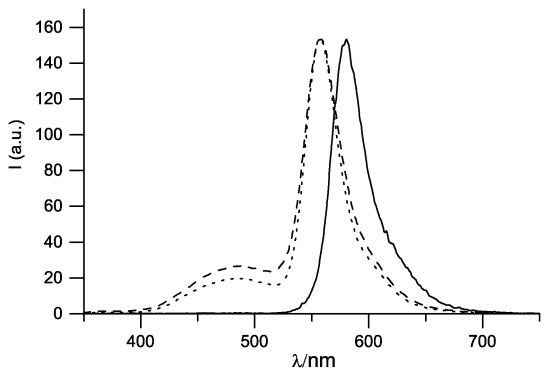

Fig. 6 Fluorescence spectra of rhodamine B hydrochloride (solid line), rhodamine B base in lactone form (dotted line) and rhodamine B hydrochloride with 1 eq. of host **1** (dashed line) in $CHCl_3$ at 286 nm excitation. Concentration 5×10^{-6} M, intensity values are normalized to rhodamine B base intensity.

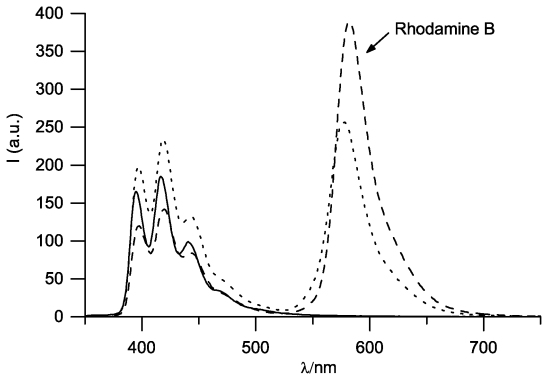

Fig. 7 Fluorescence spectra of host **2** (1×10^{-5} M in $CHCl_3$) at 258 nm excitation with addition of rhodamine B hydrochloride 0 eq. (solid line), 1 eq. (dotted line) and 2 eq. (dashed line).

Conclusions

The interaction of rhodamine B hydrochloride with aminomethylated resorcinarenes was investigated in solution using spectroscopic methods. In aprotic media, aminomethylated resorcinarenes **1–2** transformed the rhodamine B equilibrium from the zwitterion into the lactone form. Since lactonization was not observed in the presence of compounds **3–4**, we can conclude that the tertiary amine groups at the upper rim of resorcinarenes **1–2** induce lactonization by acting as a base. Lactonization was more effective with host **1** than host **2** based on the UV-vis titration, and the stoichiometric ratio was found to be 1 : 2 (host : RhB) determined by Job's method. In protic media, rhodamine B base as a zwitterion was observed.

In addition to acid–base interaction, clear evidence of π–π interaction or inclusion-type complexation between hosts and the dye was not obtained, which may partly be due to the difficulty of observing weaker changes when lactonization of rhodamine B is taking place. However, compound **3** showed aggregation ability with rhodamine B, probably *via* π–π interaction or hydrogen bonding, which was observed in hexane–water extraction and ^{1}H NMR experiments.

Experimental

General

All chemicals and solvents were purchased from Sigma-Aldrich and they were used as received. NMR spectra were recorded with a Bruker Avance DRX (500 MHz for ^{1}H and 126 MHz for ^{13}C) spectrometer at 30 °C. *J* values are given in Hz. ESI-MS spectra were measured with a Micromass LCT (ESI-TOF) instrument. Melting points were determined with a Stuart Scientific SMP3 and a Metler Toledo FP62 apparatus and are uncorrected. Elemental analyses were performed on a Vario EL III apparatus. UV-vis spectra were measured with a Varian Cary 100 Conc UV-vis spectrophotometer at RT using a 1 cm quartz cuvette, and fluorescence spectra with a Perkin Elmer Luminescence Spectrometer LS50B at RT using a 1 cm quartz cuvette.

NMR experiments

The ^{1}H NMR spectra were recorded in $CDCl_3$ or in CD_3OD at 500 MHz. The NMR titration was performed by adding

increasing amounts of compound **1** or **2** in $CDCl_3$ to an 8.7 mM solution of rhodamine B hydrochloride in $CDCl_3$ and recording the spectra.

UV-vis experiments

UV-vis titration was performed by adding increasing amounts of 1×10^{-3} M solution of **1** or **2** into 1×10^{-5} M solution of rhodamine B hydrochloride in $CHCl_3$ and recording the spectra. Titration experiments in $CHCl_3$–MeOH were performed identically.

Job plot samples were prepared by mixing 1×10^{-5} M solutions of rhodamine B hydrochloride and either **1** or **2** in $CHCl_3$ in different ratios (9 : 1, 4 : 1, 7 : 3, 3 : 2, 1 : 1, 2 : 3, 3 : 7, 1 : 4, 1 : 9) keeping the total concentration constant.

Extraction was performed by mixing 3 ml of 1×10^{-2} M rhodamine B hydrochloride in water and 3 ml of 1×10^{-3} M resorcinarene **1** or **3** in hexane for 1 h. On the following day the water phase was diluted 100 fold with water and analyzed using a UV-vis spectrophotometer. Blank samples were prepared identically as the actual samples but without resorcinarene in the hexane phase. The percent of rhodamine B transported was calculated by comparing the A_{354} of the sample against the A_{354} of the blank sample according to the equation

$$\text{transport}\% = [A_{354(\text{blank})} - A_{354(\text{sample})}]/A_{354(\text{blank})} \times 100\%.$$

Fluorescence experiments

Fluorescence spectra were recorded using 5 nm excitation and emission slits and a 350 nm emission filter for 258 and 286 nm excitation wavelengths, and a 390 nm emission filter for 350 nm excitation wavelength.

Acid titration of **2** in chloroform was performed by adding increasing amounts of 1×10^{-3} M HCl solution in $CHCl_3$ (prepared from conc. HCl) to a 1×10^{-5} M solution of **2** in $CHCl_3$ and recording the spectra at different excitation wavelengths (258, 386 and 350 nm). Titration with rhodamine B hydrochloride was performed identically.

Synthetic procedures

Aminomethylated resorcinarene **1** was prepared by Mannich condensation of formaldehyde and secondary amine into the resorcinarene aromatic ring.[25,26] Undecylresorcinarene (0.84 g, 0.76 mmol) was dissolved in a mixture of ethanol (22 ml) and 37% formaldehyde (0.28 ml, 3.76 mmol). Diethylamine (0.22 g, 3.0 mmol) was added dropwise under vigorous stirring. After the addition of amine the stirring was stopped and by next day crystals had grown. Crystals were filtered with suction and dried under vacuum to give **1** (0.94 g, 85%) as a pale powder. ^{1}H NMR ($CDCl_3$, 500 MHz) δ 0.89 (t, J = 7.0, 12H), 1.10 (t, J = 6.8, 24H), 1.27 (m, 64H), 1.37 (m, 8H), 2.17 (m, 8H), 2.59 (m, 16H), 3.81 (m, 8H), 4.28 (t, J = 7.9, 4H), 7.10 (s, 4H) ppm. ^{13}C NMR ($CDCl_3$, 126 MHz) δ 11.0, 14.1, 22.7, 28.3, 29.4, 29.74, 29.77, 29.82, 29.86, 29.87, 32.0, 33.4, 33.5, 46.4, 51.3, 107.8, 121.9, 124.0, 150.4, 153.0 ppm. MS (ESI-TOF) m/z 1446.20 $[M]^+$. Anal. calcd. for $C_{92}H_{156}N_4O_8$: C 76.40%, H 10.87%, N 3.87%. Found C 76.11%, H 10.66%, N 3.49%. Mp 82 °C.

Aminomethylated resorcinarene **2** was prepared by stirring a mixture of resorcinarene (0.3 g, 0.27 mmol), 9-(methylaminomethyl)anthracene (0.35 g, 1.6 mmol) and formaldehyde (2.0 ml, excess) in 10 ml of ethanol overnight. Yield 0.34 g (62%).^{1}H NMR ($CDCl_3$, 500 MHz) δ 0.85 (t, J = 7.1, 12H), 1.18 (m, 72H), 2.03 (m, 8H), 2.21 (s, 12H), 3.95 (m, 8H), 4.08 (t, J = 7.3, 4H), 4.64 (m, 8H), 6.95 (s, 4H), 7.55 (m, 8H), 7.61 (m, 8H), 8.05 (m, 8H), 8.36 (m, 8H), 8.46 (m, 4H) ppm. ^{13}C NMR ($CDCl_3$, 126 MHz) 14.1, 22.7, 28.2, 29.4, 29.67, 29.69, 29.71, 29.77, 29.9, 31.9, 33.4, 33.6, 41.2, 53.4, 55.1, 108.0, 121.8, 123.5, 124.0, 125.1, 126.6, 127.8, 128.4, 129.3, 131.2, 131.4, 150.4, 151.7 ppm. MS (ESI-TOF) m/z 2038.37 $[M]^+$. Anal. calcd. for $C_{140}H_{172}N_4O_8$: C 82.47%, H 8.50%, N 2.75%. Found C 82.54%, H 8.84%, N 2.79%. Mp 140 °C.

Resorcinarene **3** was synthesized according to the literature procedure.[34] To a mixture of resorcinol (4.0 g, 36.4 mmol) and 10-undecenal (7.5 ml, 36.1 mmol) in ethanol (125 ml), concentrated HCl (7.0 ml) was added dropwise under nitrogen atmosphere at 0–5 °C. The clear transparent mixture was stirred in an ice bath for 1.5 h and subsequently refluxed for 26 h. The product was precipitated from water, filtered with suction and dried under vacuum. The resulting yellowish powder was recrystallized from acetonitrile, purified by flash chromatography (SiO_2, eluent $CHCl_3$–MeOH, MeOH gradient from 0% to 10% v/v) and recrystallized again from acetonitrile–water. The resulting pale powder was filtered with suction and dried under vacuum. Yield 3.4 g (36%). ^{1}H NMR ($CDCl_3$, 500 MHz) δ 1.30 (m, 32H), 1.38 (m, 16H), 2.04 (m, 8H), 2.21 (m, 8H), 4.30 (t, J = 7.5, 4H), 4.93 (m, J = 10 and 1.2, 4H), 5.00 (m, J = 17, 2.2 and 1.6, 4H) 5.81 (m, 4H), 6.12 (s, 4H), 7.20 (s, 4H), 9.29 (m, 4H), 9.60 (m, 4H) ppm.^{13}C NMR ($CDCl_3$, 126 MHz) δ 28.0, 29.0, 29.1, 29.50, 29.54, 29.7, 33.1, 33.3, 33.8, 102.9, 114.1, 123.9, 124.9, 139.2, 150.4, 150.6 ppm. MS (ESI-TOF) m/z 1039.96 $[M - H]^-$, m/z 519.48 $[M]^{2-}$. Anal. calcd. for $C_{68}H_{96}O_8 \cdot H_2O$: C 77.09%, H 9.32%. Found C 77.14%, H 9.46%. Mp > 300 °C.

Resorcinarene **4** was prepared by heating the compound **1** (0.2 g, 0.14 mmol) at reflux with 5 eq. of concentrated hydrochloric acid (59 μl, 0.68 mmol) in ethanol (50 ml) for 1 h and removing the solvent under vacuum. The resulting pale solid was dried under vacuum. ^{1}H NMR ($CDCl_3$, 500 MHz) δ 0.88 (t, J = 6.9, 12H), 1.27 (m, 64H), 1.40 (m, 8H), 1.40 (t, J = 7.2, 24H), 2.18 (m, 8H), 3.15 (m, 16H), 4.18 (d, J = 5.8, 8H), 4.41 (t, J = 7.8, 4H), 7.30 (s, 4H), 9.33 (s, 8H), 10.2 (s, 4H) ppm. ^{13}C NMR ($CDCl_3$, 126 MHz) δ 8.9, 14.1, 22.7, 28.1, 29.4, 29.72, 29.76, 29.80, 29.81, 29.83, 32.0, 33.6, 34.8, 46.2, 47.8, 108.7, 125.6, 127.6, 151.2 ppm. MS (ESI-TOF) m/z 1446.00 $[M]^+$. Anal. calcd. for $C_{92}H_{160}N_4O_8Cl_4$: C 69.41%, H 10.13%, N 3.52%. Found C 69.38%, H 10.13%, N 3.27%. Mp 123 °C.

Acknowledgements

We are grateful to Reijo Kauppinen for his help with the NMR studies, Prof. Mika Pettersson for useful discussions related to spectroscopy, and Academy of Finland (projects 7117945 and 7116503) and Research Foundation of Orion Corporation for funding.

Notes and references

1 See for a review: B. D. Wagner, Fluorescence studies of supramolecular host-guest inclusion complexes, in *Handbook of Photochemistry and Photobiology*, ed. H. S. Nalwa, American Scientific Publishers, Stevenson Ranch, California, USA, 2003, vol. 3, pp. 1–57; M. V. Alfimov, *Russ. Chem. Bull.*, 2004, **53**, 1357–1368; D. Brühwiler and G. Galzaferri, *Microporous Mesoporous Mater.*, 2004, **72**, 1–23; B. D. Wagner, *Curr. Anal. Chem.*, 2007, **3**, 183–195.

2 D. Rodrígues-Lucena, J. M. Benito, E. Álvarez, C. Jaime, J. Perez-Miron, C. O. Mellet and J. M. G. Fernández, *J. Org. Chem.*, 2008, **73**, 2967–2979; A. A. Dawoud and N. Al-Rawashdeh, *J. Inclusion Phenom. Macrocyclic Chem.*, 2008, **60**, 293–301.

3 T. Fujimoto, C. Shimizu, O. Hayashida and Y. Aoyama, *Gazz. Chim. Ital.*, 1997, **127**, 749–752.

4 S. Kunsági-Máte, G. Nagy, P. Jurecka and L. Kollár, *Tetrahedron*, 2002, **58**, 5119–5124.

5 Y. Liu, B.-H. Han and Y.-T. Chen, *J. Org. Chem.*, 2000, **65**, 6227–6230.

6 D. Velic, M. Knapp and G. Köhler, *THEOCHEM*, 2001, **598**, 49–56.

7 Y. Liu, C.-J. Li, D.-S. Guo, Z.-H. Pan and Z. Li, *Supramol. Chem.*, 2007, **19**, 517–523.

8 Y. Ling, W. Wang and A. E. Kaifer, *Chem. Commun.*, 2007, 610–612.

9 A. Lodi, M. Caselli, A. Casnati, F. Momicchioli, F. Sansone, D. Vanossi and G. Ponterini, *THEOCHEM*, 2007, **846**, 49–54.

10 T. Fujimoto, C. Shimizu, O. Hayashida and Y. Aoyama, *J. Am. Chem. Soc.*, 1997, **119**, 6676–6677; O. Hayashida and M. Uchiyama, *Tetrahedron Lett.*, 2006, **47**, 4091–4094; O. Hayashida and M. Uchiyama, *J. Org. Chem.*, 2007, **72**, 610–616.

11 Y. He, X. Shen, H. Gao and Y. He, *J. Photochem. Photobiol., A*, 2008, **193**, 178–186.

12 E. Biavardi, G. Battistini, M. Montalti, R. M. Yebeutchou, L. Prodi and E. Dalcanale, *Chem. Commun.*, 2008, 1638–1640.

13 S. J. Dalgarno, S. A. Tucker, D. B. Bassil and J. L. Atwood, *Science*, 2005, **309**, 2037–2039.

14 I. Stoll, J. Eberhard, R. Brodbeck, W. Eisfeld and J. Mattay, *Chem.–Eur. J.*, 2008, **14**, 1155–1163.

15 R. K. Castellano, S. L. Craig, C. Nuckolls and J. Rebek, Jr, *J. Am. Chem. Soc.*, 2000, **122**, 7876–7882.

16 Y. Zhang, M. Wang, Z. Wang and G. Qian, *Mater. Lett.*, 1999, **40**, 175–179; R. Khare and S. R. Daulatabad, *Opt. Laser Technol.*, 2004, **36**, 27–30.

17 T. Suzuki, K. Fujikura, T. Higashiyama and K. Takata, *J. Histochem. Cytochem.*, 1997, **45**, 49–53; D.-W. Jung, G.-H. Tak, J.-W. Lim, C.-J. Bae, G.-Y. Kim, G.-S. Yoo and J.-K. Choi, *Anal. Biochem.*, 1998, **263**, 118–120.

18 R. W. Ramette and E. B. Sandell, *J. Am. Chem. Soc.*, 1956, **78**, 4872–4878; U. K. A. Klein and F. W. Hafner, *Chem. Phys. Lett.*, 1976, **43**, 141–145.

19 X. Wang, M. Song and Y. Long, *J. Solid State Chem.*, 2001, **156**, 325–330.

20 A. A. El-Rayyes, A. Al-Betar, T. Htun and U. K. A. Klein, *Chem. Phys. Lett.*, 2005, **414**, 287–291.

21 C. Preininger, G. J. Mohr, I. Klimant and O. S. Wolfbeis, *Anal. Chim. Acta*, 1996, **334**, 113–123.

22 I. Rosenthal, P. Peretz and K. A. Muszkat, *J. Phys. Chem.*, 1979, **83**, 350–353; D. A. Hinckley, P. G. Seybold and D. P. Borris, *Spectrochim. Acta, Part A*, 1986, **42**, 747–754; D. A. Hinckley and P. G. Seybold, *Spectrochim. Acta, Part A*, 1988, **44**, 1053–1059.

23 M. Barra and R. H. de Rossi, *Tetrahedron Lett.*, 1988, **29**, 1119–1122; M. Barra, J. J. Cosa and R. H. de Rossi, *J. Org. Chem.*, 1990, **55**, 5850–5853.

24 See for a review: P. Timmerman, W. Verboom and D. N. Reinhoudt, *Tetrahedron*, 1996, **52**, 2663–2704.

25 Y. Matsushita and T. Matsui, *Tetrahedron Lett.*, 1993, **34**, 7433–7436; S. Nummelin, D. Falábu, A. Shivanyuk and K. Rissanen, *Org. Lett.*, 2004, **6**, 2869–2872.

26 D. A. Leigh, P. Linnane, R. G. Pritchard and G. Jackson, *J. Chem. Soc., Chem. Commun.*, 1994, 389–390.

27 D. Falábu, A. Shivanyuk, M. Nissinen and K. Rissanen, *Org. Lett.*, 2002, **4**, 3019–3022.

28 A. Shivanyuk, T. P. Spaniol, K. Rissanen, E. Kolehmainen and V. Böhmer, *Angew. Chem., Int. Ed.*, 2000, **39**, 3497–3500.

29 N. K. Beyeh, D. Fehér, M. Luostarinen, C. A. Schalley and K. Rissanen, *J. Inclusion Phenom. Macrocyclic Chem.*, 2006, **56**, 381–394.

30 J. L. Atwood and A. Szumna, *Chem. Commun.*, 2003, 940–941.

31 H. Adams, F. Davis and J. M. Stirling, *J. Chem. Soc., Chem. Commun.*, 1994, 2527–2529; A. K. Hassan, A. V. Nabok, A. K. Ray, A. Lucke, K. Smith, C. J. M. Stirling and F. Davis, *Mater. Sci. Eng., C*, 1999, **8–9**, 251–255.

32 J. D. Faull and V. K. Gupta, *Langmuir*, 2001, **17**, 1470–1476.

33 R. Becker, G. Reck, R. Radeglia, A. Springer and B. Schulz, *THEOCHEM*, 2006, **784**, 157–161.

34 E. U. Thoden van Velzen, J. F. J. Engbersen and D. N. Reinhoudt, *Synthesis*, 1995, **8**, 989–997.

35 A. B. Sieval, A. L. Demirel, J. W. M. Nissink, M. R. Linford, J. H. van der Maas, W. H. de Jeu, H. Zuilhof and E. J. R. Sudhölter, *Langmuir*, 1998, **14**, 1759–1768; G. G. Condorelli, A. Motta, M. Favazza, I. L. Fragalà, M. Busi, E. Menozzi, E. Dalcanale and L. Cristofolini, *Langmuir*, 2006, **22**, 11126–11133.

36 K. Hirose, *J. Inclusion Phenom. Macrocyclic Chem.*, 2001, **39**, 193–209.

37 A. Prasanna de Silva and R. A. D. Dayasiri Rupasinghe, *J. Chem. Soc., Chem. Commun.*, 1985, 1669–1670; A. P. de Silva, S. A. de Silva, A. S. Dissaynake and K. R. A. S. Sandanayake, *J. Chem. Soc., Chem. Commun.*, 1989, 1054–1056; A. Prasanna de Silva, H. Q. N. Gunaratne and C. P. A. McCoy, *Nature*, 1993, **364**, 42–44.

DEPARTMENT OF CHEMISTRY, UNIVERSITY OF JYVÄSKYLÄ
RESEARCH REPORT SERIES

1. Vuolle, Mikko: Electron paramagnetic resonance and molecular orbital study of radical ions generated from (2.2)metacyclophane, pyrene and its hydrogenated compounds by alkali metal reduction and by thallium(III)trifluoroacetate oxidation. (99 pp.) 1976
2. Pasanen, Kaija: Electron paramagnetic resonance study of cation radical generated from various chlorinated biphenyls. (66 pp.) 1977
3. Carbon-13 Workshop, September 6-8, 1977. (91 pp.) 1977
4. Laihia, Katri: On the structure determination of norbornane polyols by NMR spectroscopy. (111 pp.) 1979
5. Nyrönen, Timo: On the EPR, ENDOR and visible absorption spectra of some nitrogen containing heterocyclic compounds in liquid ammonia. (76 pp.) 1978
6. Talvitie, Antti: Structure determination of some sesquiterpenoids by shift reagent NMR. (54 pp.) 1979
7. Häkli, Harri: Structure analysis and molecular dynamics of cyclic compounds by shift reagent NMR. (48 pp.) 1979
8. Pitkänen, Ilkka: Thermodynamics of complexation of 1,2,4-triazole with divalent manganese, cobalt, nickel, copper, zinc, cadmium and lead ions in aqueous sodium perchlorate solutions. (89 pp.) 1980
9. Asunta, Tuula: Preparation and characterization of new organometallic compounds synthesized by using metal vapours. (91 pp.) 1980
10. Sattar, Mohammad Abdus: Analyses of MCPA and its metabolites in soil. (57 pp.) 1980
11. Bibliography 1980. (31 pp.) 1981
12. Knuuttila, Pekka: X-Ray structural studies on some divalent 3d metal compounds of picolinic and isonicotinic acid N-oxides. (77 pp.) 1981
13. Bibliography 1981. (33 pp.) 1982
14. 6th National NMR Symposium, September 9-10, 1982, Abstracts. (49 pp.) 1982
15. Bibliography 1982. (38 pp.) 1983
16. Knuuttila, Hilkka: X-Ray structural studies on some Cu(II), Co(II) and Ni(II) complexes with nicotinic and isonicotinic acid N-oxides. (54 pp.) 1983
17. Symposium on inorganic and analytical chemistry May 18, 1984, Program and Abstracts. (100 pp.) 1984
18. Knuutinen, Juha: On the synthesis, structure verification and gas chromatographic determination of chlorinated catechols and guaiacols occuring in spent bleach liquors of kraft pulp mill. (30 pp.) 1984
19. Bibliography 1983. (47 pp.) 1984
20. Pitkänen, Maija: Addition of BrCl, B_2 and Cl_2 to methyl esters of propenoic and 2-butenoic acid derivatives and ^{13}C NMR studies on methyl esters of saturated aliphatic mono- and dichlorocarboxylic acids. (56 pp.) 1985
21. Bibliography 1984. (39 pp.) 1985

22. Salo, Esa: EPR, ENDOR and TRIPLE spectroscopy of some nitrogen heteroaromatics in liquid ammonia. (111 pp.) 1985
23. Humppi, Tarmo: Synthesis, identification and analysis of dimeric impurities of chlorophenols. (39 pp.) 1985
24. Aho, Martti: The ion exchange and adsorption properties of sphagnum peat under acid conditions. (90 pp.) 1985
25. Bibliography 1985 (61 pp.) 1986
26. Bibliography 1986. (23 pp.) 1987
27. Bibliography 1987. (26 pp.) 1988
28. Paasivirta, Jaakko (Ed.): Structures of organic environmental chemicals. (67 pp.) 1988
29. Paasivirta, Jaakko (Ed.): Chemistry and ecology of organo-element compounds. (93 pp.) 1989
30. Sinkkonen, Seija: Determination of crude oil alkylated dibenzothiophenes in environment. (35 pp.) 1989
31. Kolehmainen, Erkki (Ed.): XII National NMR Symposium Program and Abstracts. (75 pp.) 1989
32. Kuokkanen, Tauno: Chlorocymenes and Chlorocymenenes: Persistent chlorocompounds in spent bleach liquors of kraft pulp mills. (40 pp.) 1989
33. Mäkelä, Reijo: ESR, ENDOR and TRIPLE resonance study on substituted 9,10-anthraquinone radicals in solution. (35 pp.) 1990
34. Veijanen, Anja: An integrated sensory and analytical method for identification of off-flavour compounds. (70 pp.) 1990
35. Kasa, Seppo: EPR, ENDOR and TRIPLE resonance and molecular orbital studies on a substitution reaction of anthracene induced by thallium(III) in two fluorinated carboxylic acids. (114 pp.) 1990
36. Herve, Sirpa: Mussel incubation method for monitoring organochlorine compounds in freshwater recipients of pulp and paper industry. (145 pp.) 1991
37. Pohjola, Pekka: The electron paramagnetic resonance method for characterization of Finnish peat types and iron (III) complexes in the process of peat decomposition. (77 pp.) 1991
38. Paasivirta, Jaakko (Ed.): Organochlorines from pulp mills and other sources. Research methodology studies 1988-91. (120 pp.) 1992
39. Veijanen, Anja (Ed.): VI National Symposium on Mass Spectrometry, May 13-15, 1992, Abstracts. (55 pp.) 1992
40. Rissanen, Kari (Ed.): The 7. National Symposium on Inorganic and Analytical Chemistry, May 22, 1992, Abstracts and Program. (153 pp.) 1992
41. Paasivirta, Jaakko (Ed.): CEOEC'92, Second Finnish-Russian Seminar: Chemistry and Ecology of Organo-Element Compounds. (93 pp.) 1992
42. Koistinen, Jaana: Persistent polychloroaromatic compounds in the environment: structure-specific analyses. (50 pp.) 1993
43. Virkki, Liisa: Structural characterization of chlorolignins by spectroscopic and liquid chromatographic methods and a comparison with humic substances. (62 pp.) 1993

44. Helenius, Vesa: Electronic and vibrational excitations in some biologically relevant molecules. (30 pp.) 1993
45. Leppä-aho, Jaakko: Thermal behaviour, infrared spectra and x-ray structures of some new rare earth chromates(VI). (64 pp.) 1994
46. Kotila, Sirpa: Synthesis, structure and thermal behavior of solid copper(II) complexes of 2-amino-2- hydroxymethyl-1,3-propanediol. (111 pp.) 1994
47. Mikkonen, Anneli: Retention of molybdenum(VI), vanadium(V) and tungsten(VI) by kaolin and three Finnish mineral soils. (90 pp.) 1995
48. Suontamo, Reijo: Molecular orbital studies of small molecules containing sulfur and selenium. (42 pp.) 1995
49. Hämäläinen, Jouni: Effect of fuel composition on the conversion of fuel-N to nitrogen oxides in the combustion of small single particles. (50 pp.) 1995
50. Nevalainen, Tapio: Polychlorinated diphenyl ethers: synthesis, NMR spectroscopy, structural properties, and estimated toxicity. (76 pp.) 1995
51. Aittola, Jussi-Pekka: Organochloro compounds in the stack emission. (35 pp.) 1995
52. Harju, Timo: Ultrafast polar molecular photophysics of (dibenzylmethine)borondifluoride and 4-aminophthalimide in solution. (61 pp.) 1995
53. Maatela, Paula: Determination of organically bound chlorine in industrial and environmental samples. (83 pp.) 1995
54. Paasivirta, Jaakko (Ed.): CEOEC'95, Third Finnish-Russian Seminar: Chemistry and Ecology of Organo-Element Compounds. (109 pp.) 1995
55. Huuskonen, Juhani: Synthesis and structural studies of some supramolecular compounds. (54 pp.) 1995
56. Palm, Helena: Fate of chlorophenols and their derivatives in sawmill soil and pulp mill recipient environments. (52 pp.) 1995
57. Rantio, Tiina: Chlorohydrocarbons in pulp mill effluents and their fate in the environment. (89 pp.) 1997
58. Ratilainen, Jari: Covalent and non-covalent interactions in molecular recognition. (37 pp.) 1997
59. Kolehmainen, Erkki (Ed.): XIX National NMR Symposium, June 4-6, 1997, Abstracts. (89 pp.) 1997
60. Matilainen, Rose: Development of methods for fertilizer analysis by inductively coupled plasma atomic emission spectrometry. (41 pp.) 1997
61. Koistinen, Jari (Ed.): Spring Meeting on the Division of Synthetic Chemistry, May 15-16, 1997, Program and Abstracts. (36 pp.) 1997
62. Lappalainen, Kari: Monomeric and cyclic bile acid derivatives: syntheses, NMR spectroscopy and molecular recognition properties. (50 pp.) 1997
63. Laitinen, Eira: Molecular dynamics of cyanine dyes and phthalimides in solution: picosecond laser studies. (62 pp.) 1997
64. Eloranta, Jussi: Experimental and theoretical studies on some quinone and quinol radicals. (40 pp.) 1997
65. Oksanen, Jari: Spectroscopic characterization of some monomeric and aggregated chlorophylls. (43 pp.) 1998

66. Häkkänen, Heikki: Development of a method based on laser-induced plasma spectrometry for rapid spatial analysis of material distributions in paper coatings. (60 pp.) 1998
67. Virtapohja, Janne: Fate of chelating agents used in the pulp and paper industries. (58 pp.) 1998
68. Airola, Karri: X-ray structural studies of supramolecular and organic compounds. (39 pp.) 1998
69. Hyötyläinen, Juha: Transport of lignin–type compounds in the receiving waters of pulp mills. (40 pp.) 1999
70. Ristolainen, Matti: Analysis of the organic material dissolved during totally chlorine-free bleaching. (40 pp.) 1999
71. Eklin, Tero: Development of analytical procedures with industrial samples for atomic emission and atomic absorption spectrometry. (43 pp.) 1999
72. Välisaari, Jouni: Hygiene properties of resol-type phenolic resin laminates. (129 pp.) 1999
73. Hu, Jiwei: Persistent polyhalogenated diphenyl ethers: model compounds syntheses, characterization and molecular orbital studies. (59 pp.) 1999
74. Malkavaara, Petteri: Chemometric adaptations in wood processing chemistry. (56 pp.) 2000
75. Kujala Elena, Laihia Katri, Nieminen Kari (Eds.): NBC 2000, Symposium on Nuclear, Biological and Chemical Threats in the 21st Century. (299 pp.) 2000
76. Rantalainen, Anna-Lea: Semipermeable membrane devices in monitoring persistent organic pollutants in the environment. (58 pp.) 2000
77. Lahtinen, Manu: *In situ* X-ray powder diffraction studies of Pt/C, CuCl/C and Cu_2O/C catalysts at elevated temperatures in various reaction conditions. (92 pp.) 2000
78. Tamminen, Jari: Syntheses, empirical and theoretical characterization, and metal cation complexation of bile acid-based monomers and open/closed dimers. (54 pp.) 2000
79. Vatanen, Virpi: Experimental studies by EPR and theoretical studies by DFT calculations of α-amino-9,10-anthraquinone radical anions and cations in solution. (37 pp.) 2000
80. Kotilainen, Risto: Chemical changes in wood during heating at 150-260 °C. (57 pp.) 2000
81. Nissinen, Maija: X-ray structural studies on weak, non-covalent interactions in supramolecular compounds. (69 pp.) 2001
82. Wegelius, Elina: X-ray structural studies on self-assembled hydrogen-bonded networks and metallosupramolecular complexes. (84 pp.) 2001
83. Paasivirta, Jaakko (Ed.): CEOEC'2001, Fifth Finnish-Russian Seminar: Chemistry and Ecology of Organo-Element Compounds. (163 pp.) 2001
84. Kiljunen, Toni: Theoretical studies on spectroscopy and atomic dynamics in rare gas solids. (56 pp.) 2001
85. Du, Jin: Derivatives of dextran: synthesis and applications in oncology. (48 pp.) 2001

86. Koivisto, Jari: Structural analysis of selected polychlorinated persistent organic pollutants (POPs) and related compounds. (88 pp.) 2001
87. Feng, Zhinan: Alkaline pulping of non-wood feedstocks and characterization of black liquors. (54 pp.) 2001
88. Halonen, Markku: Lahon havupuun käyttö sulfaattiprosessin raaka-aineena sekä havupuun lahontorjunta. (90 pp.) 2002
89. Falábu, Dezsö: Synthesis, conformational analysis and complexation studies of resorcarene derivatives. (212 pp.) 2001
90. Lehtovuori, Pekka: EMR spectroscopic studies on radicals of ubiquinones Q-*n*, vitamin K_3 and vitamine E in liquid solution. (40 pp.) 2002
91. Perkkalainen, Paula: Polymorphism of sugar alcohols and effect of grinding on thermal behavior on binary sugar alcohol mixtures. (53 pp.) 2002
92. Ihalainen, Janne: Spectroscopic studies on light-harvesting complexes of green plants and purple bacteria. (42 pp.) 2002
93. Kunttu, Henrik, Kiljunen, Toni (Eds.): 4th International Conference on Low Temperature Chemistry. (159 pp.) 2002
94. Väisänen, Ari: Development of methods for toxic element analysis in samples with environmental concern by ICP-AES and ETAAS. (54 pp.) 2002
95. Luostarinen, Minna: Synthesis and characterisation of novel resorcarene derivatives. (200 pp.) 2002
96. Louhelainen, Jarmo: Changes in the chemical composition and physical properties of wood and nonwood black liquors during heating. (68 pp.) 2003
97. Lahtinen, Tanja: Concave hydrocarbon cyclophane B-prismands. (65 pp.) 2003
98. Laihia, Katri (Ed.): NBC 2003, Symposium on Nuclear, Biological and Chemical Threats – A Crisis Management Challenge. (245 pp.) 2003
99. Oasmaa, Anja: Fuel oil quality properties of wood-based pyrolysis liquids. (32 pp.) 2003
100. Virtanen, Elina: Syntheses, structural characterisation, and cation/anion recognition properties of nano-sized bile acid-based host molecules and their precursors. (123 pp.) 2003
101. Nättinen, Kalle: Synthesis and X-ray structural studies of organic and metallo-organic supramolecular systems. (79 pp.) 2003
102. Lampiselkä, Jarkko: Demonstraatio lukion kemian opetuksessa. (285 pp.) 2003
103. Kallioinen, Jani: Photoinduced dynamics of $Ru(dcbpy)_2(NCS)_2$ – in solution and on nanocrystalline titanium dioxide thin films. (47 pp.) 2004
104. Valkonen, Arto (Ed.): VII Synthetic Chemistry Meeting and XXVI Finnish NMR Symposium. (103 pp.) 2004
105. Vaskonen, Kari: Spectroscopic studies on atoms and small molecules isolated in low temperature rare gas matrices. (65 pp.) 2004
106. Lehtovuori, Viivi: Ultrafast light induced dissociation of $Ru(dcbpy)(CO)_2I_2$ in solution. (49 pp.) 2004
107. Saarenketo, Pauli: Structural studies of metal complexing schiff bases , Schiff base derived *N*-glycosides and cyclophane π-prismands. (95 pp.) 2004

108. Paasivirta, Jaakko (Ed.): CEOEC'2004, Sixth Finnish-Russian Seminar: Chemistry and Ecology of Organo-Element Compounds. (147 pp.) 2004
109. Suontamo, Tuula: Development of a test method for evaluating the cleaning efficiency of hard-surface cleaning agents. (96 pp.) 2004
110. Güneş, Minna: Studies of thiocyanates of silver for nonlinear optics. (48 pp.) 2004
111. Ropponen, Jarmo: Aliphatic polyester dendrimers and dendrons. (81 pp.) 2004
112. Vu, Mân Thi Hong: Alkaline pulping and the subsequent elemental chlorine-free bleaching of bamboo (*Bambusa procera*). (69 pp.) 2004
113. Mansikkamäki, Heidi: Self-assembly of resorcinarenes. (77 pp.) 2006
114. Tuononen, Heikki M.: EPR spectroscopic and quantum chemical studies of some inorganic main group radicals. (79 pp.) 2005
115. Kaski, Saara: Development of methods and applications of laser-induced plasma spectroscopy in vacuum ultraviolet. (44 pp.) 2005
116. Mäkinen, Riika-Mari: Synthesis, crystal structure and thermal decomposition of certain metal thiocyanates and organic thiocyanates. (119 pp.) 2006
117. Ahokas, Jussi: Spectroscopic studies of atoms and small molecules isolated in rare gas solids: photodissociation and thermal reactions. (53 pp.) 2006
118. Busi, Sara: Synthesis, characterization and thermal properties of new quaternary ammonium compounds: new materials for electrolytes, ionic liquids and complexation studies. (102 pp.) 2006
119. Mäntykoski, Keijo: PCBs in processes, products and environment of paper mills using wastepaper as their raw material. (73 pp.) 2006
120. Laamanen, Pirkko-Leena: Simultaneous determination of industrially and environmentally relevant aminopolycarboxylic and hydroxycarboxylic acids by capillary zone electrophoresis. (54 pp.) 2007
121. Salmela, Maria: Description of oxygen-alkali delignification of kraft pulp using analysis of dissolved material. (71 pp.) 2007
122. Lehtovaara, Lauri: Theoretical studies of atomic scale impurities in superfluid ^{4}He. (87 pp.) 2007
123. Rautiainen, J. Mikko: Quantum chemical calculations of structures, bonding, and spectroscopic properties of some sulphur and selenium iodine cations. (71 pp.) 2007
124. Nummelin, Sami: Synthesis, characterization, structural and retrostructural analysis of self-assembling pore forming dendrimers. (286 pp.) 2008
125. Sopo, Harri: Uranyl(VI) ion complexes of some organic aminobisphenolate ligands: syntheses, structures and extraction studies. (57 pp.) 2008
126. Valkonen, Arto: Structural characteristics and properties of substituted cholanoates and *N*-substituted cholanamides. (80 pp.) 2008
127. Lähde, Anna: Production and surface modification of pharmaceutical nano- and microparticles with the aerosol flow reactor. (43 pp.) 2008
128. Beyeh, Ngong Kodiah: Resorcinarenes and their derivatives: synthesis, characterization and complexation in gas phase and in solution. (75 pp.) 2008
129. Välisaari, Jouni, Lundell, Jan (Eds.): Kemian opetuksen päivät 2008: uusia oppimisympäristöjä ja ongelmalähtöistä opetusta. (118 pp.) 2008

130. Myllyperkiö, Pasi: Ultrafast electron transfer from potential organic and metal containing solar cell sensitizers. (69 pp.) 2009
131. Käkölä, Jaana: Fast chromatographic methods for determining aliphatic carboxylic acids in black liquors. (82 pp.) 2009
132. Koivukorpi, Juha: Bile acid-arene conjugates: from photoswitchability to cancer cell detection. (67 pp.) 2009
133. Tuuttila, Tero: Functional dendritic polyester compounds: synthesis and characterization of small bifunctional dendrimers and dyes. (74 pp.) 2009
134. Salorinne, Kirsi: Tetramethoxy resorcinarene based cation and anion receptors: synthesis, characterization and binding properties. (79 pp.) 2009
135. Rautiainen, Riikka: The use of first-thinning Scots pine (*Pinus sylvestris*) as fiber raw material for the kraft pulp and paper industry. (73 pp.) 2010
136. Ilander, Laura: Uranyl salophens: synthesis and use as ditopic receptors. (199 pp.) 2010
137. Kiviniemi, Tiina: Vibrational dynamics of iodine molecule and its complexes in solid krypton - Towards coherent control of bimolecular reactions? (73 pp.) 2010
138. Ikonen, Satu: Synthesis, characterization and structural properties of various covalent and non-covalent bile acid derivatives of N/O-heterocycles and their precursors. (105 pp.) 2010
139. Siitonen, Anni: Spectroscopic studies of semiconducting single-walled carbon nanotubes. (56 pp.) 2010
140. Raatikainen, Kari: Synthesis and structural studies of piperazine cyclophanes – Supramolecular systems through Halogen and Hydrogen bonding and metal ion coordination. (69 pp.) 2010
141. Leivo, Kimmo: Gelation and gel properties of two- and three-component Pyrene based low molecular weight organogelators. (116 pp.) 2011
142. Martiskainen, Jari: Electronic energy transfer in light-harvesting complexes isolated from *Spinacia oleracea* and from three photosynthetic green bacteria *Chloroflexus aurantiacus*, *Chlorobium tepidum*, and *Prosthecochloris aestuarii*.(55 pp.) 2011
143. Wichmann, Oula: Syntheses, characterization and structural properties of [O,N,O,X´] aminobisphenolate metal complexes. (101 pp.) 2011
144. Ilander, Aki: Development of ultrasound-assisted digestion methods for the determination of toxic element concentrations is ash samples by ICP-OES. (58 pp.) 2011
145. The Combined XII Spring Meeting of the Division of Synthetic Chemistry and XXXIII Finnish NMR Symposium. Book of Abstracts. (90 pp.) 2011
146. Valto, Piia: Development of fast analysis methods for extractives in papermaking process waters. (73 pp.) 2011
147. Andersin, Jenni: Catalytic activity of palladium-based nanostructures in the conversion of simple olefinic hydro- and chlorohydrocarbons from first principles. (78 pp.) 2011
148. Aumanen, Jukka: Photophysical properties of dansylated poly(propylene amine) dendrimers. (55 pp.) 2011